Non-Supersymmetric Heterotic Orbifolds

Thesis submitted in accordance with the requirements of the University of Liverpool for the degree of Doctor in Philosophy by

Viktor G. Matyas

Theoretical Physics
Department of Mathematical Sciences
University of Liverpool

June 2023

Abstract

Viktor G. Matyas

Non-Supersymmetric Heterotic Orbifolds

String theory is the most promising example of a unified theory of quantum gravity and provides a fertile testing ground to explore the possibilities for viable string phenomenology. The main focus of this thesis is on $\mathbb{Z}_2 \times \mathbb{Z}_2$ orbifold compactifications of the heterotic string. To date, these provide some of the best examples of exactly solvable models with many desirable properties. Much of the research in the analysis and classification of these models has centred on the study of those which possess spacetime supersymmetry. However, as known from experiments, even if present, supersymmetry must be broken. Hence, in this thesis, the analysis is extended to non-supersymmetric vacua.

An extensive overview of the methods of calculating the partition function of free fermionic models is given. This includes the possibility of reintroducing some of the moduli dependence which is lost during the construction of models in this formalism. Explicit analytic and numerical tools are provided for the analysis of the one-loop potential and cosmological constant of string vacua. Some interesting structural features of string theory and its physical spectrum are also discussed.

It is shown that starting with ten-dimensional tachyonic vacua can provide a viable starting point for the construction of stable four-dimensional models. This extends the landscape of known tachyon-free 4D vacua and opens up a new avenue in the study of non-supersymmetric string phenomenology. The extent of the vast landscape of heterotic compactifications is explored via the construction of novel four-dimensional Type 0 and Type $\bar{0}$ vacua that have a minimal number of massless fermions and bosons respectively. Some interesting edge cases are found through which the finiteness properties of string theory are explored.

The analysis is also extended to the case of asymmetric heterotic orbifold compactifications. The introduction of asymmetric shifts of the internal lattice induces the projection of some of the geometric moduli. This provides a powerful method by which the construction of stable non-supersymmetric models may become possible. A classification of all allowed shifts is given and their consequences for the phenomenological features of the resulting models are analysed.

Acknowledgements

First of all, I would like to thank my family who supported me throughout my academic journey. My parents have always given me the encouragement and means to achieve higher. Melinda has been a great support and her experiences helped me make better decisions. Mimi always keeps a keen eye on what I am doing and I am sure she will attempt to read this thesis. Good luck! Sophie has helped me every day and made my life a lot happier as a result.

I am very grateful for my supervisor, Alon, who spent much of his time over the past years discussing physics with me. He provided the support and ideas that allowed for the research that is presented within this thesis. I also feel privileged to have spent many meetings and seminars with the wider Strings Group in Liverpool and hope the fruitful discussions continue. I had the opportunity to attend many conferences and workshops where I had many interesting conversations. I would specifically like to thank Ivano, Stefan and Steve with whom I had enlightening discussions.

I shared my journey with many of my peers who I saw working endlessly every day. I believe their work deserves more recognition and so I encourage everyone to browse their research as cited. Sophie [8–11] has been of great support and her presence has made my days more enjoyable; Gabriel [12–17], who is a serious runner, has been a good friend and is always ready to explore the mountains with me; Alavya, who is not a serious runner, is always great fun to chat with and our debates are always very enjoyable; I happy to have spent a year with Mohammad who has been a great addition to the office; Ben [1–7, 18, 19] has been a great collaborator and I am grateful to have had the opportunity to work with him; I hope Alonzo [7] will carry the torch and continue the research we started; Flavio [20–25] has given me a lot of good memories and debates; Max [26, 27] and Bruno [28–33] have been good friends and I hope to keep in touch; The legend of Martin [34–37] will forever haunt the corridors of the TP wing;

List of Publications

This thesis contains material by the author that has appeared in the following publications:

[1] Alon E. Faraggi, Viktor G. Matyas, and Benjamin Percival. "Stable Three Generation Standard–like Model From a Tachyonic Ten Dimensional Heterotic–String Vacuum". In: *The European Physical Journal C* 80.4 (2020), p. 337. arXiv: 1912.00061

[2] Alon E. Faraggi, Viktor G. Matyas, and Benjamin Percival. "Towards the Classification of Tachyon-Free Models From Tachyonic Ten-Dimensional Heterotic String Vacua". In: *Nuclear Physics B* 961 (2020), p. 115231. arXiv: 2006.11340

[3] Alon E. Faraggi, Viktor G. Matyas, and Benjamin Percival. "Classification of Non-Supersymmetric Pati-Salam Heterotic String Models". In: *Physical Review D* 104.4 (2021), p. 046002. arXiv: 2011.04113

[4] Alon E. Faraggi, Viktor G. Matyas, and Benjamin Percival. "Type 0 $\mathbb{Z}_2 \times \mathbb{Z}_2$ Heterotic String Orbifolds and Misaligned Supersymmetry". In: *International Journal of Modern Physics A* 36.24 (2021), p. 2150174. arXiv: 2010.06637

[5] Alon E. Faraggi, Viktor G. Matyas, and Benjamin Percival. "Type $\bar{\mathbf{0}}$ Heterotic String Orbifolds". In: *Physics Letters B* 814 (2021), p. 136080. arXiv: 2011.12630

[6] Alon E. Faraggi, Viktor G. Matyas, and Benjamin Percival. "Towards classification of $\mathcal{N} = 1$ and $\mathcal{N} = 0$ flipped $SU(5)$ asymmetric $\mathbb{Z}_2 \times \mathbb{Z}_2$ heterotic string orbifolds". In: *Physical Review D* 106.2 (2022), p. 026011. arXiv: 2202.04507

[7] Alonzo R. Diaz Avalos, Alon E. Faraggi, Viktor G. Matyas, and Benjamin Percival. "Fayet-Iliopoulos D-Term in Non-Supersymmetric Heterotic String Orbifolds". In: (2023). arXiv: 2302.10075

In Memory of David R. Jenkins

Contents

1 Introduction

The development of *Quantum Field Theory (QFT)* and the *Standard Model (SM)* in the 20^{th} century led to a unified understanding of the forces and interactions. However, there was an outlier, gravity, which did not seem to fit into the framework of QFT in a consistent way. Ever since, the question of the unification of gravity with the other forces of nature, i.e. *Quantum Gravity*, has been at the forefront of fundamental research. To understand our world below the Planck scale, we must uncover a new consistent theory of quantum gravity.

The most promising candidate for a theory of quantum gravity to date is *String Theory*. Even though much effort has been put towards uncovering alternative formulations for the unification of gravity with the other forces of nature, nothing comes close to the successes achieved by string theory over the past few decades. The introduction of an extra degree of freedom to the fundamental objects of our theories yielded a beautifully complex framework which provides a vast landscape of consistent implementations of quantum gravity.

This new framework not only provided the only known context in which one can express the grand unification of all forces but has provoked the development of new mathematical tools with which we can gain a deeper understanding of its possibilities and limits. To this day, there remain many unanswered questions about the structure and stability of string theory and so much more work is needed to gain a deeper understanding of this wonderfully complex mathematical construction.

Despite not having a complete understanding of all structural aspects of string theory, it has provided the best working examples of models which can give a description of gravity on an equal footing with the other forces. Not only that, but it has succeeded in recovering many of the fundamental features of the standard model and beyond. Thus, string theory provides a promising new horizon in describing the world around us. The part of string theory research which aims at deriving models with such desirable phenomenological features is called *String Phenomenology* on which we focus in this thesis.

String theory provides a vast landscape of possible solutions and hence a large array of four-dimensional models can be obtained with different phenomenological features. A promising area of the landscape is $\mathbb{Z}_2 \times \mathbb{Z}_2$ orbifold compactifications of heterotic string theory which provides exactly solvable four-dimensional string vacua with many desirable features. One of the key differentiating results of these models is the ability to produce physical spectra with three generations originating from the unique underlying geometric structure. This is a crucial non-trivial step in the process of deriving viable models from string theory.

Restricting our attention to this special class of heterotic $\mathbb{Z}_2 \times \mathbb{Z}_2$ orbifold compactifications still provides a very large number of possible four-dimensional vacua. The classification of such models has been at the forefront of string phenomenology for the past two decades. One powerful approach is the use of the free fermionic formulation of the heterotic string. This allows for an explicit enumeration of large sets of models which in turn provides an

insight into the structure of the landscape of these orbifold compactifications. Due to its construction in terms of a finite number of parameters, all desired phenomenological features of the models can be used to classify $\mathcal{O}(10^9)$ models at a time with relative ease.

One of the most important early results of string theory was the emergence of spacetime supersymmetry. At the time the observation of supersymmetry was thought to be just around the corner and so string theory's success at recreating a supersymmetric spectrum was thought to be a major advantage. Since then, experiments have made it more and more unlikely that supersymmetry is realised, or at least have pushed the bound of supersymmetry breaking to higher and higher energies. This caused a resurgence in the research of supersymmetry breaking in the context of string theory in recent years.

In this thesis we attempt to unify these notions and focus on novel non-supersymmetric models in terms of the free fermionic formulation of $\mathbb{Z}_2 \times \mathbb{Z}_2$ orbifold compactifications. As we will find out, there are many ways in which one can arrive at a non-supersymmetric four-dimensional model. One way is to compactify a supersymmetric 10D theory and break supersymmetry via a stringy Sherk-Schwarz mechanism. Another way can be to start with a non-supersymmetric, possibly unstable, 10D theory and compactify to 4D while ensuring that the instabilities are cured. Either way, there are important questions about the stability of non-supersymmetric string vacua that have to be addressed.

The outline of this thesis is as follows: In Chapter 2 we begin with giving an overview of some key aspects of string theory. This helps us introduce some of the important overarching concepts and also allows us to fix some notational conventions used throughout. Chapter 3 focuses on the free fermionic formulation of the heterotic string in both ten and four-dimensions. We also provide examples of many of the well-known 10D heterotic theories using this construction. In Chapter 4 we discuss the partition function and one-loop potential of string models and develop analytic and numerical tools which allow for an explicit evaluation of these quantities. In Chapter 5 we present novel non-supersymmetric four-dimensional models that descend from tachyonic ten-dimensional heterotic vacua. This opens up a new avenue in the study of non-supersymmetric strings. Chapter 6 explores the boundaries of the heterotic landscape by studying edge-case models which have a minimal number of fermions or bosons in their massless spectra. We also observe misaligned supersymmetry in models with on-shell tachyons which raises interesting questions about the finiteness of string theory. In Chapter 7 we explore the landscape of asymmetric orbifold compactifications which have the potential to address some of the stability issues that underlie non-supersymmetric string models. Finally, in Chapter 8 we summarise our findings and draw conclusions.

2 Elements of String Theory

In this section, we give a quick introduction to some elementary concepts in string theory that will be repeatedly used in the latter part of this thesis. Our aim is not to give a pedagogical introduction to the topic, but rather to define key quantities and fix some notational conventions. String theory is a vast subject with more than four decades of research covering diverse areas ranging from string phenomenology to string field theory, holography and beyond. There are many excellent resources that provide insights from different perspectives including [38–42]. This section is broadly based on some of the material presented there.

2.1 The Classical String

String theory is a natural extension of particle physics, where instead of point particles, we consider the fundamental building block of matter to be one-dimensional objects. Consider this one-dimensional object, which we call the *fundamental string*, travelling through D-dimensional spacetime M^D. As opposed to a point particle which sweeps a world-line, the string will sweep a two-dimensional surface which we refer to as the *worldsheet* Σ. The classical action that governs the motion of the string is given by the Polyakov action

$$S = -\frac{1}{4\pi\alpha'}\int_\Sigma d^2\sigma\sqrt{h}\,h^{\alpha\beta}\partial_\alpha X^\mu\partial_\beta X^\nu\eta_{\mu\nu}, \tag{2.1}$$

where we used the following quantities:

- $\sigma^\alpha = (\tau, \sigma)$ are the coordinates of the worldsheet with $0 \leq \sigma \leq l$, where l is the length of the string.
- $X^\mu(\tau, \sigma)$ are maps $X^\mu : \Sigma \to M^D$, which provide the embedding of the worldsheet into spacetime.
- $h^{\alpha\beta}$ and $\eta^{\mu\nu}$ are the worldsheet and spacetime metric respectively, and we denote $h = -\det(h^{\alpha\beta})$.
- α' is a constant of dimensions (length)^2, which is the only dimensionful quantity in string theory. It can be used to define a characteristic string mass and length scale

$$M_s = \frac{1}{\sqrt{\alpha'}}\,, \qquad l_s = 2\pi\sqrt{\alpha'}.$$

As suggested by the choice of notation for the spacetime metric $\eta^{\mu\nu}$, throughout this thesis we will assume it to be that of flat D-dimensional Minkowski space. However, it is straightforward to generalise the above action for a general spacetime metric by replacing it with a generic metric $\eta^{\mu\nu} \to g^{\mu\nu}$. In the following, we will also restrict ourselves to discussing

closed strings, for which we must require the periodicity condition $X^\mu(\tau, \sigma + l) = X^\mu(\tau, \sigma)$.

The above action possesses some symmetries which will prove important for later discussions. Hence, it is instructive to list all symmetries under which the Polyakov action is invariant:

- *Poincaré Invariance* | This is a global symmetry of the worldsheet under the map $X^\mu \to \Lambda^\mu{}_\nu X^\nu + C^\mu$, where $\Lambda^\mu{}_\nu$ generate Lorentz transformations while C^μ generate spacetime translations.
- *Diffeomorphism Invariance* | This is a gauge symmetry of the worldsheet under the change of coordinates $\sigma^\alpha \to \tilde{\sigma}^\alpha(\sigma)$. The fields X^μ transform trivially while the worldsheet metric transforms as
$$h_{\alpha\beta} \to \frac{\partial \sigma^\gamma}{\partial \tilde{\sigma}^\alpha} \frac{\partial \sigma^\delta}{\partial \tilde{\sigma}^\beta} h_{\gamma\delta}. \tag{2.2}$$
- *Weyl Invariance* | This is a local symmetry of the action under the rescaling of the worldsheet metric
$$h_{\alpha\beta} \to \Omega^2(\sigma) h_{\alpha\beta}. \tag{2.3}$$

We can use these local symmetries to fix some degrees of freedom. The choice we make is called *conformal gauge*, which fixes the worldsheet metric to Minkowski $h^{\alpha\beta} = \eta^{\alpha\beta}$. Under this choice, the action (2.1) reduces to

$$S = -\frac{1}{4\pi\alpha'} \int_\Sigma d^2\sigma \eta^{\alpha\beta} \partial_\alpha X^\mu \partial_\beta X^\nu \eta_{\mu\nu}. \tag{2.4}$$

The equations of motion are then given by

$$\eta^{\alpha\beta} \partial_\alpha \partial_\beta X^\mu = 0, \tag{2.5}$$

but since we have fixed a gauge for the worldsheet metric, we must remember to also impose equations of motion on $h^{\alpha\beta}$ which give the two extra conditions

$$\partial_\tau X^\mu \partial_\sigma X_\mu = 0\,, \qquad \partial_\tau X^\mu \partial_\tau X_\mu + \partial_\sigma X^\mu \partial_\sigma X_\mu = 0\,, \tag{2.6}$$

which are called the *Virasoro constraints*.

The worldsheet energy-momentum tensor that arises from the variation of the action with respect to the worldsheet metric is given by

$$T_{\alpha\beta} = -4\pi\alpha' \frac{1}{\sqrt{h}} \frac{\delta S}{\delta h^{\alpha\beta}} = \partial_\alpha X^\mu \partial_\beta X_\mu - \frac{1}{2} \eta_{\alpha\beta} \eta^{\rho\sigma} \partial_\rho X^\mu \partial_\sigma X_\mu, \tag{2.7}$$

where we used the conformal gauge to fix the metric as $h^{\alpha\beta} = \eta^{\alpha\beta}$. This shows that the Virasoro constraint equations (2.6) translate to

$$T_{\alpha\beta} = 0, \tag{2.8}$$

i.e. the vanishing of the energy-momentum tensor. It is important to note that Weyl invariance implies that the energy-momentum tensor is also traceless

$$T^\alpha_\alpha = 0, \tag{2.9}$$

which must be satisfied without referring to the equations of motion.

The choice of conformal gauge does not entirely fix all local degrees of freedom. The gauge-fixed action (2.4) remains invariant under worldsheet diffeomorphisms which change the metric up to a Weyl transformation, i.e.

$$\eta_{\alpha\beta} \to \frac{\partial\sigma^\gamma}{\partial\tilde{\sigma}^\alpha}\frac{\partial\sigma^\delta}{\partial\tilde{\sigma}^\beta}\,\eta_{\gamma\delta} = \Omega^2(\sigma)\eta_{\alpha\beta}. \tag{2.10}$$

This is called a *conformal transformation* and it shows that the Polyakov action in the conformal gauge describes a two-dimensional *conformal field theory* of D free scalars. What makes string theory different from a simple two-dimensional conformal field theory is that the conformal invariance is part of a larger gauge symmetry of the theory.

2.1.1 Mode Expansions and Constraints

The equations of motion (2.5) are solved by defining the *lightcone coordinates* $\sigma^\pm \coloneqq \tau \pm \sigma$ in terms of which they become

$$\partial_+\partial_- x^\mu = 0. \tag{2.11}$$

Hence the general solution can be written as a linear combination

$$X^\mu(\tau,\sigma) = X^\mu_L(\sigma^+) + X^\mu_R(\sigma^-), \tag{2.12}$$

which are left and right-moving waves respectively. We must also remember that we are talking about closed strings and thus restricting to $0 \le \sigma \le 2\pi$, we must have $X^\mu(\tau,\sigma) = X^\mu(\tau,\sigma+2\pi)$. The most general solution can then be written as a Fourier expansion of the left and right-moving modes

$$\begin{aligned} X^\mu_L(\sigma^+) &= \frac{1}{2}x^\mu + \frac{1}{2}\alpha' p^\mu \sigma^+ + i\sqrt{\frac{\alpha'}{2}}\sum_{n\neq 0}\frac{1}{n}\alpha^\mu_n e^{-in\sigma^+} \\ X^\mu_L(\sigma^+) &= \frac{1}{2}x^\mu + \frac{1}{2}\alpha' p^\mu \sigma^- + i\sqrt{\frac{\alpha'}{2}}\sum_{n\neq 0}\frac{1}{n}\tilde{\alpha}^\mu_n e^{-in\sigma^-}, \end{aligned} \tag{2.13}$$

where x^μ and p^μ are the position and momentum of the centre of mass of the string. The α^μ and $\tilde{\alpha}^\mu$ are the Fourier modes of left and right moving oscillations and will play a crucial role in the quantisation of string theory. Constant factors such as α' and $1/n$ were chosen for later convenience.

Having found a general solution to the equations of motion (2.5) we are still required to impose the Virasoro constraints (2.6) which in lightcone coordinates become

$$T_{++} = \partial_+ X^\mu \partial_+ X_\mu = 0\,, \qquad T_{--} = \partial_- X^\mu \partial_- X_\mu = 0. \tag{2.14}$$

These will further restrict the form of our general solution (2.13) by constraining the Fourier modes via

$$\begin{aligned} T_{++} = \partial_+ X^\mu \partial_+ X_\mu = \frac{\alpha'}{2} \sum_{m,n\in\mathbb{Z}} \alpha_m \cdot \alpha_{n-m} e^{-in\sigma^-} &\coloneqq \alpha' \sum_{n\in\mathbb{Z}} L_n \, e^{-in\sigma^+} = 0 \\ T_{--} = \partial_- X^\mu \partial_- X_\mu = \frac{\alpha'}{2} \sum_{m,n\in\mathbb{Z}} \tilde{\alpha}_m \cdot \tilde{\alpha}_{n-m} e^{-in\sigma^-} &\coloneqq \alpha' \sum_{n\in\mathbb{Z}} \tilde{L}_n \, e^{-in\sigma^-} = 0, \end{aligned} \tag{2.15}$$

where we defined

$$\alpha_0^\mu = \tilde{\alpha}_0^\mu \coloneqq \sqrt{\frac{\alpha'}{2}}\, p^\mu. \tag{2.16}$$

The sum of Fourier modes L_n and $\tilde{L}_n$ defined above, referred to as *Virasoro generators*, are crucial quantities in string theory and are constrained by (2.15) as

$$L_n = \tilde{L}_n = 0 \quad \forall\, n \in \mathbb{Z}. \tag{2.17}$$

In lightcone coordinates, conformal transformations do not mix the coordinates and hence can be written as

$$\sigma^+ \to \sigma'(\sigma^+), \quad \sigma^- \to \sigma'(\sigma^-), \tag{2.18}$$

The energy-momentum tensor is conserved under these transformations

$$\partial_- T_{++} = 0, \quad \partial_+ T_{--} = 0, \tag{2.19}$$

which implies that we have two separate conserved currents

$$T_{++} = T_{++}(\sigma^+) \quad \text{and} \quad T_{--} = T_{--}(\sigma^-), \tag{2.20}$$

with the corresponding conserved charges precisely given by L_m and $\tilde{L}_m$.

To emphasise the importance of the constraints (2.17) one must notice that L_0 and $\tilde{L}_0$ can be related to the effective mass of the string by

$$M^2 = -p^\mu p_\mu = \frac{4}{\alpha'} \sum_{n=1}^{\infty} \alpha_n \cdot \alpha_{-n} = \frac{4}{\alpha'} \sum_{n=1}^{\infty} \tilde{\alpha}_n \cdot \tilde{\alpha}_{-n}. \tag{2.21}$$

This condition thus relates left and right moving modes and is known as *level-matching* and the quantity

$$\overset{(\sim)}{N} = \sum_{n=1}^{\infty} \overset{(\sim)}{\alpha}_n \cdot \overset{(\sim)}{\alpha}_{-n} \tag{2.22}$$

is often called the *occupation number*.

2.2 The Quantised String

In the previous section, we derived and solved the classical equations of motion for a closed string propagating in D-dimensional spacetime. In this section, our aim is to quantise this theory. There are three main approaches one can take to quantise the bosonic string, namely

covariant, lightcone and BRST quantisation. Each method has its own benefits and drawbacks. In the following, we outline the procedure for lightcone quantisation which is technically simpler. However, it is sufficient in order to introduce the main concepts needed to quickly progress to the main content of this thesis.

In lightcone quantisation, we make use of the residual gauge symmetry of the classical solution to fix a gauge and quantise only the physical states of our theory. What we give up in return for this simplification is manifest Lorentz symmetry which is obscured by our choice of gauge. When fixing the conformal gauge in the previous section, we did not use all gauge degrees of freedom to do so. In particular, our action and equations of motion are still invariant under diffeomorphisms which change the metric up to a Weyl transformation as expressed in (2.10). This residual symmetry can be fixed by choosing an appropriate gauge. In order to do so, we need to introduce the spacetime lightcone coordinates

$$X^{\pm} \coloneqq \frac{1}{\sqrt{2}}(X^0 \pm X^{D-1}), \tag{2.23}$$

which breaks Lorentz invariance since they pick some special directions. In these coordinates, the Minkowski metric takes the form

$$\eta_{+-} = \eta_{-+} = -1\,, \qquad \eta_{ij} = \delta_{ij}, \tag{2.24}$$

where all other components vanish and i, j to run over all non-lightcone spacetime coordinates, i.e. $i, j = 1, \cdots, D-2$. The solutions to the equations of motion for X^+ can then be written as

$$X^+ = X^+_L(\sigma^+) + X^+_R(\sigma^-). \tag{2.25}$$

We now use our residual local degrees of freedom to pick X^+ such that

$$\begin{aligned} X^+_L =& \frac{1}{2}x^+ + \frac{1}{2}\alpha' p^+ \sigma^+ \\ X^+_R =& \frac{1}{2}x^+ + \frac{1}{2}\alpha' p^+ \sigma^-, \end{aligned} \tag{2.26}$$

and so $X^+ = x^+ + \alpha' p^+ \tau$. This choice fixes all residual local symmetries and is referred to as *lightcone gauge*.

Having fixed all non-physical degrees of freedom we can solve for X^- by imposing the Virasoro constraints (2.14). Indeed the form of X^- is entirely determined up to an integration constant. For example, the oscillator modes α^-_n are given by

$$\alpha^-_n = \frac{1}{\sqrt{2\alpha'}}\frac{1}{p^+}\sum_{i=1}^{D-2}\sum_{m=-\infty}^{\infty}\alpha^i_{n-m}\alpha^i_m. \tag{2.27}$$

and so the level-matching conditions (2.21) become

$$M^2 = 2p^+p^- - \sum_{i=1}^{D-2} p^i p^i = \frac{4}{\alpha'}\sum_{i=1}^{D-2}\sum_{n=1}^{\infty}\alpha^i_n\alpha^i_{-n} = \frac{4}{\alpha'}\sum_{i=1}^{D-2}\sum_{n=1}^{\infty}\tilde{\alpha}^i_n\tilde{\alpha}^i_{-n}. \tag{2.28}$$

This means that the physical string solutions can be parametrised by x^-, p^+, x^i and p^i

together with $2(D-2)$ oscillators α^i and $\tilde{\alpha}^i$ to which we refer to as *transverse oscillators*.

Now that we have isolated all physically distinct degrees of freedom, the theory is quantised by imposing commutation relations

$$\begin{aligned} [x^i, p^j] &= i\delta^{ij}\,, \qquad [x^-, p^+] = -i \\ [\alpha_n^i, \alpha_m^j] &= [\tilde{\alpha}_n^i, \tilde{\alpha}_m^j] = n\delta^{ij}\delta_{n+m,0}, \end{aligned} \tag{2.29}$$

where the $i, j = 1, \cdots, D-2$ run over the transverse directions as before. The transverse oscillator modes provide natural creation and annihilation operators. The Hilbert space of states is formed by defining a vacuum state $|0, p\rangle$ such that

$$\hat{p}^\mu |0,p\rangle = p^\mu |0,p\rangle\,, \quad \alpha_n^i |0,p\rangle = \tilde{\alpha}_n^i |0,p\rangle = |0,p\rangle\,, \quad n > 0. \tag{2.30}$$

We can then act by subsequent creation operators α_{-n}^i and $\tilde{\alpha}_{-n}^i$, $n > 0$, to build the states of our theory.

Imposing the level-matching constraints (2.28) on the quantised theory introduces an ordering ambiguity. This is because in the presence of the commutation relations (2.29), the ordering of the transverse oscillator modes in the number operator

$$N = \sum_{i=1}^{D-2} \sum_{n=1}^{\infty} \alpha_n^i \alpha_{-n}^i, \tag{2.31}$$

is not clear. Taking all operators to be normal ordered introduces an overall shift in the number operators and hence in the level-matching conditions as

$$M^2 = \frac{4}{\alpha'}(N - a) = \frac{4}{\alpha'}(\tilde{N} - a), \tag{2.32}$$

where a is an undetermined constant. Using ζ-function regularisation methods, this constant can be evaluated as

$$a = \frac{D-2}{24}. \tag{2.33}$$

Moreover, a closer examination of Lorenz invariance in the quantised theory reveals that the quantisation is only consistent if $D = 26$. Hence the level-matching condition becomes

$$M^2 = \frac{4}{\alpha'}(N - 1) = \frac{4}{\alpha'}(\tilde{N} - 1), \tag{2.34}$$

which can be used to derive the masses of on-shell string states.

The spectrum of the bosonic sting has some interesting features. At level $N = 1$ there is a tachyon with mass

$$M^2 = -\frac{4}{\alpha'}, \tag{2.35}$$

which shows that the quantised theory is unstable. The excited states include a photon, an anti-symmetric 2-form $B_{\mu\nu}$ called the *Kalb-Ramond field*, a scalar Φ called the *dilaton* and a graviton $G_{\mu\nu}$. This shows that the string theory is indeed a theory of quantum gravity.

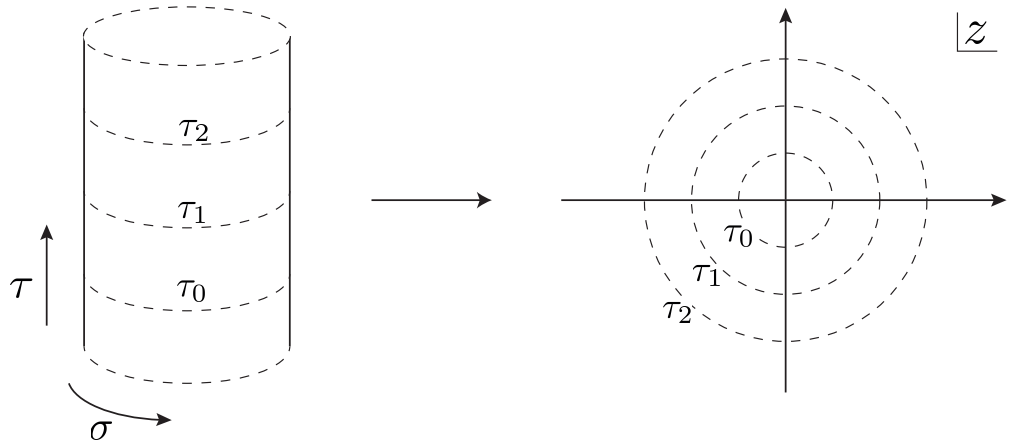

FIGURE 2.1: *The conformal map from the worldsheet cylinder to the complex plane via* (2.36)*. As shown, equal time slices on the worldsheet become circles of constant radius on the complex plane.*

2.3 The Worldsheet Prespective

We have already seen that from the worldsheet point of view, the Polyakov action in the conformal gauge describes a conformal field theory (CFT) of D free scalars in two dimensions. This means that many powerful tools we know from CFT can be readily applied to string theory.

As we are only considering closed strings, the worldsheet is a cylinder $\Sigma = I \times S^1$, where $I \subseteq \mathbb{R}$. To make connection with the CFT formalism we have to perform a Wick rotation of the worldsheet coordinate $\tau \to -i\tau$ which renders the worldsheet metric euclidean. Now we can define complex coordinates

$$z = e^{\tau + i\sigma}, \qquad \bar{z} = e^{\tau - i\sigma}, \tag{2.36}$$

which map the cylinder into the punctured complex plane. Constant time slices become circles of constant radius and so time-ordered products are replaced by radial ordering. Moreover, integration over the worldsheet becomes a problem of contour integration around the singularity at $z = 0$. An illustration of this mapping is shown in Figure 2.1

In these coordinates, the conditions on the energy-momentum tensor manifest as

$$\partial_{\bar{z}} T_{zz} = 0, \qquad \partial_z T_{\bar{z}\bar{z}} = 0, \tag{2.37}$$

which imply that the two non-vanishing components are the holomorphic and anti-holomorphic functions

$$T(z) \coloneqq T_{zz}, \qquad \bar{T}(\bar{z}) \coloneqq T_{\bar{z}\bar{z}}. \tag{2.38}$$

These conditions are analogous to (2.19) and (2.20) derived previously. This shows that the decoupling of left and right-moving modes in the Minkowski formalism translates to the independence of holomorphic and anti-holomorphic fields in the Euclidean picture.

This shows that the mode expansions of string theory in terms of left and right moving

degrees of freedom become Laurent series in the worldsheet CFT. Specifically, for the energy-momentum tensor we define the expansion

$$T(z) = \sum_n \frac{L_n}{z^{n+2}}, \qquad \bar{T}(\bar{z}) = \sum_n \frac{\tilde{L}_n}{\bar{z}^{n+2}}. \tag{2.39}$$

These can now be inverted to find expressions for the Virasoro generators using the contour integrals

$$L_n = \frac{1}{2\pi i} \oint dz\, z^{n+1} T(z), \qquad \tilde{L}_n = \frac{1}{2\pi i} \oint d\bar{z}\, \bar{z}^{n+1} \bar{T}(\bar{z}). \tag{2.40}$$

These are the conserved charges associated to conformal transformations. They obey the *Virasoro algebra* with the commutators given by

$$\begin{aligned} [L_m, L_n] &= (m-n)L_{m+n} + \frac{c}{12} m(m^2-1)\delta_{m+n,0}, \\ [\tilde{L}_m, \tilde{L}_n] &= (m-n)\tilde{L}_{m+n} + \frac{\tilde{c}}{12} m(m^2-1)\delta_{m+n,0}, \end{aligned} \tag{2.41}$$

where c and $\tilde{c}$ are known as the *central charges* of the CFT. This commutation relation follows from the operator product expansion (OPE) of the energy-momentum tensor which is a unique feature of CFTs and describes how local operators behave. The quantity c, and analogously $\tilde{c}$, then arises as a free parameter in the OPE of the energy-momentum tensor.

The central charge is a critical quantity in CFT and string theory. It captures the fact that quantum effects may render the conformal symmetry anomalous. Indeed, in theories where $c, \tilde{c} \neq 0$ the classical conformal symmetry is broken and the resulting anomaly is referred to as the *Weyl anomaly*.

2.4 The Fermionic String

There are a few key issues with the bosonic string theory discussed so far. While the theory is consistent, it lacks the presence of spacetime fermions which means that we have no chance of producing models which resemble the real world. Moreover, the presence of tachyonic degrees of freedom means that a true stable vacuum of the theory has not been found and so is not suitable for phenomenology. In this section, we aim to resolve these issues by introducing fermionic degrees of freedom on the worldsheet. As we will see this leads to the conformal symmetry of the worldsheet being complemented by worldsheet supersymmetry. This formulation of superstring theory is called the *Ramond-Neveu-Schwarz formalism* (RNS) which implements manifest worldsheet supersymmetry instead of doing so directly in the target space.

A natural approach is to introduce fermionic fields on the worldsheet to complement the bosonic fields $X^\mu(z, \bar{z})$. This can be achieved by adding a term describing D massless Majorana fermions $\psi^\mu(z, \bar{z})$ to the Polyakov action (2.4) in conformal gauge to give

$$S = -\frac{1}{4\pi\alpha'} \int_\Sigma dz d\bar{z}\, \partial_\alpha X^\mu \partial^\alpha X_\mu + \frac{1}{2\pi} \int_\Sigma dz d\bar{z}\, \left(\psi^\mu \bar{\partial}\, \psi_\mu + \bar{\psi}^\mu \partial \bar{\psi}_\mu \right), \tag{2.42}$$

where we denoted the fermions which decompose into two chiral Weyl components as

$$\psi^\mu(z,\bar{z}) = \begin{pmatrix}\psi^\mu(z)\\ \psi^\mu(\bar{z})\end{pmatrix} := \begin{pmatrix}\psi^\mu\\ \bar{\psi}^\mu\end{pmatrix}. \tag{2.43}$$

The equations of motion for the spinors are then given by the Dirac equation

$$\bar{\partial}\psi^\mu = 0, \qquad \partial\bar{\psi}^\mu = 0, \tag{2.44}$$

and so similar to the bosons, the holomorphic and anti-holomorphic sectors decouple. As mentioned above, in addition to conformal transformation, this action is now also invariant under global worldsheet supersymmetry transformations exchanging bosonic and fermionic degrees of freedom.

Since we are still considering only closed strings, the fermions must also obey the periodicity $\sigma = \sigma + 2\pi$ or $z = e^{2\pi i}z$ of the worldsheet. Unlike in the case of the boson, we now have two distinct possibilities for the boundary conditions:

$$\begin{aligned}\psi &: \begin{cases}\psi^\mu(e^{2\pi i}z) = +\psi^\mu(z) & \text{(NS)},\\ \psi^\mu(e^{2\pi i}z) = -\psi^\mu(z) & \text{(R)},\end{cases}\\ \bar{\psi} &: \begin{cases}\bar{\psi}^\mu(e^{2\pi i}\bar{z}) = +\bar{\psi}^\mu(\bar{z}) & \text{(NS)},\\ \bar{\psi}^\mu(e^{2\pi i}\bar{z}) = -\bar{\psi}^\mu(\bar{z}) & \text{(R)}.\end{cases}\end{aligned} \tag{2.45}$$

These boundary conditions are usually referred to as *Ramond* (R) and *Neveu-Schwarz* (NS) as denoted. It is important to note that the boundary condition for the holomorphic and anti-holomorphic fermions can be chosen independently so there are four distinct choices labelled as R-R, NS-NS, R-NS and NS-R depending on the choice for the holomorphic and anti-holomorphic sector respectively.

As for the bosons, the classical fermionic fields also have mode expansions in terms of left and right-moving modes. They can be written as the Laurent series

$$\begin{aligned}\psi^\mu(z) &= \sum_{r\in\mathbb{Z}+\nu}\frac{\psi^\mu_r}{z^{r+1/2}},\\ \bar{\psi}^\mu(\bar{z}) &= \sum_{r\in\mathbb{Z}+\tilde{\nu}}\frac{\tilde{\psi}^\mu_r}{\bar{z}^{r+1/2}},\end{aligned} \tag{2.46}$$

where $\nu, \tilde{\nu} = 0$ or $1/2$ for Ramond and Neveu-Schwarz boundary conditions respectively. The quantisation of these modes is implemented by imposing the anti-commutation relation

$$\{\psi^\mu_r, \psi^\nu_s\} = \{\tilde{\psi}^\mu_r, \tilde{\psi}^\nu_s\} = \eta^{\mu\nu}\delta_{r+s,0}. \tag{2.47}$$

Due to the presence of worldsheet supersymmetry and the new fields we now have the currents

$$G(z) = \sum_{r\in\mathbb{Z}+\nu}\frac{G_r}{z^{r+3/2}}, \qquad \bar{G}(\bar{z}) = \sum_{r\in\mathbb{Z}+\tilde{\nu}}\frac{\tilde{G}_r}{\bar{z}^{r+3/2}}, \tag{2.48}$$

which are the superpartners of the energy-momentum tensor with the mode expansion

$$G_r = \sum_{n\in\mathbb{Z}} \alpha_n \cdot \psi_{r-n}. \tag{2.49}$$

The Virasoro generators are modified in the presence of the new fields and are given by the mode expansion

$$\begin{aligned} L_m =& \frac{1}{2}\sum_{n\in\mathbb{Z}} \alpha_{m-n}\cdot\alpha_n + \frac{1}{4}\sum_{r\in\mathbb{Z}+\nu}(2r-m)\psi_{m-r}\cdot\psi_r, \\ L_0 =& \frac{1}{2}\alpha_0\cdot\alpha_0 + \sum_{n=1}^{\infty}\alpha_{-n}\cdot\alpha_n - a + \sum_{r\in\mathbb{Z}+\nu>0} r\psi_{-r}\cdot\psi_r - a_\nu \\ =& \frac{\alpha'}{4}p^2 + (N-a) + (N_\nu - a_\nu) \end{aligned} \tag{2.50}$$

where $a = (D-2)/24$ is the usual normal ordering constant coming from the bosonic oscillator modes. We also introduced a new normal ordering constant a_ν arising from the fermionic oscillator modes whose value differs for the NS and R sectors

$$a_\nu = \begin{cases} \frac{D-2}{48} & \nu = \frac{1}{2} \quad \text{(NS)} \\ -\frac{D-2}{24} & \nu = 0 \quad \text{(R)}. \end{cases} \tag{2.51}$$

The new modes satisfy the commutation and anti-commutation relations

$$\begin{aligned} \{G_r, G_s\} =& 2L_{r+s} + \frac{c}{3}\left(r^2 - \frac{1}{4}\right)\delta_{r+s,0} \\ [L_m, G_r] =& \left(\frac{m}{2} - r\right) G_{m+r}, \end{aligned} \tag{2.52}$$

with the $L_m, \tilde{L}_m$ still satisfying the original commutation relations of the Virasoro algebra (2.41).

Similarly to the bosonic case, one proceeds using lightcone quantisation to build the Hilbert space of physical states. In the NS sector, $\nu \in \mathbb{Z} + 1/2$ so all fermionic modes ψ_r act as either creation or annihilation operators and we can define a unique vacuum $|0,p\rangle_{\text{NS}}$ by

$$\begin{aligned} \psi_r^i |0,p\rangle_{\text{NS}} =& 0 \quad r > 0, \\ \alpha_n^i |0,p\rangle_{\text{NS}} =& 0 \quad n > 0. \end{aligned} \tag{2.53}$$

We can then build states by acting with ψ^i_{-r}, $r > 0$. Since these operators are now fermionic we can act at only once with any given operator.

In the R sector, $\nu \in \mathbb{Z}$, and so the existence of the mode ψ_0^i requires extra care. From the relations (2.47) we see that these modes satisfy the anti-commutator

$$\{\psi_0^i, \psi_0^j\} = \delta^{ij}, \tag{2.54}$$

meaning that the ground state of the R sector must form a representation of the Clifford algebra. This means that the R vacuum $|0,p\rangle_{\text{R}}$ behaves like a spinor and falls into one of

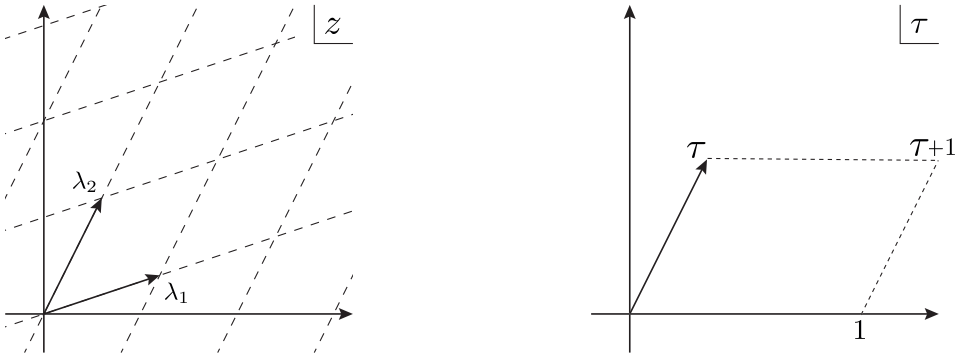

FIGURE 2.2: *(Left) The definition of the worldsheet torus on using a lattice in the complex plane using the identification* (2.55)*. (Right) The definition of a torus in terms of the modular parameter* τ *via* (2.56)*.*

two irreducible representations of the Clifford algebra. Excited states are then built using the creation operators as before.

The spectrum of the fermionic string now includes spacetime fermions which is a clear improvement over the bosonic string. A physical tachyon still arises from the ground state of the NS sector. However, as will become clear in the following section they can be consistently removed from the physical spectrum giving a stable theory. It can also be shown that the critical dimension of the superstring is $D = 10$ and so this brings us closer to the desired four-dimensional world.

2.5 The String Partition Function

In a quantum field theory, quantum corrections arrange in a perturbative series which manifests as a diagrammatic expansion in terms of spacetime loops. In string theory, the worldline of a point particle physics is replaced by the worldsheet, which in the case of the closed string, sweeps a cylindrical surface. This means that tree-level amplitudes are characterised by a sphere, one-loop amplitudes by a torus and so on. Hence, the sting perturbative series manifests as an expansion in terms of worldsheet topology. The first quantum corrections in string theory arise at one loop and so in this section, we will focus on the one-loop vacuum-to-vacuum amplitude.

2.5.1 The Worldsheet Torus and Modular Invariance

Since the one-loop vacuum amplitude corresponds to a worldsheet torus, it is crucial that we parametrise the torus such that only physically distinct configurations are taken into account. A two-dimensional torus $\mathbf{T}^2$ can be parametrised using a complex coordinate $z \in \mathbb{C}$ under the identification

$$z \simeq z + n\lambda_1 + m\lambda_2, \tag{2.55}$$

where $m, n \in \mathbb{Z}$ and $\lambda_1, \lambda_2 \in \mathbb{C}$ are two arbitrary complex numbers. The two $\lambda_{1,2}$ define a lattice in the complex plane Λ and so the torus can be written as the quotient $\mathbf{T}^2 = \mathbb{C}/\Lambda$ as depicted in Figure 2.2.

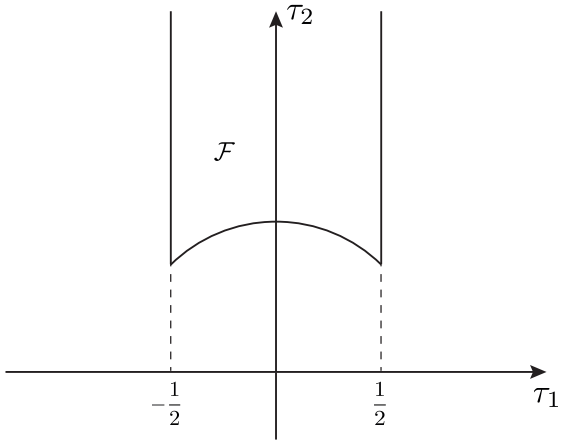

FIGURE 2.3: *(The fundamental domain $\mathcal{F}$ of the modular group defined in* (2.59)*. This region represents all allowed values for the modular parameter τ.*

Due to the conformal invariance of the worldsheet, we must assure that only conformally distinct tori are selected. Since we know that conformal transformations are ones which preserve angles, the two complex vectors λ_1, λ_2 must transform such that their relative angles stay constant. This implies that only their ratio

$$\tau \coloneqq \frac{\lambda_2}{\lambda_1} = \tau_1 + i\tau_2, \tag{2.56}$$

is modular invariant. Hence without the loss of generality, we can set $\lambda_1 = 1$. Moreover, we can restrict to cases when $\mathrm{Im}(\tau) > 0$ since all other tori can be related to by reflection. The *modular parameter* τ defined under these restrictions successfully parametrises all tori which cannot be related by infinitesimal conformal transformations. This construction is also illustrated in Figure 2.2.

There are, however, large reparametrisations of the torus which are not captured by the above construction. These correspond do *Dehn twists* which are large 2π twists at cuts along the two non-contractible loops of the torus. Such transformations along the two cycles translate to $\tau \to \tau + 1$ and $\tau \to \frac{\tau}{\tau+1}$ which generate the *modular group* $SL(2,\mathbb{Z})$, acting as

$$\tau \to \frac{a\tau + b}{c\tau + d} \quad \text{s.t.} \quad \begin{pmatrix} a & b \\ c & d \end{pmatrix} \in SL(2,\mathbb{Z}). \tag{2.57}$$

Hence requiring that the modular parameter τ defined under the constraints (2.56) be invariant under the modular group means that all described tori are now not distinct under both infinitesimal conformal transformations and global diffeomorphisms.

Instead of the generating transformations above, it is insightful to define the generators of the modular group as

$$\begin{aligned} T: &\quad \tau \to \tau + 1 \\ S: &\quad \tau \to -\frac{1}{\tau}. \end{aligned} \tag{2.58}$$

This helps to visualise the region of the complex plane covered by τ. T is a constant shift in τ while S acts as an inversion around the unit circle and a reflection at the real axis. So the modular parameter takes values in the region

$$\mathcal{F} = \{\tau \in \mathbb{C} \,|\, |\tau|^2 > 1 \ \wedge \ -1/2 < \tau_1 < 1/2\}, \tag{2.59}$$

which we refer to as the *fundamental domain* of the modular group and is shown in Figure 2.3. Summing over all inequivalent tori then amounts to a modular integration of τ over the fundamental domain which can be achieved via the modular invariant measure

$$\int_{\mathcal{F}} \frac{d^2\tau}{\tau_2^2}. \tag{2.60}$$

The integration of quantities dependent on τ using this measure will perform the required summation over only distinct tori.

2.5.2 The Partition Function

The partition function in string theory corresponds to the one-loop vacuum amplitude in Euclidean time. It is a crucial quantity and will be one of the central elements spanning this thesis. Not only can one gain crucial phenomenological features straight from the partition function, but due to its construction as the one-loop vacuum amplitude it will provide important insights into the stability of string models.

The one-loop amplitude, and hence the partition function, can be constructed as follows. Taking the one-loop worldsheet torus amounts to the two ends of the worldsheet cylinder being identified along the euclidean time direction τ. In terms of states, this corresponds to setting the same in and out states which results in the sum of all states in the Hilbert space giving a trace. Time translations along the worldsheet are generated by the worldsheet Hamiltonian

$$H = L_0 + \tilde{L}_0. \tag{2.61}$$

When identifying the final and initial states, i.e. glueing the torus, we have the choice of twisting the torus along the spacial direction σ. This corresponds to a spatial shift which is generated by the worldsheet momentum operator

$$P = L_0 - \tilde{L}_0. \tag{2.62}$$

Since in the above formulation of the worldsheet torus, τ_2 corresponds to the time-like direction and τ_1 corresponds to the space-like direction, the partition function is then given by the trace

$$Z(\tau, \bar{\tau}) = \mathrm{Tr}_{\mathcal{H}} \left(e^{-2\pi\tau_2 H} e^{2\pi i \tau_1 P} \right) = \mathrm{Tr}_{\mathcal{H}} \left(q^{L_0} \, \bar{q}^{\tilde{L}_0} \right), \tag{2.63}$$

where we defined $q \coloneqq e^{2\pi i \tau}$ and $\bar{q} \coloneqq e^{-2\pi i \bar{\tau}}$. These parameters defined carry important meaning in CFT and string theory. This is because the partition function of any model can be expanded as a series

$$Z(\tau, \bar{\tau}) = \sum_{m,n} a_{mn} q^m \bar{q}^n, \tag{2.64}$$

which we refer to as the *q-expansion*. Written as such, the coefficients a_{mn} count the degeneracy of states at any given mass level m, n. This provides a convenient way to infer many properties of a theory by looking directly at the partition function.

It is important to note that due to the way we constructed the above partition function, the zero-modes of the Virasoro generators are the ones defined on the worldsheet cylinder as opposed to the CFT on the complex plane. We have seen in Section 2.3 that the cylinder can be mapped to the complex plane via a conformal map. Under this mapping, the energy-momentum tensor and hence the zero-modes pick up an extra shift proportional to the central charge of the worldsheet CFT via

$$L_0^{\text{Cylinder}} = L_0 - \frac{c}{24}, \qquad \tilde{L}_0^{\text{Cylinder}} = \tilde{L}_0 - \frac{\tilde{c}}{24}. \tag{2.65}$$

Hence the partition function written for the worldsheet CFT also pick up this contribution and becomes

$$Z(\tau, \bar{\tau}) = \text{Tr}_{\mathcal{H}} \left(e^{-2\pi\tau_2 H} e^{2\pi i \tau_1 P} \right) = \text{Tr}_{\mathcal{H}} \left(q^{L_0 - \frac{c}{24}} \, \bar{q}^{\tilde{L}_0 - \frac{\tilde{c}}{24}} \right), \tag{2.66}$$

The appearance of this term has an interesting analogue arising from the string quantisation as the normal ordering constant $a = (D-2)/24$ as shown in (2.33). For a CFT of a holomorphic or anti-holomorphic free boson, the central charge is given by $c = 1$ and $\tilde{c} = 1$ respectively. This means that for $(D-2)$ free bosons as appearing in the gauge-fixed string action (2.42) the central charge is given by $c = (D-2)/24$ and $\tilde{c} = (D-2)/24$. Hence we see that these two quantities indeed match and we will refer to them interchangeably in this section when discussing the partition functions of string theory.

We now move on to derive the partition function for free bosons and free fermions in the worldsheet CFT. This will prove crucial in the following section to write down the partition function for string models.

2.5.3 Partition Function for Bosons

In this section, we calculate the partition function of the free bosons in the worldsheet Polyakov action (2.42). Without the loss of generality, we focus on the holomorphic sector for a single bosonic degree of freedom as the calculation for the anti-holomorphic sector is identical.

As the partition function (2.66) is given by the trace over the Hilbert space of states, recall that states are generated by the action of creation operators α_m on the vacuum state $|0\rangle$ as shown in (2.30). We can construct a basis for the Hilbert space $\mathcal{H}$ by writing

$$|m_1, m_2, \cdots, m_N\rangle = F(m_i)\, \alpha_{-1}^{m_1} \alpha_{-2}^{m_2} \cdots \alpha_{-N}^{m_N} |0, p\rangle\,, \tag{2.67}$$

where we have collected all normalisation factors if $F(m_i)$. This basis is orthonormal meaning that the inner product is

$$\langle m_1, m_2, \cdots, m_N | m_1', m_2', \cdots, m_N' \rangle = \delta_{m_1, m_1'} \delta_{m_2, m_2'} \cdots \delta_{m_N, m_N'}. \tag{2.68}$$

Given this basis, the trace over the Hilbert space in the holomorphic partition function becomes

$$\begin{aligned} Z(\tau) &= \mathrm{Tr}_{\mathcal{H}}\left(q^{L_0-\frac{c}{24}}\right) \\ &= \sum_{m_1=0}^{\infty}\sum_{m_2=0}^{\infty}\cdots\langle m_1, m_2, \cdots| \, q^{L_0-\frac{c}{24}} \, |m_1, m_2, \cdots\rangle \, . \end{aligned} \tag{2.69}$$

In order to compute this trace, recall the mode expansion of L_0 and its definition in terms of the number operator N

$$L_0 = \frac{1}{2}\alpha_0 \cdot \alpha_0 + \sum_{n=1}^{\infty}\alpha_{-n}\cdot\alpha_n = \frac{\alpha'}{4}p^2 + N, \tag{2.70}$$

Its commutator with the creation operators, which follows directly from the commutation relations (2.29), is given by

$$[N, \alpha_m] = -m\alpha_m. \tag{2.71}$$

Using the above commutator, it can be shown that the zero-mode L_0 satisfies the eigenvalue equation

$$N\,|m_1, m_2, \cdots, m_N\rangle = \sum_{k=1}^{N} k m_k \, |m_1, m_2, \cdots, m_N\rangle \, . \tag{2.72}$$

The calculation of the trace then involves the replacement of the zero-mode operator with its eigenvalue via

$$\begin{aligned} Z(\tau) =& \sum_{m_1=0}^{\infty}\sum_{m_2=0}^{\infty}\cdots\langle m_1, m_2, \cdots| \, q^{L_0-\frac{c}{24}} \, |m_1, m_2, \cdots\rangle \\ =& \sum_{m_1=0}^{\infty}\sum_{m_2=0}^{\infty}\cdots\langle m_1, m_2, \cdots| \, q^{\frac{\alpha'}{4}p^2+N-\frac{c}{24}} \, |m_1, m_2, \cdots\rangle \\ =& q^{\frac{\alpha'}{4}p^2-\frac{c}{24}}\sum_{m_1=0}^{\infty}\sum_{m_2=0}^{\infty}\cdots\prod_{k=1}^{\infty}q^{km_k} \\ =& q^{\frac{\alpha'}{4}p^2-\frac{c}{24}}\prod_{k=1}^{\infty}\frac{1}{1-q^k} = \frac{1}{\eta(\tau)}q^{\frac{\alpha'}{4}p^2}, \end{aligned} \tag{2.73}$$

where we expressed the result as the Dedekind eta-function defined in (A.3) and substituted for the fact that the CFT of one free scalar has a central charge $c = 1$ as discussed previously. Following an entirely analogous calculation for the anti-holomorphic sector, one arrives at the total partition function

$$Z(\tau, \bar{\tau}) = \frac{1}{\eta(\tau)\bar{\eta}(\bar{\tau})}q^{\frac{\alpha'}{4}p^2}\bar{q}^{\frac{\alpha'}{4}p^2}, \tag{2.74}$$

which as we see still depends on the momentum operator.

To properly take into account the effect of the momentum operator above on the partition function one has to notice that the vacuum we used only considers the oscillator modes. To calculate the contribution of the momentum we need to consider vacua containing eigenstates

of the momentum operator $|0,p\rangle$ and take a trace over them giving

$$\mathrm{Tr}\left(q^{\frac{\alpha'}{4}p^2}\bar{q}^{\frac{\alpha'}{4}p^2}\right) \simeq \int_{-\infty}^{\infty}\frac{dp}{2\pi}\,\langle 0,p|\,q^{\frac{\alpha'}{4}p^2}\bar{q}^{\frac{\alpha'}{4}p^2}\,|0,p\rangle = \int_{-\infty}^{\infty}\frac{dp}{2\pi}e^{-\pi\alpha'\tau_2 p^2} \simeq \frac{1}{\sqrt{\tau_2}}. \tag{2.75}$$

This results in the total partition function for one worldsheet scalar

$$Z(\tau,\bar{\tau}) = \frac{1}{\sqrt{\tau_2}}\frac{1}{\eta(\tau)\bar{\eta}(\bar{\tau})}. \tag{2.76}$$

The Polyakov action (2.42) contains $D = 26$ bosonic degrees of freedom. In the lightcone gauge, this gives $d = D-2 = 24$ free bosons on the worldsheet, and so the partition function of the bosonic string is given by

$$Z_B(\tau,\bar{\tau}) = \frac{1}{\tau_2^{12}}\frac{1}{\eta(\tau)^{24}\bar{\eta}(\bar{\tau})^{24}}. \tag{2.77}$$

Having found the partition function it is crucial to check whether it respects the underlying modular symmetry of the toroidal parameter. Using the transformation properties of the η-funcntion (A.4) we find that Z_B is indeed invariant under S and T-transformations and is, therefore, modular invariant.

2.5.4 Partition Function for Fermions

We now move on to calculating the partition function for the free chiral worldsheet fermions that arise from the Polyakov action (2.42). The procedure is similar to the bosonic case, but now we have to also consider the fermionic oscillator modes. We start by considering a single fermion in the holomorphic sector, we will then extend the result to all degrees of freedom in superstring action.

Starting from the expression for the toroidal one-loop CFT partition function (2.66) for the holomorphic sector

$$Z(\tau) = \mathrm{Tr}_{\mathcal{H}}\left(q^{L_0}\right), \tag{2.78}$$

we can substitute for the fermionic part of the zero-mode operators in (2.50)

$$L_0 = \sum_{r\in\mathbb{Z}+\nu>0} r\psi_{-r}\cdot\psi_r - a_\nu = N_\nu - a_\nu. \tag{2.79}$$

Entirely analogously to the bosonic case, we can then build an orthonormal basis for the fermionic Hilbert space as

$$|m_1,m_2,\cdots,m_N\rangle_\nu = \psi_{-1+\nu}^{m_1}\psi_{-2+\nu}^{m_2}\cdots\psi_{-N+\nu}^{m_N}\,|\nu\rangle\,, \tag{2.80}$$

where we identified $|\nu\rangle$ and the R and NS vacuum for $\nu = 0$ and $1/2$ respectively and $m_k \in \{0,1\}$. It satisfies the eigenvalue equation

$$N_\nu\,|m_1,m_2,\cdots,m_N\rangle_\nu = \sum_{k=1}^{N} n_k(k-\nu)\,|m_1,m_2,\cdots,m_N\rangle_\nu\,. \tag{2.81}$$

The trance over the Hilbert space can then be rewritten by replacing the number operator with its eigenvalues as

$$\begin{aligned} Z(\tau) &= \sum_{m_1}^{\infty}\sum_{m_2}^{\infty} \cdots_\nu \langle m_1, m_2, \cdots | \, q^{N_\nu - a_\nu} \, | m_1, m_2, \cdots \rangle_\nu \\ &= q^{-a_\nu} \prod_{k \in \mathbb{N}-\nu} \left(1 + q^k\right), \end{aligned} \tag{2.82}$$

where in the case of an R vacuum a subtle extra factor of two arises due to the degeneracy of the vacuum that we need to keep in mind. Using the definition of the Jacobi ϑ-functions in (A.10) and the constant a_ν in (2.51) we conclude that the partition function for one worldsheet fermion is given by

$$\begin{aligned} Z_{\mathrm{NS}}(\tau) =& q^{-\frac{1}{48}} \prod_{k\in\mathbb{N}} (1 + q^{k-\frac{1}{2}}) = \left(\frac{\vartheta_3(\tau)}{\eta(\tau)}\right)^{1/2}, \\ Z_{\mathrm{R}}(\tau) =& 2q^{\frac{1}{24}} \prod_{k\in\mathbb{N}} (1 + q^{k}) = \left(\frac{\vartheta_2(\tau)}{\eta(\tau)}\right)^{1/2}, \end{aligned} \tag{2.83}$$

for NS and R boundary conditions respectively. As discussed before, the partition function of any consistent string theory should be modular invariant. Invoking the transformation properties of the theta functions (A.6), we see that any partition function containing only ϑ_2 and ϑ_3 cannot be modular invariant.

The lack of modular invariance is due to the fact that we did not treat the fermionic boundary conditions in complete generality. The R and NS boundary conditions arise due to the periodicity and anti-periodicity of the worldsheet fermions around the compact spatial coordinate of the worldsheet torus. Since we are now considering a one-loop worldsheet torus, the second euclidean coordinate is also periodic. Thus we have the freedom of assigning separate periodicity properties to the fermions around this second cycle of the torus giving us the options

$$\begin{aligned} \psi(\tau + 2\pi, \sigma) &= e^{i\pi(1-a)}\psi(\tau, \sigma), \\ \psi(\tau, \sigma + 2\pi) &= e^{i\pi(1-b)}\psi(\tau, \sigma), \end{aligned} \tag{2.84}$$

where $b = 0, 1$ corresponds to the usual NS and R choice respectively. For the calculation of the partition function, these new choices can be implemented via the insertion of a term $(-1)^F$, where F is the fermion number operator. This acts like a projector on physical states and so is called the *Gliozzi-Scherk-Olive (GSO) projection*. The fermionic partition function can now be written as

$$Z(\tau) \begin{bmatrix} a \\ b \end{bmatrix} = \mathrm{Tr}\left(e^{i\pi b F} q^{L_0(a)}\right). \tag{2.85}$$

This results in four distinct partition functions depending on the choice of the boundary conditions a, b

$$Z\left[\begin{smallmatrix} a \\ b \end{smallmatrix}\right](\tau) = \left(\frac{\vartheta\left[\begin{smallmatrix} a \\ b \end{smallmatrix}\right](\tau)}{\eta(\tau)}\right)^{1/2}, \tag{2.86}$$

where we used the definition (A.5) for the ϑ-functions with characteristics a and b. Referring to the modular properties of the theta functions (A.6) we see that it is now possible to

construct a modular invariant partition function.

The discussion above shows that the requirement of modular invariance of the one-loop vacuum amplitude imposes a GSO projection on the physical states of superstring theories. One of the effects of this is to remove the tachyon from the spectrum rendering the vacuum of the theory stable.

2.6 Superstring Theories in 10D

For the case of the bosonic string, we have seen that there is a unique consistent theory formulated in $D = 26$ dimensions. The addition of fermions to the worldsheet results in a reduction of the critical dimension to $D = 10$ and also resolves some of the issues of the bosonic string construction. Namely, the introduction of supersymmetry on the worldsheet removed the tachyonic mode of the bosonic string and resulted in the presence of spacetime fermions in the physical spectrum. However, unlike in the case of the bosonic string, there is no longer a unique choice of ten-dimensional theory.

Restricting our attention as usual to only closed strings, this non-uniqueness arises due to the decoupling of the holomorphic and anti-holomorphic sectors in the superstring action (2.42). This gives us the freedom to introduce worldsheet fermions, and hence worldsheet supersymmetry, in either sector independently. Since from the point of view of the physical spectrum, the holomorphic and anti-holomorphic degrees of freedom are indistinguishable we are left with two distinct theories:

- *Type II String Theory*
  In this case, worldsheet fermions are introduced in both the holomorphic and anti-holomorphic sectors. This results in an $\mathcal{N} = 2$ spacetime supersymmetric theory. There is an additional choice one has to make when calculating the spectrum and partition function of Type II theories. The GSO projections can be implemented separately in the two decoupled sectors giving two distinct theories:
  - *Type IIA String Theory*
    In this case, opposite GSO projections are chosen in the holomorphic and anti-holomorphic sectors. This gives a non-chiral $\mathcal{N} = 2$ spacetime theory.
  - *Type IIB String Theory*
    In this case, the same GSO projection is chosen in both sectors giving a chiral $\mathcal{N} = 2$ spacetime theory.
- *Heterotic String Theory*
  In this case, fermions are only introduced in one of the sectors of the worldsheet theory. We usually choose to introduce the fermions and worldsheet supersymmetry in the holomorphic sector. The anti-holomorphic sector only contains the worldsheet scalars and hence is the same as for the bosonic string. Due to their construction, this theory has a critical dimension of $D = 10$ in the holomorphic and $D = 26$ in the anti-holomorphic sectors. To consistently define it in ten dimensions one has to fix the additional degrees of freedom in the bosonic sector. This can be achieved by taking the extra dimensions to be compact. During this procedure, two distinct choices arise for non-tachyonic heterotic theories:

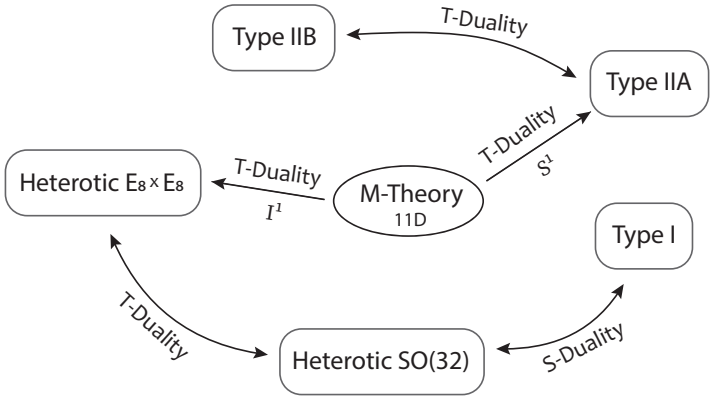

FIGURE 2.4: *The duality web of consistent supersymmetric string theories in 10D and their connection to 11D M-theory.*

- $SO(32)$ *Heterotic Theory*
  In this case, the choice of compactification of the extra bosonic degrees of freedom results in a 10D theory with $\mathcal{N} = 1$ spacetime supersymmetry. The gauge group is related to the compactification and is $SO(32)$.
- $E_8 \times E_8$ *Heterotic Theory*
  In this case, the choice of compactification also results in a 10D theory with $\mathcal{N} = 1$ spacetime supersymmetry. However, the gauge group, in this case, is $E_8 \times E_8$.

There are additional tachyonic 10D heterotic theories which are fully consistent but have a tachyonic instability in their spectrum. However, it is possible to still construct lower-dimensional theories based on these that do not suffer from these instabilities. Such constructions will be discussed later in this thesis.

If one allows for open strings, there is an additional theory called *Type I String Theory*, but we will not consider these in this thesis. These theories look a-priory unrelated other than the fact that they are all constructed from string propagating in spacetime. However, there are various transformations and dualities relating them to each other as depicted in Figure 2.4. The framework that attempts to formulate all of these string theories in terms of one higher-dimensional concept is called *M-Theory*.

In what follows, we will focus on heterotic theories as these produce some of the phenomenologically most interesting four-dimensional models that can be derived from string theory. In the coming section, we introduce a robust consistent formalism to explore the vast landscape of lower-dimensional heterotic models.

3 The Fermionic Worldsheet Construction

In the free fermionic worldsheet construction, as opposed to a geometric compactification, models are constructed directly in $D \leq 10$ dimensions. All unfixed degrees of freedom are then taken to be free fermions propagating on the worldsheet. The overall number of fermions we need to introduce is determined by the requirement that the conformal anomaly must cancel in both left and right-moving sectors. In $D < 10$, the fermionic formulation gives an unusual viewpoint of lower dimensional string models. It circumvents the discussion of compactifications and related geometry and gives rise to powerful analytic tools to explore the vast landscape of string models.

3.1 The Free Fermionic Heterotic String

We will primarily focus on heterotic theories in this thesis and so in the following, we discuss the fermionic construction for these models. However, the methods developed are readily applicable to type II theories as well. Recall, that heterotic theories correspond to a worldsheet supersymmetric theory in the holomorphic (left-moving) sector and bosonic string theory in the anti-holomorphic (right-moving) sector. To define the theory in 10D, the extra 16 bosonic degrees of freedom have to be fixed. We can denote the worldsheet fields of the right-moving sector in the lightcone gauge as

$$X^M = \{X^i, X^I\}, \tag{3.1}$$

where $i = 1, \cdots, 8$, $I = 1, \cdots 16$ and so $M = 1, \cdots, 24 = 1, \cdots, D-2$. In two dimensions, one worldsheet boson can be represented in terms of two worldsheet fermions via

$$e^{iX^I} = \psi^{2I-1} + i\psi^{2I}, \tag{3.2}$$

which is referred to as *bosonisation/fermionisation*. This relation is crucial in the understanding of fermionic constructions as will be discussed in more detail later. It is convenient to group the 32 real fermions into 16 complex fermions as

$$\lambda^I = \psi^{2I-1} + i\psi^{2I}. \tag{3.3}$$

In the fermionic formulation, the extra 16 right-moving coordinates are fermionised into 16 right-moving complex fermions via the above relation.

The Polyakov action (2.42) in conformal and lightcone gauge then becomes

$$S = -\frac{1}{4\pi\alpha'} \int_\Sigma dz d\bar{z} \left(\partial X^i \bar{\partial} X_i + i\, \psi^i \partial\, \psi_i + i\bar{\lambda}^I \bar{\partial} \bar{\lambda}_I \right), \tag{3.4}$$

where $I = 1, \cdots, 16$ counts the 16 internal complex fermions. The partition function is then given as a product of the three contributions

$$Z(\tau, \bar{\tau}) = Z_B(\tau) Z_\psi(\tau) Z_\lambda(\bar{\tau}) \tag{3.5}$$

We have already seen the partition function for bosonic coordinates in (2.76) and so the contribution of the eight transverse bosons is given by

$$Z_B = \frac{1}{\tau_2^4} \frac{1}{\eta^8(\tau)\bar{\eta}^8(\bar{\tau})}. \tag{3.6}$$

For the left-moving fermions, we can use the results derived in (2.86) so that

$$Z_\psi = \sum_{a,b=0,1} (-1)^{a+b+ab} \left(\frac{\vartheta\left[\begin{smallmatrix} a \\ b \end{smallmatrix}\right](\tau)}{\eta(\tau)} \right)^4. \tag{3.7}$$

As discussed previously, both Z_X and Z_ψ are modular invariants on their own. Hence, this constrains Z_λ to be also a modular invariant partition function of 16 right-moving fermions. Imposing this constraint results in the two possibilities

$$\begin{aligned} Z_\lambda^{SO(32)} &= \frac{1}{\bar{\eta}^{16}(\bar{\tau})} \sum_{a,b=0,1} \bar{\vartheta}\left[\begin{smallmatrix} a \\ b \end{smallmatrix}\right]^{16}(\bar{\tau}), \\ Z_\lambda^{E_8 \times E_8} &= \frac{1}{\bar{\eta}^{16}(\bar{\tau})} \sum_{a,b=0,1} \bar{\vartheta}\left[\begin{smallmatrix} a \\ b \end{smallmatrix}\right]^{8}(\bar{\tau}) \sum_{k,l=0,1} \bar{\vartheta}\left[\begin{smallmatrix} k \\ l \end{smallmatrix}\right]^{8}(\bar{\tau}), \end{aligned} \tag{3.8}$$

which correspond to the $SO(32)$ and $E_8 \times E_8$ theories discussed in the previous section. The derivation of this is purely based on modular invariance and is discussed extensively in [43].

The above discussion shows that the fermionic construction of the heterotic string in ten dimensions amounts to assigning boundary conditions to the worldsheet fermions around the two cycles of the worldsheet torus. Then the requirement of modular invariance imposes restrictions on the allowed grouping of fermions as well as overall phase factors. We follow the conventions in the literature in denoting the 16 complex right-moving fermions as

$$\bar{\lambda}^I = \{\bar{\psi}^{1\cdots5}, \bar{\eta}^{1,2,3}, \bar{\phi}^{1\cdots8}\}, \tag{3.9}$$

which has its origins in GUT model building. In order to consistently label the boundary conditions of each fermion, we introduce boundary condition vectors

$$\boldsymbol{\alpha} = \{\alpha(\psi^1), \cdots, \alpha(\psi^8) \,|\, \alpha(\bar{\psi}^1), \cdots, \alpha(\bar{\psi}^5), \alpha(\bar{\eta}^1), \alpha(\bar{\eta}^2), \alpha(\bar{\eta}^3), \alpha(\bar{\phi}^1), \cdots, \alpha(\bar{\phi}^8)\}, \tag{3.10}$$

where each entry defines the boundary condition of a fermion around a cycle of the torus. Since the fermions are complexified we have the choice of periodicities

$$\psi^i \to -e^{-i\pi\alpha(\psi^i)}\psi^i, \quad \bar{\psi}^i \to -e^{+i\pi\alpha(\bar{\psi}^i)}\bar{\psi}^i, \tag{3.11}$$

where the signs are introduced due to conventions. Real boundary conditions then mean that the elements of α are restricted to $\alpha(\psi) \in \{0, 1\}$. Sectors of models are represented in terms of pairs of boundary condition vectors $\left[\begin{smallmatrix} \boldsymbol{\alpha} \\ \boldsymbol{\beta} \end{smallmatrix}\right]$ each defining the boundary conditions

of the fermions around one of the cycles of the worldsheet torus. The partition function is then given by a sum over all possible sectors with signs chosen so that modular invariance is preserved.

3.2 Model Building with Free Fermions

This formalism can be made precise using methods developed in [44–46]. The possible boundary condition vectors $\boldsymbol{\alpha}, \boldsymbol{\beta}$ are generated by *basis vectors* $\boldsymbol{b}_i \in \mathcal{B}$ that form a basis for an additive group Ξ. All sectors can be generated by a linear combination of basis vectors

$$\boldsymbol{\alpha} = \sum_{i=1}^{N} n_i \boldsymbol{b}_i \tag{3.12}$$

generating the group, where $i = 1, \cdots, N$ runs over all basis vectors. Clearly, due to group closure, $n_i \in \{0, 1\}$ for real boundary conditions. However, in general, one can have $n_i \in \mathbb{N}$ depending on the specific choice for $\alpha(\psi)$. The partition function of a model is then expressed as

$$\begin{aligned} Z &= \int_{\mathcal{F}} \frac{d^2\tau}{\tau_2^2} Z_B \sum_{\boldsymbol{\alpha},\boldsymbol{\beta}\in\Xi} C\binom{\boldsymbol{\alpha}}{\boldsymbol{\beta}} \prod_f Z\begin{bmatrix}\alpha(f)\\ \beta(f)\end{bmatrix} \\ &= \int_{\mathcal{F}} \frac{d^2\tau}{\tau_2^2} Z_B \frac{1}{2^N}\frac{1}{\eta^4\bar{\eta}^{16}} \sum_{\boldsymbol{\alpha},\boldsymbol{\beta}\in\Xi} C\binom{\boldsymbol{\alpha}}{\boldsymbol{\beta}} \prod_f \vartheta\begin{bmatrix}\alpha(f)\\ \beta(f)\end{bmatrix} \prod_{\bar{f}} \bar{\vartheta}\begin{bmatrix}\alpha(\bar{f})\\ \beta(\bar{f})\end{bmatrix}, \end{aligned} \tag{3.13}$$

where we referred to the left and right-moving fermions as f and $\bar{f}$ respectively. The coefficients $C\binom{\boldsymbol{\alpha}}{\boldsymbol{\beta}}$ called *generalised GSO (GGSO) phases* assure the modular invariance of the entire partition function. Since we already know Z_B, given by (3.6), is modular invariant and spin-structure independent we will focus on the fermionic partition function Z_F.

The requirement of modular invariance of the fermionic partition function imposes strict constraints on both the choice of basis vectors and GGSO phases. These constraints were originally derived in [44, 46] and we adopt the notation of the former. There it is shown that basis vectors of a free fermionic model must satisfy the following modular invariance constraints:

$$\frac{1}{2} N_1 \boldsymbol{b}_1 = \mathbb{1} \tag{3.14}$$

$$N_i \boldsymbol{b}_i \cdot \boldsymbol{b}_i = 0 \mod 8, \tag{3.15}$$

$$N_{ij} \boldsymbol{b}_i \cdot \boldsymbol{b}_j = 0 \mod 4, \tag{3.16}$$

$$\prod_f b_i(f) b_j(f) b_k(f) b_l(f) = 0 \mod 2, \tag{3.17}$$

where we define the dot product of basis vectors as

$$\boldsymbol{b}_i \cdot \boldsymbol{b}_j = \left[\left(\sum_{f \text{ Comp.}} + \frac{1}{2} \sum_{f \text{ Real}} \right) - \left(\sum_{\bar{f} \text{ Comp.}} + \frac{1}{2} \sum_{\bar{f} \text{ Real}} \right) \right] b_i(f) \cdot b_j(f). \tag{3.18}$$

The integers N_i and N_{ij} are defined such that N_i is the smallest positive integer for which $N_i \boldsymbol{b}_i = 0$ and N_{ij} is the least common multiple of N_i and N_j. For purely real boundary conditions $N_i = N_{ij} = 2\ \forall i, j$. The condition (3.14) simply means that the vector $\mathbb{1} = \{1, \cdots, 1 \,|\, 1, \cdots, 1\}$ representing periodic R boundary conditions for all fermions must be in the basis. This immediately implies that $2\mathbb{1} = \{0, \cdots, 0 \,|\, 0, \cdots, 0\}$ in which all fermions have anti-periodic NS boundary conditions is also in Ξ.

To achieve a modular invariant partition function, separate conditions must be imposed on the GGSO coefficients via

$$C\begin{pmatrix}\boldsymbol{b}_i\\ \boldsymbol{b}_j\end{pmatrix} = \delta_{\boldsymbol{b}_i} e^{2\pi i n/N_j}, \tag{3.19}$$

$$C\begin{pmatrix}\boldsymbol{b}_i\\ \boldsymbol{b}_i\end{pmatrix} = -e^{i\pi \boldsymbol{b}_i\cdot\boldsymbol{b}_i/4} C\begin{pmatrix}\boldsymbol{b}_i\\ \mathbb{1}\end{pmatrix}, \tag{3.20}$$

$$C\begin{pmatrix}\boldsymbol{b}_i\\ \boldsymbol{b}_j\end{pmatrix} = e^{i\pi \boldsymbol{b}_i\cdot\boldsymbol{b}_j/2} C\begin{pmatrix}\boldsymbol{b}_j\\ \boldsymbol{b}_i\end{pmatrix}^*, \tag{3.21}$$

$$C\begin{pmatrix}\boldsymbol{b}_i\\ \boldsymbol{b}_j+\boldsymbol{b}_k\end{pmatrix} = \delta_{\boldsymbol{b}_i} C\begin{pmatrix}\boldsymbol{b}_i\\ \boldsymbol{b}_j\end{pmatrix} C\begin{pmatrix}\boldsymbol{b}_i\\ \boldsymbol{b}_k\end{pmatrix}, \tag{3.22}$$

where $\delta_{\boldsymbol{b}_i}$ is related to the boundary conditions of the left-moving fermions as

$$\delta_{\boldsymbol{b}_i} = \begin{cases} +1 & \text{if } \alpha(\psi^\mu) = 0 \\ -1 & \text{if } \alpha(\psi^\mu) = 1. \end{cases} \tag{3.23}$$

These constraints mean that any given free fermionic model defined in terms of N basis vectors has $N(N-1)/2+1$ independent GGSO phases. These are usually taken to lie in the upper or lower half triangle of the matrix of coefficients of the basis vectors $C_{ij} = C\begin{pmatrix}\boldsymbol{b}_i\\ \boldsymbol{b}_j\end{pmatrix}$ which we refer to as the *GGSO matrix*. The phase for a general sector with $\boldsymbol{\alpha} = \sum_i n_i \boldsymbol{b}_i$ and $\boldsymbol{\beta} = \sum_j m_j \boldsymbol{b}_j$ can then be determined using the formula

$$C\begin{pmatrix}\boldsymbol{\alpha}\\ \boldsymbol{\beta}\end{pmatrix} = \delta_{\boldsymbol{\alpha}}^{\sum_j m_j - 1} \delta_{\boldsymbol{\beta}}^{\sum_i n_i - 1} e^{i\pi([\boldsymbol{\alpha}]-\boldsymbol{\alpha})\cdot\boldsymbol{\beta}/2} \prod_{i,j} C\begin{pmatrix}\boldsymbol{b}_i\\ \boldsymbol{b}_j\end{pmatrix}^{n_i m_j}, \tag{3.24}$$

where we denoted by $[\boldsymbol{\alpha}]$ the reduced representation of $\boldsymbol{\alpha}$ in which its entries are taken to lie in the range $(-1, +1]$.

These constraints (3.19)-(3.21) follow directly from one-loop modular invariance and the transformation properties of ϑ-functions. However, higher-loop modular invariance must also be considered if we want our string models to be well-defined at all perturbative orders. If one considers the vacuum amplitude at genus two, i.e. at second order, an additional constraint arises requiring the factorisation property stated in (3.22). It can also be shown that no additional constraints arise at loop orders higher than two. Further discussion on the multi-loop modular invariance of string theory can be found in [47–50].

The Hilbert space of states and spectra of free fermionic models can be directly inferred from the structure of the partition function (3.13). Based on the discussion in Section 2.5, and

equations (2.85) and (2.86), we can make the identification

$$\begin{aligned} Z &= \int_{\mathcal{F}} \frac{d^2\tau}{\tau_2^2} \sum_{\boldsymbol{\alpha},\boldsymbol{\beta}\in\Xi} C\binom{\boldsymbol{\alpha}}{\boldsymbol{\beta}} \frac{1}{\tau_2^4} \frac{1}{2^N} \frac{1}{\eta^{12}\bar{\eta}^{24}} \prod_f \vartheta\begin{bmatrix}\alpha(f)\\ \beta(f)\end{bmatrix} \prod_{\bar{f}} \bar{\vartheta}\begin{bmatrix}\alpha(\bar{f})\\ \beta(\bar{f})\end{bmatrix} \\ &= \int_{\mathcal{F}} \frac{d^\tau}{\tau_2^2} \sum_{\boldsymbol{\alpha},\boldsymbol{\beta}\in\Xi} C\binom{\boldsymbol{\alpha}}{\boldsymbol{\beta}} \mathrm{Tr}_{\mathcal{H}_\alpha}\left(e^{i\pi\boldsymbol{\beta}\cdot F_\alpha} e^{i\pi\tau H_\alpha}\right), \end{aligned} \tag{3.25}$$

where H_α is the Hamiltonian in the Hilbert space $\mathcal{H}_\alpha$ of sector α. F_α is the vector formed from the fermion number operator $F_\alpha(f)$ counting f and f^* with opposite signs. Using the factorisation property of the GGSO phase (3.22) we can rewrite the trace over the Hilbert space as

$$Z = \int_{\mathcal{F}} \frac{d^2\tau}{\tau_2^2} \sum_{\boldsymbol{\alpha}\in\Xi} \delta_{\boldsymbol{\alpha}} \mathrm{Tr}\left(\prod_{\boldsymbol{b}_i}\left(1 + \delta_\alpha C\binom{\boldsymbol{\alpha}}{\boldsymbol{b}_i} e^{i\pi\boldsymbol{b}_i F_\alpha} + \cdots + \left[\delta_\alpha C\binom{\boldsymbol{\alpha}}{\boldsymbol{b}_i} e^{i\pi\boldsymbol{b}_i F_\alpha}\right]^{N_i-1}\right) e^{i\pi\tau H_\alpha}\right). \tag{3.26}$$

This shows that the entire Hilbert space is constructed by summing over all sectors subject to

$$\mathcal{H} = \bigoplus_{\boldsymbol{\alpha}\in\Xi} \prod_i \left\{ e^{i\pi\boldsymbol{b}_i\cdot F_\alpha} = \delta_\alpha C\binom{\boldsymbol{\alpha}}{\boldsymbol{b}_i}^* \right\} \mathcal{H}_\alpha, \tag{3.27}$$

where the condition in the brackets imposes the projection. This means states in the sectors must satisfy the GGSO condition

$$e^{i\pi\boldsymbol{b}_i\cdot F_\alpha} |S_\alpha\rangle = \delta_\alpha C\binom{\boldsymbol{\alpha}}{\boldsymbol{b}_i}^* |S_\alpha\rangle, \tag{3.28}$$

where $|S_\alpha\rangle$ is a state in sector $\boldsymbol{\alpha}$. If a state satisfies this condition then it will contribute to the one-loop partition function and appear in the physical spectrum. On the other hand, states that do not satisfy this condition are said to be *projected out* and do not contribute.

The masses of states in the spectrum are calculated using zero-mode of the Virasoro generator using (2.79). For the heterotic string, left and right-moving masses are determined separately before imposing the level-matching condition for physical states. In the above formalism, the mass of a state in sector $\boldsymbol{\alpha}$ is given by

$$\begin{aligned} M_L^2 &= -\frac{1}{2} + \frac{\boldsymbol{\alpha}_L\cdot\boldsymbol{\alpha}_L}{8} + N_L, \\ M_R^2 &= -1 + \frac{\boldsymbol{\alpha}_R\cdot\boldsymbol{\alpha}_R}{8} + N_R, \end{aligned} \tag{3.29}$$

where we define separate left and right vectors as $\boldsymbol{\alpha} = \{\boldsymbol{\alpha}_L|\boldsymbol{\alpha}_R\}$ with a Euclidean inner product. The $N_{L,R}$ are sums over the left and right-moving oscillator frequencies

$$\begin{aligned} N_L &= \sum_{f_L} \nu_{f_L} + \sum_{f_L^*} \nu_{f_L^*}, \\ N_L &= \sum_{f_R} \nu_{f_R} + \sum_{f_R^*} \nu_{f_R^*}, \end{aligned} \tag{3.30}$$

where the frequencies are determined in terms of the boundary conditions via

$$\nu_f = \frac{1+\alpha(f)}{2}, \qquad \nu_{f^*} = \frac{1-\alpha(f)}{2}. \tag{3.31}$$

The level matching condition (2.21) then imposes the constraint $M_L^2 = M_R^2$ which must be satisfied by all on-shell states.

3.3 10D Heterotic String Theories

In this section, we present some examples of 10D heterotic string models constructed using the free fermionic formalism presented above. We will cover some supersymmetric and non-supersymmetric models and discuss their key features. We will then provide a classification and outline of all possible 10D heterotic models. More details on specific models and more general considerations regarding model building in the fermionic formulation can be found in [43].

Tachyonic $SO(32)$ Model

The simplest case one can think of in the fermionic formulation is the inclusion of only the vector $\mathbb{1}$ in the basis set which is required by consistency. Hence we have the basis set $\mathcal{B} = \{\mathbb{1}\}$ given by

$$\mathbb{1} = \{\psi^\mu \mid \bar{\phi}^{1,\dots,16}\}, \tag{3.32}$$

where for simplicity we denoted all 16 right-moving complex fermions as $\bar{\phi}^{1,\dots,16}$. Writing the left moving fermions as ψ^μ is due to notational conventions, however, we still implicitly understand that the only independent oscillators are the transverse ones in the lightcone gauge. The fermionic partition function can then be expressed using (3.13) and is given by

$$Z_F = \frac{1}{\eta^4\bar{\eta}^{16}}\frac{1}{2}\sum_{a,b}(-1)^{a+b+\mu ab}\vartheta\left[\begin{smallmatrix}a\\b\end{smallmatrix}\right]^4\bar{\vartheta}\left[\begin{smallmatrix}a\\b\end{smallmatrix}\right]^{16}. \tag{3.33}$$

For both choices of $\mu = 0, 1$ this produces a nonzero q-expansion for the total partition function

$$Z = \frac{8}{\bar{q}} + \frac{128\,q}{\bar{q}} + \frac{32}{q^{1/2}\bar{q}^{-1/2}} + \frac{1152\,q^{1/2}}{\bar{q}^{-1/2}} + \frac{5248\,\bar{q}^{1/2}}{q^{-1/2}} + 4032 + 188928\,q^{1/2}\bar{q}^{1/2}, \tag{3.34}$$

where we displayed all terms up to $\mathcal{O}(q^{1/2}\bar{q}^{1/2})$. This is indeed modular invariant, but we must notice the presence of the term $\sim q^{-1/2}\bar{q}^{-1/2}$ which is an on-shell tachyon. Hence the model defined by this basis is unstable and has a divergent one-loop vacuum energy.

Out of the two sector $\mathbb{1}$ and $\mathbb{1}+\mathbb{1}$ = NS only the NS sector give raise to massless states. They can be written as

$$\begin{aligned}\psi^i\bar{\Phi}^I\bar{\Phi}^J\left|0\right\rangle_{\text{NS}},\\ \psi^i\partial\bar{X}^j\left|0\right\rangle_{\text{NS}},\end{aligned} \tag{3.35}$$

where $i, j = 1, \cdots, 8$, $I, J = 1, \dots, 16$ and we used $\bar{\Phi}^I$ to denote the 16 right-moving complex fermions. We also adopted the notation where we denote the bosonic creation operators as

∂X^i. The on-shell tachyon also arises from this sector as the state

$$\bar{\Phi}^I \left|0\right\rangle_{\rm NS} . \tag{3.36}$$

All states stated above survive the GSO projections and hence appear in the physical spectrum. We also note the presence of a model-independent of-shell tachyon that contributes the term $\sim \bar{q}^{-1}$ to the partition function. This state is always part of the spectra of heterotic models and so provides a nice consistency check on the partition function and spectrum [51].

Supersymmetric $SO(32)$ Model

To generate another ten-dimensional model, we can add an additional vector to the set. What basis vectors we can add are constrained by the modular invariance rules (3.14)-(3.17) meaning that we only have a finite number of distinct choices. One of these is to introduce the vector

$$S = \{\psi^\mu\} \tag{3.37}$$

which splits the left and right-moving fermions in the partition function now given by

$$Z_F = \frac{1}{\eta^4\bar{\eta}^{16}}\frac{1}{2}\sum_{a,b}\frac{1}{2}\sum_{k,l}(-1)^{a+b+\mu ab+\nu kl}\vartheta\left[\begin{smallmatrix}a\\b\end{smallmatrix}\right]^4\bar{\vartheta}\left[\begin{smallmatrix}k\\l\end{smallmatrix}\right]^{16} . \tag{3.38}$$

The two independent choices of GGSO coefficients translate into the independent choices for $\mu, \nu = 0, 1$. This translation will be explicitly discussed in Chapter 4 and forms a pivotal part of this thesis.

From the generalised Jacobi identity (A.13), we can derive a simplified version given by

$$\frac{1}{2}\sum_{a,b\in\{0,1\}}(-1)^{a+b}\vartheta\left[\begin{smallmatrix}a\\b\end{smallmatrix}\right]^4 = \vartheta\left[\begin{smallmatrix}1\\1\end{smallmatrix}\right]^4 = 0. \tag{3.39}$$

This implies that the above partition function vanishes for all choices of μ and ν and hence the model is supersymmetric. From the point of view of the partition function, supersymmetry is always realised through this generalised Jacobi identity and so supersymmetric configurations are easy to isolate.

The addition of the new basis vector introduces a new GSO projection which projects out the NS tachyon. In addition to the purely R and NS sectors of the non-supersymmetric $SO(32)$ model above, we now have the additional sectors S and $\mathbb{1}+S$ contributing states to the physical spectrum. Only the S sector contributes massless states which can be written as

$$\begin{aligned}\partial\bar{X}^i \left|0\right\rangle_{\rm R} ,\\ \bar{\Phi}^I\bar{\Phi}^J \left|0\right\rangle_{\rm R} .\end{aligned} \tag{3.40}$$

These give the superpartners of the massless states (3.35) arising from the NS sector realising the $\mathcal{N} = 1$ spacetime supersymmetry.

Supersymmetric $E_8 \times E_8$ and Non-Supersymmetric $SO(16) \times SO(16)$ Model

The modular invariance rules of the basis vectors (3.14)-(3.17) allows for the addition of another basis vector

$$x_1 = \{\bar{\phi}^{1-8}\} \tag{3.41}$$

so that we now have $\mathcal{B} = \{\mathbb{1}, S, x_1\}$. The addition of this vector splits the boundary conditions of the 16 complex right-moving fermions resulting in the partition function

$$Z_F = \frac{1}{\eta^4\bar{\eta}^{16}}\frac{1}{2}\sum_{\substack{a\\b}}\frac{1}{2^2}\sum_{\substack{\gamma,\epsilon\\\delta,\xi}}(-1)^{a+b+\Phi\left[\begin{smallmatrix}a&\gamma&\epsilon\\b&\delta&\xi\end{smallmatrix}\right]}\vartheta\left[\begin{smallmatrix}a\\b\end{smallmatrix}\right]^4\vartheta\left[\begin{smallmatrix}\gamma\\\delta\end{smallmatrix}\right]^8\vartheta\left[\begin{smallmatrix}\epsilon\\\xi\end{smallmatrix}\right]^8, \tag{3.42}$$

where we have introduced the phase $\Phi\left[\begin{smallmatrix}a&\gamma&\epsilon\\b&\delta&\xi\end{smallmatrix}\right]$ that ensures modular invariance and implements the various GGSO projections. The specific form of this phase will be discussed extensively in Chapter 4. Two distinct scenarios arise, one in which the choice Φ preserves supersymmetry and one in which supersymmetry is broken. This is specifically explicitly by the inclusion of the term $\sigma(a+k)+l(a+\rho)+b(k+\rho)$ in the phase Φ which renders the Jacobi identity (A.13) unsatisfiable. These give the supersymmetric $E_8 \times E_8$ and non-supersymmetric $SO(16) \times SO(16)$ models respectively.

There are now also additional massless states arising from the $\mathbb{1}+x_1$ and $\mathbb{1}+S+x_1$ sectors, however, we will not discuss these explicitly here. It is important to note that in both models the NS tachyon is projected. In the case of the non-supersymmetric $SO(16) \times SO(16)$ model, this provides the first example of a non-supersymmetric model that is tachyon-free and hence has finite vacuum energy. These models will be further discussed in Chapter 5.

Classification 10D Heterotic Theories

The discussion above shows that new ten-dimensional heterotic models are either generated by the inclusion of an additional basis vector or by the choice of a specific GGSO phase. It is then natural to ask what all possible 10D heterotic models are and how one can construct them in this formulation. As we will see shortly, there are precisely eight distinct modular invariant heterotic theories in ten dimensions, two supersymmetric and six non-supersymmetric. They all differ in many of their phenomenological features and all possess a different gauge group which we usually use to identify them. A list of all of these models can be found in Table 3.1. Of the six that lack spacetime supersymmetry, only one is void of physical tachyons the rest contain such on-shell states making the one-loop cosmological constant divergent.

Most of these theories were originally constructed using the bosonic formulation in [52, 53] (SUSY $E_8 \times E_8$ & $SO(32)$), [54] (Non-SUSY $SO(16) \times SO(16)$, $SO(32)$, $SO(16) \times E_8$, $SO(8) \times SO(24)$, $E_7^2 \times SU(2)^2$ & $U(16)$), [55] (Non-SUSY $SO(16) \times SO(16)$) and [56] (Non-SUSY $SO(32)$ & $SO(16) \times E_8$). These models were then also found and classified using the fermionic formulation in [57] where an additional model with an E_8 gauge group was also found. This model does not pair the worldsheet fermions rendering the bosonisation non-trivial making in hard-to-find using the bosonic formulation.

A classification of all 10D heterotic models can be neatly done using the free fermionic formulation. The modular invariance conditions (3.14)-(3.17) heavily constrain the possible

Basis Vectors	Gauge Group	#Fermions	#Tachyons	SUSY
$\mathbb{1}$, S	$SO(32)$	496	0	Yes
$\mathbb{1}$, S, x_1	$E_8 \times E_8$	496	0	Yes
$\mathbb{1}$, S, x_1	$SO(16) \times SO(16)$	512	0	No
$\mathbb{1}$	$SO(32)$	0	32	No
$\mathbb{1}$, x_1	$SO(16) \times E_8$	256	16	No
$\mathbb{1}$, $S + x_2$	$SO(8) \times SO(24)$	384	8	No
$\mathbb{1}$, $S + x_1$, $x_1 + x_2$	$E_7^2 \times SU(2)^2$	448	4	No

TABLE 3.1: All modular invariant 10D heterotic theories that can be generated using the four basis vectors $\{\mathbb{1}, S, x_1, x_2\}$ with the number of massless fermionic states and on-shell tachyonic states explicitly written.

choices of basis vectors. Indeed, using a combination of the four basis vectors

$$\begin{aligned} \mathbb{1} &= \{\psi^\mu \mid \bar{\phi}^{1,\dots,16}\}, \\ S &= \{\psi^\mu\}, \\ x_1 &= \{\bar{\phi}^{1,\dots,8}\}, \\ x_2 &= \{\bar{\phi}^{7,\dots,10}\}, \end{aligned} \tag{3.43}$$

we can generate all but one of the possible 10-dimensional models. In Table 3.1 we give a summary of which combination of these basis vectors generates which 10D model. For simplicity, we chose to denote the right-moving complex fermions as $\phi^{1,\dots,16}$.

Using the basis vectors (3.43) and equation (2.86) we can express the partition functions of all distinct theories as

$$\begin{aligned} Z_F^{SO(32)} &= \frac{1}{\eta^4\bar{\eta}^{16}}\frac{1}{2}\sum_{\substack{a\\b}}(-1)^{a+b+\Phi\left[\begin{smallmatrix}a\\b\end{smallmatrix}\right]}\vartheta\left[\begin{smallmatrix}a\\b\end{smallmatrix}\right]^4\bar{\vartheta}\left[\begin{smallmatrix}a\\b\end{smallmatrix}\right]^{16}, \\ Z_F^{SO(32)} &= \frac{1}{\eta^4\bar{\eta}^{16}}\frac{1}{4}\sum_{\substack{a\,k\\b\,l}}(-1)^{a+b+\Phi\left[\begin{smallmatrix}a&k\\b&l\end{smallmatrix}\right]}\vartheta\left[\begin{smallmatrix}a\\b\end{smallmatrix}\right]^4\bar{\vartheta}\left[\begin{smallmatrix}k\\l\end{smallmatrix}\right]^{16}, \\ Z_F^{E_8\times SO(16)} &= \frac{1}{\eta^4\bar{\eta}^{16}}\frac{1}{4}\sum_{\substack{a\,k\\b\,l}}(-1)^{a+b+\Phi\left[\begin{smallmatrix}a&k\\b&l\end{smallmatrix}\right]}\vartheta\left[\begin{smallmatrix}a\\b\end{smallmatrix}\right]^4\bar{\vartheta}\left[\begin{smallmatrix}a\\b\end{smallmatrix}\right]^8\bar{\vartheta}\left[\begin{smallmatrix}k\\l\end{smallmatrix}\right]^8, \\ Z_F^{SO(8)\times SO(24)} &= \frac{1}{\eta^4\bar{\eta}^{16}}\frac{1}{4}\sum_{\substack{a\,k\\b\,l}}(-1)^{a+b+al+kb+\Phi\left[\begin{smallmatrix}a&k\\b&l\end{smallmatrix}\right]}\vartheta\left[\begin{smallmatrix}a\\b\end{smallmatrix}\right]^4\bar{\vartheta}\left[\begin{smallmatrix}a\\b\end{smallmatrix}\right]^4\bar{\vartheta}\left[\begin{smallmatrix}k\\l\end{smallmatrix}\right]^{12}, \\ Z_F^{\substack{E_8\times E_8\\SO(16)\times SO(16)}} &= \frac{1}{\eta^4\bar{\eta}^{16}}\frac{1}{8}\sum_{\substack{a\,k\,\rho\\b\,l\,\sigma}}(-1)^{a+b+\Phi\left[\begin{smallmatrix}a&k&\rho\\b&l&\sigma\end{smallmatrix}\right]}\vartheta\left[\begin{smallmatrix}a\\b\end{smallmatrix}\right]^4\bar{\vartheta}\left[\begin{smallmatrix}k\\l\end{smallmatrix}\right]^8\bar{\vartheta}\left[\begin{smallmatrix}\rho\\\sigma\end{smallmatrix}\right]^8, \\ Z_F^{E_7^2\times SU(2)^2} &= \frac{1}{\eta^4\bar{\eta}^{16}}\frac{1}{8}\sum_{\substack{a\,k\,\rho\\b\,l\,\sigma}}(-1)^{a+b+kb+\rho l+\Phi\left[\begin{smallmatrix}a&k&\rho\\b&l&\sigma\end{smallmatrix}\right]}\vartheta\left[\begin{smallmatrix}a\\b\end{smallmatrix}\right]^4\bar{\vartheta}\left[\begin{smallmatrix}a\\b\end{smallmatrix}\right]^2\bar{\vartheta}\left[\begin{smallmatrix}a+k\\b+l\end{smallmatrix}\right]^6\bar{\vartheta}\left[\begin{smallmatrix}\rho\\\sigma\end{smallmatrix}\right]^2\bar{\vartheta}\left[\begin{smallmatrix}\rho+k\\\sigma+l\end{smallmatrix}\right]^6. \end{aligned} \tag{3.44}$$

The included phases ensure modular invariance and Φ implements the desired GGSO projections. This formulation of writing the partition functions will be extensively discussed in Chapter 4. We see that as explicitly discussed before, the supersymmetric $E_8 \times E_8$ model and the non-supersymmetric $SO(16) \times SO(16)$ are related by a change of GGSO phase and are hence generated by the same basis set as seen in Table 3.1. The expressions above also clearly show that in the case of supersymmetric theories, the left-moving $\vartheta\left[\begin{smallmatrix} a \\ b \end{smallmatrix}\right]^4$ term clearly separates facilitating the cancellation via the Jacobi Identity (A.13).

There are two additional consistent ten-dimensional heterotic models that can arise which are not written in Table 3.1. An additional $U(16)$ model occurs when we consider adding a fifth basis vector to the set (3.43). Moreover, an E_8 model arises in cases when not all complex fermions are paired. We will not cover this in detail here, but more on it can be found in [57]. The possibility of deriving most models from only four basis vectors shows the main power of the fermionic formulation. More details on the spectra and other properties of these models can be found in [43, 46, 57].

3.4 4D Heterotic String via Free Fermions

So far, we discussed the free fermionic formulation of the heterotic string in ten dimensions. To make a connection to the real world and hence develop the framework for a viable string phenomenology, we must formulate our models in four dimensions. In the bosonic picture, this is done by a so-called *compactification* in which six of the ten dimensions are taken to live on a compact manifold. The choice of this compact manifold then determines many of the features of the lower-dimensional model. Some of the most promising choices when it comes to string phenomenology are toroidal orbifolds. They are exactly solvable since we have a good geometric understanding of them and give interesting and viable models in four dimensions. These orbifold compactifications are also easily described using the free fermionic language and were originally formulated in [44–46].

In Section 3.1 we showed that in the free fermionic formulation of 10D heterotic string theory, the extra bosonic degrees of freedom from the additional 16 dimensions of the bosonic string are treated as free worldsheet fermions with assigned boundary conditions. If we now want to formulate the theory in 4D, we have to deal with the extra 6 right and left-moving bosonic degrees of freedom. Analogously to the 10D case, these can be fermionised and assigned boundary conditions around the two cycles of the worldsheet torus. In customary to denote these new "internal" fermions as

$$\{y^{1,\cdots,6},\, w^{1,\cdots,6} \,|\, \bar{y}^{1,\cdots,6},\, \bar{w}^{1,\cdots,6}\}, \tag{3.45}$$

where, as usual, the bar denotes the anti-holomorphic side. Additionally, since we are now formulating the model in four spacetime dimensions, the field with a spacetime index X^μ and ψ^μ will now have $\mu = 1, 2$ in the lightcone gauge. This means that we must introduce six left-moving fermions this compensate for this change. Altogether this results in the worldsheet content of 4D free fermionic stings being

$$\{\psi^\mu,\, \chi^{1,\cdots,6},\, y^{1,\cdots,6},\, w^{1,\cdots,6} \,|\, \bar{y}^{1,\cdots,6},\, \bar{w}^{1,\cdots,6},\, \bar{\eta}^{1,2,3},\, \bar{\psi}^{1,\ldots,5},\, \bar{\phi}^{1,\ldots,8}\}, \tag{3.46}$$

where the $\psi, \chi, y, w, \bar{y}, \bar{w}$ are real while $\bar{\psi}, \bar{\eta}, \bar{\phi}$ are complex. With these choices, the model-building rules are identical to the ten-dimensional case with sums and products now running over the additional fermions as well.

This means that 4D free fermionic modes are defined by a set of basis vectors which satisfy (3.14)-(3.17) and collection of GGSO coefficients restricted by modular invariance via the rules (3.19)-(3.22). I going to four dimensions an additional subtlety arises with regards to worldsheet supersymmetry. We must ensure that the worldsheet supercurrent is consistently defined via

$$T_F = i\psi^\mu \partial X_\mu + i \sum_{I=1}^{6} \chi^I y^I w^I, \tag{3.47}$$

which corresponds to a nonlinear realisation. More detailed discussion on this can be found in [58]. The partition function for 4D is then calculated via (3.13) giving consistent modular invariant models in 4D.

This formulation of the four-dimensional heterotic string gives a powerful tool to explore the landscape of possible string models. As we will show in the coming sections, we can use this formalism to derive models with many interesting properties. Moreover, due to the way these models are constructed, the free fermionic formulation provides some of the best know methods to classify the famously numerous four-dimensional string vacua. There are, of course, some downsides to this description too. Choosing to fermionise all bosonic degrees of freedom we lose the information about the underlying geometric structure of the compactification. Even though some of this information can be recovered as we will show in Chapter 4, this does not amount to complete geometric understanding. There have been similar efforts in developing model-building techniques in the bosonic language like [59]. The exact relation between the geometric compactifications in the bosonic language and the free fermionic construction has also been studied as a result. More on this can be found in [60]. In what follows we focus on the exploration of the heterotic landscape using this free fermionic formulation.

4 String Partition Functions, Moduli and The Cosmological Constant

In the previous section, we discussed extensively the free fermionic worldsheet construction of heterotic strings. In this section, we develop techniques and tools that will give us deeper insight into these models. We develop a systematic approach to expressing the partition function of fermionic models in such a way that allows for the underlying geometric structure to be readily visible. In turn, this allows us to deform the theory away from the self-dual fermionic point and explore other regions of the geometric moduli space. Using these tools, we will uncover some intriguing properties of the behaviour of superstring theories and their spectra.

4.1 From Free Fermions to Orbifolds

In Chapter 3, we defined the partition function of a heterotic string in a fermionic worldsheet construction as

$$Z_{Tot} = \int_{\mathcal{F}} \frac{d^2\tau}{\tau_2^2} \frac{1}{2^N} Z_B \sum_{Sp.Str.} C\begin{pmatrix}\boldsymbol{\alpha}\\ \boldsymbol{\beta}\end{pmatrix} \prod_f Z\begin{bmatrix}\boldsymbol{\alpha}(f)\\ \boldsymbol{\beta}(f)\end{bmatrix}, \tag{4.1}$$

where the sum runs over all sectors of our theory and the product runs over all worldsheet fermions. The sectors α, β are defined as elements of an additive group spanned by the basis vectors b_i of the fermionic construction. The phases $C\left(\begin{smallmatrix}\alpha\\ \beta\end{smallmatrix}\right)$ are set such that the partition function is modular invariant, and can be determined according to the rules (3.19)-(3.22). These rules do not fix the partition function exactly, for a model with N basis vectors, we are left with $N(N-1)/2+1$ independent GGSO phases which we are free to use. This means that each set of N basis vectors can potentially generate $2^{N(N-1)/2+1}$ distinct models.

Having reminded ourselves of the free fermionic construction and its partition function we discuss some of its shortcomings. Most importantly as we have seen earlier, the fermionisation of bosonic degrees of freedom is only possible at a special point in moduli space. This means that the partition function (4.1) lacks explicit dependence on the geometric moduli. Moreover, the form of the partition function is written in such a way that it obscures the underlying geometric structure making any reference to moduli dependence hard to see. Our aim in this section is to develop a consistent and general methodology for rewriting free fermionic partition functions to a form which accurately represents the geometric structures underpinning them. Such methods will also allow us to examine how the dependence on the geometric moduli can be reinstated. This gives us powerful tools with which the stability of these models can be better examined.

The above discussion can be made more concrete by defining what we mean by rewriting the partition function. Taking the part of (4.1) corresponding to the worldsheet fermions,

we write

$$Z_F = \frac{1}{2^N}\sum_{\boldsymbol{\alpha},\boldsymbol{\beta}} C\begin{pmatrix}\boldsymbol{\alpha}\\ \boldsymbol{\beta}\end{pmatrix} Z\begin{bmatrix}\boldsymbol{\alpha}\\ \boldsymbol{\beta}\end{bmatrix} = \sum_{\substack{a,k,\cdots\\ b,l,\cdots}} (-1)^{\Psi\left[\begin{smallmatrix}a & k & \cdots\\ b & l & \cdots\end{smallmatrix}\right]}\; Z\begin{bmatrix}a & k & \cdots\\ b & l & \cdots\end{bmatrix}, \tag{4.2}$$

where the product over the fermions is now implicit and contained within $Z\left[\begin{smallmatrix}\boldsymbol{\alpha}\\ \boldsymbol{\beta}\end{smallmatrix}\right]$. The right-hand side requires some further comments. The term $Z\left[\begin{smallmatrix}a & k & \cdots\\ b & l & \cdots\end{smallmatrix}\right]$ is our new way of representing the theta functions in terms of the summation indices $a, b, k, l, \cdots$. The phase $(-1)^{\Psi\left[\begin{smallmatrix}a & k & \cdots\\ b & l & \cdots\end{smallmatrix}\right]}$ is the analogue of the GGSO phase in this new formulation. Our task at hand is therefore to both find an appropriate form for $Z\left[\begin{smallmatrix}a & k & \cdots\\ b & l & \cdots\end{smallmatrix}\right]$ and develop a formalism which allows a one-to-one translation between $\Psi\left[\begin{smallmatrix}a & k & \cdots\\ b & l & \cdots\end{smallmatrix}\right]$ and $C\left(\begin{smallmatrix}\boldsymbol{\alpha}\\ \boldsymbol{\beta}\end{smallmatrix}\right)$.

4.1.1 The Modular Invariant Phase

To develop the formalism under which to find the right-hand side of (4.2), it is most instructive to choose an example set of basis vectors which will allow us to fully demonstrate the methods used. To do so consider the free fermionic basis

$$\begin{aligned}
\mathbb{1} &= \left\{\psi^\mu, \chi^{1,\ldots,6}, y^{1,\ldots,6}, \omega^{1,\ldots,6} \mid \bar{y}^{1,\ldots,6}, \bar{\omega}^{1,\ldots,6}, \bar{\eta}^{1,2,3}, \bar{\psi}^{1,\ldots,5}, \bar{\phi}^{1,\ldots,8}\right\}\\
S &= \left\{\psi^\mu, \chi^{1,\ldots,6}\right\}\\
T_1 &= \left\{y^{12}, w^{12} \mid \bar{y}^{12}, \bar{w}^{12}\right\}\\
T_2 &= \left\{y^{34}, w^{34} \mid \bar{y}^{34}, \bar{w}^{34}\right\}\\
T_3 &= \left\{y^{56}, w^{56} \mid \bar{y}^{56}, \bar{w}^{56}\right\}\\
b_1 &= \left\{\chi^{34}, \chi^{56}, y^{34}, y^{56} \mid \bar{y}^{34}, \bar{y}^{56}, \bar{\psi}^{1,\ldots,5}, \bar{\eta}^1\right\}\\
b_2 &= \left\{\chi^{12}, \chi^{56}, y^{12}, y^{56} \mid \bar{y}^{12}, \bar{y}^{56}, \bar{\psi}^{1,\ldots,5}, \bar{\eta}^2\right\}\\
z_1 &= \left\{\bar{\phi}^{1,\ldots,4}\right\}\\
z_2 &= \left\{\bar{\phi}^{5,\ldots,8}\right\}.
\end{aligned} \tag{4.3}$$

We now must choose the form of $Z\left[\begin{smallmatrix}a & k & \cdots\\ b & l & \cdots\end{smallmatrix}\right]$ such that the structure of theta functions performs the roles we require. For this example, we make the choice

$$\begin{aligned}
Z =& \frac{1}{\eta^{10}\bar{\eta}^{22}}\frac{1}{2^2}\sum_{\substack{a,k\\ b,l}}\frac{1}{2^3}\sum_{\substack{H_1,H_2,H_3\\ G_1,G_2,G_3}}\frac{1}{2^4}\sum_{\substack{h_1,h_2,P_1,P_2\\ g_1,g_2,Q_1,Q_2}}(-1)^{\Psi\left[\begin{smallmatrix}a & k & H_1 & H_2 & H_3 & h_1 & h_2 & P_1 & P_2\\ b & l & G_1 & G_2 & G_3 & g_1 & g_2 & Q_1 & Q_2\end{smallmatrix}\right]}\\
&\times \vartheta\begin{bmatrix}a\\ b\end{bmatrix}_{\psi^\mu}\vartheta\begin{bmatrix}a+h_1\\ b+g_1\end{bmatrix}_{\chi^{12}}\vartheta\begin{bmatrix}a+h_2\\ b+g_2\end{bmatrix}_{\chi^{34}}\vartheta\begin{bmatrix}a-h_1-h_2\\ b-g_1-g_2\end{bmatrix}_{\chi^{56}}\\
&\times \vartheta\begin{bmatrix}H_1\\ G_1\end{bmatrix}_{w^{12}}\vartheta\begin{bmatrix}H_1+h_1\\ G_1+g_1\end{bmatrix}_{y^{12}}\bar{\vartheta}\begin{bmatrix}H_1\\ G_1\end{bmatrix}_{\bar{w}^{12}}\bar{\vartheta}\begin{bmatrix}H_1+h_1\\ G_1+g_1\end{bmatrix}_{\bar{y}^{12}}\\
&\times \vartheta\begin{bmatrix}H_2\\ G_2\end{bmatrix}_{w^{34}}\vartheta\begin{bmatrix}H_2+h_2\\ G_2+g_2\end{bmatrix}_{y^{34}}\bar{\vartheta}\begin{bmatrix}H_2\\ G_2\end{bmatrix}_{\bar{w}^{34}}\bar{\vartheta}\begin{bmatrix}H_2+h_2\\ G_2+g_2\end{bmatrix}_{\bar{y}^{34}}\\
&\times \vartheta\begin{bmatrix}H_3\\ G_3\end{bmatrix}_{w^{56}}\vartheta\begin{bmatrix}H_3-h_1-h_2\\ G_3-g_1-g_2\end{bmatrix}_{y^{56}}\bar{\vartheta}\begin{bmatrix}H_3\\ G_3\end{bmatrix}_{\bar{w}^{56}}\bar{\vartheta}\begin{bmatrix}H_3-h_1-h_2\\ G_3-g_1-g_2\end{bmatrix}_{\bar{y}^{56}}\\
&\times \bar{\vartheta}\begin{bmatrix}k\\ l\end{bmatrix}^5_{\bar{\psi}^{1-5}}\bar{\vartheta}\begin{bmatrix}k+h_1\\ l+g_1\end{bmatrix}_{\bar{\eta}^1}\bar{\vartheta}\begin{bmatrix}k+h_2\\ l+g_2\end{bmatrix}_{\bar{\eta}^2}\bar{\vartheta}\begin{bmatrix}k-h_1-h_2\\ l-g_1-g_2\end{bmatrix}_{\bar{\eta}^3}\bar{\vartheta}\begin{bmatrix}k+P_1\\ l+Q_1\end{bmatrix}^4_{\bar{\phi}^{1-4}}\bar{\vartheta}\begin{bmatrix}k+P_2\\ l+Q_2\end{bmatrix}^4_{\bar{\phi}^{5-8}}.
\end{aligned} \tag{4.4}$$

where we have explicitly denoted which worldsheet fermion each theta function corresponds to. The form of this partition function is essentially mostly due to notational conventions. It is important to note that the index a is always taken to correspond to the boundary

condition of ψ^μ, the reason for which will become evident later. There are many consistent ways the partition function can be represented in terms of indices, the above choice is one which makes the underlying orbifold structure most evident.

To see all possible choices of indices, which in turn fix the form of $Z\left[\begin{smallmatrix} a & k & \cdots \\ b & l & \cdots \end{smallmatrix}\right]$, we note that to represent a partition function of a model with N basis vectors requires the use of N summation indices. This can purely be seen by matching the number of terms on each side of (4.2). Thus the translation of the form of the partition function simply entails a choice of basis, and hence the structure of the indices in (4.4) is uniquely determined by the choice of a change of basis matrix, S, in this case given by

$$S = \begin{array}{c} \\ \mathbb{1} \\ S \\ T_1 \\ T_2 \\ T_3 \\ b_1 \\ b_2 \\ z_1 \\ z_2 \end{array} \begin{array}{c} \begin{array}{ccccccccc} a & k & H_1 & H_2 & H_3 & h_1 & h_2 & P_1 & P_2 \end{array} \\ \begin{pmatrix} 1 & 1 & 1 & 1 & 1 & 0 & 0 & 0 & 0 \\ 1 & 0 & 0 & 0 & 0 & 0 & 0 & 0 & 0 \\ 0 & 0 & 1 & 0 & 0 & 0 & 0 & 0 & 0 \\ 0 & 0 & 0 & 1 & 0 & 0 & 0 & 0 & 0 \\ 0 & 0 & 0 & 0 & 1 & 0 & 0 & 0 & 0 \\ 0 & 1 & 0 & 0 & 0 & 0 & 1 & 1 & 1 \\ 0 & 1 & 0 & 0 & 0 & 1 & 0 & 1 & 1 \\ 0 & 0 & 0 & 0 & 0 & 0 & 0 & 1 & 0 \\ 0 & 0 & 0 & 0 & 0 & 0 & 0 & 0 & 1 \end{pmatrix} \end{array} \tag{4.5}$$

where we have indicated which rows and columns correspond to which basis vector and index respectively. All invertible $N \times N$ matrices whose entries take values in $\mathbb{Z}_2$ are valid choices. However, the above choice is the one which most emphasises the geometry of the underlying compactification. Choosing $S = I_N$, the N-dimensional identity matrix, would render the translation trivial and the form of $Z\left[\begin{smallmatrix} a & k & \cdots \\ b & l & \cdots \end{smallmatrix}\right]$ and $(-1)^{\Psi\left[\begin{smallmatrix} a & k & \cdots \\ b & l & \cdots \end{smallmatrix}\right]}$ would match that of $Z\left[\begin{smallmatrix} \boldsymbol{\alpha} \\ \boldsymbol{\beta} \end{smallmatrix}\right]$ and $C\left(\begin{smallmatrix} \boldsymbol{\alpha} \\ \boldsymbol{\beta} \end{smallmatrix}\right)$ respectively modulo some subtleties we discuss in the following section.

Once a choice for a valid S is made and the partition function is written in its index form as in (4.4), we can start making the connection between the GGSO Phases $C\left(\begin{smallmatrix} \boldsymbol{\alpha} \\ \boldsymbol{\beta} \end{smallmatrix}\right)$ and the modular invariant phase Ψ. We assume that Ψ can be expressed as a polynomial in the summation variables. Then, two-loop modular invariance imposed on the GGSO phases via the rule (3.22)

$$C\begin{pmatrix} \boldsymbol{b}_i \\ \boldsymbol{b}_j + \boldsymbol{b}_k \end{pmatrix} = \delta_{\boldsymbol{b}_i} C\begin{pmatrix} \boldsymbol{b}_i \\ \boldsymbol{b}_j \end{pmatrix} C\begin{pmatrix} \boldsymbol{b}_i \\ \boldsymbol{b}_k \end{pmatrix}, \tag{4.6}$$

implies that $\Psi\left[\begin{smallmatrix} a & k & H_i & h_i & P_i \\ b & l & G_i & g_i & Q_i \end{smallmatrix}\right]$ is at most second order in its variables. Moreover, the presence of δ_{b_i} restricts the first-order terms. That is Ψ must include a term a and cannot contain other terms like it. More precisely, (4.6) implies

$$\begin{cases} \Psi \ni a, \\ \Psi \not\ni k, h_i, H_i, P_i, \end{cases} \tag{4.7}$$

where we take "$\in$" to mean a term in the sum. These conditions can be implemented in a compact form by requiring the phase to be of the form

$$\Psi\left[\begin{smallmatrix} a & k & H_i & h_i & P_i \\ b & l & G_i & g_i & Q_i \end{smallmatrix}\right] = a + \beta_i \Delta_i + \Gamma_i \Omega_{ij} \Delta_j, \tag{4.8}$$

where we defined

$$\begin{aligned}\Gamma &= (a,\ k,\ H_1,\ H_2,\ H_3,\ h_1,\ h_2,\ P_1,\ P_2),\\ \Delta &= (b,\ l,\ G_1,\ G_2,\ G_3,\ g_1,\ g_2,\ Q_1,\ Q_2),\end{aligned} \tag{4.9}$$

to be the vectors containing top and bottom indices respectively.

We now impose one-loop modular invariance by requiring that the partition function (4.4) remains invariant under S and T-transformations, under which the theta functions transform according to (A.6) as

$$\begin{aligned}S:\ \ \vartheta\begin{bmatrix}a\\ b\end{bmatrix} &\longrightarrow\ e^{i\pi ab/2}\,\vartheta\begin{bmatrix}b\\ -a\end{bmatrix},\\ T:\ \ \vartheta\begin{bmatrix}a\\ b\end{bmatrix} &\longrightarrow\ e^{i\pi a(a-2)/4}\,\vartheta\begin{bmatrix}a\\ a+b-1\end{bmatrix}.\end{aligned} \tag{4.10}$$

By using a compact notation for the theta and eta function terms as in (4.2), i.e.

$$Z_F = \frac{1}{2^2}\sum_{\substack{a,k\\ b,l}}\frac{1}{2^7}\sum_{\substack{H_i,h_i,P_i\\ G_i,g_i,Q_i}}(-1)^{\Psi\left[\begin{smallmatrix}a&k&H_i&h_i&P_i\\ b&l&G_i&g_i&Q_i\end{smallmatrix}\right]}Z\left[\begin{smallmatrix}a&k&H_i&h_i&P_i\\ b&l&G_i&g_i&Q_i\end{smallmatrix}\right], \tag{4.11}$$

we can express the modular transformations more readily. In particular, under modular transformations

$$\begin{aligned}Z\left[\begin{smallmatrix}a&k&H_i&h_i&P_i\\ b&l&G_i&g_i&Q_i\end{smallmatrix}\right] &\xrightarrow{S} Z\left[\begin{smallmatrix}b&l&G_i&g_i&Q_i\\ -a&-k&-H_i&-h_i&-P_i\end{smallmatrix}\right],\\ Z\left[\begin{smallmatrix}a&k&H_i&h_i&P_i\\ b&l&G_i&g_i&Q_i\end{smallmatrix}\right] &\xrightarrow{T} (-1)^{1+a+P_1+P_2}\,Z\left[\begin{smallmatrix}a&k&H_i&h_i&P_i\\ a+b-1&k+l-1&H_i+G_i-1&h_i+g_i&P_i+Q_i\end{smallmatrix}\right],\end{aligned}$$

where the extra factor of -1 in the T-transformation comes from the η-functions. By noting that the phase Ψ transforms trivially as it is just a constant factor and that under two consecutive S and T-transformations, the above expressions close on themselves, i.e.

$$\begin{aligned}Z\left[\begin{smallmatrix}a&k&H_i&h_i&P_i\\ b&l&G_i&g_i&Q_i\end{smallmatrix}\right] &\xrightarrow{S}\cdots\xrightarrow{S} Z\left[\begin{smallmatrix}a&k&H_i&h_i&P_i\\ b&l&G_i&g_i&Q_i\end{smallmatrix}\right],\\ Z\left[\begin{smallmatrix}a&k&H_i&h_i&P_i\\ b&l&G_i&g_i&Q_i\end{smallmatrix}\right] &\xrightarrow{T}\cdots\xrightarrow{T} Z\left[\begin{smallmatrix}a&k&H_i&h_i&P_i\\ b&l&G_i&g_i&Q_i\end{smallmatrix}\right],\end{aligned} \tag{4.12}$$

we can conclude that to be modular invariant the phase must satisfy

$$\begin{aligned}\Psi\left[\begin{smallmatrix}a&k&H_i&h_i&P_i\\ b&l&G_i&g_i&Q_i\end{smallmatrix}\right] &\overset{S}{=} \Psi\left[\begin{smallmatrix}b&l&G_i&g_i&Q_i\\ -a&-k&-H_i&-h_i&-P_i\end{smallmatrix}\right],\\ \Psi\left[\begin{smallmatrix}a&k&H_i&h_i&P_i\\ b&l&G_i&g_i&Q_i\end{smallmatrix}\right] &\overset{T}{=} 1+a+P_1+P_2+\Psi\left[\begin{smallmatrix}a&k&H_i&h_i&P_i\\ a+b-1&k+l-1&H_i+G_i-1&h_i+g_i&P_i+Q_i\end{smallmatrix}\right].\end{aligned} \tag{4.13}$$

The first equation, i.e. S-invariance, shows that Ψ must be symmetric under the exchange of lower and upper indices, which together with (4.8) implies that

$$\Psi\left[\begin{smallmatrix}a&k&H_i&h_i&P_i\\ b&l&G_i&g_i&Q_i\end{smallmatrix}\right] = a+b+\Gamma_i\Omega_{ij}\Delta_j, \tag{4.14}$$

with $\Omega_{ij} = \Omega_{ji}$. Implementing the condition for T-invariance in (4.13) further restricts the form of Ω imposing the conditions on its elements

$$\begin{aligned}
\sum_{j=1}^{5} \Omega_{ij}(1-\delta_{ij}) = 0 \qquad & \text{for} \quad i = 1, \cdots, 5, \\
\sum_{j=1}^{5} \Omega_{ij} = \Omega_{ii} \qquad & \text{for} \quad i = 6, 7, \\
\sum_{j=1}^{5} \Omega_{i,j} = 1 + \Omega_{ii} \qquad & \text{for} \quad i = 8, 9,
\end{aligned} \tag{4.15}$$

where all equalities are understood modulo 2 and δ_{ij} is the Kronecker delta. These fix a further 8 components of $\Omega_{i,j}$. Together with the condition form S-invariance $\Omega_{ij} = \Omega_{ji}$, we are left with $(9^2/2 + 9/2) - 8 = 37$ independent choices for the Ω_{ij}. This precisely matches the number of independent GGSO phases for a 9 basis vector model.

What we achieved here is precisely the derivation of the modular invariance conditions, equivalent to (3.19)-(3.22), for the phase Ψ. All remaining independent components of Ω can be freely chosen as $\Omega_{ij} \in \{0, 1\}$ with each choice giving a new consistent model. Hence, these matrix elements perform the same role as the independent GGSO phases $C\binom{\alpha}{\beta}$ and therefore a one-to-one matching between them should exist.

4.1.2 The Translation

Now that we have found a consistent modular invariant way of representing a model in terms of a phase Ψ, what remains is to find a translation between the GGSO phases and Ψ as set out in (4.2). With the above setup, this means finding a correspondence between the independent GGSO phases $C\binom{\alpha}{\beta}$ and the matrix elements Ω_{ij}. We have already established that the number of these elements is in agreement on both sides and both quantities perform the same role so such a translation should be possible in principle.

To make the connection, one has to notice that the forms of the theta functions on the left and right-hand sides of (4.2) do not match. In particular the expression

$$\sum_{\substack{a,k,\cdots \\ b,l,\cdots}} (-1)^{\Psi\left[\begin{smallmatrix} a & k & \cdots \\ b & l & \cdots \end{smallmatrix}\right]} \; Z \begin{bmatrix} a & k & \cdots \\ b & l & \cdots \end{bmatrix} \tag{4.16}$$

involves theta functions which are not strictly one of $\theta_{1,2,3,4}$ due to the presence of terms like $\vartheta\left[\begin{smallmatrix} 1 \\ -1 \end{smallmatrix}\right], \vartheta\left[\begin{smallmatrix} 3 \\ 0 \end{smallmatrix}\right], \cdots$. We can, however, use the periodicity properties (A.8) of the theta functions

$$\begin{aligned}
\vartheta \begin{bmatrix} a+2 \\ b \end{bmatrix} &= \vartheta \begin{bmatrix} a \\ b \end{bmatrix} \\
\vartheta \begin{bmatrix} a \\ b+2 \end{bmatrix} &= e^{i\pi a} \vartheta \begin{bmatrix} a \\ b \end{bmatrix}
\end{aligned} \tag{4.17}$$

to rewrite (4.16) in terms of the standard theta functions. This will allow for consistent term-by-term matching. By denoting the "fundamental" form of the theta functions as

$$\vartheta_f \begin{bmatrix} a \\ b \end{bmatrix} \equiv \vartheta \begin{bmatrix} a & \mod 2 \\ b & \mod 2 \end{bmatrix}, \tag{4.18}$$

we can find equations using (4.17) that help bring all theta functions to this reduced form, e.g.

$$\begin{aligned} \vartheta \begin{bmatrix} a+h_1 \\ b+g_1 \end{bmatrix} &= (-1)^{(a+h_1)bg_1}\ \vartheta_f \begin{bmatrix} a+h_1 \\ b+g_1 \end{bmatrix} \\ \vartheta \begin{bmatrix} a+h_1+h_2 \\ b+g_1+g_2 \end{bmatrix} &= (-1)^{(a+h_1+h_2)(bg_1+bg_2+g_1g_2)}\ \vartheta_f \begin{bmatrix} a+h_1+h_2 \\ b+g_1+g_2 \end{bmatrix} \\ \vartheta \begin{bmatrix} a-h_1-h_2 \\ b-g_1-g_2 \end{bmatrix} &= (-1)^{(a-h_1-h_2)(g_1+g_2+bg_1+bg_2+g_1g_2)}\ \vartheta_f \begin{bmatrix} a-h_1-h_2 \\ b-g_1-g_2 \end{bmatrix}. \end{aligned} \tag{4.19}$$

These relations can always be found by writing $\vartheta\left[\begin{smallmatrix} a & \cdots \\ b & \cdots \end{smallmatrix}\right] = (-1)^{F(a,b,\cdots)}\vartheta_f\left[\begin{smallmatrix} a & \cdots \\ b & \cdots \end{smallmatrix}\right]$, with $F(a,b,\cdots)$ a suitably general polynomial, and restricting the form of F by requiring (4.17) to hold.

Utilising these expressions, we can rewrite the right-hand side of (4.2), i.e. (4.4), fully in terms of the theta functions $\theta_{1,2,3,4}$ as

$$Z = \sum_{\substack{a,k,\cdots \\ b,l,\cdots}} (-1)^{\chi\left[\begin{smallmatrix} a & k & \cdots \\ b & l & \cdots \end{smallmatrix}\right]+\Psi\left[\begin{smallmatrix} a & k & \cdots \\ b & l & \cdots \end{smallmatrix}\right]}\ Z_f \begin{bmatrix} a & k & \cdots \\ b & l & \cdots \end{bmatrix}, \tag{4.20}$$

where we defined the compensating phase factor χ. For our specific model it is given by

$$\chi\left[\begin{smallmatrix} a & k & H_i & h_i & P_i \\ b & l & G_i & g_i & Q_i \end{smallmatrix}\right] = (a+k)(g_1+g_2+g_1g_2) + (b+l)(h_1g_2+h_2g_1), \tag{4.21}$$

which enforces the rules (4.19). Here, by Z_f we denote that all theta functions have been brought to their mod 2 form as written in (4.18). This compensating phase is crucial for the matching of the partition functions.

We are now ready to make the connection between the two formalisms. To compare the two sides of (4.2) we must re-express the GGSO matrix C in the form

$$C_{ij} = (-1)^{G_{ij}}, \tag{4.22}$$

this allows for a direct comparison of Ψ and G. Furthermore, it will be convenient to separate Ψ into its first and second order terms, that is we define

$$\Psi\left[\begin{smallmatrix} a & k & H_i & h_i & P_i \\ b & l & G_i & g_i & Q_i \end{smallmatrix}\right] = a+b+\Gamma_i\Omega_{ij}\Delta_j \coloneqq a+b+\Phi\left[\begin{smallmatrix} a & k & H_i & h_i & P_i \\ b & l & G_i & g_i & Q_i \end{smallmatrix}\right]. \tag{4.23}$$

We can now express the factor of $a+b+\chi$ in the basis formed by the basis vectors (4.3) as a matrix P whose elements are

$$P_{ij} = \{a+b+\chi\left[\begin{smallmatrix} a & k & \cdots \\ b & l & \cdots \end{smallmatrix}\right] \mid \Gamma_k = S_{ik} \text{ and } \Delta_k = S_{jk}\}. \tag{4.24}$$

All that remains is to express Φ, i.e. Ω, in the same basis so we can equate the two. We can do this by noticing that

$$\{\Phi\left[\begin{smallmatrix} a & k & \cdots \\ b & l & \cdots \end{smallmatrix}\right] \mid \Gamma_k = S_{ik} \text{ and } \Delta_k = S_{jk}\} = S_{ik}\,\Omega_{kl}\,S_{jl} = S\,\Omega\,S^T, \tag{4.25}$$

and so $\tilde{\Omega} = S\,\Omega\,S^T$ is the phase expressed in the basis formed by the basis vectors of the free fermionic model. Since all quantities are now expressed in the same basis we can write down the equality which implements the translation, namely

$$G + P = S\,\Omega\,S^T, \tag{4.26}$$

where the equality is understood modulo 2. Solving the above equation means finding values for all Ω_{ij} and so fixing Ω. Once the solution is found to the linear system, the final phase can be expressed using (4.23), that is

$$\Psi\left[\begin{smallmatrix} a & k & H_i & h_i & P_i \\ b & l & G_i & g_i & Q_i \end{smallmatrix}\right] = a + b + \Gamma\,\Omega\,\Delta. \tag{4.27}$$

This gives a precise one-to-one correspondence between the modular invariant phase and the GGSO matrix.

It is important to note that the above methods only cover the case for real boundary conditions, i.e. models where the periodicities of the fermions are either R or NS. This in turn implies that all GGSO phases are real. It is, however, possible to generalise this construction to allow for more general choices of boundary condition vectors and GGSO matrices. This, however, is beyond the scope of this thesis and requires a more careful treatment of the derived relations.

4.2 Moduli Dependence in Free Fermionic Models

We have already eluded to the fact that a major drawback of the fermionic worldsheet construction is the lack of explicit dependence on the geometric moduli of the underlying geometry. However, this is in fact also one of the major benefits of the construction. By making no reference to the compactification geometry, we can explore parts of the landscape which may be hard to access via other bosonic methods. In this section, we aim to show that this drawback is one that can be addressed by reintroducing the moduli dependence by hand in cases where the underlying geometry allows us to do so. This would allow us to use the full power of the fermionic construction without compromise.

There are two main approaches to getting moduli-dependent models within the free fermionic construction. The *coordinate-dependent compactification* framework, developed in [61–64] and later used for example in [51, 65], relies on constructing models via worldsheet fermions in higher than required dimensions. Then, the remaining degrees of freedom are bosonised and compactified via bosonic methods to give explicit dependence on the geometric moduli in those directions. An alternative method is to construct the model via a fermionic construction directly in the required spacetime dimension. Then, *Thirring interactions* [66] are introduced for some of the worldsheet fermions which deform the model away from the fermionic point. These deformations precisely correspond to the moduli of the underlying geometry [66, 67]. These two methods are of course equivalent, but each one offers some benefits and drawbacks over the other. In what follows, we will employ the latter formulation

as this allows us to reinstate the moduli dependence of models built entirely in the fermionic construction, however, it is instructive to keep the other picture in sight as it provides a more intuitive description of the process.

This statement can be made more concrete by using the bosonisation/fermionisation relation (3.2) to rewrite the internal fermionic degrees of freedom as bosonic ones. Models which incorporate the twist vectors b_k naturally implement a $\mathbb{Z}_2 \times \mathbb{Z}_2$ orbifolding the that leave an untwisted moduli space

$$\left(\frac{SO(2,2)}{SO(2) \times SO(2)}\right)^3 \tag{4.28}$$

where each of the three factors is parameterised by the moduli scalar fields from the NS sector

$$h_{ij} = |\chi^i\rangle_L \otimes |\bar{y}^j \bar{w}^j\rangle_R = \begin{cases} (i,j=1,2) \\ (i,j=3,4) \\ (i,j=5,6) \end{cases}, \tag{4.29}$$

as discussed in detail in [67]. In free fermionic models, these untwisted moduli are in one-to-one correspondence with marginal operators that generate Abelian Thirring Interactions.

In order to make the connection between the fields h_{ij} and the familiar three Kähler and three complex structure moduli of the $\mathbb{Z}_2 \times \mathbb{Z}_2$ orbifold we can construct six complex moduli from the six real ones of (4.29). For the first complex plane, we can write

$$\begin{aligned} H_1^{(1)} &= \frac{1}{\sqrt{2}}(h_{11} + i h_{21}) = \frac{1}{\sqrt{2}} |\chi^1 + i\chi^2\rangle_L \otimes |\bar{y}^1 \bar{w}^1\rangle_R \\ H_2^{(1)} &= \frac{1}{\sqrt{2}}(h_{12} + i h_{22}) = \frac{1}{\sqrt{2}} |\chi^1 + i\chi^2\rangle_L \otimes |\bar{y}^2 \bar{w}^2\rangle_R \,, \end{aligned} \tag{4.30}$$

which can then be combined to define the Kähler and complex structure moduli for the first complex plane

$$\begin{aligned} T^{(1)} &= \frac{1}{\sqrt{2}}(H_1^{(1)} - i H_2^{(1)}) = \frac{1}{\sqrt{2}} |\chi^1 + i\chi^2\rangle_L \otimes |\bar{y}^1 \bar{w}^1 - i\bar{y}^2 \bar{w}^2\rangle_R \\ U^{(1)} &= \frac{1}{\sqrt{2}}(H_1^{(1)} + i H_2^{(1)}) = \frac{1}{\sqrt{2}} |\chi^1 + i\chi^2\rangle_L \otimes |\bar{y}^1 \bar{w}^1 + i\bar{y}^2 \bar{w}^2\rangle_R \end{aligned} \tag{4.31}$$

and similarly for $T^{(2),(3)}$ and $U^{(2),(3)}$.

The power of the translation methodology developed in the previous section is that one can readily separate the parts of the partition function corresponding to the internal geometry. We can already see this for our example model (4.3), for which we re-wrote the free fermionic

partition function in (4.4) as

$$\begin{aligned} Z =& \frac{1}{\eta^{10}\bar{\eta}^{22}} \frac{1}{2^2} \sum_{\substack{a,k \\ b,l}} \frac{1}{2^3} \sum_{\substack{H_1,H_2,H_3 \\ G_1,G_2,G_3}} \frac{1}{2^4} \sum_{\substack{h_1,h_2,P_1,P_2 \\ g_1,g_2,Q_1,Q_2}} (-1)^{\Psi\left[\begin{smallmatrix} a & k & H_1 & H_2 & H_3 & h_1 & h_2 & P_1 & P_2 \\ b & l & G_1 & G_2 & G_3 & g_1 & g_2 & Q_1 & Q_2 \end{smallmatrix}\right]} \\ & \times \vartheta\left[\begin{smallmatrix} a \\ b \end{smallmatrix}\right]_{\psi^\mu} \vartheta\left[\begin{smallmatrix} a+h_1 \\ b+g_1 \end{smallmatrix}\right]_{\chi^{12}} \vartheta\left[\begin{smallmatrix} a+h_2 \\ b+g_2 \end{smallmatrix}\right]_{\chi^{34}} \vartheta\left[\begin{smallmatrix} a-h_1-h_2 \\ b-g_1-g_2 \end{smallmatrix}\right]_{\chi^{56}} \\ & \times Z^{(1)}_{2,2}\left[\begin{smallmatrix} H_1 \\ G_1 \end{smallmatrix}\middle|\begin{smallmatrix} h_1 \\ g_1 \end{smallmatrix}\right] \times Z^{(2)}_{2,2}\left[\begin{smallmatrix} H_2 \\ G_2 \end{smallmatrix}\middle|\begin{smallmatrix} h_2 \\ g_2 \end{smallmatrix}\right] \times Z^{(3)}_{2,2}\left[\begin{smallmatrix} H_3 \\ G_3 \end{smallmatrix}\middle|\begin{smallmatrix} h_1+h_2 \\ g_1+g_2 \end{smallmatrix}\right] \\ & \times \bar{\vartheta}\left[\begin{smallmatrix} k \\ l \end{smallmatrix}\right]^5_{\bar{\psi}^{1-5}} \bar{\vartheta}\left[\begin{smallmatrix} k+h_1 \\ l+g_1 \end{smallmatrix}\right]_{\bar{\eta}^1} \bar{\vartheta}\left[\begin{smallmatrix} k+h_2 \\ l+g_2 \end{smallmatrix}\right]_{\bar{\eta}^2} \bar{\vartheta}\left[\begin{smallmatrix} k-h_1-h_2 \\ l-g_1-g_2 \end{smallmatrix}\right]_{\bar{\eta}^3} \bar{\vartheta}\left[\begin{smallmatrix} k+P_1 \\ l+Q_1 \end{smallmatrix}\right]^4_{\bar{\phi}^{1-4}} \bar{\vartheta}\left[\begin{smallmatrix} k+P_2 \\ l+Q_2 \end{smallmatrix}\right]^4_{\bar{\phi}^{5-8}} . \end{aligned} \tag{4.32}$$

where we have now separated the internal parts corresponding to the $\{y^i, w^i \mid \bar{y}^i, \bar{w}^i\}$, which are given by

$$\begin{aligned} Z^{(1)}_{2,2}\left[\begin{smallmatrix} H_1 \\ G_1 \end{smallmatrix}\middle|\begin{smallmatrix} h_1 \\ g_1 \end{smallmatrix}\right] &= \left|\vartheta\left[\begin{smallmatrix} H_1 \\ G_1 \end{smallmatrix}\right] \vartheta\left[\begin{smallmatrix} H_1+h_1 \\ G_1+g_1 \end{smallmatrix}\right]\right|^2 \\ Z^{(2)}_{2,2}\left[\begin{smallmatrix} H_2 \\ G_2 \end{smallmatrix}\middle|\begin{smallmatrix} h_2 \\ g_2 \end{smallmatrix}\right] &= \left|\vartheta\left[\begin{smallmatrix} H_2 \\ G_2 \end{smallmatrix}\right] \vartheta\left[\begin{smallmatrix} H_2+h_2 \\ G_2+g_2 \end{smallmatrix}\right]\right|^2 \\ Z^{(3)}_{2,2}\left[\begin{smallmatrix} H_3 \\ G_3 \end{smallmatrix}\middle|\begin{smallmatrix} h_1+h_2 \\ g_1+g_2 \end{smallmatrix}\right] &= \left|\vartheta\left[\begin{smallmatrix} H_3 \\ G_3 \end{smallmatrix}\right] \vartheta\left[\begin{smallmatrix} H_3-h_1-h_2 \\ G_3-g_1-g_2 \end{smallmatrix}\right]\right|^2 . \end{aligned} \tag{4.33}$$

To keep the upcoming discussion as general as possible, it is instructive to also introduce different orbifold shifts acting on the internal coordinates of our models. We have so far developed the translation methodology for using the T_i which consolidate shift around each individual cycle of the underlying six-dimensional torus by grouping shifts in each $\mathbf{T}^2$ factor. A more general setting in fermionic construction can be achieved by the inclusion of basis vectors

$$e_i = \{y^i, w^i \,|\, \bar{y}^i, \bar{w}^i\} \qquad i = 1, \cdots, 6. \tag{4.34}$$

These produce shifts along each individual circle of the internal $\mathbf{T}^6$ torus. Even though in the development of the translation methodology above we used the T_i, everything discussed till now readily generalises to the case of the e_i. One can always reduce the model to the T_i case starting from the e_i by identifying boundary conditions for the $\{y^i, w^i \mid \bar{y}^i, \bar{w}^i\}$ within each $\mathbf{T}^2$ factor. Hence we will consider the more general case of the e_i for the discussion to follow, but will also give examples of how the methodology applies to the T_i.

Adding the six extra basis vectors to the set (4.3) modifies only the internal part of the partition function (4.32) since the e_i only contain the y's and w's, however, their addition will, of course, introduce a summation over additional indices which we denote $H_i, G_i \in \{0, 1\}$ $i = 4, \cdots, 6$, together with an additional factor of 2^{-3}. The internal partition function now takes the form

$$\begin{aligned} Z^{(1)}_{2,2}\left[\begin{smallmatrix} H_1 & H_2 \\ G_1 & G_2 \end{smallmatrix}\middle|\begin{smallmatrix} h_1 \\ g_1 \end{smallmatrix}\right] &= \left|\vartheta\left[\begin{smallmatrix} H_1 \\ G_1 \end{smallmatrix}\right] \vartheta\left[\begin{smallmatrix} H_1+h_1 \\ G_1+g_1 \end{smallmatrix}\right] \vartheta\left[\begin{smallmatrix} H_2 \\ G_2 \end{smallmatrix}\right] \vartheta\left[\begin{smallmatrix} H_2+h_1 \\ G_2+g_1 \end{smallmatrix}\right]\right| \\ Z^{(2)}_{2,2}\left[\begin{smallmatrix} H_3 & H_4 \\ G_3 & G_4 \end{smallmatrix}\middle|\begin{smallmatrix} h_2 \\ g_2 \end{smallmatrix}\right] &= \left|\vartheta\left[\begin{smallmatrix} H_3 \\ G_3 \end{smallmatrix}\right] \vartheta\left[\begin{smallmatrix} H_3+h_2 \\ G_3+g_2 \end{smallmatrix}\right] \vartheta\left[\begin{smallmatrix} H_4 \\ G_4 \end{smallmatrix}\right] \vartheta\left[\begin{smallmatrix} H_4+h_2 \\ G_4+g_2 \end{smallmatrix}\right]\right| \\ Z^{(3)}_{2,2}\left[\begin{smallmatrix} H_5 & H_6 \\ G_5 & G_6 \end{smallmatrix}\middle|\begin{smallmatrix} h_1+h_2 \\ g_1+g_2 \end{smallmatrix}\right] &= \left|\vartheta\left[\begin{smallmatrix} H_5 \\ G_5 \end{smallmatrix}\right] \vartheta\left[\begin{smallmatrix} H_5-h_1-h_2 \\ G_5-h_1-h_2 \end{smallmatrix}\right] \vartheta\left[\begin{smallmatrix} H_6 \\ G_6 \end{smallmatrix}\right] \vartheta\left[\begin{smallmatrix} H_6-h_1-h_2 \\ G_6-h_1-h_2 \end{smallmatrix}\right]\right| . \end{aligned} \tag{4.35}$$

A model defined as above with basis vectors (4.3) and the additional e_i gives us all the required complexity to discuss the moduli role of the geometric moduli in detail and this is

what we turn to in the coming section.

4.2.1 The One-Dimensional Lattice

To start with, we will reintroduce the dependence on one real modulus for a model constructed in four dimensions. As discussed above, this is equivalent to a model constructed in five dimensions where then the remaining degrees of freedom are bosonised and compactified on a circle. This results in the first torus having two real moduli controlling the radii of each circle which are arranged perpendicular to one another. To leave only one real parameter, we fix all moduli other than the radius of the first circle to their free-fermionic values.

In terms of these assumptions, $Z^{(2)}_{2,2}$ and $Z^{(3)}_{2,2}$ reduce to their fermionic representations given in (4.35). Moreover, due to the assumption that the first torus factorises into two S^1 factors, we must have

$$Z^{(1)}_{2,2}\left[\begin{smallmatrix} H_1 & H_2 \\ G_1 & G_2 \end{smallmatrix}\middle|\begin{smallmatrix} h_1 \\ g_1 \end{smallmatrix}\right](T^{(1)}_*, U^{(1)}_*) = Z^{(1)}_{1,1}\left[\begin{smallmatrix} H_1 \\ G_1 \end{smallmatrix}\middle|\begin{smallmatrix} h_1 \\ g_1 \end{smallmatrix}\right](R)\;\; Z^{(2)}_{1,1}\left[\begin{smallmatrix} H_2 \\ G_2 \end{smallmatrix}\middle|\begin{smallmatrix} h_1 \\ g_1 \end{smallmatrix}\right](R_*), \tag{4.36}$$

where we fixed the radius of the second circle at its fermionic point as discussed above. This means that the $Z_{1,1}$ block corresponding to the second circle will also reduce to

$$Z^{(2)}_{1,1}\left[\begin{smallmatrix} H_2 \\ G_2 \end{smallmatrix}\middle|\begin{smallmatrix} h_1 \\ g_1 \end{smallmatrix}\right](R_*) = \left|\vartheta\left[\begin{smallmatrix} H_2 \\ G_2 \end{smallmatrix}\right]\vartheta\left[\begin{smallmatrix} H_2+h_1 \\ G_2+g_1 \end{smallmatrix}\right]\right|, \tag{4.37}$$

which we have taken from (4.35).

What remains is to analyse the R-dependence of the block $Z^{(1)}_{1,1}$. At this point, it is important to note that the dependence on geometric moduli is entirely contained in the untwisted sector of the model. Since the first orbifold plane is twisted by h_1, this means that the partition function separates into the form

$$Z^{(1)}_{1,1}\left[\begin{smallmatrix} H_1 \\ G_1 \end{smallmatrix}\middle|\begin{smallmatrix} h_2 \\ g_2 \end{smallmatrix}\right](R) = \begin{cases} Z^{(1)}_{1,1}\left[\begin{smallmatrix} H_1 \\ G_1 \end{smallmatrix}\middle|\begin{smallmatrix} 0 \\ 0 \end{smallmatrix}\right](R) & h_2 = g_2 = 0 \\ Z^{(1)}_{1,1}\left[\begin{smallmatrix} H_1 \\ G_1 \end{smallmatrix}\middle|\begin{smallmatrix} h_1 \\ g_1 \end{smallmatrix}\right] & h_2 \neq 0 \text{ or } g_2 \neq 0. \end{cases} \tag{4.38}$$

Hence the sector in which h_2 and g_2 are not both 0 mod 2, the fermionic block $Z^{(1)}_{1,1}$ again reduces to its theta function form given in (4.35).

Since we know that to go from the bosonic orbifold picture to the fermionic one, we must fermionise a bosonic coordinate to two fermionic ones, the task at hand is to rewrite the block $Z^{(1)}_{1,1}$ in terms of the partition function of a compactified boson. The partition function for a boson compactified on a circle of radius R is given by

$$\Gamma_{1,1}(R) = \frac{R}{\sqrt{\tau_2}} \sum_{m,n\in\mathbb{Z}} e^{-\frac{\pi R^2}{\tau_2}|m+n\tau|^2}. \tag{4.39}$$

However, since our basis contains e_1, which is a shift precisely on the circle we are considering, we have to take the shifted lattice sum

$$\Gamma_{1,1}\left[\begin{smallmatrix} H \\ G \end{smallmatrix}\right](R) = \frac{R}{\sqrt{\tau_2}} \sum_{m,n\in\mathbb{Z}} e^{-\frac{\pi R^2}{\tau_2}|(m+\frac{G}{2})+(n+\frac{H}{2})\tau|^2}. \tag{4.40}$$

We now have to show that this lattice sum can indeed reduce to the theta function representation of the partition function at a special radius R_*. To do this, we generalise the above construction and invoke additional characters γ, δ that will assist in the matching of the shifted lattice and the free-fermionic partition function. Using the definition of the theta function (A.5), we can rewrite the term corresponding to the worldsheet fermions as

$$\begin{aligned}\vartheta\left[\begin{smallmatrix}\gamma-H\\ \delta-G\end{smallmatrix}\right]\bar{\vartheta}\left[\begin{smallmatrix}\gamma+H\\ \delta+G\end{smallmatrix}\right] = \sum_{m,n\in\mathbb{Z}} & q^{\frac{1}{2}(m-\frac{1}{2}(\gamma-H))^2}\bar{q}^{\frac{1}{2}(n-\frac{1}{2}(\gamma+H))^2} \\ & \times e^{-i\pi\left[(m-\frac{1}{2}(\gamma-H))(\delta-G)-(n-\frac{1}{2}(\gamma+H))(\delta+G)\right]}.\end{aligned} \tag{4.41}$$

To bring this to the same Lagrangian form as the lattice sum, we must perform a Poisson resummation of m using (A.14) giving

$$\vartheta\left[\begin{smallmatrix}\gamma-H\\ \delta-G\end{smallmatrix}\right]\bar{\vartheta}\left[\begin{smallmatrix}\gamma+H\\ \delta+G\end{smallmatrix}\right] = \frac{1}{\sqrt{2\tau_2}}\sum_{m,n\in\mathbb{Z}} e^{-\frac{\pi}{2\tau_2}|(m+G)+(n+H)\tau|^2}e^{i\pi(mn+m\gamma-n\delta-H\delta)}. \tag{4.42}$$

We note that in order to derive the above equality, other than the resummation of $m \to m$, we also re-scaled the summation variables $m \to -m$ and $n \to -m-n$. To connect this expression to the lattice sum, we must sum over γ, δ. By doing so we can derive the relations

$$\frac{1}{2}\sum_{\gamma,\delta}\vartheta\left[\begin{smallmatrix}\gamma-H\\ \delta-G\end{smallmatrix}\right]\bar{\vartheta}\left[\begin{smallmatrix}\gamma+H\\ \delta+G\end{smallmatrix}\right]e^{-i\pi H\delta} = \frac{1}{2}\sum_{\gamma,\delta}\frac{1}{\sqrt{2\tau_2}}\sum_{m,n\in\mathbb{Z}} e^{-\frac{\pi}{2\tau_2}|(m+G)+(n+H)\tau|^2}e^{i\pi(mn+m\gamma-n\delta)} \tag{4.43}$$

$$= \frac{\sqrt{2}}{\sqrt{\tau_2}}\sum_{m,n\in\mathbb{Z}} e^{-\frac{2\pi}{\tau_2}\left|(m+\frac{G}{2})+(n+\frac{H}{2})\tau\right|^2} \tag{4.44}$$

$$= \Gamma_{1,1}\left[\begin{smallmatrix}H\\ G\end{smallmatrix}\right](\sqrt{2}). \tag{4.45}$$

Some clarifying comments are due here. The equality (4.43) is precisely the one we got in (4.42). The derivation of (4.44) is a non-trivial step. One must separate the sum over m, n into their even and odd components and notice that

$$\sum_{\delta,\gamma} e^{i\pi(mn+m\gamma-n\delta)} = \begin{cases} 4 & \text{if} \quad m,n \in 2\mathbb{Z} \\ 0 & \text{else.}\end{cases} \tag{4.46}$$

Thus the sum over γ, δ is equivalent to rewriting $m, n \to 2m, 2n$ and multiplying by a factor of 4, and so we arrive at (4.44). We have now made the connection between the theta functions and toroidal lattice sums, however, one might notice that the form of the theta functions we have been using, i.e. the one defined in (4.41), does not match with the one in our fermionic partition function in (5.5) and (4.35). We can solve this problem by utilising the periodicity properties of the theta functions stated in (A.8) to write

$$\vartheta\left[\begin{smallmatrix}\gamma-H\\ \delta-G\end{smallmatrix}\right] = e^{-i\pi(\gamma+H)G}\vartheta\left[\begin{smallmatrix}\gamma+H\\ \delta+G\end{smallmatrix}\right], \tag{4.47}$$

and so substituting this into (4.43)-(4.45) gives the required form.

We can summarise the above results as follows. To reintroduce the dependence on the geometric modulus R for the free fermionic model defined by the basis (4.3), with the e_i

included, and partition function (4.4), one must write the $Z^{(1)}_{1,1}$ fermionic block as

$$Z^{(1)}_{1,1}\left[\begin{smallmatrix} H \\ G \end{smallmatrix}\middle|\begin{smallmatrix} h \\ g \end{smallmatrix}\right](R) = Z^{(1)}_{1,1}\left[\begin{smallmatrix} H \\ G \end{smallmatrix}\middle|\begin{smallmatrix} 0 \\ 0 \end{smallmatrix}\right](R) + \left|\vartheta\left[\begin{smallmatrix} H \\ G \end{smallmatrix}\right]\vartheta\left[\begin{smallmatrix} H+h \\ G+g \end{smallmatrix}\right]\right|_{h,g\neq 0}. \tag{4.48}$$

The radius dependent untwisted block is then given by

$$Z^{(1)}_{1,1}\left[\begin{smallmatrix} k & H \\ l & G \end{smallmatrix}\middle|\begin{smallmatrix} 0 \\ 0 \end{smallmatrix}\right](R) = \sum_{m,n\in\mathbb{Z}} q^{\frac{1}{2}|\mathcal{P}_L(R)|^2}\bar{q}^{\frac{1}{2}|\mathcal{P}_R(R)|^2} e^{i\pi((m+n+H)G)}, \tag{4.49}$$

where

$$\begin{aligned} \mathcal{P}_L(R) =& \frac{1}{\sqrt{2}}\left[\frac{1}{2R}(m+n) + R(m-n+H)\right] \\ \mathcal{P}_R(R) =& \frac{1}{\sqrt{2}}\left[\frac{1}{2R}(m+n) - R(m-n+H)\right]. \end{aligned} \tag{4.50}$$

This expression is derived by Poisson resumming (4.43) via (A.14), which allows us to write it in a Hamiltonian q-expanded form.

It is important to note that the above expression reduces to its fermionic theta function representation at a radius $R_* = 1/\sqrt{2}$, however, when written in terms of the $\Gamma_{1,1}$ toroidal lattice sum this point is at $R_* = \sqrt{2}$. This doubling of the radius as we sum over γ, δ is evident from (4.43)-(4.45). Hence it is crucial that we keep good track of which radius we refer to when talking about the moduli at the free fermionic point.

4.2.2 The Two-Dimensional Lattice

Having discussed in detail how to reintroduce the dependence on the radius modulus of a circle in free fermionic construction, we now move on to generalise this concept to the case of a 2-dimensional torus. This allows us to discuss the moduli structure of $\mathbb{Z}_2\times\mathbb{Z}_2$ in full detail considering all geometric moduli. As before, we consider our fermionic basis (4.3) with the e_i and focus on the first torus corresponding to the worldsheet coordinates $\{y^{12}, w^{12} \mid \bar{y}^{12}, \bar{w}^{12}\}$.

Recall that for the torus one can parametrise the metric G_{ij} and anti-symmetric tensor B_{ij} in terms of the Kähler and complex structure moduli as

$$G_{ij} = \frac{T_2}{U_2}\begin{pmatrix} 1 & U_1 \\ U_1 & U_1^2+U_2^2 \end{pmatrix} \qquad B_{ij} = T_1\begin{pmatrix} 0 & -1 \\ 1 & 0 \end{pmatrix}. \tag{4.51}$$

As in the one-dimensional case, the task at hand is to relate the part of the fermionic partition function corresponding to the compact degrees of freedom, $Z^{(1)}_{2,2}$, to the partition function of two shifted bosons compactified on a torus given by

$$\Gamma_{2,2}\left[\begin{smallmatrix} H_1 & H_2 \\ G_1 & G_2 \end{smallmatrix}\right] = \frac{\sqrt{\det G_{ij}}}{\tau_2}\sum_{m_i,n_i\in\mathbb{Z}} e^{-\frac{\pi}{\tau_2}[(m_i+G_i/2)+(n_i+H_i/2)\tau]\,[G+B]_{ij}\,[(m_j+G_j/2)+(n_j+H_j/2)\bar{\tau}]}. \tag{4.52}$$

Following identical arguments as for the one-dimensional case, we only need to consider the untwisted sector in which $h_2 = g_2 = 0$ as the partition function of the twisted sectors is independent of the geometric moduli and is equivalent to the one at the fermionic point.

We proceed as before by expressing the relevant theta function terms in terms of their definitions (A.5) as infinite sums

$$\begin{aligned}\Theta\left[\begin{smallmatrix}\gamma\\ \delta\end{smallmatrix}\middle|\begin{smallmatrix}H_1 & H_2\\ G_1 & G_2\end{smallmatrix}\right] &\coloneqq \vartheta\left[\begin{smallmatrix}\gamma-H_1\\ \delta-G_1\end{smallmatrix}\right]\vartheta\left[\begin{smallmatrix}\gamma-H_2\\ \delta-G_2\end{smallmatrix}\right]\bar{\vartheta}\left[\begin{smallmatrix}\gamma+H_1\\ \delta+G_1\end{smallmatrix}\right]\bar{\vartheta}\left[\begin{smallmatrix}\gamma+H_2\\ \delta+G_2\end{smallmatrix}\right]\\ &= \sum_{m_i,n_i\in\mathbb{Z}} q^{\sum_i \frac{1}{2}(m_i-\frac{1}{2}(\gamma-H_i))^2}\bar{q}^{\sum_i \frac{1}{2}(n_i-\frac{1}{2}(\gamma+H_i))^2}\\ &\qquad\times e^{-i\pi\left[\sum_i(m_i-\frac{1}{2}(\gamma-H_i))(\delta-G_i)-\sum_i(n_i-\frac{1}{2}(\gamma+H_i))(\delta+G_i)\right]}.\end{aligned} \tag{4.53}$$

We can now perform a Poisson resummation (A.14) of m_1 and m_2 to express them in the Lagrangian form. This allows us to derive the set of equalities

$$\frac{1}{4}\sum_{\gamma,\delta}\Theta\left[\begin{smallmatrix}\gamma\\ \delta\end{smallmatrix}\middle|\begin{smallmatrix}H_1 & H_2\\ G_1 & G_2\end{smallmatrix}\right]e^{-i\pi\delta(H_1+H_2)} \tag{4.54}$$

$$= \frac{1}{4}\sum_{\gamma,\delta}\frac{1}{2\tau_2}\sum_{m_i,n_i\in\mathbb{Z}} e^{-\frac{\pi}{\tau_2}[(m_i+G_i)+(n_i+H_i)\tau]\,[(G_{ij}+B_{ij})(T_*,U_*)]\,[(m_j+G_j)+(n_j+H_j)\bar{\tau}]}\times e^{i\pi(m_in_i+\sum_i m_i\gamma-\sum_i n_i\delta)} \tag{4.55}$$

$$= \frac{2}{\tau_2}\sum_{m_i,n_i\in\mathbb{Z}} e^{-\frac{4\pi}{\tau_2}[(m_i+\frac{G_i}{2})+(n_i+\frac{H_i}{2})\tau]\,[(G_{ij}+B_{ij})(T_*,U_*)]\,[(m_j+\frac{G_j}{2})+(n_j+\frac{H_j}{2})\bar{\tau}]} \tag{4.56}$$

$$= \Gamma_{2,2}\left[\begin{smallmatrix}H_1 & H_2\\ G_1 & G_2\end{smallmatrix}\right](4T_*,U_*), \tag{4.57}$$

relating the shifted toroidal lattice sums at the fermionic point to the theta functions. Thus we have found that $(T_*,U_*)=(i/2,i)$ is the point in moduli space where the bosonisation-fermionisation becomes possible. The equalities (4.56)-(4.57) are obtained by performing the summation over γ,δ using tricks similar to the case of the one-dimensional lattice in (4.45).

As before, these expressions do not precisely represent the theta functions we used in the definition of the partition function (4.4) and (4.35). To do so, we must re-express (4.53) using the periodicity properties of the theta function (A.8), which give

$$e^{i\pi[(\gamma+H_1)G_1+(\gamma+H_2)G_2]}\,\Theta\left[\begin{smallmatrix}\gamma\\ \delta\end{smallmatrix}\middle|\begin{smallmatrix}H_1 & H_2\\ G_1 & G_2\end{smallmatrix}\right] = \vartheta\left[\begin{smallmatrix}\gamma+H_1\\ \delta+G_1\end{smallmatrix}\right]\vartheta\left[\begin{smallmatrix}\gamma+H_2\\ \delta+G_2\end{smallmatrix}\right]\bar{\vartheta}\left[\begin{smallmatrix}\gamma+H_1\\ \delta+G_1\end{smallmatrix}\right]\bar{\vartheta}\left[\begin{smallmatrix}\gamma+H_2\\ \delta+G_2\end{smallmatrix}\right], \tag{4.58}$$

where the right-hand side now gives precisely the required form. We now have all the tools to express the untwisted fermionic block in a moduli-dependent and modular invariant way. Poisson resumming (4.56) and implementing (4.58) we arrive at the final expression

$$Z_{2,2}\left[\begin{smallmatrix}\gamma & H_1 & H_2\\ \delta & G_1 & G_2\end{smallmatrix}\middle|\begin{smallmatrix}0\\ 0\end{smallmatrix}\right](T,U) = \sum_{m,n\in\mathbb{Z}} q^{\frac{1}{2}|\mathcal{P}_L(T,U)|^2}\bar{q}^{\frac{1}{2}|\mathcal{P}_R(T,U)|^2}e^{i\pi((m_i+n_i+H_i)G_i}, \tag{4.59}$$

with

$$\begin{aligned}\mathcal{P}_L(T,U) = \frac{1}{\sqrt{2T_2U_2}}\Bigg[&\frac{U}{2}(m_1+n_1) - \frac{1}{2}(m_2+n_2) \\ &+ T(m_1 - n_1 + H_1) + TU(m_2 - n_2 + H_2)\Bigg] \\ \mathcal{P}_R(T,U) = \frac{1}{\sqrt{2T_2U_2}}\Bigg[&\frac{U}{2}(m_1+n_1) - \frac{1}{2}(m_2+n_2) \\ &+ \bar{T}(m_1 - n_1 + H_1) - TU(m_2 - n_2 + H_2)\Bigg].\end{aligned} \tag{4.60}$$

It is important to note the ambiguity of the value of the moduli when talking about the fermionic point. From expression (4.55)-(4.57) we see that there is a change $T \to 4T$ when we perform the sum over γ, δ. Therefore it is important to keep track of which value we refer to. In what follows, we make the notational choice to refer to the value of the moduli at the fermionic point at

$$\begin{aligned}T_* &= i/2 \\ U_* &= i,\end{aligned} \tag{4.61}$$

but one can always refer to (4.57) to recover the true value.

The expression (4.59) gives a general and consistent way in which one may reintroduce the dependence on the geometric moduli of any free fermionic model. We have described the case on only the first torus, but these methods can be readily applied to the two other internal tori. Thus in principle, the dependence on all moduli can be reintroduced in this way. A more detailed discussion on the classification of various shifts one can implement, although using a slightly different framework, can be found in [68]. What we presented above is simply just a working example of a specific implementation.

4.3 Cosmological Constant and One-Loop Potential

As we have seen in Section 2.5, the one-loop worldsheet vacuum energy is calculated via summing over all inequivalent worldsheet tori. This can be achieved by performing a modular invariant integration of the partition function over the fundamental domain of the modular group as expressed in (2.60). In this section, we discuss how explicitly to evaluate these integrals and relate the results to the spacetime cosmological constant and one-loop potential.

First, it is important to note that for all partition functions discussed so far in this section, we only considered the part corresponding to the free worldsheet fermions. We must, however, also include in the partition function the contribution of the bosons which in D-dimensions is given by

$$Z_B = (\sqrt{\tau_2}\eta\bar{\eta})^{-(D-2)}. \tag{4.62}$$

This will multiply the terms coming from the worldsheet fermions (4.4) giving us a total partition function $Z(\tau, \bar{\tau}, T^{(i)}, U^{(i)})$. In general, one must integrate overall inequivalent worldsheet tori via a modular invariant integral

$$V_{\text{One-Loop}}(T^{(i)}, U^{(i)}) = -\frac{1}{2}\left(\frac{M_s}{2\pi}\right)^D \int_{\mathcal{F}} \frac{d^2\tau}{\tau_2^2}\, Z(\tau, \bar{\tau}, T^{(i)}, U^{(i)}), \tag{4.63}$$

where

$$\mathcal{F} = \{\tau \in \mathbb{C} \mid |\tau| > 1\,,\, |\tau_1| < 1/2\} \tag{4.64}$$

is the fundamental domain of the modular group $SL(2,\mathbb{Z})$. This gives the spacetime cosmological constant and thus the one-loop potential as a function of the geometric moduli. The dimensionful constant factor in front of the integral can be derived using field theoretic arguments [69]. It is common to abbreviate it with the notation $\mathcal{M} = M_s/2\pi$.

Our task at hand is to evaluate this integral as a function of the moduli. There are, however, no currently known techniques which allow for an analytic evaluation of such integrals over the entire moduli space. Much effort has gone into the development of such techniques and there are some recent developments, e.g. [70–73], that rely on the unfolding of the modular domain. However, these techniques are not yet ripe enough to be able to apply in generality and are currently only able to evaluate such integrals in the asymptotic regions of moduli space. Therefore, in what follows we will approach the problem from a more practical and numerical point of view.

To find the behaviour of the one-loop potential around the fermionic point, one must evaluate the partition function on a grid of moduli values. For each fixed value $(T,U) = (T_0,U_0)$, the partition function can be written in a q-expanded form by employing the appropriate definitions, (A.3) and (4.53), of the ϑ and η-functions as well as the moduli dependent fermionic block (4.59). Utilising these, we have

$$V_{\text{One-Loop}}(T_0,U_0) = \int_{\mathcal{F}} \frac{d^2\tau}{\tau_2^3} \sum_{n.m} a_{mn}\, q^m \bar{q}^n = \sum_{n.m} a_{mn} \int_{\mathcal{F}} \frac{d^2\tau}{\tau_2^3}\, q^m \bar{q}^n \tag{4.65}$$

at the specific chosen point $(T,U) = (T_0,U_0)$. The extra factor of τ_2^{-1} compared to (4.63) is coming from the contribution of the bosons in (4.62). Hence the value of the potential relies on the evaluation of integrals of the form

$$I_{mn} = \int_{\mathcal{F}} \frac{d^2\tau}{\tau_2^3}\, q^m \bar{q}^n = \int_{\mathcal{F}} \frac{d^2\tau}{\tau_2^3}\, e^{-2\pi\tau_2(m+n)} e^{2\pi i \tau_1 (n-m)}. \tag{4.66}$$

As the fundamental domain $\mathcal{F}$ is symmetric with respect to τ_1, only the even part of the τ_1 exponential will contribute giving

$$I_{nm} = \int_{\mathcal{F}} \frac{d^2\tau}{\tau_2^3}\, e^{-2\pi\tau_2(m+n)} \cos(2\pi\tau_1(m-n)). \tag{4.67}$$

The integral over τ_1 can be done analytically while the τ_2 integral has to be done numerically.

The analytic integral is calculated by splitting $\mathcal{F}$ into the two regions

$$\mathcal{F} \;\to \begin{cases} \mathcal{F}_1 = \{\tau \in \mathbb{C} \,|\, \tau_2 \geq 1 \;\wedge\; |\tau_1| < 1/2\} \\ \mathcal{F}_2 = \{\tau \in \mathbb{C} \,|\, |\tau| > 1 \;\wedge\; \tau_2 < 1 \;\wedge\; |\tau_1| < 1/2\}, \end{cases} \tag{4.68}$$

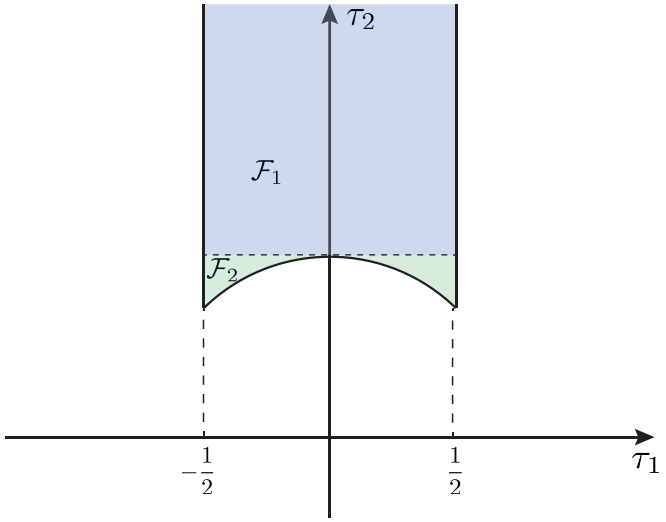

FIGURE 4.1: *The two regions $\mathcal{F}_1$ and $\mathcal{F}_2$ of the fundamental domain $\mathcal{F}$. The modular integrals* (4.67) *behave differently in these two domains.*

such that $\mathcal{F} = \mathcal{F}_1 \cup \mathcal{F}_2$. These two subregions of the fundamental domain are depicted in Figure 4.1. We then have the integrals I_{mn} splitting as

$$\begin{aligned} I_{mn}^{\mathcal{F}_1} &= \int_1^\infty \frac{d\tau_2}{\tau_2^3}\, e^{-2\pi\tau_2(m+n)} \int_{-1/2}^{1/2} d\tau_1\, \cos(2\pi\tau_1(m-n)) \\ I_{mn}^{\mathcal{F}_2} &= \int_{\sqrt{3}/2}^1 \frac{d\tau_2}{\tau_2^3}\, e^{-2\pi\tau_2(m+n)} \int_{\sqrt{1-\tau_2^2}}^{1/2} d\tau_1\, \cos(2\pi\tau_1(m-n)) \\ &\quad + \int_{\sqrt{3}/2}^1 \frac{d\tau_2}{\tau_2^3}\, e^{-2\pi\tau_2(m+n)} \int_{-1/2}^{-\sqrt{1-\tau_2^2}} d\tau_1\, \cos(2\pi\tau_1(m-n)) \end{aligned} \tag{4.69}$$

and so performing the τ_1 integration results in

$$\begin{aligned} I_{mn}^{\mathcal{F}_1} &= \frac{\sin(\pi(m-n))}{\pi(m-n)} \int_1^\infty \frac{d\tau_2}{\tau_2^3}\, e^{-2\pi\tau_2(m+n)} \\ I_{mn}^{\mathcal{F}_2} &= \frac{1}{\pi(m-n)} \int_{\sqrt{3}/2}^1 \frac{d\tau_2}{\tau_2^3} \left(\sin(\pi(m-n)) - \sin(2\pi\sqrt{1-\tau_2^2}(m-n)) \right) e^{-2\pi\tau_2(m+n)}. \end{aligned} \tag{4.70}$$

This shows that the integrals behave very differently in cases when $m = n$, which correspond to on-shell degrees of freedom. Hence, we must consider this case separately and evaluate the limits accordingly, giving

$$\begin{aligned} I_{mn}^{\mathcal{F}_1} &= \begin{cases} \int_1^\infty \frac{d\tau_2}{\tau_2^3}\, e^{-2\pi\tau_2(m+n)} & \text{if } m = n \\ \frac{\sin(\pi(m-n))}{\pi(m-n)} \int_1^\infty \frac{d\tau_2}{\tau_2^3}\, e^{-2\pi\tau_2(m+n)} & \text{if } m \neq n \end{cases} \\ I_{mn}^{\mathcal{F}_2} &= \begin{cases} \int_{\sqrt{3}/2}^1 \frac{d\tau_2}{\tau_2^3} \left(1 - 2\sqrt{1-\tau_2^2} \right) e^{-2\pi\tau_2(m+n)} & \text{if } m = n \\ \int_{\sqrt{3}/2}^1 \frac{d\tau_2}{\tau_2^3} \left(\sin(\pi(m-n)) - \sin(2\pi\sqrt{1-\tau_2^2}(m-n)) \right) \frac{e^{-2\pi\tau_2(m+n)}}{\pi(m-n)} & \text{if } m \neq n. \end{cases} \end{aligned} \tag{4.71}$$

	m=n	$m \neq n$ $m-n \in \mathbb{Z}$	else
$m+n<0$	$\mathcal{F}_1: \infty$ $\mathcal{F}_2$: finite allowed	$\mathcal{F}_1: 0$ $\mathcal{F}_2$: finite allowed	$\mathcal{F}_1: \infty$ $\mathcal{F}_2$: finite disallowed
$m+n\geq 0$	$\mathcal{F}_1$: finite $\mathcal{F}_2$: finite allowed	$\mathcal{F}_1: 0$ $\mathcal{F}_2$: finite allowed	$\mathcal{F}_1$: finite $\mathcal{F}_2$: finite disallowed

TABLE 4.1: The values of the integrals in the q-expanded partition function sum (4.65) in the subregions $\mathcal{F}_1$ and $\mathcal{F}_2$. We have also indicated whether the specific term is allowed or disallowed by modular invariance.

The remaining τ_2 integral has to be done using numerical methods, but this does not cause any major difficulties as standard numerical techniques suffice.

At this point, we can draw some conclusions about the overall convergence of the above integrals. All contributions from the region $\mathcal{F}_2$ are finite and in general non-zero, however the same is not true about $\mathcal{F}_1$. As expected, on-shell tachyonic states with $m=n<0$ give a divergent contribution. The same is true for terms in which $m+n<0$ and $m-n\notin\mathbb{Z}$. Moreover, of-shell states with $m\neq n$ and $m-n\in\mathbb{Z}$ integrate to zero in this $\mathcal{F}_2$ region. We can summarise these findings as follows:

$$I^{\mathcal{F}_1}_{mn}=\begin{cases}0 & \text{if} \quad m\neq n \text{ and } m-n\in\mathbb{Z}\\ \infty & \text{if} \quad m+n<0 \text{ and } m-n\notin\mathbb{Z}\backslash\{0\}\\ \text{finite nonzero} & \text{else}\end{cases}$$
$$I^{\mathcal{F}_2}_{mn}=\Big\{\text{finite nonzero} \qquad \forall m,n. \tag{4.72}$$

Thus for partition functions which are absent of divergent terms, the above integrals can be consistently evaluated using numerical methods.

Other than on-shell tachyonic states, (4.72) shows that divergences may arise from of-shell tachyonic terms in the q-expansion of the form $q^m\bar{q}^n$ with $m-n\notin\mathbb{Z}$. However, considering the q-expanded partition function, one may notice that under T-transformations

$$T: \quad \sum_{m,n} a_{mn}q^m\bar{q}^n \longrightarrow \sum_{m,n} a_{mn}e^{2\pi i(m-n)}q^m\bar{q}^n. \tag{4.73}$$

This shows that in order to have a modular invariant partition function, the q-expansion must only contain terms that satisfy $m-n\in\mathbb{Z}$. This is a fully general result that applies to all closed-string theories. Therefore, this result together with (4.72) implies that the only possible divergent terms in the integral sum of the one-loop potential (4.65) are the on-shell tachyons. We summarise the discussion above in Table 4.1, where we display all possible terms in the partition function q-expansion and whether they arise or not.

We have shown that other than on-shell tachyonic terms, each individual term in the one-loop potential sum (4.65) is finite. This, however, does not mean that the sum itself is convergent. To analyse its behaviour one can easily see that asymptotically, the on-shell integrals behave as

$$\lim_{n \text{ large}} I_{nn} \sim e^{-4\pi n}. \tag{4.74}$$

This can be compared to the well-known result [74], that in general for string theories the number of states at each mass level asymptotically follows the relation

$$\lim_{n \text{ large}} a_{nn} \sim n^{-b} e^{c\sqrt{n}}, \tag{4.75}$$

where b and c are model-dependent constants. For example, in some well know models they take the following values [74]

$$\begin{aligned} \text{Bosonic String:} \quad & b = \frac{27}{4}, \quad c = 4\pi, \\ SO(32) \text{ or } E_8 \times E_8 \text{ Heterotic:} \quad & b = \frac{11}{12}, \quad c = 2\pi(2+\sqrt{2}). \end{aligned} \tag{4.76}$$

General methods for deriving these parameters can be found in [75, 76]. Comparing the asymptotic results (4.74) and (4.75) we see that the product $a_{nn}I_{nn}$ tends to zero for large n and so the infinite sum in the partition function (4.65) will converge given the absence of physical tachyons. This powerful result shows that the one-loop vacuum energy in string theory is indeed finite.

A feature of all non-supersymmetric string theories that we have not mentioned so far is that all of them feature a non-vanishing dilaton tadpole. This happens in all models with non-vanishing one-loop vacuum energy. This, however, does not necessarily mean an inconsistency of the underlying theory. Indeed, it was shown in [77, 78] that this is just a sign that our theory is no longer defined in a flat background and the dilaton tadpole can be removed by a suitable redefinition of the background geometry. Hence to entirely solve a non-supersymmetric theory one has to take into account this non-trivial back-reaction of a non-zero cosmological constant on the metric as discussed in more detail in [79, 80]. This is, however, very difficult in most cases and does not form a part of this thesis. In what follows, we keep in mind that all calculated values of the cosmological constant are not actually the observable ones since this effect is not taken into account.

Much of this thesis will centre around the discussion of physical tachyonic degrees of freedom in non-supersymmetric models. Table 4.1 shows that on-shell tachyonic states are allowed in string models and do not cause any underlying structural issues. However, they do cause a divergence in the vacuum energy at the points in moduli space where they do emerge. This does not mean that models with tachyons should be discarded. They can still be viable models for string phenomenology and can even be useful when considering some cosmological scenarios [81]. In the context of this thesis what we should care about is that tachyons do not emerge in regions of moduli space around the minimum of the potential. Solutions at this minimum should still be considered viable solutions since they are not directly affected by tachyons that may emerge elsewhere far in moduli space.

4.4 Partition Function and Potential: An Example

We now move on to demonstrating the powerful tool developed in this section through an example. We start from a free fermionic model constructed in four dimensions and eventually arrive at the one-loop potential as a function of some of the geometric moduli.

Our starting point is the free fermionic model in 4-dimensions defined by the basis vectors

$$\begin{aligned}
\mathbf{1} &= \left\{\psi^{\mu}, \chi^{1,\ldots,6}, y^{1,\ldots,6}, \omega^{1,\ldots,6} \mid \bar{y}^{1,\ldots,6}, \bar{\omega}^{1,\ldots,6}, \bar{\eta}^{1,2,3}, \bar{\psi}^{1,\ldots,5}, \bar{\phi}^{1,\ldots,8}\right\} \\
S &= \left\{\psi^{\mu}, \chi^{1,\ldots,6}\right\} \\
T_1 &= \left\{y^{12}, w^{12} \mid \bar{y}^{12}, \bar{w}^{12}\right\} \\
T_2 &= \left\{y^{34}, w^{34} \mid \bar{y}^{34}, \bar{w}^{34}\right\} \\
T_3 &= \left\{y^{56}, w^{56} \mid \bar{y}^{56}, \bar{w}^{56}\right\} \\
b_1 &= \left\{\chi^{34}, \chi^{56}, y^{34}, y^{56} \mid \bar{y}^{34}, \bar{y}^{56}, \bar{\psi}^{1,\ldots,5}, \bar{\eta}^{1}\right\} \\
b_2 &= \left\{\chi^{12}, \chi^{56}, y^{12}, y^{56} \mid \bar{y}^{12}, \bar{y}^{56}, \bar{\psi}^{1,\ldots,5}, \bar{\eta}^{2}\right\} \\
z_1 &= \left\{\bar{\phi}^{1,\ldots,4}\right\} \\
z_2 &= \left\{\bar{\phi}^{5,\ldots,8}\right\},
\end{aligned} \tag{4.77}$$

which is the set we considered in Section 4.1. It also coincides with the one used in [82] and possesses an $SO(10)$ observable gauge group. To define a model, we must also specify a set of GGSO phases that fix the partition function and ensure modular invariance. For this example, we will consider the model with

$$C\begin{pmatrix}\mathbf{b}_i\\ \mathbf{b}_j\end{pmatrix} = \begin{array}{c} \\ \mathbb{1} \\ S \\ T_1 \\ T_2 \\ T_3 \\ b_1 \\ b_2 \\ z_1 \\ z_2 \end{array} \begin{array}{c} \begin{array}{ccccccccc} \mathbb{1} & S & T_1 & T_2 & T_3 & b_1 & b_1 & z_1 & z_2 \end{array} \\ \begin{pmatrix} -1 & -1 & -1 & -1 & -1 & +1 & -1 & +1 & -1 \\ -1 & -1 & -1 & -1 & -1 & +1 & +1 & +1 & +1 \\ -1 & -1 & +1 & +1 & +1 & +1 & -1 & -1 & -1 \\ -1 & -1 & +1 & +1 & -1 & +1 & -1 & +1 & +1 \\ -1 & -1 & +1 & -1 & +1 & -1 & +1 & -1 & +1 \\ +1 & -1 & +1 & +1 & -1 & +1 & -1 & +1 & -1 \\ -1 & -1 & -1 & -1 & +1 & -1 & -1 & -1 & -1 \\ +1 & +1 & -1 & +1 & -1 & +1 & -1 & +1 & +1 \\ -1 & +1 & -1 & +1 & +1 & -1 & -1 & +1 & -1 \end{pmatrix} \end{array} \tag{4.78}$$

Having defined a model in the free fermionic construction, we now proceed to implement the methodology developed in Section 4.1 to write down the partition function in an efficient a practical way.

We have to start by choosing a change of basis matrix S such that we get a form of the partition function that best showcases the geometric structure of our model. We make the

choice

$$S = \begin{array}{c} \\ \mathbb{1} \\ S \\ T_1 \\ T_2 \\ T_3 \\ b_1 \\ b_2 \\ z_1 \\ z_2 \end{array} \begin{array}{c} \begin{array}{ccccccccc} a & k & H_1 & H_2 & H_3 & h_1 & h_2 & P_1 & P_2 \end{array} \\ \left(\begin{array}{ccccccccc} 1 & 1 & 1 & 1 & 1 & 0 & 0 & 0 & 0 \\ 1 & 0 & 0 & 0 & 0 & 0 & 0 & 0 & 0 \\ 0 & 0 & 1 & 0 & 0 & 0 & 0 & 0 & 0 \\ 0 & 0 & 0 & 1 & 0 & 0 & 0 & 0 & 0 \\ 0 & 0 & 0 & 0 & 1 & 0 & 0 & 0 & 0 \\ 0 & 1 & 0 & 0 & 0 & 0 & 1 & 1 & 1 \\ 0 & 1 & 0 & 0 & 0 & 1 & 0 & 1 & 1 \\ 0 & 0 & 0 & 0 & 0 & 0 & 0 & 1 & 0 \\ 0 & 0 & 0 & 0 & 0 & 0 & 0 & 0 & 1 \end{array} \right) \end{array} \tag{4.79}$$

and a quick check gives $\det S \neq 0$, which confirms that this is indeed a valid one. This fixes the form of the partition function which is now given by

$$\begin{aligned} Z =& \frac{1}{\eta^{10}\bar{\eta}^{22}} \frac{1}{2^2} \sum_{\substack{a,k \\ b,l}} \frac{1}{2^3} \sum_{\substack{H_1,H_2,H_3 \\ G_1,G_2,G_3}} \frac{1}{2^4} \sum_{\substack{h_1,h_2,P_1,P_2 \\ g_1,g_2,Q_1,Q_2}} (-1)^{\Psi \left[\begin{smallmatrix} a & k & H_1 & H_2 & H_3 & h_1 & h_2 & P_1 & P_2 \\ b & l & G_1 & G_2 & G_3 & g_1 & g_2 & Q_1 & Q_2 \end{smallmatrix} \right]} \\ & \times \vartheta \left[\begin{smallmatrix} a \\ b \end{smallmatrix} \right]_{\psi^\mu} \vartheta \left[\begin{smallmatrix} a+h_1 \\ b+g_1 \end{smallmatrix} \right]_{\chi^{12}} \vartheta \left[\begin{smallmatrix} a+h_2 \\ b+g_2 \end{smallmatrix} \right]_{\chi^{34}} \vartheta \left[\begin{smallmatrix} a-h_1-h_2 \\ b-g_1-g_2 \end{smallmatrix} \right]_{\chi^{56}} \\ & \times \left| \vartheta \left[\begin{smallmatrix} H_1 \\ G_1 \end{smallmatrix} \right] \vartheta \left[\begin{smallmatrix} H_1+h_1 \\ G_1+g_1 \end{smallmatrix} \right] \right|^2_{yw^{12}\bar{y}\bar{w}^{12}} \\ & \times \left| \vartheta \left[\begin{smallmatrix} H_2 \\ G_2 \end{smallmatrix} \right] \vartheta \left[\begin{smallmatrix} H_2+h_2 \\ G_2+g_2 \end{smallmatrix} \right] \right|^2_{yw^{34}\bar{y}\bar{w}^{34}} \\ & \times \left| \vartheta \left[\begin{smallmatrix} H_3 \\ G_3 \end{smallmatrix} \right] \vartheta \left[\begin{smallmatrix} H_3-h_1-h_2 \\ G_3-g_1-g_2 \end{smallmatrix} \right] \right|^2_{yw^{56}\bar{y}\bar{w}^{56}} \\ & \times \bar{\vartheta} \left[\begin{smallmatrix} k \\ l \end{smallmatrix} \right]^5_{\bar{\psi}^{1-5}} \bar{\vartheta} \left[\begin{smallmatrix} k+h_1 \\ l+g_1 \end{smallmatrix} \right]_{\bar{\eta}^1} \bar{\vartheta} \left[\begin{smallmatrix} k+h_2 \\ l+g_2 \end{smallmatrix} \right]_{\bar{\eta}^2} \bar{\vartheta} \left[\begin{smallmatrix} k-h_1-h_2 \\ l-g_1-g_2 \end{smallmatrix} \right]_{\bar{\eta}^3} \bar{\vartheta} \left[\begin{smallmatrix} k+P_1 \\ l+Q_1 \end{smallmatrix} \right]^4_{\bar{\phi}^{1-4}} \bar{\vartheta} \left[\begin{smallmatrix} k+P_2 \\ l+Q_2 \end{smallmatrix} \right]^4_{\bar{\phi}^{5-8}} . \end{aligned} \tag{4.80}$$

where we have again indicated which ϑ-functions correspond to which worldsheet fermion. As discussed at length is Section 4.1.1 we have written the modular invariant phase as $\Psi = a + b + \Phi$.

Imposing S and T-invariance as in (4.13) implies that the phase must satisfy (4.13). This shows that, as before, Ψ must be symmetric under the exchange of upper and lower indices and so $\Psi = a + b + \Omega_{ij}$ with $\Omega_{ij} = \Omega_{ji}$. We also get extra conditions on the Ω_{ij} from T-invariance given by (4.15) so we are left with 37 independent Ω_{ij} which, as expected, coincides with the number of independent GGSO phases for a 9 basis vector model.

As discussed in Section 4.1.2, to implement the translation of the GGSO phase (4.78) to the modular invariant phase Ψ we must calculate the compensating phase that arises due to the periodicity properties of the theta functions. Implementing the relations (4.19) gives

$$\chi = (a+k)(g_1 + g_2 + g_1 g_2) + (b+l)(h_1 g_2 + h_2 g_1), \tag{4.81}$$

based on which we can calculate the matrix P via (4.24).

Now, that we have isolated the independent phases and calculated the periodicity offset matrix P, we can consistently implement the translation equation (4.26) which reads

$$G + P = S\,\Omega\,S^T, \tag{4.82}$$

where G is calculated form the GGSO matrix by (4.22). In our case, since we are interested in calculating the phase from the GGSO matrix, we can invert this equation to give

$$\Omega = S^{-1}(G + P)S^{T,-1}. \tag{4.83}$$

Inputting the values for G from (4.22) and P from (4.81) gives the modular invariant phase

$$\begin{aligned}\Psi\left[\begin{smallmatrix} a & k & H_i & h_i & P_i \\ b & l & G_i & g_i & Q_i \end{smallmatrix}\right] = {} & a + b + b(a + P_1 + P_2) + l(H_2 + H_3) \\ & + G_1(h_1 + P_1 + P_2) + G_2(h_2 + H_3 + k) \\ & + G_3(h_2 + H_2 + k + P_1) \\ & + g_1(h_1 + h_2 + H_1 + P_1) + g_2(h_1 + H_2 + H_3) \\ & + Q_1(a + h_1 + H_1 + H_3) + Q_2(a + H_1 + P_2),\end{aligned} \tag{4.84}$$

where we have used (4.27). This phase ensures the modular invariance of the partition function and sets all signs in the sum such that it is equivalent to the one defined in the free fermionic construction.

Using this phase we can now evaluate the partition function (4.80) for this specific model. As we discussed previously, the most insightful way to do so is in terms of a q-expansion which in this case gives

$$\begin{aligned}Z = {} & \frac{2}{q} - 16\frac{q^{1/4}}{\bar{q}^{-3/4}} + 256\frac{q^{1/2}}{\bar{q}^{1/2}} + 224\frac{\bar{q}^{1/2}}{q^{1/2}} \\ & + 520 - 4128 q^{1/4}\bar{q}^{1/4} + 14336 q^{1/2}\bar{q}^{1/2},\end{aligned} \tag{4.85}$$

where we displayed all terms up to order $q^{1/2}$ and $\bar{q}^{1/2}$. The first line encompasses all off-shell terms and the second line gives all on-shell terms. Using the analytic and numeric integration methods of Section 4.3, we can integrate this q-expansion to gain a value

$$\lambda = -99.34\,\mathcal{M}^4 = -0.064\,M_s^4 \tag{4.86}$$

for the spacetime cosmological constant at the fermionic point. Of course, this value generally depends on the geometric moduli which are frozen at the free fermion point. Thus it is not guaranteed that this is a stable value. To analyse the stability of this model in the geometric moduli space, we have to deform the model away from the fermionic point

We now move on to reinstating the moduli dependence of our model according to the techniques developed in Section 4.2. In this example, we choose to restore the dependence on the volume of the first torus of the underlying $\mathbf{T}^2 \times \mathbf{T}^2 \times \mathbf{T}^2$, which is given by $T_2^{(1)}$. This choice is made as in models that correspond to a Scherk-Schwarz breaking of supersymmetry, one can choose a configuration in which the scale of the breaking is controlled by the volume of

the first torus [82, 83]. We assume all other moduli are kept at their self-dual values meaning

$$\begin{aligned} T^{(1)} &= iT_2 \\ T^{(2),(3)} &= T_* = \frac{i}{2} \\ U^{(1),(2),(3)} &= U_* = i, \end{aligned} \tag{4.87}$$

and so our partition function now depends on one real modulus $Z = Z(\tau, \bar{\tau}, T_2)$.

As shown in Section 4.2 we have to rewrite the internal lattice corresponding to the first torus in terms of the toroidal lattice sums (4.52). This means that the part of the partition function corresponding to $\{y^{12}, w^{12} \,|\, \bar{y}^{12}, \bar{w}^{12}\}$ should be rewritten as

$$\left|\vartheta \begin{bmatrix} H_1 \\ G_1 \end{bmatrix} \vartheta \begin{bmatrix} H_1+h_1 \\ G_1+g_1 \end{bmatrix}\right|^2 \longrightarrow Z_{2,2} \left[\begin{array}{c|c} H_1 & h_1 \\ G_1 & g_1 \end{array}\right](T,U) \tag{4.88}$$

such that the fermionic block $Z_{2,2}$ reduces back to its theta function form at the fermionic point $(T,U) = (T_*, U_*)$.

Recall from Section 4.2 that only the untwisted sector depends on the moduli and so sectors in which either h_1 or g_1 are nonzero, $Z_{2,2}$ will be represented entirely in terms of its theta function form throughout the entire moduli space. Hence we only need to consider the case when $h_2 = g_2 = 0$. This is precisely what (4.59) achieves, but now we must make sure to correctly identify the two independent shifts implemented there. This is because in our case both circles of the first torus are shifted by the same H_1. Therefore, identifying $H_1 = H_2$ in (4.59) and implementing our assumptions on the moduli (4.87) we get

$$Z_{2,2} \left[\begin{array}{cc|c} \gamma & H_1 \; H_2 & 0 \\ \delta & G_1 \; G_2 & 0 \end{array}\right](T_2) = \sum_{m,n\in\mathbb{Z}} q^{\frac{1}{2}|\mathcal{P}_L(T_2)|^2} \bar{q}^{\frac{1}{2}|\mathcal{P}_R(T_2)|^2} e^{i\pi((m_i+n_i+H_i)G_i}, \tag{4.89}$$

with

$$\begin{aligned} \mathcal{P}_L(T_2) = \frac{1}{\sqrt{2iT_2}} \Bigg[& \frac{i}{2}(m_1+n_1) - \frac{1}{2}(m_2+n_2) \\ & + iT_2(m_1 - n_1 + H_1) - T_2(m_2 - n_2 + H_2) \Bigg] \\ \mathcal{P}_R(T_2) = \frac{1}{\sqrt{2iT_2}} \Bigg[& \frac{i}{2}(m_1+n_1) - \frac{1}{2}(m_2+n_2) \\ & - iT_2(m_1 - n_1 + H_1) + T_2(m_2 - n_2 + H_2) \Bigg]. \end{aligned} \tag{4.90}$$

This allows us to express the complete moduli-dependent partition function. We can then define a lattice in T_2 over which we evaluate the potential via a modular invariant integral using the method presented in Section 4.3. This results in the one-loop potential shown in Figure 4.2. We see that the potential exhibits a local minimum at $T_2 = i/2$ which is precisely the free fermionic point. Moreover, at large volume $T_2 \to \infty$ the vacuum energy tends to zero and so supersymmetry is restored. This is exactly what one would expect in the case of a stringy Scherk-Schwarz scenario and so this model corresponds to such a case. The potential interestingly also exhibits a T-duality symmetry in this direction of moduli space.

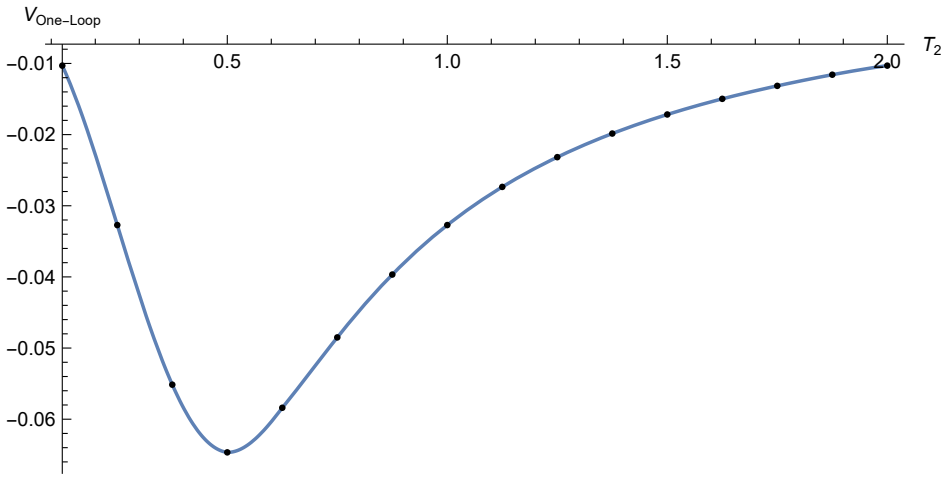

FIGURE 4.2: *The one-loop potential for the model defined by basis* (4.77) *and GGSO matrix* (4.78) *evaluated as a function of the volume modulus* T_2 *of the first torus in string units* M_s^4. *The dots show the lattice on which the evaluations were made while the line is a polynomial interpolation.*

4.5 Finiteness and Misaligned Supersymmetry

Having discussed the partition function and one-loop potential for heterotic theories in detail, we now turn to elaborate on an intriguing feature of all non-supersymmetric string models called *misaligned supersymmetry*. This quality of string models was initially discovered in [69, 84] and has been subject to rigorous research ever since. In what follows we introduce this phenomenon and also give examples from models we discussed so far.

Recall that the one-loop partition function for heterotic string models can always be expanded in the form

$$Z = \int_{\mathcal{F}} \frac{d^2\tau}{\tau_2^3} \sum_{n.m} a_{mn}\, q^m \bar{q}^n, \tag{4.91}$$

where the coefficients a_{mn} give the difference in fermionic and bosonic degrees of freedom at any given mass level m, n. More specifically $a_{mn} = N_b^{mn} - N_f^{mn}$, where N_b and N_f are the number of bosonic and fermionic states at each mass level respectively. In theories with spacetime supersymmetry, it is ensured that the bosonic and fermionic degrees of freedom are exactly matched at each mass level. That is, we necessarily have that $a_{mn} = 0$ for all m and n, which in turn causes the vanishing of the partition function and cosmological constant as one expects. For our non-supersymmetric models, this level-by-level cancellation is not ensured and so such theories in general produce a non-zero value for Λ. It is, therefore, not obviously clear that they should produce finite partition functions, or what form the state degeneracies should take. It has, however, been shown [69, 84, 85], that the partition functions of non-supersymmetric closed string theories possess a special feature called misaligned supersymmetry.

As one expects, the degeneracy of states grows rapidly going up the infinite tower of massive states. This growth, in theory, could counteract the suppression received from the decreasing contributions from the integrals of (4.91) and cause divergences. As we have seen in (4.74) and (4.75) this proliferation of states is, however, always overcome due to the exponential

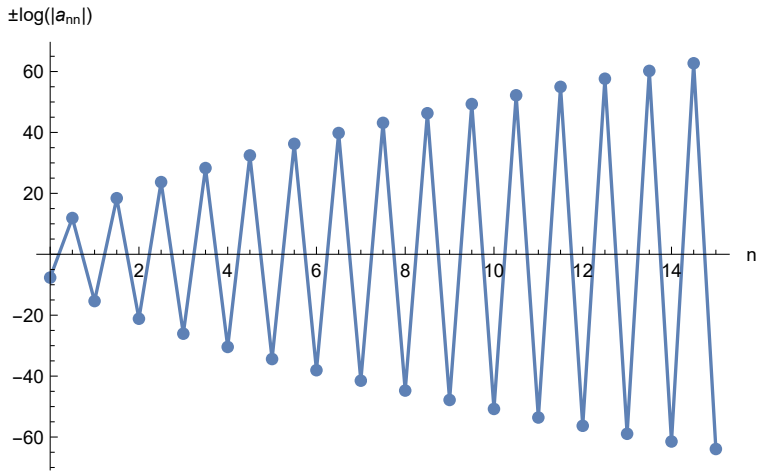

FIGURE 4.3: *The boson-fermion oscillation of misaligned supersymmetry for the* $SO(16) \times SO(16)$ *heterotic string in 10D. The state degeneracies are plotted on a logarithmic scale while preserving the overall sign of each term.*

suppression of the modular integral terms. This can be seen as a direct consequence of modular invariance since the mapping of the integrals to the fundamental domain of the modular group removes the divergences. However. it has been discovered in [69, 84] and rigorously proven in [85] that for some closed string theories, modular invariance also causes the states in the massive tower to oscillate between an excess of bosons and an excess of fermions. This behaviour is referred to as boson-fermion oscillation. An example of this for the 10D $SO(16) \times SO(16)$ heterotic string is shown in Figure 4.3. Instead of cancelling level-by-level as in the supersymmetric case, the cancellation is misaligned causing the oscillation meaning a large positive contribution is followed by an even larger negative contribution and so on.

The above discussion shows that the finiteness of string theory is a direct consequence of modular invariance, which also causes the oscillatory behaviour of the massive spectrum. The two concepts are inseparable and one cannot have a finite closed string model that doesn't exhibit both modular invariance and misaligned supersymmetry. In fact, it has been recently shown in [5] and extensively discussed in [86] that even closed string models with tachyonic instabilities exhibit this misalignment. This provides further evidence that the finiteness of string models should not be thought of as a direct consequence of misaligned supersymmetry and that this phenomenon is simply an imprint of modular invariance on the physical spectrum.

Having discussed the moduli dependence of fermionic models in the previous section, it is an interesting question to ask how this influences the misalignment of the on-shell spectrum. It is clear from the outline above that at all points in moduli space where supersymmetry is broken, the oscillatory behaviour should be present and this is indeed the case. However, in many models, as one approaches asymptotic regions of moduli space, supersymmetry is restored. This happens, for example, in the case of Scherk-Schwarz supersymmetry breaking as shown in Figure 4.2. In these cases, the way supersymmetry is asymptotically restored gives us deeper insight into how misaligned supersymmetry manifests itself on the physical spectrum. As an example, we take a generic free fermionic model corresponding to a Scherk-Schwarz breaking and reinstate the dependence on the one real modulus governing the scale of the SUSY breaking. The resulting boson-fermion oscillation pattern is depicted

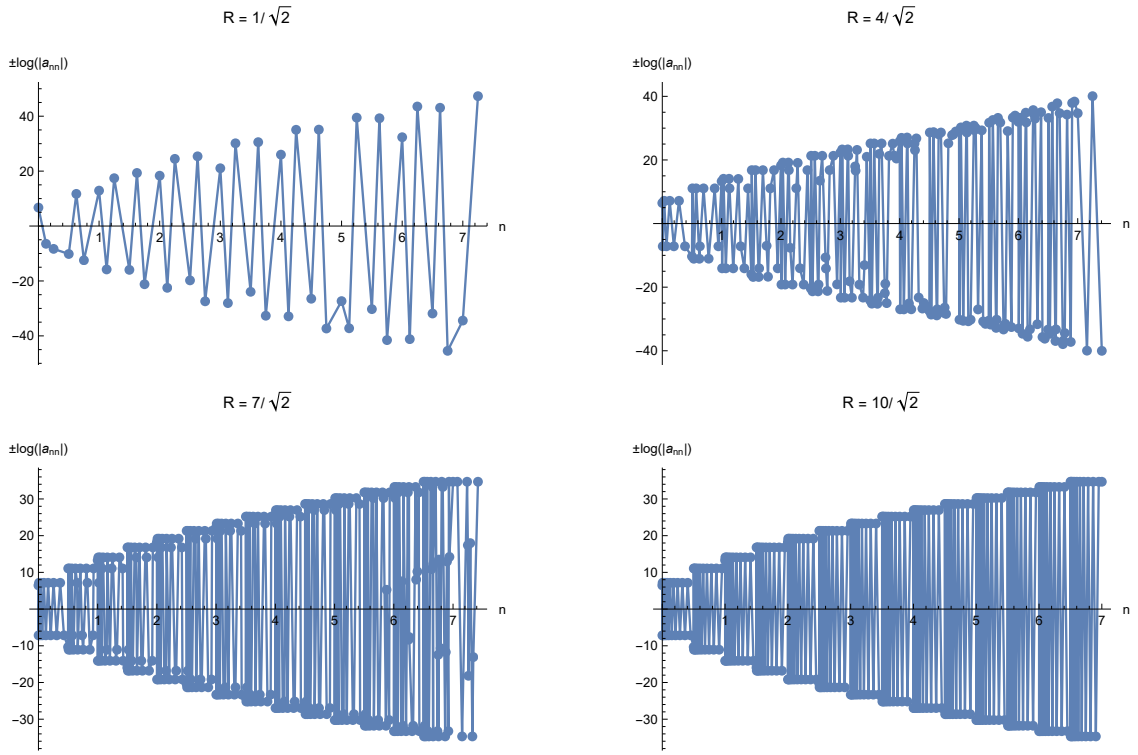

FIGURE 4.4: *The boson-fermion oscillation of misaligned supersymmetry for a generic Scherk-Schwarz model plotted at various points in moduli space. The real modulus R is the radius of the circle controlling the scale of the SUSY breaking.*

in Figure 4.4 at various points of moduli space. This shows that as we approach large, or small volumes in cases with unbroken T-duality, the misalignment becomes more and more aligned. This means that the state degeneracies arrange in a way that asymptotically results in direct cancellations between bosonic and fermionic degrees of freedom thereby effectively restoring supersymmetry.

So far we have only discussed the case of closed string models in which modular invariance is required by consistency and showed that this is the origin of misaligned SUSY. What is even more remarkable is that it has been recently shown in [21, 23] that some open string models also exhibit this behaviour. In open string theories, the one-loop amplitude does not correspond to the torus and so modular invariance is not required. However as shown in these papers, the misalignment is caused by a residual symmetry that forms a subgroup of the modular group. This shows that there is still much to learn about this intriguing feature of string theory.

5 Tachyon-Free Models from Tachyonic 10D Heterotic Vacua

Over the past few decades of string phenomenology, much attention has been devoted to studying four-dimensional models. Initially, the main focus fell on the landscape of supersymmetric vacua which arise from the compactification of one of the consistent supersymmetric tachyon-free 10D string theories. Due to the lack of experimental signals for the presence of supersymmetry at higher and higher energies, the focus has recently shifted to the exploration of non-supersymmetric vacua. In the case of models with broken supersymmetry, much care has to be taken to ensure that tachyonic instabilities are not present in the physical spectrum. The main approach to construct such models in 4D has been to start with a supersymmetric 10D model and then break supersymmetry in the process of compactification ensuring that tachyons don't arise by suitable choices of projections. Another option is to start with the known tachyon-free non-supersymmetric 10D models and compactify to 4D. In this section, we highlight another possibility first discussed in [87] and further elaborated in [1–3] in which one starts with a tachyonic 10D vacua. We show that it is possible to construct viable models based on these in four-dimension. This in turn implies that the tachyonic 10D vacua should be treated on an equal footing with their tachyon-free and supersymmetric counterparts when discussing four-dimensional string phenomenology. This section is based on the paper [2] by the author.

This section is organised as follows: In Section 5.1 we recap the main structure of the models that descend from the ten-dimensional tachyonic vacua. The free fermionic classification method utilises a common set of boundary condition basis vectors, which is presented in Section 5.1, and the enumeration of the models is obtained by varying the one–loop Generalised GSO projection coefficients. We discuss in sections 5.1 and 5.4 two generic maps that play important roles in our analysis, the $\tilde{S}$-map (Section 5.1), and the $\tilde{x}$-map. In Section 5.2 we discuss the gauge symmetry arising in our models and the sectors contributing to it. In sections 5.3 and 5.4 we set up the tools for the systematic analysis of the tachyonic and massless sectors of our models. In Section 5.5 we discuss the systematic analysis of the partition function and the vacuum energy. In Section 5.6 we present the results of our classification. Section 5.8 concludes the section with a discussion of the results and outlook for future directions.

5.1 Heterotic Vacua and the $\widetilde{S}$-Map

Recall from Section 3.3 that the $E_8 \times E_8$ and $SO(16) \times SO(16)$ heterotic–models in ten dimensions are defined in terms of a common set of basis vectors

$$\begin{aligned} v_1 = \mathbb{1} =& \{\psi^\mu,\ \chi^{1,\dots,6} \mid \overline{\eta}^{1,2,3}, \overline{\psi}^{1,\dots,5}, \overline{\phi}^{1,\dots,8}\}, \\ v_2 = z_1 =& \{\overline{\psi}^{1,\dots,5}, \overline{\eta}^{1,2,3}\}, \\ v_3 = z_2 =& \{\overline{\phi}^{1,\dots,8}\}. \end{aligned} \tag{5.1}$$

The spacetime supersymmetry generator arises from the combination

$$S = \mathbb{1} + z_1 + z_2 = \{\psi^\mu, \chi^{1,\dots,6}\}. \tag{5.2}$$

The choice of GGSO phase $C\left[\begin{smallmatrix} z_1 \\ z_2 \end{smallmatrix}\right] = \pm 1$ differentiates between the $SO(16) \times SO(16)$ or $E_8 \times E_8$ heterotic strings in ten dimensions. The vector (5.2) dictates that in ten dimensions the breaking of spacetime supersymmetry is correlated with the breaking pattern $E_8 \times E_8 \to SO(16) \times SO(16)$. However, this does not hold in lower dimensions, and the two breakings are not correlated. On the other hand, these vacua with broken and unbroken supersymmetry can be interpolated [65, 88].

On the level of the partition function, we can represent these ten-dimensional fermionic models entirely in terms of theta functions using methods discussed in Section 4.1 as

$$Z = \frac{1}{\eta^4 \bar{\eta}^{16}} \frac{1}{2} \sum_{\substack{a \\ b}} \frac{1}{2^2} \sum_{\substack{\gamma,\epsilon \\ \delta,\xi}} (-1)^{a+b+\Phi\left[\begin{smallmatrix} a & \gamma & \epsilon \\ b & \delta & \xi \end{smallmatrix}\right]} \vartheta\left[\begin{smallmatrix} a \\ b \end{smallmatrix}\right]^4 \vartheta\left[\begin{smallmatrix} \gamma \\ \delta \end{smallmatrix}\right]^8 \vartheta\left[\begin{smallmatrix} \epsilon \\ \xi \end{smallmatrix}\right]^8 . \tag{5.3}$$

The choice of modular invariant phase Φ then selects between the $SO(16) \times SO(16)$ and $E_8 \times E_8$ models. In the case of the non-supersymmetric $SO(16) \times SO(16)$ model, this phase explicitly breaks supersymmetry resulting in a nonzero q-expansion

$$Z_{SO(16)\times SO(16)} = \frac{8}{\bar{q}} + \frac{4096\sqrt{\bar{q}}}{\sqrt{q}} - 2112 + 147456\sqrt{q}\sqrt{\bar{q}} + \cdots , \tag{5.4}$$

where we have displayed all terms up to order $\sqrt{\bar{q}}\sqrt{q}$. Of course, in the case of the $E_8 \times E_8$ string, supersymmetry is realised via the generalised Jacobi Identity (A.13) resulting in a vanishing one-loop partition function.

The tachyonic states in the $E_8 \times E_8$ and $SO(16) \times SO(16)$ heterotic strings in ten dimensions are projected out. The would-be tachyons in these models are obtained from the Neveu-Schwarz (NS) sector, by acting on the right–moving vacuum with a single fermionic oscillator

$$|0\rangle_L \otimes \bar{\phi}^a |0\rangle_R, \tag{5.5}$$

where in ten dimensions $a = 1, \cdots, 16$. The GSO projection induced by the S–vector projects out the untwisted tachyons, producing tachyon-free models in both cases. As discussed in refs. [1, 87], obtaining the ten-dimensional tachyonic vacua in the free fermionic formulation amounts to the removal of the S–vector from the construction. The ten-dimensional configurations are obtained by substituting the z_1 basis vector with $z_1 = \{\bar{\phi}^{1,\cdots,\ 4}\}$ and adding

similar z_i basis vectors, with four periodic fermions, and at most two overlapping. These vacua are connected by interpolations or orbifolds along the lines of ref. [89], and, in general, contain tachyons in their spectrum.

In the free fermionic formulation, the four-dimensional models that descend from the ten-dimensional tachyonic vacua amount to removing the vector S from the set of basis vectors that are used to generate the models. In four spacetime dimensions the set $\{\mathbb{1}, z_1, z_2\}$ produces a non–supersymmetric model with $SU(2)^6 \times SO(12) \times E_8 \times E_8$ or $SU(2)^6 \times SO(12) \times SO(16) \times SO(16)$. An alternative to removing the S–vector from the construction is to augment it with periodic right–moving fermions. A convenient choice is given by

$$\tilde{S} = \{\psi^{1,2}, \chi^{1,2}, \chi^{3,4}, \chi^{5,6} \mid \bar{\phi}^{3,\cdots,\ 6}\}. \tag{5.6}$$

In this case, there are no massless gravitinos and the untwisted tachyonic states

$$|0\rangle_L \otimes \bar{\phi}^{3,\cdots,\ 6}|0\rangle_R \tag{5.7}$$

are invariant under the $\tilde{S}$–vector projection. These untwisted tachyons are those that descend from the ten-dimensional vacuum, hence confirming that the model can be regarded as a compactification of a ten-dimensional tachyonic vacuum.

We, therefore, observe a general map, which is induced by the exchange

$$S \longleftrightarrow \tilde{S}, \tag{5.8}$$

in the construction of the heterotic string models that descend from the ten-dimensional tachyonic vacua. We refer to this map as the $S - \tilde{S}$–map. It was discussed and used in the construction of the $\overline{\text{NAHE}}$–based model in [1]. We remark that the $S-\tilde{S}$–map is reminiscent of the map used to induce the spinor–vector duality in [90–94], in the sense that both utilise a block of four periodic right–moving worldsheet fermions. We may term these sorts of maps as modular maps, in the sense that they involve a block of four periodic complex worldsheet fermions.

We, therefore, have another instance where such a modular map is reflected in the symmetry structure of the string vacua. Be it the spacetime supersymmetry in the models in which the S–basis vector is the supersymmetry spectral flow operator, or in the spinor–vector dual models in which a similar spectral flow operator operates in the observable E_8 sector and induces the spinor–vector duality map [90–92, 95]. Here, a similar operation is at play in the four-dimensional models inducing the transformation from the supersymmetric (and non–supersymmetric) models that contain the S–basis vector, to the non–supersymmetric models that contain the $\tilde{S}$–basis vector. As discussed in [96], this may be a reflection of a larger symmetry structure that underlies these models and string compactifications in general.

It is important to comment on the difference between the S and $\tilde{S}$ maps, and the $S \to \tilde{S}$ map. The addition of the basis vector S to a set is often referred to as a supersymmetry or S-mapping. This is because adding S to any state of the theory generates its superpartner and hence this basis vector can be thought of as a map on the states of any given model. If one introduces $\tilde{S}$ instead of S this mapping of states will no longer generate the superpartners. Instead, these would-be superpartner states now acquire mass and hence supersymmetry is no longer present. In contrast, the $S \to \tilde{S}$ map is understood as a mapping on the basis

vectors on the models and in turn a map of the partition function as discussed above. This distinction is important to keep in mind when discussing such maps.

5.2 Non–Supersymmetric $SO(10)$ Models in 4D

Let us now define the classification structure for the $SO(10)$ models we consider, which employ the $S - \tilde{S}$–map. The first ingredient we need is a set of basis vectors that generate the space of $SO(10)$ $\tilde{S}$-models. We can choose the set

$$\begin{aligned}
\mathbb{1} &= \{\psi^\mu,\ \chi^{1,\ldots,6}, y^{1,\ldots,6}, w^{1,\ldots,6} \mid \overline{y}^{1,\ldots,6}, \overline{w}^{1,\ldots,6}, \overline{\psi}^{1,\ldots,5}, \overline{\eta}^{1,2,3}, \overline{\phi}^{1,\ldots,8}\},\\
\tilde{S} &= \{\psi^\mu, \chi^{1,\ldots,6} \mid \overline{\phi}^{3,4,5,6}\},\\
e_i &= \{y^i, w^i \mid \overline{y}^i, \overline{w}^i\}, \quad i = 1, ..., 6\\
b_1 &= \{\psi^\mu, \chi^{12}, y^{34}, y^{56} \mid \overline{y}^{34}, \overline{y}^{56}, \overline{\eta}^1, \overline{\psi}^{1,\ldots,5}\},\\
b_2 &= \{\psi^\mu, \chi^{34}, y^{12}, y^{56} \mid \overline{y}^{12}, \overline{y}^{56}, \overline{\eta}^2, \overline{\psi}^{1,\ldots,5}\},\\
b_3 &= \{\psi^\mu, \chi^{56}, y^{12}, y^{34} \mid \overline{y}^{12}, \overline{y}^{34}, \overline{\eta}^3, \overline{\psi}^{1,\ldots,5}\},\\
z_1 &= \{\overline{\phi}^{1,\ldots,4}\},
\end{aligned} \tag{5.9}$$

which is a similar basis set to $\overline{\text{NAHE}} = \{\mathbb{1}, \tilde{S}, b_1, b_2, b_3\}$ employed in [1], except with the inclusion of z_1 to break the hidden gauge group and of e_i to obtain all symmetric shifts of the internal $\Gamma_{6,6}$ lattice. We note that the vector b_3 which spans the third twisted plane and facilitates the analysis of the observable spinorial representations is typically formed as a linear combination in previous supersymmetric classifications [18, 90–92, 97–104]. Furthermore, we note the existence of a vector combination z_2

$$z_2 = \mathbb{1} + \sum_{i=1}^{6} e_i + \sum_{k=1}^{3} b_k + z_1 = \{\bar{\phi}^{5,6,7,8}\} \tag{5.10}$$

in our models, which is typically its own basis vector in previous classifications.

Models may then be defined through the specification of GGSO phases $C\left[\begin{smallmatrix} v_i \\ v_j \end{smallmatrix}\right]$, which for our $SO(10)$ models are 66 free phases with all others specified by modular invariance. Hence, the full space of models is of size $2^{66} \sim 10^{19.9}$ models. This is a notably enlarged space compared with the supersymmetric $SO(10)$ case where the requirement that the spectrum is supersymmetric fixes some GGSO phases.

The untwisted sector gauge vector bosons for this choice of basis vectors give rise to a gauge group

$$SO(10) \times U(1)_1 \times U(1)_2 \times U(1)_3 \times SO(4)^4 \tag{5.11}$$

where our desired GUT $SO(10)$ is generated by the spacetime vector bosons $\psi^\mu \bar{\psi}^a \bar{\psi}^b |0\rangle$, the $U(1)_{i=1,2,3}$ are those generated by the worldsheet currents $: \bar{\eta}^i \bar{\eta}^{i*} :$ and the $SO(4)^4$ is the hidden sector generated by spacetime vector bosons from the pairs of $\bar{\phi}^a$ with common boundary conditions for each basis vector: $\{\bar{\phi}^{1,2}, \bar{\phi}^{3,4}, \bar{\phi}^{5,6}, \bar{\phi}^{7,8}\}$.

The gauge group of a model may be enhanced by additional gauge bosons which may arise from the z_1, z_2 and $z_1 + z_2$ sectors with appropriate oscillators, i.e.

$$\left\{ \begin{array}{c} \psi^\mu \left|z_1\right\rangle_L \otimes \{\bar{\lambda}^i\} \left|z_1\right\rangle_R \\ \psi^\mu \left|z_2\right\rangle_L \otimes \{\bar{\lambda}^i\} \left|z_2\right\rangle_R \\ \psi^\mu \left|z_1+z_2\right\rangle_L \otimes \left|z_1+z_2\right\rangle_R \end{array} \right\} \tag{5.12}$$

where $\bar{\lambda}^i$ are all possible right moving Neveu-Schwarz oscillators.

Whether these gauge bosons appear is model-dependent since it depends on their survival under the GGSO projections. These enhancement sectors are also present in the familiar supersymmetric classification set-ups used in [18, 90–92, 97–104]. However, in those cases, there is also an observable enhancement from the vector $x = \{\overline{\psi}^{1,\ldots,5}, \overline{\eta}^{1,2,3}\}$, which arises as a linear combination in these models.If present, this vector induces the enhancement$SO(10) \times U(1) \to E_6$, where the $U(1) = U(1)_1 + U(1)_2 + U(1)_3$ combination is typically anomalous [105],unless such an enhancement is present.This result was first discussed in the context of the NAHE models, where including x in the basis was shown to similarly produce E_6 GUT models [106, 107]. We therefore can see that one effect of our $\tilde{S}$ models with the basis (5.9) is to preclude the possibility of an E_6 enhancement in these models.

From (5.12) we can deduce that enhancements of the observable $SO(10)$ gauge group may arise from the sectors $\psi^\mu\{\bar{\psi}^a\}\left|z_1\right\rangle, \psi^\mu\{\bar{\psi}^a\}\left|z_2\right\rangle$, $a = 1, ..., 5$. Interestingly, the sectors: $\left|z_1\right\rangle, \left|z_2\right\rangle$ (with no oscillators) produce level-matched tachyons with conformal weight $(-1/2, -1/2)$ and so the appearance of these enhancements is correlated with the projection of level-matched tachyons. The full analysis of the level-matched tachyonic sectors is presented in the following section.

5.3 Tachyonic Sectors Analysis

Due to the absence of the supersymmetry generating vector S in our construction, analysing whether on-shell tachyons arise in the spectrum of our models becomes crucial. On-shell tachyons arise when

$$M_L^2 = M_R^2 < 0, \tag{5.13}$$

which corresponds to left and right products of $\alpha_L \cdot \alpha_L = 0, 1, 2, 3$ and $\alpha_R \cdot \alpha_R = 0, 1, \cdots, 7$. The presence of such tachyonic sectors in the physical spectrum indicates the instability of the string vacuum. There are 126 of these sectors in our models which are summarised compactly in Table 5.1. We will find that models in which all 126 on-shell tachyons are projected by the GGSO projections appear with a probability of ~ 0.0054 and so in our classification we will filter all but around 1 in 185 models.

In [82, 108] a basis was chosen such that, rather than having the six internal shift vectors e_i, the combinations $T_1 = e_1 + e_2$, $T_2 = e_3 + e_4$ and $T_3 = e_5 + e_6$ were employed. Such a grouping does not allow for sectors to arise for all shifts in the internal space and, for example, means that spinorial $\mathbf{16}/\overline{\mathbf{16}}$ sectors have a degeneracy of 4 making 3 particle generations impossible once the $SO(10)$ group is broken. However, choosing $T_{i=1,2,3}$ did have the advantage of restricting the number of tachyonic sectors and allowing for a more simplified set-up to perform an analysis of the structure of the 1-loop potential in these models.

Mass Level	Vectorials	Spinorials
$(-1/2,-1/2)$	$\{\bar{\lambda}^m\}\,\|0\rangle$	$z_1,\ z_2$
$(-3/8,-3/8)$	$\{\bar{\lambda}^m\}e_i$	$e_i+z_1,\ e_i+z_2$
$(-1/4,-1/4)$	$\{\bar{\lambda}^m\}e_i+e_j$	$e_i+e_j+z_1,\ e_i+e_j+z_2$
$(-1/8,-1/8)$	$\{\lambda^m\}e_i+e_j+e_k$	$e_i+e_j+e_k+z_1,\ e_i+e_j+e_k+z_2$

TABLE 5.1: *Level-matched tachyonic sectors and their mass level, where* $i\neq j\neq k=1,...,6$ and $\bar{\lambda}^m$ is any right-moving complex fermion with NS boundary condition for the relevant tachyonic sector.

Sector	$C\left[\begin{smallmatrix}z_1\\e_1\end{smallmatrix}\right]$	$C\left[\begin{smallmatrix}z_1\\e_2\end{smallmatrix}\right]$	$C\left[\begin{smallmatrix}z_1\\e_3\end{smallmatrix}\right]$	$C\left[\begin{smallmatrix}z_1\\e_4\end{smallmatrix}\right]$	$C\left[\begin{smallmatrix}z_1\\e_5\end{smallmatrix}\right]$	$C\left[\begin{smallmatrix}z_1\\e_6\end{smallmatrix}\right]$	$C\left[\begin{smallmatrix}z_1\\b_1\end{smallmatrix}\right]$	$C\left[\begin{smallmatrix}z_1\\b_2\end{smallmatrix}\right]$	$C\left[\begin{smallmatrix}z_1\\b_3\end{smallmatrix}\right]$	$C\left[\begin{smallmatrix}z_1\\z_2\end{smallmatrix}\right]$
z_1	+	+	+	+	+	+	+	+	+	+

TABLE 5.2: *Conditions on GGSO coefficients for survival of the on-shell tachyons* $|z_1\rangle$.

Since finding models in which all on-shell tachyons are projected is crucial with regard to all questions of stability of our string vacua we will delineate the methodology used in our analysis. In order to perform this analysis a computer algorithm had to be developed which could scan samples of $\mathcal{O}(10^9)$ models or more for on-shell tachyons. A detailed analysis of how to check whether our on-shell tachyons are projected is outlined in what follows.

Tachyons of Conformal Weight $(-\frac{1}{2},-\frac{1}{2})$

The first on-shell tachyons we will inspect are those with conformal weight $(-\frac{1}{2},-\frac{1}{2})$. Firstly we have the aforementioned untwisted tachyons (5.7) which are always projected since $\binom{z_1}{NS}=\binom{z_2}{NS}=-\binom{b_i}{NS}=1$. There are then two spinorial tachyonic sectors at this mass level: z_1 and z_2. The conditions for their survival can be displayed as in Tables 5.2 and 5.3.

These tell us that only when all 10 of the column phases are $+1$ do the sectors remain in the spectrum. Interestingly, this has a bearing on the existence of the gauge group enhancements mentioned in the previous section. In particular, the only observable enhancements $\psi^\mu\,|z_1\rangle_L\otimes\bar{\psi}^a\,|z_1\rangle$ and $\psi^\mu\,|z_2\rangle_L\otimes\bar{\psi}^a\,|z_2\rangle$ have the same survival conditions as the z_1, z_2 tachyonic sectors. Therefore we find that for our construction, there are no tachyon-free models in which the $SO(10)$ is enhanced. This is evident in the classification results shown in Table 5.14 of Section 5.6.

Tachyons of Conformal Weight $(-\frac{3}{8},-\frac{3}{8})$

Now moving up the mass levels to $(-\frac{3}{8},-\frac{3}{8})$, we have vectorial tachyons from the 6 sectors: $\{\bar{\lambda}^i\}\,|e_i\rangle,\ i=1,...,6$ and spinorial tachyons from 12 sectors: $|e_i+z_1\rangle$ and $|e_i+z_2\rangle$. To demonstrate how to check the survival of these sectors we take the case of $\{\bar{\lambda}^i\}\,|e_1\rangle$, $|e_1+z_1\rangle$ and $|e_1+z_2\rangle$, which we show in the Tables 5.4, 5.5 and 5.6. The other cases with $e_{2,...,6}$ are much the same except for a simple permutation of the projection phases.

Sector	$C\left[\begin{smallmatrix} z_2 \\ e_1 \end{smallmatrix}\right]$	$C\left[\begin{smallmatrix} z_2 \\ e_2 \end{smallmatrix}\right]$	$C\left[\begin{smallmatrix} z_2 \\ e_3 \end{smallmatrix}\right]$	$C\left[\begin{smallmatrix} z_2 \\ e_4 \end{smallmatrix}\right]$	$C\left[\begin{smallmatrix} z_2 \\ e_5 \end{smallmatrix}\right]$	$C\left[\begin{smallmatrix} z_2 \\ e_6 \end{smallmatrix}\right]$	$C\left[\begin{smallmatrix} z_2 \\ b_1 \end{smallmatrix}\right]$	$C\left[\begin{smallmatrix} z_2 \\ b_2 \end{smallmatrix}\right]$	$C\left[\begin{smallmatrix} z_2 \\ b_3 \end{smallmatrix}\right]$	$C\left[\begin{smallmatrix} z_2 \\ z_1 \end{smallmatrix}\right]$
z_2	+	+	+	+	+	+	+	+	+	+

TABLE 5.3: *Conditions on GGSO coefficients for survival of the on-shell tachyons* $|z_2\rangle$.

$\|e_1\rangle$ **Oscillator**	$C\left[\begin{smallmatrix} e_1 \\ \tilde{S} \end{smallmatrix}\right]$	$C\left[\begin{smallmatrix} e_1 \\ e_2 \end{smallmatrix}\right]$	$C\left[\begin{smallmatrix} e_1 \\ e_3 \end{smallmatrix}\right]$	$C\left[\begin{smallmatrix} e_1 \\ e_4 \end{smallmatrix}\right]$	$C\left[\begin{smallmatrix} e_1 \\ e_5 \end{smallmatrix}\right]$	$C\left[\begin{smallmatrix} e_1 \\ e_6 \end{smallmatrix}\right]$	$C\left[\begin{smallmatrix} e_1 \\ b_1 \end{smallmatrix}\right]$	$C\left[\begin{smallmatrix} e_1 \\ \tilde{x} \end{smallmatrix}\right]$	$C\left[\begin{smallmatrix} e_1 \\ z_1 \end{smallmatrix}\right]$	$C\left[\begin{smallmatrix} e_1 \\ z_2 \end{smallmatrix}\right]$
$\{\bar{y}^2\}$	+	-	+	+	+	+	-	+	+	+
$\{\bar{w}^2\}$	+	-	+	+	+	+	+	+	+	+
$\{\bar{y}^3\}$	+	+	-	+	+	+	-	+	+	+
$\{\bar{w}^3\}$	+	+	-	+	+	+	+	+	+	+
$\{\bar{y}^4\}$	+	+	+	-	+	+	-	+	+	+
$\{\bar{w}^4\}$	+	+	+	-	+	+	+	+	+	+
$\{\bar{y}^5\}$	+	+	+	+	-	+	-	+	+	+
$\{\bar{w}^5\}$	+	+	+	+	-	+	+	+	+	+
$\{\bar{y}^6\}$	+	+	+	+	+	-	-	+	+	+
$\{\bar{w}^6\}$	+	+	+	+	+	-	+	+	+	+
$\{\bar{\psi}^{1/2/3/4/5(*)}\}$ $/\{\bar{\eta}^{1(*)}\}$	+	+	+	+	+	+	-	-	+	+
$\{\bar{\eta}^{2,3(*)}\}$	+	+	+	+	+	+	+	-	+	+
$\{\bar{\phi}^{1,2(*)}\}$	+	+	+	+	+	+	+	+	-	+
$\{\bar{\phi}^{3,4(*)}\}$	-	+	+	+	+	+	+	+	-	+
$\{\bar{\phi}^{5,6(*)}\}$	-	+	+	+	+	+	+	+	+	-
$\{\bar{\phi}^{7,8(*)}\}$	+	+	+	+	+	+	+	+	+	-

TABLE 5.4: *Conditions on GGSO coefficients for survival of the on-shell vectorial tachyons* $\{\bar{\lambda}^i\}\,|e_1\rangle$. *We have made use of the combination* $\tilde{x} = b_1+b_2+b_3 = \{\psi^\mu, \chi^{1,\ldots,6} \mid \bar{\psi}^{1,2,3,4,5}, \bar{\eta}^{1,2,3}\}$, *which will be discussed more in the next section.*

Sector	$C\left[\begin{smallmatrix} e_1+z_1 \\ e_2 \end{smallmatrix}\right]$	$C\left[\begin{smallmatrix} e_1+z_1 \\ e_3 \end{smallmatrix}\right]$	$C\left[\begin{smallmatrix} e_1+z_1 \\ e_4 \end{smallmatrix}\right]$	$C\left[\begin{smallmatrix} e_1+z_1 \\ e_5 \end{smallmatrix}\right]$	$C\left[\begin{smallmatrix} e_1+z_1 \\ e_6 \end{smallmatrix}\right]$	$C\left[\begin{smallmatrix} e_1+z_1 \\ b_1 \end{smallmatrix}\right]$	$C\left[\begin{smallmatrix} e_1+z_1 \\ \tilde{x} \end{smallmatrix}\right]$	$C\left[\begin{smallmatrix} e_1+z_1 \\ z_2 \end{smallmatrix}\right]$
$\|e_1+z_1\rangle$	+	+	+	+	+	+	+	+

TABLE 5.5: *Conditions on GGSO coefficients for survival of the on-shell tachyons* $|e_1+z_1\rangle$

Sector	$C\left[\begin{smallmatrix} e_1+z_2 \\ e_2 \end{smallmatrix}\right]$	$C\left[\begin{smallmatrix} e_1+z_2 \\ e_3 \end{smallmatrix}\right]$	$C\left[\begin{smallmatrix} e_1+z_2 \\ e_4 \end{smallmatrix}\right]$	$C\left[\begin{smallmatrix} e_1+z_2 \\ e_5 \end{smallmatrix}\right]$	$C\left[\begin{smallmatrix} e_1+z_2 \\ e_6 \end{smallmatrix}\right]$	$C\left[\begin{smallmatrix} e_1+z_2 \\ b_1 \end{smallmatrix}\right]$	$C\left[\begin{smallmatrix} e_1+z_2 \\ \tilde{x} \end{smallmatrix}\right]$	$C\left[\begin{smallmatrix} e_1+z_2 \\ z_1 \end{smallmatrix}\right]$
$\|e_1+z_2\rangle$	+	+	+	+	+	+	+	+

TABLE 5.6: *Conditions on GGSO coefficients for survival of the on-shell tachyons* $|e_1+z_2\rangle$.

Tachyons of Conformal Weight $(-\frac{1}{4}, -\frac{1}{4})$

Carrying on up the mass levels we have $(-\frac{1}{4}, -\frac{1}{4})$ in which vectorial tachyons arise from 15 sectors: $\{\bar{\lambda}^i\}\,|e_i+e_j\rangle$, $i \neq j = 1,...,6$ and spinorial tachyons arise from 30 sectors: $|e_i+e_j+z_1\rangle$ and $|e_i+e_j+z_2\rangle$. Again, we will present the conditions on the survival of $\{\bar{\lambda}^i\}\,|e_1+e_2\rangle$, $|e_1+e_2+z_1\rangle$ and $|e_1+e_2+z_2\rangle$ in Tables 5.7, 5.8 and 5.9 below and note that the other sectors with other e_i combinations are easily obtainable from these.

Tachyons of Conformal Weight $(-\frac{1}{8}, -\frac{1}{8})$

The final mass level we obtain on-shell tachyons from is $(-\frac{1}{8}, -\frac{1}{8})$, where vectorial tachyons arise from 20 sectors: $\{\bar{\lambda}^i\}\,|e_i+e_j+e_k\rangle$, $i \neq j \neq k = 1,...,6$ and spinorial tachyons arise

$\|e_1+e_2\rangle$ **Oscillators**	$C\left[\begin{smallmatrix}e_1+e_2\\ \tilde{S}\end{smallmatrix}\right]$	$C\left[\begin{smallmatrix}e_1+e_2\\ e_3\end{smallmatrix}\right]$	$C\left[\begin{smallmatrix}e_1+e_2\\ e_4\end{smallmatrix}\right]$	$C\left[\begin{smallmatrix}e_1+e_2\\ e_5\end{smallmatrix}\right]$	$C\left[\begin{smallmatrix}e_1+e_2\\ e_6\end{smallmatrix}\right]$	$C\left[\begin{smallmatrix}e_1+e_2\\ b_1\end{smallmatrix}\right]$	$C\left[\begin{smallmatrix}e_1+e_2\\ \tilde{x}\end{smallmatrix}\right]$	$C\left[\begin{smallmatrix}e_1+e_2\\ z_1\end{smallmatrix}\right]$	$C\left[\begin{smallmatrix}e_1+e_2\\ z_2\end{smallmatrix}\right]$
$\{\bar{y}^3\}$	+	-	+	+	+	-	+	+	+
$\{\bar{w}^3\}$	+	-	+	+	+	+	+	+	+
$\{\bar{y}^4\}$	+	+	-	+	+	-	+	+	+
$\{\bar{w}^4\}$	+	+	-	+	+	+	+	+	+
$\{\bar{y}^5\}$	+	+	+	-	+	-	+	+	+
$\{\bar{w}^5\}$	+	+	+	-	+	+	+	+	+
$\{\bar{y}^6\}$	+	+	+	+	-	-	+	+	+
$\{\bar{w}^6\}$	+	+	+	+	-	+	+	+	+
$\{\bar{\psi}^{1/\ldots/5(*)}\}$ $/\{\bar{\eta}^{1(*)}\}$	+	+	+	+	+	-	-	+	+
$\{\bar{\eta}^{2,3(*)}\}$	+	+	+	+	+	+	-	+	+
$\{\bar{\phi}^{1,2(*)}\}$	+	+	+	+	+	+	+	-	+
$\{\bar{\phi}^{3,4(*)}\}$	-	+	+	+	+	+	+	-	+
$\{\bar{\phi}^{5,6(*)}\}$	-	+	+	+	+	+	+	+	-
$\{\bar{\phi}^{7,8(*)}\}$	+	+	+	+	+	+	+	+	-

TABLE 5.7: *Conditions on GGSO coefficients for survival of the on-shell vectorial tachyons* $\{\bar{\lambda}^i\}\,|e_1+e_2\rangle$. *We have made use of the combination* $\tilde{x} = b_1+b_2+b_3 = \{\psi^\mu, \chi^{1,\ldots,6} \mid \bar{\psi}^{1,2,3,4,5}, \bar{\eta}^{1,2,3}\}$, *which will be discussed more in the next section.*

Sector	$C\left[\begin{smallmatrix}e_1+e_2+z_1\\ e_3\end{smallmatrix}\right]$	$C\left[\begin{smallmatrix}e_1+e_2+z_1\\ e_4\end{smallmatrix}\right]$	$C\left[\begin{smallmatrix}e_1+e_2+z_1\\ e_5\end{smallmatrix}\right]$	$C\left[\begin{smallmatrix}e_1+e_2+z_1\\ e_6\end{smallmatrix}\right]$	$C\left[\begin{smallmatrix}e_1+e_2+z_1\\ b_1\end{smallmatrix}\right]$	$C\left[\begin{smallmatrix}e_1+e_2+z_1\\ \tilde{x}\end{smallmatrix}\right]$	$C\left[\begin{smallmatrix}e_1+e_2+z_1\\ z_2\end{smallmatrix}\right]$
$\|e_1+e_2+z_1\rangle$	+	+	+	+	+	+	+

TABLE 5.8: *Conditions on GGSO coefficients for survival of the on-shell tachyons* $|e_1+e_2+z_1\rangle$.

Sector	$C\left[\begin{smallmatrix}e_1+e_2+z_2\\ e_3\end{smallmatrix}\right]$	$C\left[\begin{smallmatrix}e_1+e_2+z_2\\ e_4\end{smallmatrix}\right]$	$C\left[\begin{smallmatrix}e_1+e_2+z_2\\ e_5\end{smallmatrix}\right]$	$C\left[\begin{smallmatrix}e_1+e_2+z_2\\ e_6\end{smallmatrix}\right]$	$C\left[\begin{smallmatrix}e_1+e_2+z_2\\ b_1\end{smallmatrix}\right]$	$C\left[\begin{smallmatrix}e_1+e_2+z_2\\ \tilde{x}\end{smallmatrix}\right]$	$C\left[\begin{smallmatrix}e_1+e_2+z_2\\ z_1\end{smallmatrix}\right]$
$\|e_1+e_2+z_2\rangle$	+	+	+	+	+	+	+

TABLE 5.9: *Conditions on GGSO coefficients for survival of the on-shell tachyons* $|e_1+e_2+z_2\rangle$.

from 40 sectors: $|e_i+e_j+e_k+z_1\rangle$ and $|e_i+e_j+e_k+z_2\rangle$. We present the conditions on the survival of $\{\bar{\lambda}^i\}\,|e_1+e_2+e_3\rangle$, $|e_1+e_2+e_3+z_1\rangle$ and $|e_1+e_2+e_3+z_2\rangle$ in the Tables 5.10, 5.11 and 5.12 below and note again that the conditions for other sectors with other e_i combinations are easily obtainable from these.

Using this structure of the conditions on the GGSO phases for the survival of tachyonic sectors at each mass level our computer algorithm runs through and checks whether any configuration of the phases that leaves the tachyon in the spectrum is satisfied. If none are satisfied then all 126 are projected and the model is retained for further analysis.

5.4 Massless Sectors

Having dealt with the $M_L^2 = M_R^2 < 0$ level-matched sectors we turn our attention to the more familiar discussion of the structure of the massless sectors $M_L^2 = M_R^2 = 0$ in this section. Although some aspects of the massless spectrum look similar to the supersymmetric case, the structure of our $\tilde{S}$-models are very different. In particular, we can contrast our models with those in which supersymmetry is spontaneously broken (by a GGSO phase) where in

$\lvert e_1+e_2+e_3\rangle$ **Oscillator**	$C\left[\begin{smallmatrix}e_1+e_2+e_3\\ \tilde{S}\end{smallmatrix}\right]$	$C\left[\begin{smallmatrix}e_1+e_2+e_3\\ e_4\end{smallmatrix}\right]$	$C\left[\begin{smallmatrix}e_1+e_2+e_3\\ e_5\end{smallmatrix}\right]$	$C\left[\begin{smallmatrix}e_1+e_2+e_3\\ e_6\end{smallmatrix}\right]$	$C\left[\begin{smallmatrix}e_1+e_2+e_3\\ \tilde{x}\end{smallmatrix}\right]$	$C\left[\begin{smallmatrix}e_1+e_2+e_3\\ z_1\end{smallmatrix}\right]$	$C\left[\begin{smallmatrix}e_1+e_2+e_3\\ z_2\end{smallmatrix}\right]$
$\{\bar{y}^4/\bar{w}^4\}$	+	-	+	+	+	+	+
$\{\bar{y}^5/\bar{w}^5\}$	+	+	-	+	+	+	+
$\{\bar{y}^6/\bar{w}^6\}$	+	+	+	-	+	+	+
$\{\bar{\psi}^{1/\ldots/5}\}$ $/\{\bar{\eta}^{1/2/3(*)}\}$	+	+	+	+	-	+	+
$\{\bar{\phi}^{1,2(*)}\}$	+	+	+	+	+	-	+
$\{\bar{\phi}^{3,4(*)}\}$	-	+	+	+	+	-	+
$\{\bar{\phi}^{5,6(*)}\}$	-	+	+	+	+	+	-
$\{\bar{\phi}^{7,8(*)}\}$	+	+	+	+	+	+	-

TABLE 5.10: *Conditions on GGSO coefficients for survival of the on-shell vectorial tachyons* $\{\bar{\lambda}^i\}\,\lvert e_1+e_2+e_3\rangle$.

Sector	$C\left[\begin{smallmatrix}e_1+e_2+e_3+z_1\\ e_4\end{smallmatrix}\right]$	$C\left[\begin{smallmatrix}e_1+e_2+e_3+z_1\\ e_5\end{smallmatrix}\right]$	$C\left[\begin{smallmatrix}e_1+e_2+e_3+z_1\\ e_6\end{smallmatrix}\right]$	$C\left[\begin{smallmatrix}e_1+e_2+e_3+z_1\\ \tilde{x}\end{smallmatrix}\right]$	$C\left[\begin{smallmatrix}e_1+e_2+e_3+z_1\\ z_2\end{smallmatrix}\right]$
$\lvert e_1+e_2+e_3+z_1\rangle$	+	+	+	+	+

TABLE 5.11: *Conditions on GGSO coefficients for survival of the on-shell tachyons* $\lvert e_1+e_2+e_3+z_1\rangle$.

Sector	$C\left[\begin{smallmatrix}e_1+e_2+e_3+z_2\\ e_4\end{smallmatrix}\right]$	$C\left[\begin{smallmatrix}e_1+e_2+e_3+z_2\\ e_5\end{smallmatrix}\right]$	$C\left[\begin{smallmatrix}e_1+e_2+e_3+z_2\\ e_6\end{smallmatrix}\right]$	$C\left[\begin{smallmatrix}e_1+e_2+e_3+z_2\\ \tilde{x}\end{smallmatrix}\right]$	$C\left[\begin{smallmatrix}e_1+e_2+e_3+z_2\\ z_1\end{smallmatrix}\right]$
$\lvert e_1+e_2+e_3+z_2\rangle$	+	+	+	+	+

TABLE 5.12: *Conditions on GGSO coefficients for survival of the on-shell tachyons* $\lvert e_1+e_2+e_3+z_2\rangle$.

general some parts of the spectrum remain supersymmetric. This was, for example, demonstrated in [109] in terms of invariant orbits of the partition function for orbifold models with spontaneously broken supersymmetry. Similarly, our models are very different than those of the broken supersymmetry models discussed in [110] where observable spinorial sectors of the models still exhibit a supersymmetric–like structure, *i.e.* in these sectors the bosonic and fermionic states only differ by their charges under some $U(1)$ symmetries that are broken at a high scale.

As we explore this new structure in the massless spectrum we will see that the role of the $\tilde{S}$-map is of central importance. Further to this, we will also uncover the importance of a vector combination $\tilde{x}$ which induces another interesting map. Without the presence of the supersymmetry generator S we must also handle a number of extra massless sectors which would not arise in supersymmetric setups due to the GGSO projections induced by S.

Observable Sectors

The chiral spinorial **16**/$\overline{\mathbf{16}}$ representations arise from the 48 sectors (16 from each orbifold plane)

$$\begin{aligned} B^{(1)}_{pqrs} &= b_1 + pe_3 + qe_4 + re_5 + se_6 \\ &= \{\psi^\mu, \chi^{1,2}, (1-p)y^3\bar{y}^3, pw^3\bar{w}^3, (1-q)y^4\bar{y}^4, qw^4\bar{w}^4, \\ &\quad (1-r)y^5\bar{y}^5, rw^5\bar{w}^5, (1-s)y^6\bar{y}^6, sw^6\bar{w}^6, \bar{\eta}^1, \bar{\psi}^{1,\ldots,5}\} \\ B^{(2)}_{pqrs} &= b_2 + pe_1 + qe_2 + re_5 + se_6 \\ B^{(3)}_{pqrs} &= b_3 + pe_1 + qe_2 + re_3 + se_4 \end{aligned} \tag{5.14}$$

where $p, q, r, s = 0, 1$ account for all combinations of shift vectors of the internal fermions $\{y^i, w^i \mid \bar{y}^i, \bar{w}^i\}$. As in previous classifications, we can now write down generic algebraic equations to determine the number **16** and $\overline{\mathbf{16}}$, N_{16} and $N_{\overline{16}}$, as a function of the GGSO coefficients. To do this we first utilize the following projectors to determine which of the 48 spinorial sectors survive

$$\begin{aligned} P^1_{pqrs} &= \frac{1}{2^4}\prod_{i=1,2}\left(1 - C\left[\begin{smallmatrix} B^1_{pqrs} \\ e_i \end{smallmatrix}\right]^*\right)\prod_{a=1,2}\left(1 - C\left[\begin{smallmatrix} B^1_{pqrs} \\ z_a \end{smallmatrix}\right]^*\right) \\ P^2_{pqrs} &= \frac{1}{2^4}\prod_{i=3,4}\left(1 - C\left[\begin{smallmatrix} B^2_{pqrs} \\ e_i \end{smallmatrix}\right]^*\right)\prod_{a=1,2}\left(1 - C\left[\begin{smallmatrix} B^2_{pqrs} \\ z_a \end{smallmatrix}\right]^*\right) \\ P^3_{pqrs} &= \frac{1}{2^4}\prod_{i=5,6}\left(1 - C\left[\begin{smallmatrix} B^3_{pqrs} \\ e_i \end{smallmatrix}\right]^*\right)\prod_{a=1,2}\left(1 - C\left[\begin{smallmatrix} B^3_{pqrs} \\ z_a \end{smallmatrix}\right]^*\right) \end{aligned} \tag{5.15}$$

where, we recall that the vector $z_2 = \{\overline{\phi}^{5,6,7,8}\}$ is the combination defined in eq. (5.10). Then we define the chirality phases

$$\begin{aligned} X^1_{pqrs} &= -C\left[\begin{smallmatrix} B^1_{pqrs} \\ b_2+(1-r)e_5+(1-s)e_6 \end{smallmatrix}\right]^* \\ X^2_{pqrs} &= -C\left[\begin{smallmatrix} B^2_{pqrs} \\ b_1+(1-r)e_5+(1-s)e_6 \end{smallmatrix}\right]^* \\ X^3_{pqrs} &= -C\left[\begin{smallmatrix} B^3_{pqrs} \\ b_1+(1-r)e_3+(1-s)e_4 \end{smallmatrix}\right]^* \end{aligned} \tag{5.16}$$

to determine whether a sector will give rise to a **16** or a $\overline{\mathbf{16}}$. With these definitions we can write compact expressions for N_{16} and $N_{\overline{16}}$

$$\begin{aligned} N_{16} &= \frac{1}{2}\sum_{\substack{A=1,2,3 \\ p,q,r,s=0,1}} P^A_{pqrs}\left(1 + X^A_{pqrs}\right) \\ N_{\overline{16}} &= \frac{1}{2}\sum_{\substack{A=1,2,3 \\ p,q,r,s=0,1}} P^A_{pqrs}\left(1 - X^A_{pqrs}\right). \end{aligned} \tag{5.17}$$

Up to here, these equations are familiar from previous supersymmetric classifications. However, there is a fundamental difference from the supersymmetric case where $B^{1,2,3}$, along with all model sectors, appear in supermultiplets with superpartners obtained through the addition of S, which exchanges spacetime bosons with spacetime fermions but leaves the

gauge group representations unchanged. In our set-up, the fermionic $B^{1,2,3}$ sectors have no such bosonic sector counterparts. Indeed, the addition of our basis vector $\tilde{S}$ would give rise to massive states with non-trivial representations under the hidden sector gauge group. As mentioned above, we can also compare with the broken supersymmetry models of [110] where the bosonic counterparts of $B^{1,2,3}$ only differ from their fermionic superpartners by their charges under some $U(1)$ symmetries that are broken at a high scale.

A further new important feature of our construction is the inclusion of the vector

$$\tilde{x} = b_1 + b_2 + b_3 \tag{5.18}$$

which we name in analogy to the x–vector from the supersymmetric classifications [18, 90–92, 97–104]. We note that $\tilde{x}$ is the same as the vector $S + x$ which arises in supersymmetric models. In these models, the states from the x–sector enhance the observable gauge symmetry from $SO(10)$ to E_6, so $S+x$ arises when such an enhancement is present. The vector $\tilde{x}$ is important in our models since it plays the role of mapping between the observable spinorial and vectorial representations of $SO(10)$, as well as a map between bosonic and fermionic states. More specifically, the $\tilde{x}$–vector maps sectors that produce spacetime fermions in the spinorial representation of $SO(10)$, from which the Standard Model matter states are obtained, to sectors that produce spacetime bosons in its vectorial representation, from which the Standard Model Higgs state is obtained. Thus, the $\tilde{x}$–map induces simultaneously the fermion–boson map of the S–vector, as well as the spinor–vector map of the x–vector.

Without S to provide the simple symmetry at each mass level between bosons and fermions the question of the relationship between bosons and fermions is unclear. It appears that the structure is controlled in some sense by the $\tilde{S}$-map and the $\tilde{x}$-map taking us between mass levels as both these maps often change the mass level of the sector they act on. We also note that the $\tilde{x}$–sector also affects the observable spectrum since its presence in the Hilbert space results in an extra 4 **16**'s and $\overline{\mathbf{16}}$'s of $SO(10)$.The $\tilde{x}$–sector corresponds to the sector producing the fermionic superpartners of the states from the x–sector, *i.e.* $S + x$, which enhance the $SO(10)$ symmetry to E_6. The $\tilde{x}$–sector, therefore, gives rise to the fermionic superpartners of the spacetime vector bosons from the x–sector, which are in fact absent from the spectrum.

Vectorial Sectors

As mentioned above, the vector $\tilde{x}$ in (5.18) maps between the spinorial sectors $B^{1,2,3}_{pqrs}$ and vectorial sectors:

$$\begin{aligned} V^{(1)}_{pqrs} &= B^{(1)}_{pqrs} + \tilde{x} \\ &= b_2 + b_3 + pe_3 + qe_4 + re_5 + se_6 \\ &= \{\chi^{3,4,5,6}, (1-p)y^3\bar{y}^3, pw^3\bar{w}^3, (1-q)y^4\bar{y}^4, qw^4\bar{w}^4, \\ &\quad (1-r)y^5\bar{y}^5, rw^5\bar{w}^5, (1-s)y^6\bar{y}^6, sw^6\bar{w}^6, \bar{\eta}^{2,3}\} \\ V^{(2)}_{pqrs} &= B^{(2)}_{pqrs} + \tilde{x} \\ V^{(3)}_{pqrs} &= B^{(3)}_{pqrs} + \tilde{x} \end{aligned} \tag{5.19}$$

The observable vectorial **10** representations of $SO(10)$ arise when the right moving oscillator is a $\overline{\psi}^{a(*)}$, $a = 1, ..., 5$. To determine the number of such observable vectorial sectors we use

the projectors

$$\begin{aligned} R^{(1)}_{pqrs} &= \frac{1}{2^4}\prod_{i=1,2}\left(1+C\left[\begin{smallmatrix} e_i \\ V^{(1)}_{pqrs}\end{smallmatrix}\right]\right)\prod_{a=1,2}\left[1+C\left[\begin{smallmatrix} z_a \\ V^{(1)}_{pqrs}\end{smallmatrix}\right]\right) \\ R^{(2)}_{pqrs} &= \frac{1}{2^4}\prod_{i=3,4}\left(1+C\left[\begin{smallmatrix} e_i \\ V^{(2)}_{pqrs}\end{smallmatrix}\right]\right)\prod_{a=1,2}\left(1+C\left[\begin{smallmatrix} z_a \\ V^{(2)}_{pqrs}\end{smallmatrix}\right]\right) \\ R^{(3)}_{pqrs} &= \frac{1}{2^4}\prod_{i=5,6}\left(1+C\left[\begin{smallmatrix} e_i \\ V^{(3)}_{pqrs}\end{smallmatrix}\right]\right)\prod_{a=1,2}\left(1+C\left[\begin{smallmatrix} z_a \\ V^{(3)}_{pqrs}\end{smallmatrix}\right]\right). \end{aligned} \tag{5.20}$$

Using these we can write the number of vectorial **10**'s arising from these sectors as

$$N_{10} = \sum_{\substack{A=1,2,3 \\ p,q,r,s=0,1}} R^A_{pqrs}. \tag{5.21}$$

Further to these observable vectorials arising from $V^{1,2,3}$ there are the additional states arising for the other choices of oscillator $\bar{y}^i_{NS}, \bar{w}^i_{NS}, \bar{\phi}^{1,2}, \bar{\phi}^{3,4}, \bar{\phi}^{5,6}, \bar{\phi}^{7,8}$, which only transform under the hidden group.

In contrast to the supersymmetric case, our models come with additional vectorial sectors, which can give rise to states transforming under the observable gauge group as well as the hidden. Firstly we observe 4 additional sectors that can give rise to vectorial states transforming under both the observable and the hidden or solely the hidden. These sectors are

$$\tilde{V} = \{\{\bar{\lambda}^i\}|\tilde{S}\rangle, \{\bar{\lambda}^i\}|\tilde{S}+z_1\rangle, \{\bar{\lambda}^i\}|\tilde{S}+z_2\rangle, \{\bar{\lambda}^i\}|\tilde{S}+z_1+z_2\rangle\} \tag{5.22}$$

which are spacetime fermions. There are two cases to distinguish when one of these sectors is present:

- $\{\bar{y}^i/\bar{w}^i\}|\tilde{V}\rangle$ which are charged under the hidden sector only.
- $\{\bar{\psi}^{1,\ldots,5}, \bar{\eta}^{1,2,3}, \bar{\phi}_{NS}\}|\tilde{V}\rangle$ with $\bar{\phi}_{NS}$ being the four Neveu-Schwarz oscillators such that $\bar{\phi}_{NS} \cap \tilde{V} = \emptyset$. These transform in mixed representations of the observable and hidden sectors which means we should analyse them further. We realise that the condition for one of these to remain in the spectrum is:

$$C\left[\begin{smallmatrix} \tilde{V} \\ e_i\end{smallmatrix}\right] = -1, \quad \forall\, i \in \{1,2,3,4,5,6\} \tag{5.23}$$

  for one of the $\tilde{V}$. In ref. [1] it was suggested that such states appearing in these models may be instrumental in implementing electroweak symmetry breaking by hidden sector condensates.

Similar to the $\tilde{x}$–sector, it is interesting to compare the $\tilde{S}$–sector with the S–sector in supersymmetric models.The S–sector in the supersymmetric models produces the spacetime fermionic superpartners of the states from the NS–sector, *i.e.* it gives rise to the gauginos. The $\tilde{S}$–sector gives rise to spacetime fermions that could transform as, *e.g.* electroweak doublets and triplets, but also transforms as doublets of the hidden gauge group, due to the $S-\tilde{S}$–map noted in Section 5.1.In this respect the $\tilde{S}$–models exhibit a sort of split supersymmetry, in the sense that the states from the sectors $B_{1,2,3}$ are massive, but the sector that produces the would–be gauginos, *i.e.* $\tilde{S}$, still produces massless states transforming

under the observable gauge symmetry. It will be of interest to explore how this phenomenon affects the phenomenological characteristics of the models.

Finally, there are further vectorials that may be observable or hidden arising from the 15 sectors

$$\gamma^{k=1,...,15} = \{\bar{\lambda}^i\}\,|e_i + e_j + e_k + e_l\rangle \tag{5.24}$$

for $i \neq j \neq k \neq l = 1, ..., 6$. We note that these sectors can give rise to vectorial **10**'s when the oscillators $\bar{\psi}^a$, $a = 1, ..., 5$, are present. In this case, the projector is

$$P_{\gamma^k} = \frac{1}{2^5}\prod_{i=m,n}\left(1 + C\left[\begin{smallmatrix}\gamma^k\\ e_i\end{smallmatrix}\right]\right)\prod_{a=1,2}\left(1 + C\left[\begin{smallmatrix}\gamma^k\\ z_a\end{smallmatrix}\right]\right)\left(1 - C\left[\begin{smallmatrix}\gamma^k\\ \tilde{x}\end{smallmatrix}\right]\right) \tag{5.25}$$

where $m \neq n \neq i \neq j \neq k \neq l$. We can count the number of such sectors through the expression

$$N_\gamma^{\{\bar{\psi},\bar{\eta}\}} = \sum_{k=1}^{15} P_{\gamma^k}. \tag{5.26}$$

These additional vectorials can evidently play a role in the phenomenology of our models, so their couplings and charge contributions must be considered carefully for specific models. We can note that γ^k will not couple at leading order to the observable spinorial representations due to their additional charges, and so at leading order the only vectorial 10 representations to generate realistic Standard Model fermion mass spectrum, remain those from $V^{1,2,3}$.

Hidden Sectors

We find that there are a relatively large number of hidden massless sectors in our model, which is another effect of the $\tilde{S}$-map we have chosen since its right-moving complex fermions generate representations of the hidden group.

Firstly, we can identify 96 spinorial sectors that give rise to spacetime bosons arising through the addition of z_1 or z_2 onto the vectorial sectors $V^{1,2,3}$

$$\begin{aligned}
H^{(1)}_{pqrs} &= V^{(1)}_{pqrs} + z_1\\
H^{(2)}_{pqrs} &= V^{(2)}_{pqrs} + z_1\\
H^{(3)}_{pqrs} &= V^{(3)}_{pqrs} + z_1\\
H^{(4)}_{pqrs} &= V^{(1)}_{pqrs} + z_2\\
H^{(5)}_{pqrs} &= V^{(2)}_{pqrs} + z_2\\
H^{(6)}_{pqrs} &= V^{(3)}_{pqrs} + z_2
\end{aligned} \tag{5.27}$$

which evidently transform under the hidden $SO(4)^4$ only. A further four groups of 48 sectors are generated through the addition of the combinations $\{\tilde{S}, \tilde{S} + z_1, \tilde{S} + z_2, \tilde{S} + z_1 + z_2\}$ which

give rise to spacetime fermionic hidden sectors

$$\begin{aligned}
H^{(7)}_{pqrs} &= \tilde{S} + V^{(1)}_{pqrs} \\
H^{(8)}_{pqrs} &= \tilde{S} + V^{(2)}_{pqrs} \\
H^{(9)}_{pqrs} &= \tilde{S} + V^{(3)}_{pqrs} \\
H^{(10)}_{pqrs} &= \tilde{S} + V^{(1)}_{pqrs} + z_1 \\
H^{(11)}_{pqrs} &= \tilde{S} + V^{(2)}_{pqrs} + z_1 \\
H^{(12)}_{pqrs} &= \tilde{S} + V^{(3)}_{pqrs} + z_1 \\
H^{(13)}_{pqrs} &= \tilde{S} + V^{(1)}_{pqrs} + z_2 \\
H^{(14)}_{pqrs} &= \tilde{S} + V^{(2)}_{pqrs} + z_2 \\
H^{(15)}_{pqrs} &= \tilde{S} + V^{(3)}_{pqrs} + z_2 \\
H^{(16)}_{pqrs} &= \tilde{S} + V^{(1)}_{pqrs} + z_1 + z_2 \\
H^{(17)}_{pqrs} &= \tilde{S} + V^{(2)}_{pqrs} + z_1 + z_2 \\
H^{(18)}_{pqrs} &= \tilde{S} + V^{(3)}_{pqrs} + z_1 + z_2
\end{aligned} \tag{5.28}$$

Essentially we see that by adding on the combinations $\tilde{h}_n = \{z_1, z_2, \tilde{S}, \tilde{S}+z_1, \tilde{S}+z_2, \tilde{S}+z_1+z_2\}$ we generate the 6 ways of having 2 doublet representations of the four hidden $SO(4)$ groups.

There are additional hidden sectors, on top of those counted by N_H, that don't live on the orbifold planes. These 30 sectors are

$$\delta^{1,\ldots,30} = \begin{cases} e_i + e_j + e_k + e_l + z_1 \\ e_i + e_j + e_k + e_l + z_2 \end{cases} \tag{5.29}$$

for $i \neq j \neq k \neq l = 1, ..., 6$. Similar to (5.22), (5.24) these are examples of sectors which are not found in supersymmetric models since the S–vector would project them out.

Knowing the number of hidden sectors will mainly be useful when looking at the size of the massless coefficient in the q-expansion of the partition function, which is equivalent to a counting of the number of massless states. We will return to this in Section 5.5.

5.5 Partition Function and Cosmological Constant

The partition function of string models encapsulates most information one knows about its structure, symmetries and spectrum. Thus to fully understand our model it is essential to get a handle on the calculation and form of its partition function. The analysis of the partition function is particularly instrumental in non–supersymmetric constructions since it gives a complementary tool to count the total number of massless states, and its integration over the fundamental domain corresponds to the cosmological constant.

For free fermionic models, the partition function can be calculated using techniques developed in Section 2.5 and Chapter 4. In terms of the basis vectors, the partition function is given

by

$$Z = \int_{\mathcal{F}} \frac{d^2\tau}{\tau_2^2}\, Z_B \sum_{Sp.Str.} C\binom{\alpha}{\beta} \prod_f Z\left[\begin{smallmatrix}\alpha(f)\\ \beta(f)\end{smallmatrix}\right], \tag{5.30}$$

where $d^2\tau/\tau_2^2$ is the modular invariant measure. The expression (4.63) specifically represents the one-loop vacuum energy of our theory at the fermionic point and so we may refer to it as the cosmological constant Λ. As we have seen the part of this expression corresponding to the worldsheet fermions can be re-expressed in a compact and insightful way using methods developed in Section 4.1. Implementing these for this model results in the fermionic partition

$$\begin{aligned} Z_F =& \frac{1}{\eta^{10}\bar{\eta}^{22}} \frac{1}{2^2} \sum_{\substack{a,k\\ b,l}} \frac{1}{2^6} \sum_{\substack{H_i\\ G_i}} \frac{1}{2^4} \sum_{\substack{h_i,P_i\\ g_i,Q_i}} (-1)^{\Psi\left[\begin{smallmatrix} a & k & H_i & h_i & P_i\\ b & l & G_i & g_i & Q_i\end{smallmatrix}\right]} \\ &\times \vartheta\left[\begin{smallmatrix}a\\ b\end{smallmatrix}\right]_{\psi^\mu} \vartheta\left[\begin{smallmatrix}a+h_1\\ b+g_1\end{smallmatrix}\right]_{\chi^{12}} \vartheta\left[\begin{smallmatrix}a+h_2\\ b+g_2\end{smallmatrix}\right]_{\chi^{34}} \vartheta\left[\begin{smallmatrix}a-h_1-h_2\\ b-g_1-g_2\end{smallmatrix}\right]_{\chi^{56}} \\ &\times Z^{(1)}_{2,2}\left[\begin{smallmatrix}H_1\\ G_1\end{smallmatrix}\middle|\begin{smallmatrix}h_1\\ g_1\end{smallmatrix}\right] \times Z^{(2)}_{2,2}\left[\begin{smallmatrix}H_2\\ G_2\end{smallmatrix}\middle|\begin{smallmatrix}h_2\\ g_2\end{smallmatrix}\right] \times Z^{(3)}_{2,2}\left[\begin{smallmatrix}H_3\\ G_3\end{smallmatrix}\middle|\begin{smallmatrix}h_1+h_2\\ g_1+g_2\end{smallmatrix}\right] \\ &\times \bar{\vartheta}\left[\begin{smallmatrix}k\\ l\end{smallmatrix}\right]^5_{\bar{\psi}^{1-5}} \bar{\vartheta}\left[\begin{smallmatrix}k+h_1\\ l+g_1\end{smallmatrix}\right]_{\bar{\eta}^1} \bar{\vartheta}\left[\begin{smallmatrix}k+h_2\\ l+g_2\end{smallmatrix}\right]_{\bar{\eta}^2} \bar{\vartheta}\left[\begin{smallmatrix}k-h_1-h_2\\ l-g_1-g_2\end{smallmatrix}\right]_{\bar{\eta}^3} \\ &\times \bar{\vartheta}\left[\begin{smallmatrix}k+P_1\\ l+Q_1\end{smallmatrix}\right]^2_{\bar{\phi}^{12}} \bar{\vartheta}\left[\begin{smallmatrix}a+P_1\\ b+Q_1\end{smallmatrix}\right]^2_{\bar{\phi}^{34}} \bar{\vartheta}\left[\begin{smallmatrix}a+P_2\\ b+Q_2\end{smallmatrix}\right]^2_{\bar{\phi}^{56}} \bar{\vartheta}\left[\begin{smallmatrix}k+P_2\\ l+Q_2\end{smallmatrix}\right]^2_{\bar{\phi}^{78}}. \end{aligned} \tag{5.31}$$

with the internal lattice given by the usual $\boldsymbol{e}_i$ shifted lattice at the fermionic point

$$\begin{aligned} Z^{(1)}_{2,2}\left[\begin{smallmatrix}H_1 & H_2\\ G_1 & G_2\end{smallmatrix}\middle|\begin{smallmatrix}h_1\\ g_1\end{smallmatrix}\right] &= \left|\vartheta\left[\begin{smallmatrix}H_1\\ G_1\end{smallmatrix}\right] \vartheta\left[\begin{smallmatrix}H_1+h_1\\ G_1+g_1\end{smallmatrix}\right] \vartheta\left[\begin{smallmatrix}H_2\\ G_2\end{smallmatrix}\right] \vartheta\left[\begin{smallmatrix}H_2+h_1\\ G_2+g_1\end{smallmatrix}\right]\right| \\ Z^{(2)}_{2,2}\left[\begin{smallmatrix}H_3 & H_4\\ G_3 & G_4\end{smallmatrix}\middle|\begin{smallmatrix}h_2\\ g_2\end{smallmatrix}\right] &= \left|\vartheta\left[\begin{smallmatrix}H_3\\ G_3\end{smallmatrix}\right] \vartheta\left[\begin{smallmatrix}H_3+h_2\\ G_3+g_2\end{smallmatrix}\right] \vartheta\left[\begin{smallmatrix}H_4\\ G_4\end{smallmatrix}\right] \vartheta\left[\begin{smallmatrix}H_4+h_2\\ G_4+g_2\end{smallmatrix}\right]\right| \\ Z^{(3)}_{2,2}\left[\begin{smallmatrix}H_5 & H_6\\ G_5 & G_6\end{smallmatrix}\middle|\begin{smallmatrix}h_1+h_2\\ g_1+g_2\end{smallmatrix}\right] &= \left|\vartheta\left[\begin{smallmatrix}H_5\\ G_5\end{smallmatrix}\right] \vartheta\left[\begin{smallmatrix}H_5-h_1-h_2\\ G_5-h_1-h_2\end{smallmatrix}\right] \vartheta\left[\begin{smallmatrix}H_6\\ G_6\end{smallmatrix}\right] \vartheta\left[\begin{smallmatrix}H_6-h_1-h_2\\ G_6-h_1-h_2\end{smallmatrix}\right]\right|. \end{aligned} \tag{5.32}$$

It is instructive to look at the effect of the $\tilde{S}$-map on the partition function. Comparing with (4.32) we see that the addition of the $\bar{\phi}^{3-6}$ to S translate to the replacement of $k \to a$ and $l \to b$ in the theta function characteristics corresponding to $\bar{\phi}^{3-6}$. This is significant since this renders the Jacobi identity (A.13) irrelevant and so the partition function is nonzero for all GGSO configurations as expected.

The most practical way to perform the modular integration of the total partition function (5.30) is as presented in Section 4.3 using the expansion of the η and ϑ functions in terms of the modular parameters q and $\bar{q}$. This leads to a series expansion of the one-loop partition function which converges quickly as demonstrated in Figure 5.1 for a set of non-tachyonic GGSO configurations. This provides a nice empirical check for the convergence properties discussed in Section 4.3.

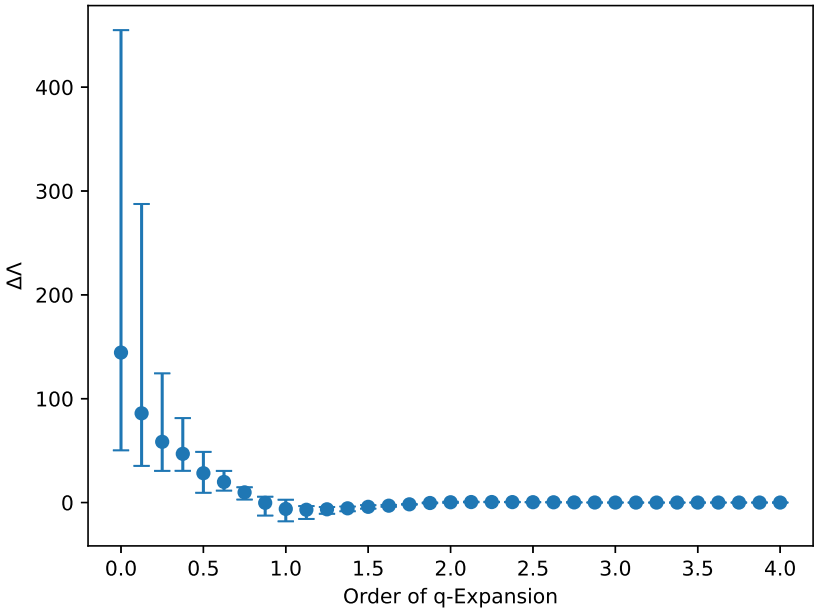

FIGURE 5.1: *The convergence of* Λ *order-by-order in the* q*-expansion, where* $\Delta\Lambda$ *is the difference between* Λ *at a specific order and* Λ *at 4th order. The dots represent the average over a sample of 2000 tachyon-free models and the bars give the maximum deviation from this average.*

As discussed previously, modular invariance constraint $m-n \in \mathbb{Z}$ means that the q-expansion of the partition function (4.65) neatly arranges into the form

$$a_{mn} = \begin{pmatrix} 0 & 0 & a_{-\frac{1}{2}-\frac{1}{2}} & 0 & 0 & 0 & a_{-\frac{1}{2}\frac{1}{2}} & 0 & 0 & 0 \\ 0 & 0 & 0 & a_{-\frac{1}{4}-\frac{1}{4}} & 0 & 0 & 0 & a_{-\frac{1}{4}\frac{3}{4}} & 0 & 0 \\ a_{0-1} & 0 & 0 & 0 & a_{00} & 0 & 0 & 0 & a_{01} & 0 \\ 0 & a_{\frac{1}{4}-\frac{3}{4}} & 0 & 0 & 0 & a_{\frac{1}{4}\frac{1}{4}} & 0 & 0 & 0 & \ddots \\ 0 & 0 & a_{\frac{1}{2}-\frac{1}{2}} & 0 & 0 & 0 & a_{\frac{1}{2}\frac{1}{2}} & 0 & 0 & 0 \\ 0 & 0 & 0 & a_{\frac{3}{4}-\frac{1}{4}} & 0 & 0 & 0 & a_{\frac{3}{4}\frac{3}{4}} & 0 & 0 \\ a_{1-1} & 0 & 0 & 0 & a_{10} & 0 & 0 & 0 & a_{11} & 0 \\ 0 & \ddots & 0 & 0 & 0 & \ddots & 0 & 0 & 0 & \ddots \end{pmatrix} \tag{5.33}$$

i.e. into series of states with $n - m = p \in \mathbb{Z}$. This gives a convenient way to examine the different contributions to the cosmological constant (5.30) and compare the effect of on and off-shell states. We have mentioned previously in Section 4.3 that off-shell contributions to the potential and cosmological constant are in general suppressed compared to the on-shell ones. We can use these models to confirm this is indeed the case as shown in Figure 5.2 where we have chosen a model with a suppressed value for the vacuum energy.

We see that the suppressed value of Λ is due to the cancellation between the large positive contributions from the on-shell states and the negative contributions from the off-shell states. Indeed, in general, we find that for our set of models, the only positive contributions to Λ come from on-shell states and so these states can give us a handle on the expected value of

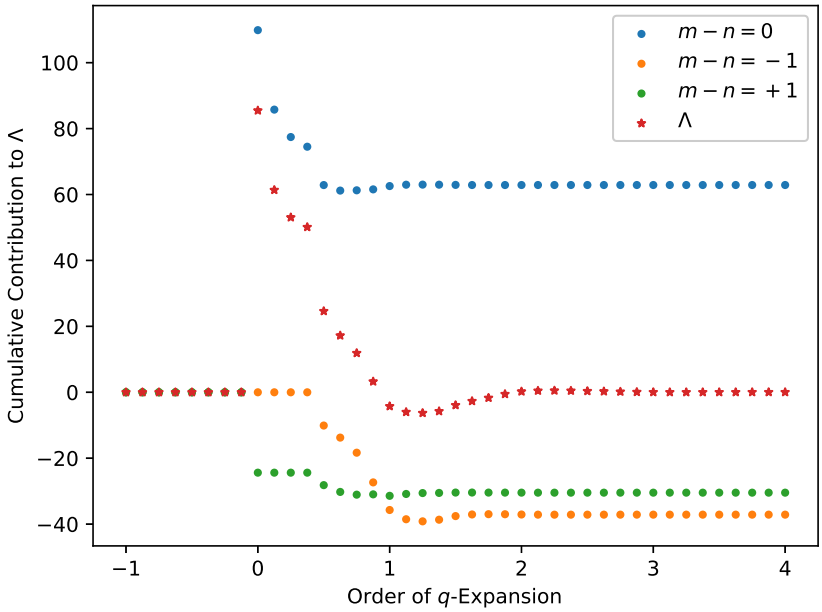

FIGURE 5.2: *A comparison of different contributions to* Λ *for a model with* $\Lambda = 0.03$ *arranged as in (5.33). We see that the large positive contributions of the on-shell states are compensated by the negative contributions of the off-shell states.*

the cosmological constant.

As we have seen in Figure 5.1, for our tachyon-free models, Λ always converges and does so rapidly starting from 2nd order in q and $\bar{q}$. Based on the discussion in Section 4.5 this is a direct consequence of modular invariance which removes the divergent regions of the integration domain. Since all our four-dimensional models are of course modular invariant we expect them to also exhibit misaligned supersymmetry regardless of the unconventional breaking of supersymmetry. This is indeed the case and all models exhibit the oscillatory behaviour of the physical spectrum as shown in Figure 5.3.

The discussion above shows that while for non-supersymmetric theories there is no mechanism which ensures the vanishing of a_{mn} at any allowed level, there is, however, nothing preventing it from happening. It is indeed possible to find models within our classification set-up detailed in Section 5.2 which have $a_{00} = 0$, i.e. $N_b^0 = N_f^0$, at the massless level.

In the analysis of the one-loop potential in [82], no models were found that exhibit $N_b^0 = N_f^0$ at the free fermionic point in the sample explored. Instead, they use techniques developed in Chapter 4 to move away from the free fermionic point by reintroducing the moduli dependence and find models with $N_b^0 = N_f^0$ at other points in moduli space. In our analysis, we stay at the free fermionic point and it turns out that we do find models with $N_b^0 = N_f^0$ and an example model is presented in Section 5.7.

It is convenient to summarise the various contributions to a_{00} in the form of Table 5.13. We use the notation for sectors laid out in Section 5.4. For simplicity, and since we restrict our classification to models with no enhancements, the contributions of vector bosons from sectors $z_1, z_2, z_1 + z_2$ are ignored.

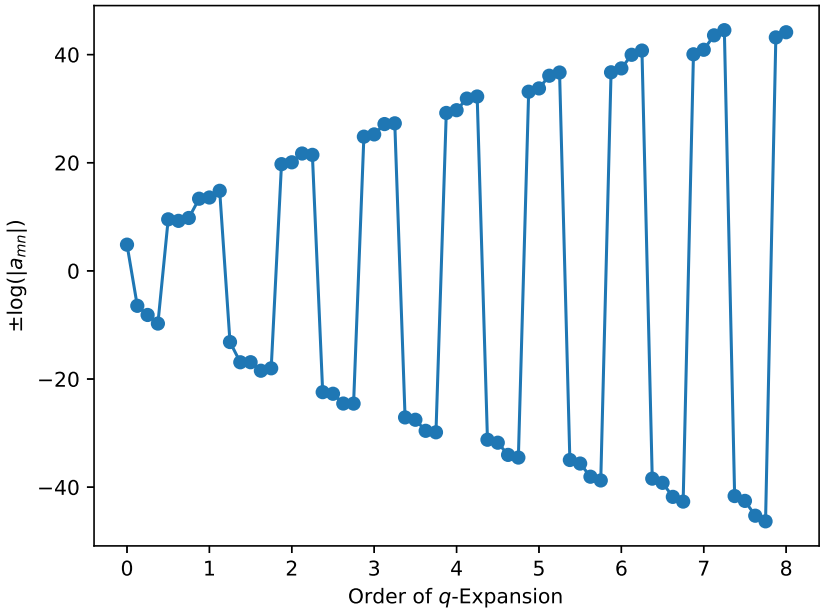

FIGURE 5.3: *The boson-fermion oscillation of misaligned supersymmetry for the on-shell states of one of our models to 8^{th} order in the q-expansion. The overall sign of $\pm\log(|\ a_{mn}\ |)$ is chosen according to the sign of a_{mn}.*

5.6 Results of Classification

Having discussed how to determine key features of the massless spectrum and how to calculate the partition function and cosmological constant for our $\tilde{S}$ -models we can now present some statistics derived from a sample in the space of models. As mentioned in Section 5.2, the space of all models is $2^{66} \sim 10^{19.9}$ and so a complete classification is far beyond the computing power at our disposal. Instead, we explore a sample of 2×10^9 models of which only around 1 in 185 are tachyon-free that we take forward for further analysis. We will start with some results of key aspects of the massless spectrum.

5.6.1 Results for the Massless Spectrum

From our sample of 2×10^9 models we choose 10^7 tachyon-free models and display the results for their $SO(10)$ observable representations. In Figure 5.4 the net chirality, $N_{16} - N_{\overline{16}}$, distribution is displayed and in Figure 5.5 the distribution of their number of vectorial **10** representations is displayed. From Figure 5.5 we see that the large majority of models contain at least one vectorial **10**. The familiar normal distribution also found in all other classifications for the supersymmetric cases is uncovered. This is not surprising since the structure of the fermionic $\mathbf{16}/\overline{\mathbf{16}}$ is unchanged for our models.

In order to see more clearly the statistics from our 2×10^9 sample we display the frequency of $SO(10)$ models as several phenomenological constraints are considered in Table 5.14. These

Sector	$N_b - N_f$	Sector	$N_b - N_f$
$\|NS\rangle$	304	$\{\bar{y}^i_{NS}/\bar{w}^i_{NS}\}\|\tilde{V}\rangle$	-8
$\|B^{1,2,3}\rangle$	-32	$\delta^{1,\ldots,30}$	16
$\|\tilde{x}\rangle$	-256	$\{\bar{\psi}^{a(*)}/\bar{\eta}^{b(*)}\}\|\gamma^{1,\ldots,15}\rangle$	64
$\{\bar{\psi}^{a(*)}\}\|V^{1,2,3}\rangle$	32	$\{\bar{y}^i_{NS}/\bar{w}^i_{NS}\}\|\gamma^{1,\ldots,15}\rangle$	4
$\{\bar{\phi}^{\{1,2\}/\{3,4\}/\{5,6\}/\{7,8\}(*)}\}\|V^{1,2,3}\rangle$	8	$\{\bar{\phi}^{\{1,2\}/\{3,4\}/\{5,6\}/\{7,8\}(*)}\}\|\gamma^{1,\ldots,15}\rangle$	8
$\{\bar{y}^i/\bar{w}^i\}\|V^{1,2,3}\rangle$	4	$\{y^i_{NS}/w^i_{NS}\}\{\bar{y}^j_{NS}/\bar{w}^j_{NS}\}\|z_{1/2}\rangle$	8
$\|H^{1,\ldots,6}\rangle$	16	$\{y^i_{NS}/w^i_{NS}\}\{\bar{\eta}^{b(*)}\}\|z_{1/2}\rangle$	32
$\|H^{7,\ldots,18}\rangle$	-8	$\{y^i_{NS}/w^i_{NS}\}\{\bar{\phi}^{\{5,6,7,8\}/\{1,2,3,4\}(*)}\}\|z_{1/2}\rangle$	16
$\{\bar{\psi}^{1,\ldots,5(*)},\bar{\eta}^{1,2,3(*)},\bar{\phi}^{(*)}_{NS}\}\|\tilde{V}\rangle$	-192	$\{y^i_{NS}/w^i_{NS}\}\|z_1+z_2\rangle$	8

TABLE 5.13: *Contributions of massless sectors to a_{00} when present in Hilbert space of a model. As noted $a_{00} = N^0_b - N^0_f$, so bosonic contributions are positive and fermionic are negative. The superscripts used here are $i \neq j = 1, ..., 6$, $a = 1, ..., 5$ and $b = 1, 2, 3$. The NS subscript means that the oscillator has Neveu-Schwarz boundary conditions in the sector.*

	Constraints	Total models in sample	Probability
	No Constraints	2×10^9	1
(1)	+ Tachyon-Free	10741667	5.37×10^{-3}
(2)	+ No Observable Enhancements	10741667	5.37×10^{-3}
(3)	+ No Hidden Enhancements	9921843	4.96×10^{-3}
(4)	+ $N_{16} - N_{\overline{16}} \geq 6$	69209	3.46×10^{-5}
(5)	+ $N_{10} \geq 1$	69013	3.45×10^{-5}
(6)	+ $a_{00} = N^0_b - N^0_f = 0$	3304	1.65×10^{-6}

TABLE 5.14: *Phenomenological statistics from sample of 2×10^9 $SO(10)$ $\tilde{S}$ -models.*

results confirm the observation made in previous sections that there are no tachyon-free models in our construction which have observable enhancements. In phenomenological terms, we do not need to worry about enhancements of the hidden sector gauge group, but they are included in the table for completeness. The next constraints we add are much like the so-called 'fertility constraints' implemented in [18, 103, 104]. The constraint on the net chirality $N_{16} - N_{\overline{16}} \geq 6$ is a necessary, but not sufficient, condition for the existence of 3 or more chiral generations at the level of the standard model.

The condition $N_{10} \geq 1$ ensures at least one state exists that can produce a Standard Model Higgs doublet and can be used to break the electroweak symmetry. Finally, we implement a condition on the q-expansion coefficient $a_{00} = 0$ which corresponds to finding models with $N_b = N_f$ at the massless level as discussed in Section 5.5.

The 3304 models satisfying all these constraints are notable, particularly in regard to this final condition of $N^0_b = N^0_f$. Inspecting the patterns in the spectra of these 3304 models revealed that $\sim 58\%$ contain the vector $\tilde{x}$ in their spectrum. In these cases, the large negative contribution of -256 that $\tilde{x}$ contributes to a_{00} is helpful in ensuring $N^0_b = N^f_0$. Of those models not containing $\tilde{x} \sim 70\%$ obtained the large negative contribution of -192 from one of the additional vectorials $\tilde{V} = \tilde{S}, \tilde{S} + z_1, \tilde{S} + z_2, \tilde{S} + z_1 + z_2$ with mixed charges under the observable and hidden groups, i.e. the sectors $\{\bar{\psi}^{1,\ldots,5}, \bar{\eta}^{1,2,3}, \bar{\phi}_{NS}\}\|\tilde{V}\rangle$. Again this large negative contribution helps in matching the number of massless fermions to massless bosons.

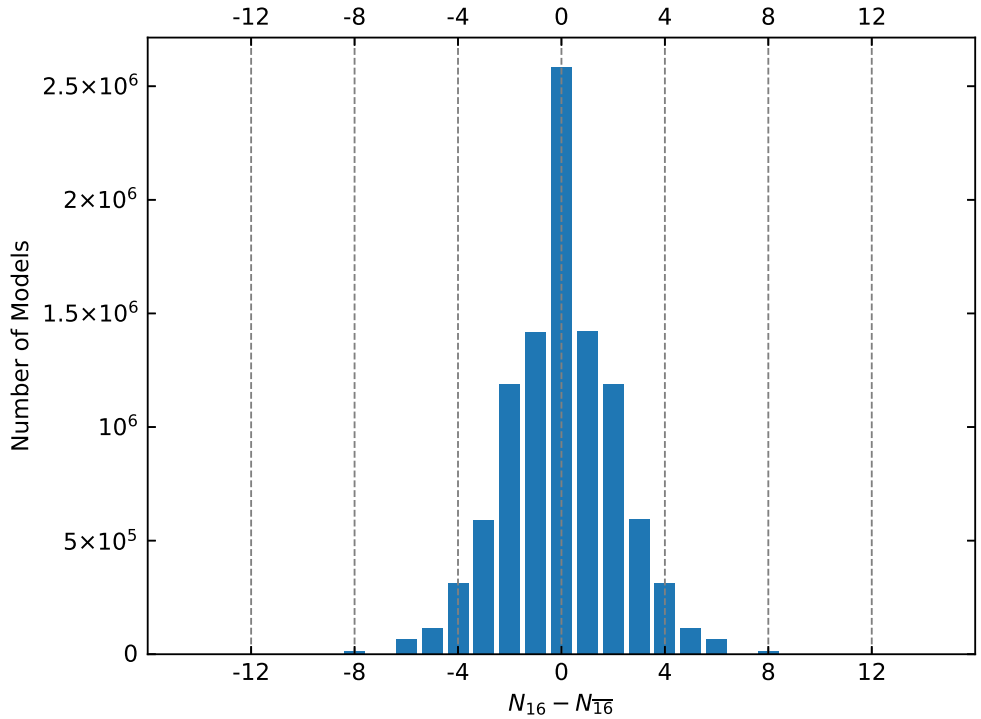

FIGURE 5.4: *Number of models versus net chiral generations from a random sample of* 10^7 *tachyon free* $SO(10)$ *models.*

5.6.2 Results for the Cosmological Constant

As the value of the constant term $a_{00} = N_b^0 - N_f^0$ and the cosmological constant Λ vary from model to model, it is interesting to see what range of values these non-supersymmetric models can produce.

The distribution of the cosmological constant Λ is shown in Figure 5.6, for a sample of 10^4 non-tachyonic and 10^4 fertile models. By non-tachyonic, we mean that only condition (1) of Table 5.14 is satisfied, while fertile models satisfy all conditions (1)-(5). It is important to note that values presented in Figure 5.6 are at the special free fermionic point in moduli space. This means that moving away from this point will change these values and if there are unfixed moduli, there is nothing preventing this from happening. This is indeed the case for our class of models. A full stability analysis would include the deformation of the model away from the fermionic point in all directions of the geometric moduli space using the methods of Section 4.2, however, this is beyond the scope of this thesis.

Another interesting quantity in the partition functions is boson-fermion degeneracy at the massless level. As discussed in Section 5.5, the on-shell states provide the majority of positive contributions to the partition function, the largest of which is the massless term. Thus the value of a_{00} gives a good handle on the value of the cosmological constant. It is also, of course, interesting for the discussion of phenomenological features and stability as explained in Section 5.5. The distribution of values of $a_{00} = N_b^0 - N_f^0$ for a sample of 10^4 non-tachyonic and 10^4 fertile models is shown in Figure 5.7.

From Figures 5.6 and 5.7 we see that the fertility conditions have a measurable effect on the distribution of Λ and a_{00}, that is, they slightly shift the values of both to the negative.

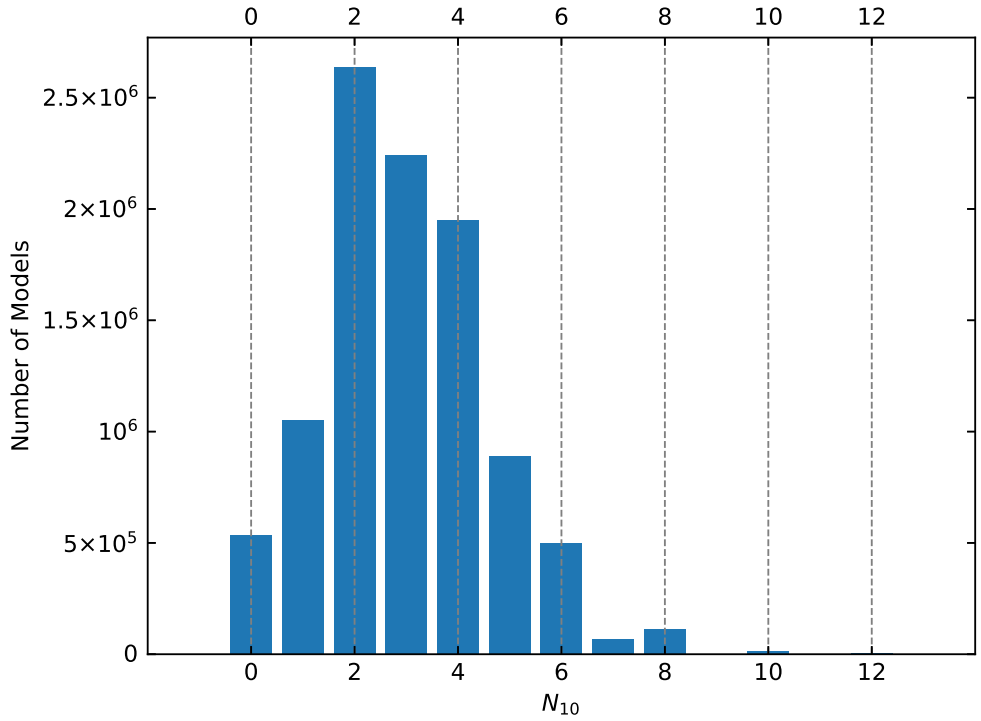

FIGURE 5.5: *Number of models versus number of vectorial* **10** *sectors from a random sample of* 10^7 *tachyon free* $SO(10)$ *models.*

This is an interesting effect and is likely due to condition (4) in Table 5.14. Even though the fertility condition (4) is directed at ensuring the difference $N_{16} - N_{\overline{16}}$ is greater than 6, doing so also results in fertile models having a larger average total $N_{16} + N_{\overline{16}}$ compared to non-fertile models. As specified in Table 5.13, these sectors contribute a value of -32 to a_{00} and thus appear to cause the shift toward smaller values for a_{00} and as a consequence also for Λ.

5.7 An Example Model with Bose-Fermi Degeneracy

From the 3304 fertile models with $N_b^0 = N_f^0$ we present an analysis of the key features of the massless spectrum for one example model, as well as presenting its partition function and

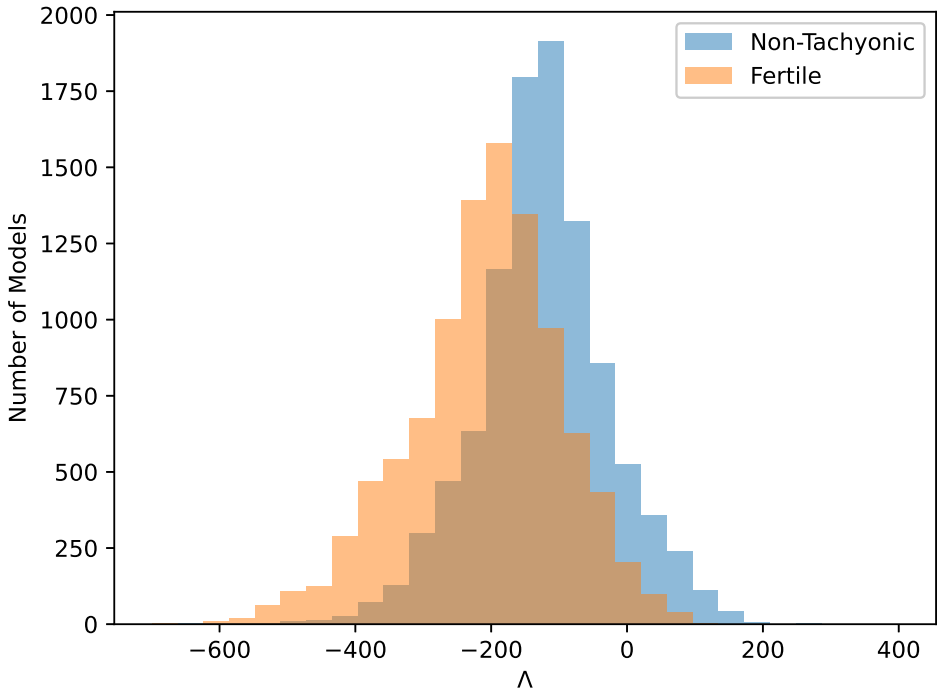

FIGURE 5.6: *The distribution of the cosmological constant for a sample of* 10^4 *non-tachyonic and* 10^4 *fertile models models.*

cosmological constant. The model we choose has the GGSO matrix

$$C\left[\begin{smallmatrix} v_i \\ v_j \end{smallmatrix}\right] = \begin{array}{c} \\ \mathbf{1} \\ \tilde{S} \\ e_1 \\ e_2 \\ e_3 \\ e_4 \\ e_5 \\ e_6 \\ b_1 \\ b_2 \\ b_3 \\ z_1 \end{array} \begin{array}{c} \begin{array}{cccccccccccc} \mathbf{1} & \tilde{S} & e_1 & e_2 & e_3 & e_4 & e_5 & e_6 & b_1 & b_2 & b_3 & z_1 \end{array} \\ \begin{pmatrix} -1 & -1 & 1 & -1 & -1 & -1 & 1 & 1 & 1 & 1 & -1 & -1 \\ -1 & 1 & -1 & -1 & -1 & 1 & 1 & 1 & 1 & -1 & -1 & 1 \\ 1 & -1 & -1 & -1 & -1 & -1 & -1 & -1 & -1 & -1 & -1 & 1 \\ -1 & -1 & -1 & 1 & -1 & 1 & 1 & -1 & 1 & -1 & 1 & -1 \\ -1 & -1 & -1 & -1 & 1 & -1 & -1 & 1 & 1 & 1 & -1 & -1 \\ -1 & 1 & -1 & 1 & -1 & 1 & 1 & 1 & 1 & -1 & 1 & 1 \\ 1 & 1 & -1 & 1 & -1 & 1 & -1 & 1 & -1 & 1 & 1 & -1 \\ 1 & 1 & -1 & -1 & 1 & 1 & 1 & -1 & -1 & 1 & 1 & 1 \\ 1 & -1 & -1 & 1 & 1 & 1 & -1 & -1 & 1 & -1 & 1 & 1 \\ 1 & 1 & -1 & -1 & 1 & -1 & 1 & 1 & -1 & 1 & -1 & 1 \\ -1 & 1 & -1 & 1 & -1 & 1 & 1 & 1 & 1 & -1 & -1 & -1 \\ -1 & -1 & 1 & -1 & -1 & 1 & -1 & 1 & 1 & 1 & -1 & -1 \end{pmatrix} \end{array} \tag{5.34}$$

This model has $N_{16} = 7$, $N_{\overline{16}} = 1$ and $N_{10} = 8$ and thus satisfies the constraints imposed in Table 5.14. Furthermore, in this model the $\tilde{x}$–sector produces massless states, which in the supersymmetric models would correspond to the presence of the $S + x$ sector when x enhances the $SO(10)$ symmetry to E_6. In that case, the $S + x$ include the superpartners of the gauge vector bosons of the sector x, i.e. the gauginos. So in this case, we have the gauginos but not the vector bosons.

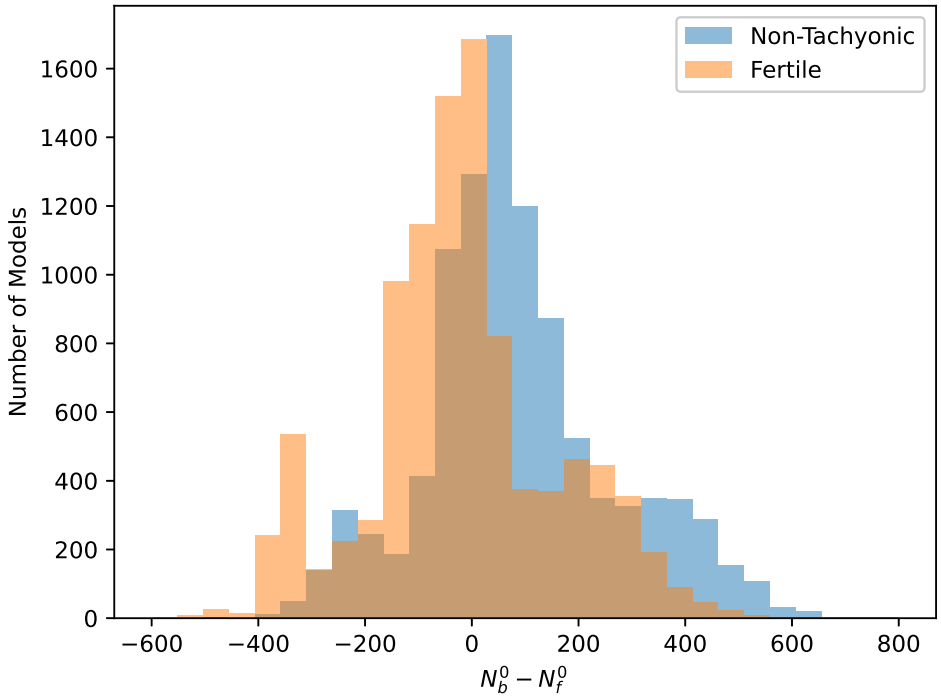

FIGURE 5.7: *The distribution of the constant term* $a_{00} = N_b^0 - N_f^0$ *for a sample of* 10^4 *non-tachyonic and* 10^4 *fertile models.*

Our model also contains 6 bosonic hidden states from the sectors $H^{1,\dots,6}$ and 48 fermionic hidden states from the $H^{7,\dots,18}$. There are additional vectorials from the sectors $e_3 + e_4 + e_5 + e_6$, $e_1 + e_2 + e_3 + e_6$ and $e_1 + e_2 + e_3 + e_4$ with observable oscillators $\{\bar{\psi}^a, \bar{\eta}^b\}$, $a = 1, ..., 5$, $b = 1, 2, 3$ which cannot couple with observable states from $B^{1,2,3}$ since it cannot conserve the charges of the $U(1)_{1,2,3}$ in particular. However, these three sectors may provide couplings at higher order.

The partition function is calculated in terms of its q-expansion and so it can be specified by a matrix of coefficients a_{mn} as in (5.33). For our example model, these values are presented in Table 5.15. We see that indeed this model has $a_{00} = N_b^0 - N_f^0 = 0$ as advertised and the series of states arrange according to (5.33). The absence of on-shell tachyons is explicit and the contribution from off-shell tachyonic states is non-zero as expected. We also find that the consistency condition $a_{0-1} = 2$ for the proto-graviton as described in [51, 84] is also satisfied.

The cosmological constant can also be calculated according to Section 4.3 and 5.5 with the modular integral quickly converging after 2^{nd} order in q. In this case, it takes the value

$$\Lambda = \sum_{m,n} a_{mn} I_{mn} = -149.77 \tag{5.35}$$

at the free fermionic point. As we see it is negative which is the case for most models with $N_b^0 = N_f^0$. This is due to the fact that the largest positive contributions to the partition function come from the light on-shell states and in particular from the massless states. If

q\ qb	-1	-7/8	-3/4	-5/8	-1/2	-3/8	-1/4	-1/8	0	1/8	1/4	3/8	1/2	5/8	3/4	7/8
-1/2	0	0	0	0	0	0	0	0	0	0	0	0	320	0	0	0
-3/8	0	0	0	0	0	0	0	0	0	0	0	0	0	896	0	0
-1/4	0	0	0	0	0	0	0	0	0	0	0	0	0	0	5696	0
-1/8	0	0	0	0	0	0	0	0	0	0	0	0	0	0	0	29312
0	2	0	0	0	0	0	0	0	0	0	0	0	0	0	0	0
1/8	0	0	0	0	0	0	0	0	0	-288	0	0	0	0	0	0
1/4	0	0	0	0	0	0	0	0	0	0	-4512	0	0	0	0	0
3/8	0	0	0	16	0	0	0	0	0	0	0	-9808	0	0	0	0
1/2	0	0	0	0	224	0	0	0	0	0	0	0	1344	0	0	0
5/8	0	0	0	0	0	416	0	0	0	0	0	0	0	36640	0	0
3/4	0	0	0	0	0	0	576	0	0	0	0	0	0	0	78080	0
7/8	0	0	0	0	0	0	0	-320	0	0	0	0	0	0	0	212928
1	32	0	0	0	0	0	0	0	-1440	0	0	0	0	0	0	0

TABLE 5.15: *The q-expansion of the partition function for our example model. Each entry in the table represents the coefficient a_{mn} in the partition function sum (4.65), with the first column and row being the mass levels for the left and right moving sectors respectively.*

$N_b^0 - N_f^0 = 0$, this is zero and the negative contributions from the light off-shell tachyons produce a negative value for Λ. This is indeed the case for all 3304 such models in our scan.

Looking at Figure 5.6 one may wonder what the meaning of the models around $\Lambda = 0$ mean. Indeed it is important to note that none of the models here has a vanishing cosmological constant. The smallest values range in $\mathcal{O}(10^{-3})$ in string scale which is still a very large value when thought of in cosmological scenarios. The total vanishing of the cosmological constant in non-supersymmetric orbifolds in four dimensions is very hard if not impossible to achieve as discussed extensively in [111].

5.8 Discussion and Conclusion

In this section, we developed systematic computerised tools to classify large spaces of free fermion heterotic string vacua that correspond to compactifications of ten-dimensional tachyonic vacua. From the point of view of the four-dimensional constructions this is achieved by the general $S - \tilde{S}$–map. Our previous $\overline{\text{NAHE}}$–based model [1] was similarly constructed from the model published in [112], which raises the question of what are the consequences of applying the map to generic models, *i.e.* what are the relations between the spectra of the two mapped models, and what are the general patterns. This relation is similar to the general relation exhibited by the spinor–vector duality map, and the two may in fact be manifestations of a much larger symmetry structure [96].

Adopting the classification methodology developed for supersymmetric free fermionic models entails the proliferation of tachyon-producing sectors in the $S - \tilde{S}$–mapped models. The systematic classification, therefore, requires a detailed analysis of these sectors that was discussed in Section 5.3. In the analysis of the massless sectors separate attention to bosonic and fermionic sectors is required and was discussed in Section 5.4. In Section 5.5 we discussed the general analysis of the partition function and its q–expansion in left and right moving energy modes. The analysis of the partition function is particularly instrumental in the case of non–supersymmetric string vacua as it gives a direct handle on the physical

states at different mass levels. Of particular interest in the q–expansion is the $a_{00} = N_b^0 - N_f^0$ term, which counts the difference between massless bosons and fermions in the spectrum of the string vacuum. In supersymmetric models, the number of fermionic and bosonic degrees of freedom are matched at all mass levels, and hence the partition function and the vacuum energy are identically zero. In non–supersymmetric models there is a generic mismatch at different mass levels, which is partially compensated by the so-called misaligned supersymmetry [84]. It has been argued that in tachyon–free non–supersymmetric models with $a_{00} = 0$ the vacuum energy may be suppressed by the volume of the compactified dimensions [113].

In Section 5.6 we presented the results of the classification of the order of 2×10^9 random GGSO phases that generate the space of vacua spanned by the basis vectors in eq. (5.9) and the 66 independent one–loop GGSO phases. The analysis reveals that tachyon–free models occur with $\sim 5 \times 10^{-3}$ probability. Furthermore, we analysed this data by further imposing some fertility conditions $N_{16} - N_{\overline{16}} \geq 6$ and $N_{10} \geq 1$ and found fertile models with $a_{00} = 0$ with frequency $\sim 2 \times 10^{-6}$ in our sample. In Figures 5.7 and 5.6 a notable shift in values of the cosmological constant and the a_{00} term were detected for fertile models compared with a random sample of non-tachyonic vacua.

These results reveal that extracting interesting phenomenological models necessitates the development of more sophisticated computerised methods than the random generation method. This is particularly true in light of the fact that generating a viable symmetry-breaking pattern may necessitate breaking the $SO(10)$ symmetry to the Standard Model subgroup. The $S - \tilde{S}$–map entails that scalar degrees of freedom in the spinorial sixteen representation of $SO(10)$ are shifted to the massive spectrum. The consequence is that the spectrum does not contain the neutral component in the 16 of $SO(10)$ required to break the remnant unbroken gauge symmetry down to the Standard Model gauge group. The only available states are exotic states that carry fractional $U(1)_{Z'}$ charge and appear in the heterotic string Standard–like Models [114–116]. This assertion requires of course further investigation that will be scrutinised in future work. The lesson may be that quasi-realistic models in this class may only be possible for a very restricted and narrow set of models, rather than the more generic set, which is the prevalent experience with supersymmetric constructions.

In subsequent work [3], these questions were investigated in tachyon–free Pati–Salam models, including the inclusion of fertility conditions. The increased space of vacua, in particular in the case of Standard–like models, requires adaptation of novel computational techniques [18].

Following from [1] the analysis and results presented in this section open up new vistas in string phenomenology. It reveals the potential relevance of string vacua that have been previously considered to be irrelevant. The number of questions to explore is large and may potentially provide insight into some of the prevailing problems in string phenomenology. Interpolation between the supersymmetric vacua and our tachyon–free constructions, as well as with the two-dimensional MSDS constructions [117–119], may shed some light on the problem of supersymmetry breaking and vacuum energy in string theory. This can be carried out in a subset of the basis vectors *e.g.* $\{1, \tilde{S}, b_1\}$ or $\{1, \tilde{S}, \tilde{x}\}$. Another question of interest is the question of stability of the tachyon–free models. This question is necessarily tied to the non–vanishing one–loop vacuum energy in these models. Finally, further understanding of the symmetries that underlie the partition function at all mass levels, as exhibited at the massless level by the $\tilde{S}$ and $\tilde{x}$ maps, are important to extract.

6 Corners of The Landscape: Heterotic Type 0 and Type $\bar{0}$ Vacua

In this section, we explore some of the extremities of the landscape of heterotic string theories. We show that it is possible to construct models in four-dimension which are free of fermions or of twisted bosons in their massless spectra. Motivated by the usual 10D Type 0 string theory, we call these the 4D *Type 0* and *Type* $\bar{0}$ *heterotic string vacua*. The material presented in this section is based on the papers [4, 5] by the author.

To begin with, in Section 6.1 we present the construction of four-dimensional Type 0 heterotic string vacua. We will consider two separate cases based on both the S and $\tilde{S}$ vectors of the previous section and provide a classification of possible vacua. We also highlight the novel observation of the existence of misaligned supersymmetry in these classes of models. We then move on to discuss the possibility of four-dimensional Type $\bar{0}$ heterotic vacua in Section 6.2 and perform a similar classification of possible scenarios.

6.1 Type 0 Heterotic Vacua

In this section, we extend the analysis of the classification of free fermionic vacua to the class of Type 0 models. Our interest here is in the existence of models that do not contain any fermions at all. Such models are of particular interest to explore the boundaries of the space of $\mathbb{Z}_2 \times \mathbb{Z}_2$ orbifold compactifications. It is plausible that progress on some of the phenomenological issues in string theory, in particular in relation to cosmological evolution and vacuum selection, will be obtained by an improved understanding of these vacua. Moreover, it is likely that further insight can be achieved by exploring some of the features of these vacua in connection with the phenomenological string vacua. In this section, we pursue this line of investigation. We present several type 0 models in this class. We further adapt the systematic classification method that was developed using the free fermionic formulation [68, 90, 97–101, 103, 104] to this class of models. This requires careful analysis of tachyonic states that proliferate in these configurations. While we do not find any model which is completely free of tachyonic states, we present a model with a minimal set of tachyonic states. Using the methods of Chapter 4, we may explore the possibility that these tachyonic states become massive when the moduli are moved away from the free fermionic point. Another issue that we analyse in detail is the calculation of the vacuum energy and the finiteness properties of the string one–loop amplitude. Naturally, these are divergent due to the existence of tachyonic states, however, we still observe a form of misaligned supersymmetry.

The first model that we present uses the $\overline{\text{NAHE}}$-set that was introduced in [1, 87] and Chapter 5. In this set the basis vector S that generates spacetime supersymmetry in NAHE–based models [120, 121] is augmented with four periodic right–moving fermions, which amounts to making the gravitinos massive. This introduces a general $S \to \tilde{S}$ map in the space of models

that was discussed in detail in Chapter 5. The set of basis vectors is given by

$$\begin{aligned}
\mathbb{1} &= \{\psi^\mu,\ \chi^{1,\ldots,6}, y^{1,\ldots,6}, w^{1,\ldots,6} \mid \overline{y}^{1,\ldots,6}, \overline{w}^{1,\ldots,6}, \overline{\psi}^{1,\ldots,5}, \overline{\eta}^{1,2,3}, \overline{\phi}^{1,\ldots,8}\},\\
\tilde{S} &= \{\psi^\mu, \chi^{1,\ldots,6} \mid \overline{\phi}^{3,4,5,6}\},\\
b_1 &= \{\chi^{34}, \chi^{56}, y^{34}, y^{56} \mid \overline{y}^{34}, \overline{y}^{56}, \overline{\eta}^{1}, \overline{\psi}^{1,\ldots,5}\},\\
b_2 &= \{\chi^{12}, \chi^{56}, y^{12}, w^{56} \mid \overline{y}^{12}, \overline{w}^{56}, \overline{\eta}^{2}, \overline{\psi}^{1,\ldots,5}\},\\
b_3 &= \{\chi^{12}, \chi^{34}, w^{12}, w^{34} \mid \overline{w}^{12}, \overline{w}^{34}, \overline{\eta}^{3}, \overline{\psi}^{1,\ldots,5}\},\\
z_1 &= \{\overline{\phi}^{1,\ldots,4}\},\\
x &= \{\overline{\psi}^{1,\ldots,5}, \overline{\eta}^{1,2,3}\}.
\end{aligned} \tag{6.1}$$

A model may then be specified through the assignment of modular invariant GGSO phase between the basis vectors. An example of a Type 0 configuration arises for the specific choice

$$C\binom{\boldsymbol{b}_i}{\boldsymbol{b}_j} = \begin{array}{c} \\ \mathbf{1} \\ \tilde{S} \\ b_1 \\ b_2 \\ b_3 \\ z_1 \\ x \end{array} \begin{array}{c} \begin{array}{ccccccc} \mathbf{1} & \tilde{S} & b_1 & b_2 & b_3 & z_1 & x \end{array} \\ \begin{pmatrix} 1 & 1 & -1 & -1 & -1 & -1 & -1 \\ 1 & -1 & -1 & -1 & -1 & 1 & 1 \\ -1 & 1 & -1 & -1 & -1 & 1 & 1 \\ -1 & 1 & -1 & -1 & -1 & 1 & 1 \\ -1 & 1 & -1 & -1 & -1 & 1 & 1 \\ -1 & -1 & 1 & 1 & 1 & -1 & 1 \\ -1 & 1 & -1 & -1 & -1 & 1 & 1 \end{pmatrix} \end{array} \tag{6.2}$$

which we consider later on.

All models in this basis will have gauge bosons arising from the Neveu–Schwarz (NS) sector that produce the vector bosons of a $SO(10) \times U(1)^3 \times SO(4)^3 \times SU(2)^8$ gauge symmetry. Additional vector bosons may arise from the sectors in the z_1, $z_3 = \mathbf{1} + \tilde{S} + b_1 + b_2 + b_3 = \{\bar{\phi}^{1,2,7,8}\}$ and $z_4 = \mathbf{1}+\tilde{S}+b_1+b_2+b_3+z_1 = \{\bar{\phi}^{3,4,7,8}\}$, which can affect the observable and the hidden gauge group factors or just the hidden, depending on the right-moving oscillator. A solely observable gauge enhancement may also arise from the sector x. In the above model, the hidden $SU(2)^8$ gauge symmetry is enhanced to $SO(16)$ by vector bosons arising in z_1, z_3 and z_4. The four-dimensional gauge group is, therefore, given by

$$SO(10) \times U(1)^3 \times SO(4)^3 \times SO(16). \tag{6.3}$$

The NS–sector and the three enhancement sectors above produce in total sixteen tachyonic states that transform in the 16 representation of the hidden $SO(16)$ gauge symmetry. The vectorial fermionic sectors in the model are

$$\begin{aligned}
&\tilde{S};\\
&\tilde{S} + z_1;\\
&\tilde{S} + z_4 \sim S + z_2,
\end{aligned} \tag{6.4}$$

while the massless fermionic spinorial sectors are

$$\begin{aligned}
&\tilde{S} + b_{1,2,3} + x;\\
&\tilde{S} + b_{1,2,3} + x + z_1;\\
&\tilde{S} + b_{1,2,3} + x + z_4;\\
&\tilde{S} + z_3 \sim S + z_1 + z_2;
\end{aligned} \tag{6.5}$$

where we defined $z_2 = \{\bar{\phi}^{5,\cdots,8}\}$ and $S = \{\psi^{1,2}, \chi^{1,\cdots,6}\}$, neither of which are basis vector combinations in the additive group. We note that the S–vector coincides with the supersymmetry generator in supersymmetric free fermionic models, as well as those that are compactifications of the ten-dimensional $SO(16)\times SO(16)$ heterotic string. These definitions comply with the terminology used in the classification of the supersymmetric free fermionic heterotic string models. We emphasise that the absence of the S–vector from the additive group is the crucial feature of the $\tilde{S}$–models. As discussed in refs. [1, 2, 87] the absence of the S–vector is the characteristic property of vacua that descend from the tachyonic ten-dimensional vacua.

The massless states from all the fermionic sectors are projected out from the physical spectrum by the choice of GGSO phases in (6.2). In addition to the NS–sector, sectors giving rise to spacetime massless bosonic states are

$$\begin{aligned}
&x;\\
&z_{1,3,4};\\
&b_{1,2,3};\\
&b_{1,2,3} + x;\\
&b_{1,2,3} + x + z_1;\\
&b_{1,2,3} + x + z_3;\\
&b_{1,2,3} + x + z_1 + z_3.
\end{aligned} \tag{6.6}$$

They give rise to scalar spacetime bosons that transform in representations of the four-dimensional gauge symmetry. They are of no particular interest here and we do not list their detail explicitly.

In Sections 6.1.2 and 6.1.3 we perform a more general search for similar Type 0 heterotic string models using the free fermionic classification methodology. In particular, we search for Type 0 models without tachyons. Our search is conducted using the $\tilde{S}$ based models as well as models that use S. First, however, it is interesting to study a bit more closely the basis (6.1), and what additional constraints Type 0 vacua may satisfy.

6.1.1 Analytic Conditions on Type 0 Vacua

Since we are interested in the construction and analysis of Type 0 vacua, we focus on the massless fermionic sectors and will seek to project them out, leaving only bosonic states at the massless level. The Hilbert space in the free fermionic construction is given by the

collection of GGSO-projected states $|S_\xi\rangle$

$$\mathcal{H} = \bigoplus_{\xi\in\Xi}\prod_{i=1}^{k}\left\{ e^{i\pi v_i\cdot F_\xi}\,|S_\xi\rangle = \delta_\xi C\begin{pmatrix}\xi\\ v_i\end{pmatrix}^{*}|S_\xi\rangle\right\}. \tag{6.7}$$

For the Type 0 case, this will only have contributions from sectors ξ in the additive space Ξ with bosonic spin statistic index $\delta_\xi = +1$ at the massless level.

For the basis (6.1), These definitions comply with the terminology used in the classification of the supersymmetric free fermionic heterotic string models. In particular, we note that the S–vector coincides with the supersymmetry generator in supersymmetric free fermionic models, as well as those that are compactifications of the ten-dimensional $SO(16)\times SO(16)$ heterotic string which we analyse in Section 6.1.3. However, since we want to find choices of GGSO phases for which the fermionic sectors may be projected out to leave Type 0 vacua, it is worth exploring explicitly the analytic conditions on their projection. Another important part of the analysis will be to consider the presence of tachyonic sectors in our models which we turn to in Section 6.1.1. Due to our basis being relatively simple, writing down analytic conditions for generating Type 0 models seems tractable *a priori* and we will see that, indeed, it is entirely solvable.

In order to project the fermionic massless sectors given in equations (6.4) and (6.5) we can write down analytic conditions from the GGSO projection equation for the existence of Type 0 models. For the fermionic vectorial sectors (6.4)

$$\{\bar{y},\bar{w}\}\,|\tilde{S}\rangle \text{ projected } \iff \left(1-C\left(\begin{smallmatrix}\tilde{S}\\ x\end{smallmatrix}\right)\right)\left(1-C\left(\begin{smallmatrix}\tilde{S}\\ z_3\end{smallmatrix}\right)\right)=0 \tag{6.8}$$

$$\{\bar{\psi}^{1,\dots,5},\bar{\eta}^{1,2,3}\}\,|\tilde{S}\rangle \text{ projected } \iff \left(1+C\left(\begin{smallmatrix}\tilde{S}\\ x\end{smallmatrix}\right)\right)\left(1-C\left(\begin{smallmatrix}\tilde{S}\\ z_3\end{smallmatrix}\right)\right)=0 \tag{6.9}$$

$$\{\bar{\phi}^{1,2,7,8}\}\,|\tilde{S}\rangle \text{ projected } \iff \left(1-C\left(\begin{smallmatrix}\tilde{S}\\ x\end{smallmatrix}\right)\right)\left(1+C\left(\begin{smallmatrix}\tilde{S}\\ z_3\end{smallmatrix}\right)\right)=0 \tag{6.10}$$

$$\{\bar{y},\bar{w}\}\,|\tilde{S}+z_1\rangle \text{ projected } \iff \left(1-C\left(\begin{smallmatrix}\tilde{S}+z_1\\ x\end{smallmatrix}\right)\right)\left(1-C\left(\begin{smallmatrix}\tilde{S}+z_1\\ z_4\end{smallmatrix}\right)\right)=0 \tag{6.11}$$

$$\{\bar{\psi}^{1,\dots,5},\bar{\eta}^{1,2,3}\}\,|\tilde{S}+z_1\rangle \text{ projected } \iff \left(1+C\left(\begin{smallmatrix}\tilde{S}+z_1\\ x\end{smallmatrix}\right)\right)\left(1-C\left(\begin{smallmatrix}\tilde{S}+z_1\\ z_4\end{smallmatrix}\right)\right)=0 \tag{6.12}$$

$$\{\bar{\phi}^{3,4,7,8}\}\,|\tilde{S}+z_1\rangle \text{ projected } \iff \left(1-C\left(\begin{smallmatrix}\tilde{S}+z_1\\ x\end{smallmatrix}\right)\right)\left(1+C\left(\begin{smallmatrix}\tilde{S}+z_1\\ z_4\end{smallmatrix}\right)\right)=0 \tag{6.13}$$

$$\{\bar{y},\bar{w}\}\,|\tilde{S}+z_4\rangle \text{ projected } \iff \left(1-C\left(\begin{smallmatrix}\tilde{S}+z_4\\ x\end{smallmatrix}\right)\right)\left(1-C\left(\begin{smallmatrix}\tilde{S}+z_4\\ z_1\end{smallmatrix}\right)\right)=0 \tag{6.14}$$

$$\{\bar{\psi}^{1,\dots,5},\bar{\eta}^{1,2,3}\}\,|\tilde{S}+z_4\rangle \text{ projected } \iff \left(1+C\left(\begin{smallmatrix}\tilde{S}+z_4\\ x\end{smallmatrix}\right)\right)\left(1-C\left(\begin{smallmatrix}\tilde{S}+z_4\\ z_1\end{smallmatrix}\right)\right)=0 \tag{6.15}$$

$$\{\bar{\phi}^{1,2,3,4}\}\,|\tilde{S}+z_4\rangle \text{ projected } \iff \left(1-C\left(\begin{smallmatrix}\tilde{S}+z_4\\ x\end{smallmatrix}\right)\right)\left(1+C\left(\begin{smallmatrix}\tilde{S}+z_4\\ z_1\end{smallmatrix}\right)\right)=0 \tag{6.16}$$

Using the ABK rules on equations (6.8), (6.9) and (6.10) we deduce that

$$C\left(\begin{smallmatrix}\tilde{S}\\ x\end{smallmatrix}\right)=1 \;\text{ and }\; C\left(\begin{smallmatrix}\tilde{S}\\ b_1\end{smallmatrix}\right)C\left(\begin{smallmatrix}\tilde{S}\\ b_2\end{smallmatrix}\right)C\left(\begin{smallmatrix}\tilde{S}\\ b_3\end{smallmatrix}\right)=-1 \tag{6.17}$$

using these results and the ABK rules on equations (6.11), (6.12) and (6.13) gives the further results

$$C\left(\begin{smallmatrix}z_1\\ x\end{smallmatrix}\right)=1 \;\text{ and }\; C\left(\begin{smallmatrix}z_1\\ b_1\end{smallmatrix}\right)C\left(\begin{smallmatrix}z_1\\ b_2\end{smallmatrix}\right)C\left(\begin{smallmatrix}z_1\\ b_3\end{smallmatrix}\right)=1. \tag{6.18}$$

Finally, the first bracket of equations (6.14), (6.15) and (6.16) implies the result

$$C\left(\begin{smallmatrix}x\\ 1\end{smallmatrix}\right)C\left(\begin{smallmatrix}x\\ b_1\end{smallmatrix}\right)C\left(\begin{smallmatrix}x\\ b_2\end{smallmatrix}\right)C\left(\begin{smallmatrix}x\\ b_3\end{smallmatrix}\right)=1. \tag{6.19}$$

Meanwhile, for the fermionic spinorial sectors (6.5) we have

$$\tilde{S}+b_i+x \text{ projected} \iff \left(1-C\left(\begin{smallmatrix}\tilde{S}+b_i+x\\ b_j+b_k+x\end{smallmatrix}\right)\right)\left(1-C\left(\begin{smallmatrix}\tilde{S}+b_i+x\\ z_3\end{smallmatrix}\right)\right)=0 \quad (6.20)$$

$$\tilde{S}+b_i+z_1+x \text{ projected} \iff \left(1-C\left(\begin{smallmatrix}\tilde{S}+b_i+z_1+x\\ b_j+b_k+x\end{smallmatrix}\right)\right)\left(1-C\left(\begin{smallmatrix}\tilde{S}+b_i+z_1+x\\ z_4\end{smallmatrix}\right)\right)=0 \quad (6.21)$$

$$\tilde{S}+b_i+z_4+x \text{ projected} \iff \left(1-C\left(\begin{smallmatrix}\tilde{S}+b_i+z_4+x\\ b_j+b_k+x\end{smallmatrix}\right)\right)\left(1-C\left(\begin{smallmatrix}\tilde{S}+b_i+z_4+x\\ z_1\end{smallmatrix}\right)\right)=0 \quad (6.22)$$

$$\tilde{S}+z_3 \text{ projected} \iff \left(1-C\left(\begin{smallmatrix}\tilde{S}+z_3\\ b_1+b_2+b_3+x\end{smallmatrix}\right)\right)\left(1-C\left(\begin{smallmatrix}\tilde{S}+z_3\\ x\end{smallmatrix}\right)\right)=0 \quad (6.23)$$

where $i\neq j\neq k=1,2,3$. Using results (6.17),(6.18) and (6.19) in equation (6.22) implies that

$$C\left(\begin{smallmatrix}z_1\\ b_1\end{smallmatrix}\right)=C\left(\begin{smallmatrix}z_1\\ b_2\end{smallmatrix}\right)=C\left(\begin{smallmatrix}z_1\\ b_3\end{smallmatrix}\right)=1 \quad (6.24)$$

and using results (6.17) and (6.19) in equation (6.20) allows us to deduce the results

$$\begin{aligned} C\left(\begin{smallmatrix}\tilde{S}\\ b_1\end{smallmatrix}\right)C\left(\begin{smallmatrix}b_1\\ b_2\end{smallmatrix}\right)C\left(\begin{smallmatrix}b_1\\ b_3\end{smallmatrix}\right)&=-1\\ C\left(\begin{smallmatrix}\tilde{S}\\ b_2\end{smallmatrix}\right)C\left(\begin{smallmatrix}b_2\\ b_1\end{smallmatrix}\right)C\left(\begin{smallmatrix}b_2\\ b_3\end{smallmatrix}\right)&=-1\\ C\left(\begin{smallmatrix}\tilde{S}\\ b_3\end{smallmatrix}\right)C\left(\begin{smallmatrix}b_3\\ b_1\end{smallmatrix}\right)C\left(\begin{smallmatrix}b_3\\ b_2\end{smallmatrix}\right)&=-1. \end{aligned} \quad (6.25)$$

Since (6.17) means there are only two independent equations here, we can use this result to fix two of the phases: $C\left(\begin{smallmatrix}b_1\\ b_2\end{smallmatrix}\right), C\left(\begin{smallmatrix}b_1\\ b_3\end{smallmatrix}\right)$ and $C\left(\begin{smallmatrix}b_2\\ b_3\end{smallmatrix}\right)$.

Gathering the results (6.17), (6.18), (6.19), (6.24) and (6.25) we find the following necessary and sufficient conditions on the projection of massless fermions within models derived from the basis (6.1)

$$\begin{aligned} C\left(\begin{smallmatrix}\tilde{S}\\ x\end{smallmatrix}\right)=C\left(\begin{smallmatrix}z_1\\ x\end{smallmatrix}\right)=C\left(\begin{smallmatrix}z_1\\ b_1\end{smallmatrix}\right)=C\left(\begin{smallmatrix}z_1\\ b_2\end{smallmatrix}\right)=C\left(\begin{smallmatrix}z_1\\ b_3\end{smallmatrix}\right)&=1\\ C\left(\begin{smallmatrix}\tilde{S}\\ b_1\end{smallmatrix}\right)&=-C\left(\begin{smallmatrix}\tilde{S}\\ b_2\end{smallmatrix}\right)C\left(\begin{smallmatrix}\tilde{S}\\ b_3\end{smallmatrix}\right)\\ C\left(\begin{smallmatrix}x\\ 1\end{smallmatrix}\right)&=C\left(\begin{smallmatrix}x\\ b_1\end{smallmatrix}\right)C\left(\begin{smallmatrix}x\\ b_2\end{smallmatrix}\right)C\left(\begin{smallmatrix}x\\ b_3\end{smallmatrix}\right)\\ C\left(\begin{smallmatrix}b_2\\ b_3\end{smallmatrix}\right)&=-C\left(\begin{smallmatrix}\tilde{S}\\ b_2\end{smallmatrix}\right)C\left(\begin{smallmatrix}b_1\\ b_2\end{smallmatrix}\right)\\ C\left(\begin{smallmatrix}b_3\\ b_1\end{smallmatrix}\right)&=-C\left(\begin{smallmatrix}\tilde{S}\\ b_2\end{smallmatrix}\right)C\left(\begin{smallmatrix}\tilde{S}\\ b_3\end{smallmatrix}\right)C\left(\begin{smallmatrix}b_1\\ b_2\end{smallmatrix}\right). \end{aligned} \quad (6.26)$$

These conditions mean that 9 of the 21 GGSO phases are fixed in order to obtain Type 0 vacua. Hence, the number of possible Type 0 models is reduced to $2^{12}=4096$.

Armed with the conditions (6.26) we can look now at the bosonic sectors (6.6) and in fact prove that all these sectors must appear in all 4096 possible Type 0 models. To prove this we can go through the projection conditions as we did above for the fermionic sectors. In particular, taking the sectors b_i, for $i=1,2,3$ we get

$$b_i \text{ survives} \iff C\left(\begin{smallmatrix}b_i\\ \tilde{S}+b_j+b_k\end{smallmatrix}\right)=1 \quad \text{and} \quad C\left(\begin{smallmatrix}b_i\\ z_1\end{smallmatrix}\right)=1 \quad (6.27)$$

these conditions coincide exactly with conditions (6.25) and (6.24), respectively, from the projection of fermions analysis above. A similar result can easily be found for the other spinorial bosonic sectors: $b_{1,2,3}+x+z_1, b_{1,2,3}+x+z_3$ and $b_{1,2,3}+x+z_4$. For the bosonic

vectorial sectors $b_i + x$, $i = 1, 2, 3$, we have the conditions

$$\{\bar{y}, \bar{w}, \bar{\psi}^{1,\ldots,5}, \bar{\eta}^i, \bar{\phi}^{5,6}\} |b_i + x\rangle \text{ survives } \Longrightarrow \frac{1}{4}\left(1 + C\binom{b_i+x}{z_3}\right)\left(1 + C\binom{b_i+x}{z_1}\right) = 1 \quad (6.28)$$

$$\{\bar{\phi}^{1,2}\} |b_i + x\rangle \text{ survives } \Longrightarrow \frac{1}{4}\left(1 - C\binom{b_i+x}{z_3}\right)\left(1 - C\binom{b_i+x}{z_1}\right) = 1 \quad (6.29)$$

$$\{\bar{\phi}^{3,4}\} |b_i + x\rangle \text{ survives } \Longrightarrow \frac{1}{4}\left(1 + C\binom{b_i+x}{z_3}\right)\left(1 - C\binom{b_i+x}{z_1}\right) = 1 \quad (6.30)$$

$$\{\bar{\phi}^{7,8}\} |b_i + x\rangle \text{ survives } \Longrightarrow \frac{1}{4}\left(1 - C\binom{b_i+x}{z_3}\right)\left(1 + C\binom{b_i+x}{z_1}\right) = 1 \quad (6.31)$$

The Type 0 conditions (6.26) guarantee that $C\binom{b_i+x}{z_3} = 1$ and $C\binom{b_i+x}{z_1} = 1$ and thus the first case survives.

Finally, let us show that the bosonic sector x survives. In order to make this sector massless there must be a left-moving oscillator, which could make it a gauge boson if this oscillator is ψ^μ. However, since for Type 0 models $C\binom{x}{S} = 1$ only the states of the Type $\{y^i/w^i\}_{1/2} |x\rangle$ can survive, which they must do due to $C\binom{x}{z_1} = C\binom{x}{z_3} = 1$.

For the z_1 massless sector the conditions for Type 0 models necessitate that states of the Type $\{y/w\}\{\bar{y}/\bar{w}\} |z_1\rangle$ and extra gauge bosons of the Type $\{\psi^\mu\}\{\bar{\phi}^{5,6,7,8}\} |z_1\rangle$ survive. Similarly for the z_3 massless sector Type 0 models must have states of the Type $\{y/w\}\{\bar{y}/\bar{w}\} |z_3\rangle$ and extra gauge bosons of the Type $\{\psi^\mu\}\{\bar{\phi}^{3,4,5,6}\} |z_3\rangle$. Finally, for the z_4 massless sector Type 0 models must have states of the Type $\{y/w\}\{\bar{y}/\bar{w}\} |z_4\rangle$ and extra gauge bosons of the Type $\{\psi^\mu\}\{\bar{\phi}^{1,2,5,6}\} |z_4\rangle$. Therefore, all Type 0 models derived from this basis (6.1) have a hidden sector enhancement of $SU(2)^4 \to SO(16)$.

This analysis tells us that all 4096 possible Type 0 models contain all bosonic sectors 6.6 with the specific set of oscillators given above. In other words, their massless spectra are identical. Doing the counting of all the bosonic states can be shown to give 4264, which is thus the constant term in the q-expansion of the partition function in all 4096 cases. Having seen how restrictive the Type 0 conditions (6.26) are at the massless level it makes sense to analyse what happens with the tachyonic sectors for our Type 0 models.

Tachyon Analysis for Type 0 Vacua

The tachyonic sectors for models derived from the basis (6.1) come from the sectors $|z_1\rangle$, $|z_3\rangle$ and $|z_4\rangle$ as well as the untwisted tachyon of the NS sector. We can immediately see that all vacua in this basis will contain an untwisted tachyon $\{\bar{\phi}^{5,6}\} |NS\rangle$. This can be seen as being related to the absence of $z_2 = \{\bar{\phi}^{5,6,7,8}\}$ in the basis which would allow for the projection of this tachyon since we would be equipped with the GGSO projection with the phase $C\binom{NS}{z_2} = 1$.

In regard to the tachyons from the sectors $|z_1\rangle$, $|z_3\rangle$ and $|z_4\rangle$, we see that the Type 0 conditions (6.26) necessitate their presence. For example, all phases that could project the z_1 tachyon: $C\binom{z_1}{b_1}, C\binom{z_1}{b_2}, C\binom{z_1}{b_3}, C\binom{z_1}{x}$ are all equal to $+1$ and thus leave it in the Hilbert space. Therefore, we conclude that all Type 0 in this construction contain the tachyons from the sectors $|z_1\rangle$, $|z_3\rangle$ and $|z_4\rangle$, along with the model-independent untwisted tachyon $\bar{\phi}^{5,6} |NS\rangle$.

Equivalence of Type 0 Models

Having shown that the massless spectrum and tachyonic sectors are identical for all the 4096 choices of GGSO phases consistent with the Type 0 conditions (6.26), we might wonder whether these models are in fact identical at all massive levels. Calculating the partition function for all 4096 Type 0 models gives the same

$$Z = 2\bar{q}^{-1} + 16q^{-1/2}\bar{q}^{-1/2} + 4264 + 45056q^{1/4}\bar{q}^{1/4} + \cdots \tag{6.32}$$

with degeneracy 4096. Note that this does not necessarily imply that all these models are the same. They may still differ in their charges under some of the symmetries of the theory. However, this is still a good example of the non-uniqueness of the free fermionic construction since the partition function (5.5) is invariant under the 12 phases: $C\binom{1}{\tilde{S}}$, $C\binom{1}{b_1}$, $C\binom{1}{b_2}$, $C\binom{1}{b_3}$, $C\binom{1}{z_1}$, $C\binom{\tilde{S}}{b_2}$, $C\binom{\tilde{S}}{b_3}$, $C\binom{\tilde{S}}{z_1}$, $C\binom{b_1}{b_2}$, $C\binom{x}{b_1}$, $C\binom{x}{b_2}$, $C\binom{x}{b_3}$. This result will ultimately be related to the many symmetries underlying models defined by the basis (6.1).

6.1.2 Classification of Type 0 $\tilde{S}$-Models

Having found that Type 0, tachyonic models exist for the simple basis (6.1), we can consider a more general basis

$$\begin{aligned}
\mathbb{1} &= \{\psi^\mu,\ \chi^{1,\ldots,6}, y^{1,\ldots,6}, w^{1,\ldots,6} \mid \overline{y}^{1,\ldots,6}, \overline{w}^{1,\ldots,6}, \overline{\psi}^{1,\ldots,5}, \overline{\eta}^{1,2,3}, \overline{\phi}^{1,\ldots,8}\},\\
\tilde{S} &= \{\psi^\mu, \chi^{1,\ldots,6} \mid \overline{\phi}^{3,4,5,6}\},\\
T_1 &= \{y^{1,2}, w^{1,2} \mid \overline{y}^{1,2}, \overline{w}^{1,2}\},\\
T_2 &= \{y^{3,4}, w^{3,4} \mid \overline{y}^{3,4}, \overline{w}^{3,4}\},\\
T_3 &= \{y^{5,6}, w^{5,6} \mid \overline{y}^{5,6}, \overline{w}^{5,6}\},\\
b_1 &= \{\chi^{34}, \chi^{56}, y^{34}, y^{56} \mid \overline{y}^{34}, \overline{y}^{56}, \overline{\eta}^{1}, \overline{\psi}^{1,\ldots,5}\},\\
b_2 &= \{\chi^{12}, \chi^{56}, y^{12}, w^{56} \mid \overline{y}^{12}, \overline{w}^{56}, \overline{\eta}^{2}, \overline{\psi}^{1,\ldots,5}\},\\
b_3 &= \{\chi^{12}, \chi^{34}, w^{12}, w^{34} \mid \overline{w}^{12}, \overline{w}^{34}, \overline{\eta}^{3}, \overline{\psi}^{1,\ldots,5}\},\\
z_1 &= \{\overline{\phi}^{1,\ldots,4}\},
\end{aligned} \tag{6.33}$$

where the T_i, $i = 1, 2, 3$ allow for internal symmetric shifts in the compactified coordinates around the 3 tori. The only other difference to the basis (6.1) is that x is now a linear combination given by

$$x = b_1 + b_2 + b_3 + T_1 + T_2 + T_3, \tag{6.34}$$

and we have the same combinations $z_3 = 1 + \tilde{S} + b_1 + b_2 + b_3$ and $z_4 = z_3 + z_1$. We can further note that the space of independent GGSO phase configuration is now $2^{36} \sim 6 \times 10^{10}$ for this basis.

The addition of the T_i's has some key consequences in relation to finding tachyon-free Type 0 vacua. It multiplies the number of massless fermionic sectors and also increases the number of ways to project the (fermionic) sectors. Furthermore, we now have 15 tachyonic sectors: $z_1, z_3, z_4, T_i, z_1 + T_i, z_3 + T_i$ and $z_4 + T_i$, $i = 1, 2, 3$ rather than just the 3 for basis (6.1). We

can notice that the model-independent NS tachyon $\{\bar{\phi}^{5,6}\}\,|NS\rangle$ remains in this construction so the minimal number of tachyons is to only have the NS tachyon.

Fermionic Sector Analysis

Using a similar methodology to Section 6.1.1, we wish to analyse the conditions on the projection of all fermionic sectors from these models. Due to the increased size of the space of models from the added complexity of having of $T_{i=1,2,3}$ in the basis, we developed a computer algorithm to scan efficiently over the space of vacua and check for the absence of fermionic massless states.

We note that massless fermionic vectorials in these models arise from the sectors

$$\begin{aligned} &\tilde{S};\\ &\tilde{S}+z_1;\\ &\tilde{S}+z_4 \end{aligned} \tag{6.35}$$

and the massless fermionic spinorial sectors from

$$\begin{aligned} &\tilde{S}+b_i+b_j+T_k+pT_i+qT_j;\\ &\tilde{S}+b_i+b_j+z_1+T_k+pT_i+qT_j;\\ &\tilde{S}+b_{1,2,3}+x+z_4;\\ &\tilde{S}+z_3. \end{aligned} \tag{6.36}$$

Our computer algorithm can then be further applied to analyse the tachyonic sectors arising in Type 0 models. The results of this computerised scan are presented in the following section.

Results of Classification

By implementing the projection conditions on the massless fermionic sectors (6.35) and (6.36) in a computer scan we can collect data for the number of fermionic states remaining in the Hilbert Space of a model and see how many are fermion-free and thus Type 0. The distribution of the number of fermionic states for a scan of 10^7 is displayed in Figure 6.1. In this sample, we find a total of 24508 which are free of fermionic states.

In order to gather a slightly larger sample of Type 0 models in this basis we take a larger sample of 10^8 models which still does not take much computing time. From this sample, we find 245685 Type 0 models which gives a probability $\sim 2.46\times10^{-3}$ for Type 0 vacua in the total space. We now wish to classify these Type 0 configurations according to which tachyonic sectors remain in their spectra (along with the model-independent untwisted tachyon), as shown in Table 6.1. These results clearly show that all Type 0 models have both the model-independent untwisted tachyon and some combination of at least 2 twisted tachyonic sectors. One might wonder how general this result is since our sample size of 10^8 only covers about $1:687$ models in the total space of GGSO phase configurations. Recalling the 4096 degeneracy factor from the analysis of models in the basis (6.1), we can reasonably suppose that Type 0 models are highly constrained and degenerate also in the current construction where the $T_{i=1,2,3}$ are incorporated in the basis.

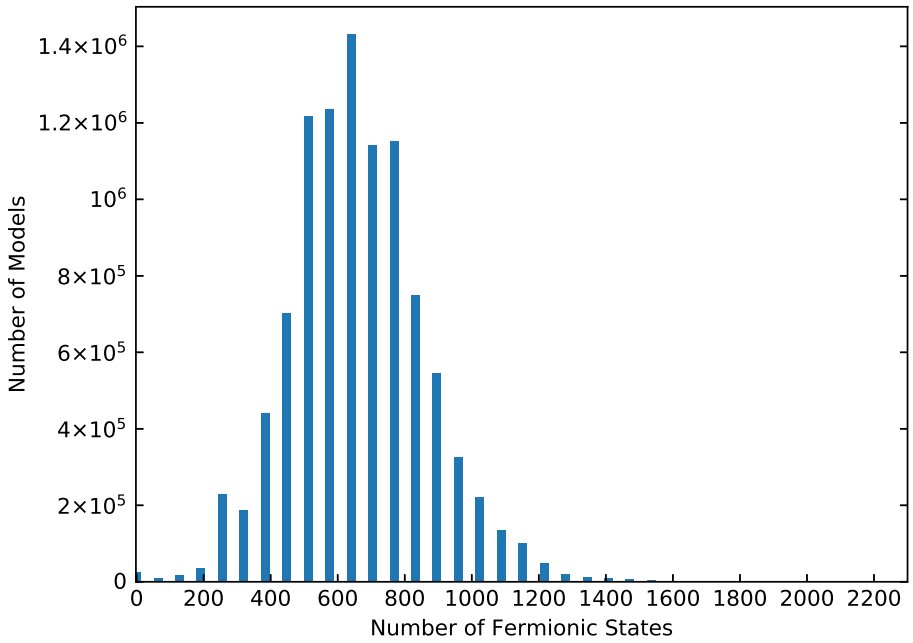

FIGURE 6.1: *Frequency plot for the number of fermionic states in a model from a sample of* 10^7 *randomly generated GGSO configurations.*

To see this we took 10^4 Type 0 models out from the 245685 total sample and calculated their partition functions and found a total of 109 distinct ones. In Figure 6.2 a comparison between the degeneracy of these 10^4 Type 0 models and those of a random sample of 10^4 models is shown and the number of different Type 0 models is seen to converge fast to just over 100, This shows, just as in the earlier case, that the subspace of Type 0 vacua is highly symmetric. This result strongly justifies the generality of our results from the 10^8 sample for the tachyonic analysis and makes it highly likely that our 245685 Type 0 models from the 10^8 sample capture all such unique models. In Section 6.1.4, we will further discuss the structure of these Type 0 models from the point of view of the partition function and one-loop vacuum energy.

6.1.3 Classification of Type 0 S-Models

Having explored a space of $\tilde{S}$-models in the previous section we now wish to do the same analysis for models deriving from the ten-dimensional $SO(16) \times SO(16)$ non-supersymmetric

z_k Tachyon	$z_k + T_i$ Tachyon	$\{\bar{\lambda}^a\}\,\|T_i\rangle$ Tachyon	Frequency
0	2	2	42773
1	2	1	33513
1	2	2	19402
1	0	2	17405
1	0	1	17140
1	1	2	12056
0	3	1	11996
3	0	1	7141
0	1	3	6044
3	0	2	5708
1	2	3	5575
1	2	0	5175
1	1	1	5170
1	4	2	5071
0	4	2	5017
0	0	2	4262
0	2	3	4253
1	4	1	4226
3	0	0	3827
0	3	2	3405
0	1	1	3389
1	4	0	3322
1	1	3	2625
1	3	3	2179
0	3	3	1774
0	4	3	1724
3	3	2	1713
1	3	2	1631
3	0	3	1529
3	3	3	1168
1	5	2	913
1	5	3	888
0	4	1	854
1	0	3	840
1	4	3	795
1	6	3	583
0	0	3	308
3	6	3	291

TABLE 6.1: *Number of tachyonic sectors for 245685 Type 0* $\tilde{S}$*-models, where* $k = 1, 3, 4$*,* $i = 1, 2, 3$ *and* $\bar{\lambda}^a$ *is any right-moving oscillator with NS boundary condition.*

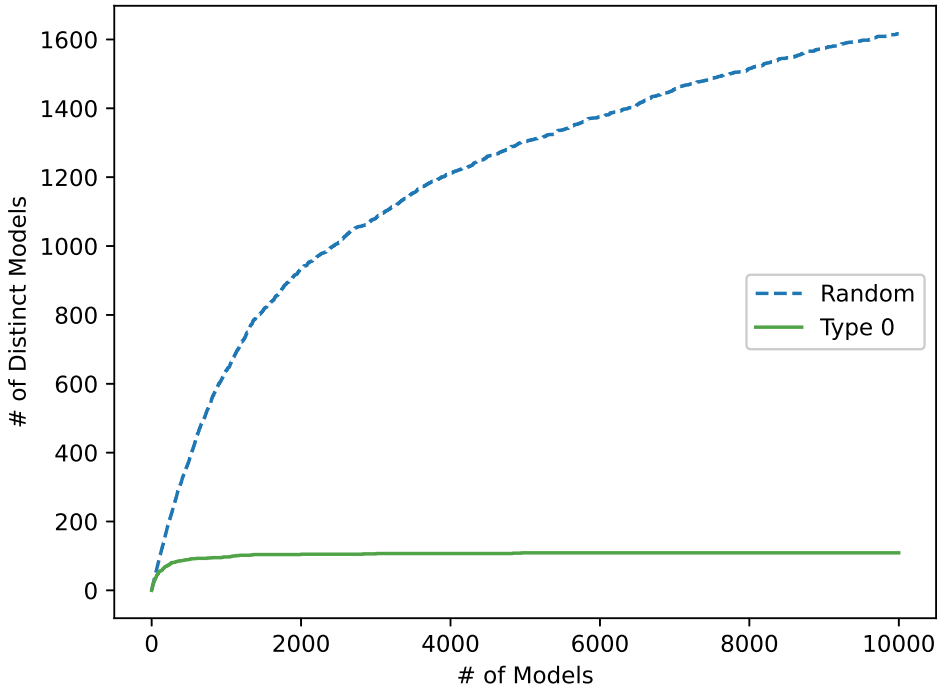

FIGURE 6.2: *The degeneracy of models for a random sample of models versus Type 0 models for a sample of 10^4 models each. We see that the space of Type 0 models is indeed highly degenerate.*

heterotic string, which we will refer to as S-models since their basis contains the SUSY–generating vector S. The precise basis we use is given by

$$\begin{aligned}
\mathbb{1} &= \{\psi^{\mu},\ \chi^{1,\dots,6}, y^{1,\dots,6}, w^{1,\dots,6} \mid \overline{y}^{1,\dots,6}, \overline{w}^{1,\dots,6}, \overline{\psi}^{1,\dots,5}, \overline{\eta}^{1,2,3}, \overline{\phi}^{1,\dots,8}\},\\
S &= \{\psi^{\mu}, \chi^{1,\dots,6}\},\\
T_1 &= \{y^{1,2}, w^{1,2} \mid \overline{y}^{1,2}, \overline{w}^{1,2}\},\\
T_2 &= \{y^{3,4}, w^{3,4} \mid \overline{y}^{3,4}, \overline{w}^{3,4}\},\\
T_3 &= \{y^{5,6}, w^{5,6} \mid \overline{y}^{5,6}, \overline{w}^{5,6}\},\\
b_1 &= \{\chi^{34}, \chi^{56}, y^{34}, y^{56} \mid \overline{y}^{34}, \overline{y}^{56}, \overline{\eta}^{1}, \overline{\psi}^{1,\dots,5}\},\\
b_2 &= \{\chi^{12}, \chi^{56}, y^{12}, y^{56} \mid \overline{y}^{12}, \overline{y}^{56}, \overline{\eta}^{2}, \overline{\psi}^{1,\dots,5}\},\\
z_1 &= \{\overline{\phi}^{1,\dots,4}\},\\
z_2 &= \{\overline{\phi}^{5,\dots,8}\},
\end{aligned} \tag{6.37}$$

which is in fact identical to that used in ref. [82] and the same as that used in the supersymmetric classifications of [68, 90, 97–101, 103, 104] up to the swap $T_{1,2,3} \to e_{1,\dots,6}$. As noted in these works, we will make regular use of the important linear combination x [106, 107],

which appears as the combination

$$x = 1 + S + \sum_{i=1}^{3} T_i + z_1 + z_2 \tag{6.38}$$

in this basis and we further have the combination $b_3 = b_1 + b_2 + x$ to give the generator of the third orbifold plane.

The untwisted gauge bosons in this construction generate a gauge group of $U(1)^6 \times SO(10) \times U(1)^3 \times SO(8)^2$ and the full space of models is again given by the combinations of modular invariant GGSO phase configurations $2^{36} \sim 6 \times 10^{10}$. An important difference from the $\tilde{S}$-construction is that we do not have a model-independent tachyon as the NS tachyon is automatically projected. This leaves the door open for possible tachyon-free Type 0 models.

Now we turn to the massless fermionic vectorial sectors which for our S-models arise from

$$\begin{aligned} &S \\ &S + z_1; \\ &S + z_2 \\ &S + b_i + x + pT_j + qT_k \end{aligned} \tag{6.39}$$

and the massless fermionic spinorial sectors from

$$\begin{aligned} &S + x \\ &S + z_1 + z_2 \\ &S + b_i + pT_j + qT_k; \\ &S + b_i + z_1 + x + pT_j + qT_k; \\ &S + b_i + z_2 + x + pT_j + qT_k; \end{aligned} \tag{6.40}$$

where $i \neq j \neq k \in \{1, 2, 3\}$ and $p, q \in \{0, 1\}$. We note that there are more fermionic sectors in this construction than in the $\tilde{S}$ case. In particular, the familiar $\mathbf{16}/\overline{\mathbf{16}}$ of $SO(10)$ from the sectors $S + b_i + pT_j + qT_k$ and vectorial $\mathbf{10}$ of $SO(10)$ from the sectors $(S+)b_i + x + pT_j + qT_k$ arise in this construction. However, for the $\tilde{S}$-models they were deliberately chosen to be absent and there are in fact no spinorial fermionic sectors with non-trivial representation under the $SO(10)$ observable gauge group factor.

As in the case of the $\tilde{S}$-models we use a computer algorithm to scan for Type 0 configurations where these fermionic sectors are projected out. The results are presented in the following section.

Results of Classification

As in the case of the $\tilde{S}$-models we generate a distribution for the number of fermionic states across a sample of 10^7 randomly generated GGSO phase configurations. This is shown in Figure 6.3. Comparing this to Figure 6.1 for the $\tilde{S}$ case we see a more dense distribution with more possible values for the fermionic states.

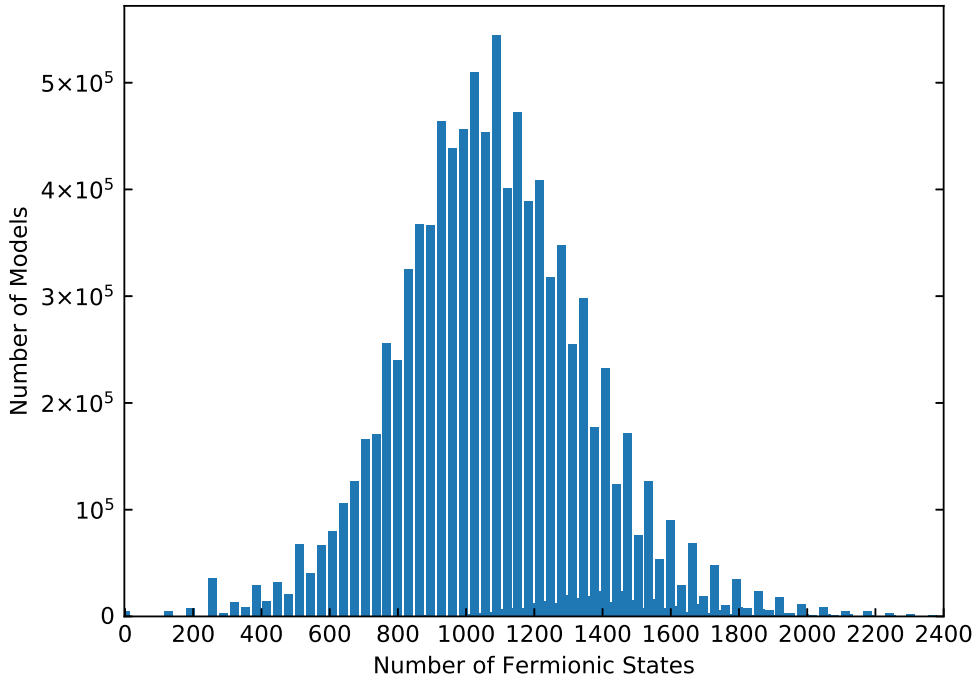

FIGURE 6.3: *Frequency plot for the number of fermionic states for S-models from a random sample of 10^7 GGSO configurations.*

As in the $\tilde{S}$ case, we generate a larger sample of Type 0 models by taking a scan of 10^8 GGSO configurations. From this scan, we find 54590 Type 0 models with probability $\sim 5.46 \times 10^{-4}$ which makes them approximately 5 times rarer than in the $\tilde{S}$ case. The likely reason for this and the main difference in general between the S case and $\tilde{S}$ case is the already mentioned fact that in the S-models we have more fermionic massless sectors to project.

Despite being rarer we already noted that we do not have any model-independent tachyons for these S-models which leave the possibility of tachyon-free Type 0 vacua open. The data for the numbers of tachyons is shown in Table 6.2 and we see again that no tachyon-free models exist and that the minimal number of tachyonic sectors is 2, which always includes at least 1 vectorial tachyon of the Type $\{\bar{\lambda}^a\}\,|T_i\rangle$. As in the case of the $\tilde{S}$-models, we observe a degeneracy in the space of Type 0 models and from the sample of 54590 Type 0 S-models, we found just 89 independent partition functions and the same convergence pattern as shown in Figure 6.2, therefore we can confidently claim that the lack of tachyon-free Type 0 models is a generic result in this class of vacua. It is however worth remembering that our models are defined at a free fermionic point in moduli space and so it may be that such tachyonic instabilities may disappear when a model is translated into a bosonic language and defined away from the fermionic point. The process for doing this in the same basis as we are employing here for the S-models is detailed in ref. [82].

6.1.4 Misaligned Supersymmetry in Type 0 Models

The partition function of string models encapsulates most information one knows about its structure and spectrum. Thus to fully understand these Type 0 models it is essential to get a handle on their partition function. The analysis of the partition function is particularly

z_k Tachyon	$z_k + T_i$ Tachyon	$\{\bar{\lambda}^a\}\,\|T_i\rangle$ Tachyon	Frequency
1	1	2	11605
1	0	2	10471
1	1	1	4431
1	0	3	4388
2	0	2	4066
2	0	1	3749
1	0	1	3363
1	1	3	2384
1	2	2	1870
2	0	3	1509
1	2	3	1318
1	2	1	1080
2	2	1	871
2	2	2	538
0	1	3	488
0	1	2	454
0	2	1	299
1	3	1	291
1	3	2	290
0	0	2	236
1	3	3	189
0	4	3	151
0	2	3	151
0	2	2	135
0	0	3	135
2	4	1	128

TABLE 6.2: *Number of tachyonic sectors for 54860 Type 0 S-models, where* $k = 1, 2$ *and* $i = 1, 2, 3$.

instrumental in non-supersymmetric constructions since it gives a complementary tool to count the total number of massless states, and its integration over the fundamental domain corresponds to the cosmological constant.

As explicitly shown in Chapter 4, on-shell tachyonic states, *i.e.* states with $m = n < 0$, have an infinite contribution. On the other hand off–shell tachyonic states may contribute a finite value to the partition function. It is also important to note that modular invariance only allows states with $m - n \in \mathbb{Z}$.

In the case of Type 0 models presented above, due to the presence of on-shell tachyonic states, the partition function diverges. However, this divergence is contained purely in the tachyonic mode, i.e. the degeneracy of states a_{mn} for $m, n > 0$ still behaves in a similar fashion to any other non-tachyonic heterotic theory. This is also emphasised by the presence of misaligned supersymmetry in the massive spectra of our models. Such misalignment of the physical spectrum in heterotic theories is well documented in the literature [2, 51, 69, 84]. It however remains to see whether this mechanism is replicated for Type 0 heterotic

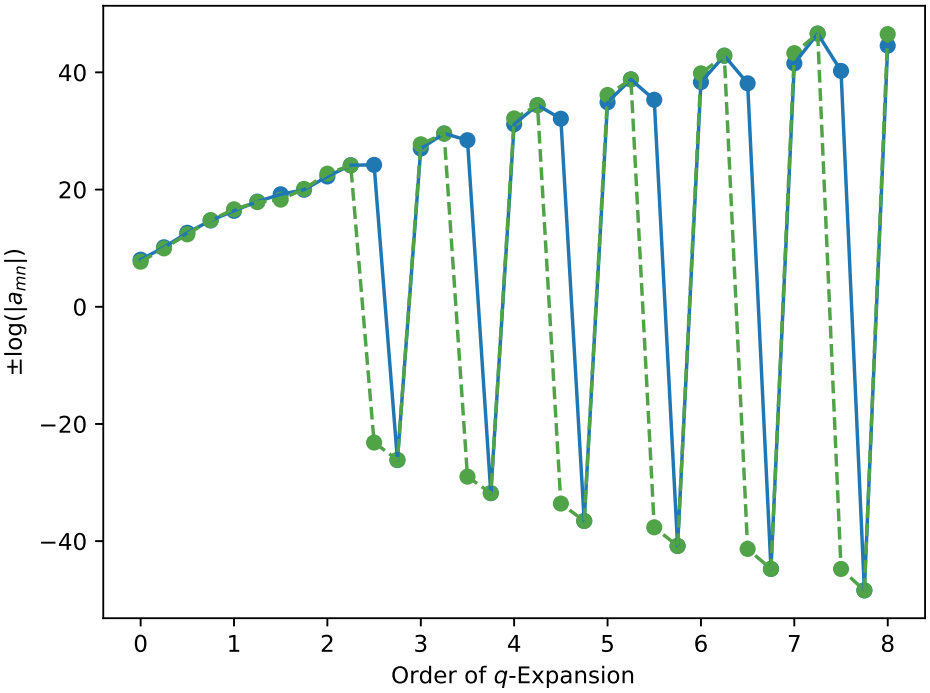

FIGURE 6.4: *The boson-fermion oscillation of misaligned supersymmetry for the on-shell states of two $\tilde{S}$ models to 8^{th} order in the q-expansion. The overall sign of $\pm\log(|\ a_{mn}\ |)$ is chosen according to the sign of a_{mn}.*

theories described in previous sections. We find that indeed both sets of Type 0 models generated by (6.1) and (6.33) exhibit such misalignment of their on-shell massive tower of states. The misalignment pattern appears to have no correlation to whether a specific model has massless fermions or not.

It was proved in [85] that non-SUSY heterotic strings without physical tachyons should always produce such misalignment of their massive spectra. In our case, due to the presence of on-shell tachyons the emergence of misaligned supersymmetry may seem somewhat unexpected. The analysis presented in the proof of misaligned supersymmetry in [85] relies on modular invariance together with the stated lack of physical tachyons. Since our theory is of course still modular invariant, we can speculate that the emergence of the misalignment should be a consequence of this, however, rigorous analysis is still lacking under these conditions. For the time being, we only present this as an observations for the theories under consideration in this section, but further investigation may lead to a deeper understanding of the relationship between on-shell tachyons and misaligned SUSY.

As an example, for the $\tilde{S}$-models of Section 6.1.2 we observe the two general patterns shown in Figure 6.4, or in general a combination of these two. This is true whether or not the choice of GGSO coefficients projects all massless fermions. The only observable difference we find for Type 0 models from the partition function point of view is the larger value of a_{00}. This is of course fully expected due to the lack of fermions at the massless level. The misalignment pattern is mostly similar for the S–models of Section 6.1.3. It is important to

note that, unlike for tachyon–free non–supersymmetric theories, this oscillatory behaviour does not result in a finite value for the cosmological constant due to the presence of the physical tachyons described in Sections 6.1.2 and 6.1.3.

This discussion shows that there is still much to learn about the relationship between finiteness, modular invariance and misaligned supersymmetry. This example gives an important example which can give us more insight. The Type 0 models above are fully modular invariant and also exhibit misaligned supersymmetry as shown explicitly. However, due to the presence of physical tachyons, they are not finite. Thus modular invariance does not necessarily imply finiteness. On the other hand, there are consistent string models, like the bosonic string, which do not exhibit misaligned supersymmetry but are still modular invariant. Hence modular invariance does not necessarily cause misaligned supersymmetry. Of course in the case of heterotic models, the relation between modular invariance and misaligned supersymmetry seems to be more concrete there is a lot to understand from these concepts.

6.2 Type $\bar{0}$ Heterotic Vacua

In this section, we extend the analysis to tachyon–free heterotic string models that do not contain any twisted bosonic degrees of freedom. In analogy with Type 0 models, we refer to such configurations as Type $\bar{0}$ models. It is apparent that such models contain untwisted bosonic degrees of freedom that correspond to the gravitational, gauge and untwisted scalar fields. However, in the Type $\bar{0}$ configurations that we present all the bosonic degrees of freedom from the twisted sectors of the $Z_2 \times Z_2$ orbifold are projected out. As a consequence, in such vacua, there is an excess of fermionic over bosonic degrees of freedom and the models possess a positive cosmological constant. Furthermore, in contrast to the Type 0 models of Section 6.1 that necessarily contain some tachyonic degrees of freedom, we find that most cases of Type $\bar{0}$ models are free of tachyonic states. We present Type $\bar{0}$ models that belong to the class of $\tilde{S}$-models of ref. [1–3, 87], as well as the class of S–models, where the first class are those models that descend from a tachyonic ten-dimensional vacuum, whereas the second are those that can be regarded as compactifications of the non–supersymmetric $SO(16) \times SO(16)$ ten-dimensional tachyon–free vacuum. We also note the existence of a supersymmetric vacuum that does not contain massless twisted bosons that has indeed appeared in previous classifications [90–92, 97, 100, 102]. In these cases the partition function is vanishing, whereas the Type $\bar{0}$ of interest are those that are not supersymmetric and with an excess of fermionic over bosonic states. In such configurations the vacuum energy is positive. Though they are unstable they may serve as laboratories to explore the possible string dynamics in the early universe.

The first Type $\bar{0}$ model we found is built off the $\overline{\text{NAHE}}$–set that was employed in [1, 87]. In this set, the basis vector S that generates spacetime supersymmetry in NAHE–based models [120, 121] is augmented with four periodic right–moving fermions, which amounts to making the gravitinos massive. This introduces a general $S \to \tilde{S}$ map in the space of models that

were discussed in detail in Chapter 5 and ref. [1–3]. The set of basis vectors is given by

$$\begin{aligned}
\mathbb{1} &= \{\psi^\mu,\ \chi^{1,\ldots,6}, y^{1,\ldots,6}, w^{1,\ldots,6} \mid \overline{y}^{1,\ldots,6}, \overline{w}^{1,\ldots,6}, \overline{\psi}^{1,\ldots,5}, \overline{\eta}^{1,2,3}, \overline{\phi}^{1,\ldots,8}\},\\
\tilde{S} &= \{\psi^\mu, \chi^{1,\ldots,6} \mid \overline{\phi}^{3,4,5,6}\},\\
b_1 &= \{\psi^\mu, \chi^{12}, y^{34}, y^{56} \mid \overline{y}^{34}, \overline{y}^{56}, \overline{\eta}^1, \overline{\psi}^{1,\ldots,5}\},\\
b_2 &= \{\psi^\mu, \chi^{34}, y^{12}, w^{56} \mid \overline{y}^{12}, \overline{w}^{56}, \overline{\eta}^2, \overline{\psi}^{1,\ldots,5}\},\\
b_3 &= \{\psi^\mu, \chi^{56}, w^{12}, w^{34} \mid \overline{w}^{12}, \overline{w}^{34}, \overline{\eta}^3, \overline{\psi}^{1,\ldots,5}\},\\
z_1 &= \{\overline{\phi}^{1,\ldots,4}\},\\
G &= \{y^{1,\ldots,6}, w^{1,\ldots,6} \mid \overline{y}^{1,\ldots,6}, \overline{w}^{1,\ldots,6}\},
\end{aligned} \tag{6.41}$$

and we further define the important linear combination

$$z_2 = 1 + b_1 + b_2 + b_3 + z_1 = \{\bar{\phi}^{5,6,7,8}\}. \tag{6.42}$$

A model may then be specified through the assignment of modular invariant GGSO phases between the basis vectors. An example of a Type $\bar{0}$ configuration arises for the choice

$$C\begin{pmatrix}\boldsymbol{b}_i\\ \boldsymbol{b}_j\end{pmatrix} = \begin{array}{c} \\ \mathbf{1}\\ \tilde{S}\\ b_1\\ b_2\\ b_3\\ z_1\\ G\end{array}\begin{array}{c}\begin{array}{ccccccc}\mathbf{1} & \tilde{S} & b_1 & b_2 & b_3 & z_1 & G\end{array}\\ \begin{pmatrix} 1 & 1 & -1 & -1 & 1 & 1 & 1\\ 1 & -1 & 1 & -1 & 1 & -1 & -1\\ -1 & -1 & -1 & 1 & 1 & 1 & -1\\ -1 & 1 & 1 & -1 & 1 & 1 & -1\\ 1 & -1 & 1 & 1 & 1 & 1 & 1\\ 1 & 1 & 1 & 1 & 1 & 1 & -1\\ 1 & -1 & -1 & -1 & 1 & -1 & -1\end{pmatrix}\end{array} \tag{6.43}$$

and so we can discuss some features of this model.

The model is free of on-shell tachyons and the gauge group is given by the model-independent contribution from the NS (untwisted) sector giving the vector bosons of $SO(10) \times U(1)^3 \times SO(4)^3 \times SU(2)^8$, as well as the additional gauge bosons arising from the presence of $\psi^\mu\,|z_1 + z_2\rangle$ in the massless spectrum, as well as additional scalars from the $\{\lambda^a\}\{\bar{\lambda}^b\}\,|z_k\rangle$, $k = 1, 2$ and λ^a is some left-moving oscillator not equal to ψ^μ and $\bar{\lambda}^b$ is any right-moving oscillator with NS boundary conditions in z_k. These additional scalars arise in the untwisted sector necessarily to give the scalar moduli degrees of freedom. With the gauge enhancement, the full gauge group of the model becomes

$$SO(10) \times U(1)^3 \times SO(4)^3 \times SO(8)^2. \tag{6.44}$$

Apart from these untwisted sector gauge bosons and scalars though, the massless spectrum contains exclusively fermionic states, as advertised for a Type $\bar{0}$ configuration. These

fermionic sectors are

$$\begin{aligned}
&\tilde{S},\quad \tilde{S}+z_1,\quad \tilde{S}+z_1+z_2,\quad \tilde{S}+z_2,\\
&b_1+b_2+b_3+G,\\
&\tilde{S}+b_i+b_j+G,\\
&\tilde{S}+b_i+b_j+z_1+G,\\
&\mathbb{1}+\tilde{S}+b_i+G,\\
&\mathbb{1}+\tilde{S}+b_i+z_1+G,
\end{aligned} \tag{6.45}$$

where $i\neq j\neq k\in\{1,2,3\}$. This is notably all the possible fermionic massless sectors except $b_{1,2,3}$ which generate the $\mathbf{16}/\overline{\mathbf{16}}$ of $SO(10)$.

Within the class of models with the minimal basis (6.41), possible twisted bosons may arise from the vectorial sectors

$$\begin{aligned}
V^1&=b_2+b_3+G,\\
V^2&=b_1+b_3+G,\\
V^3&=b_1+b_2+G,
\end{aligned} \tag{6.46}$$

which come with a right–moving oscillator, and the fermionic spinorial sectors

$$\begin{aligned}
B^1&=b_2+b_3+z_1+G,\\
B^2&=b_1+b_3+z_1+G,\\
B^3&=b_1+b_2+z_1+G,\\
B^4&=\mathbb{1}+b_1+z_1+G,\\
B^5&=\mathbb{1}+b_2+z_1+G,\\
B^6&=\mathbb{1}+b_3+z_1+G.
\end{aligned} \tag{6.47}$$

Type $\bar{0}$ models will be those in which the Hilbert space of GGSO-projected states $|S_\xi\rangle$

$$\mathcal{H}=\bigoplus_{\xi\in\Xi}\prod_{i=1}^{k}\left\{e^{i\pi v_i\cdot F_\xi}\,|S_\xi\rangle=\delta_\xi C\binom{\xi}{v_i}^*|S_\xi\rangle\right\}, \tag{6.48}$$

only has contributions from sectors ξ in the additive space Ξ with fermionic spin statistic index $\delta_\xi=-1$ at the massless level, except for the aforementioned untwisted sectors. Thus, using GGSO projections, we can derive the conditions on the GGSO phases in order to realise Type $\bar{0}$ configurations.

One easy way to derive these conditions is to first inspect the projection of the sector B^4 which can only be projected by z_1 such that

$$C\binom{\mathbb{1}+b_1+z_1+G}{z_1}=-1\quad\Longleftrightarrow\quad C\binom{z_1}{b_1}C\binom{z_1}{G}=-1. \tag{6.49}$$

Similarly, projecting B^5 and B^6 requires

$$C\binom{z_1}{b_2}C\binom{z_1}{G}=-1=C\binom{z_1}{b_3}C\binom{z_1}{G}. \tag{6.50}$$

The projection of B^1 then requires that

$$\left(1+C\binom{B^1}{b_1+G}\right)\left(1+C\binom{B^1}{z_2}\right)=0, \tag{6.51}$$

and so expanding z_2 in terms of basis vectors and using the ABK rules for these two phases results in

$$\begin{aligned} C\left(\begin{smallmatrix} B^1 \\ b_1+G \end{smallmatrix}\right) &= -C\left(\begin{smallmatrix} b_2 \\ b_1 \end{smallmatrix}\right) C\left(\begin{smallmatrix} b_2 \\ G \end{smallmatrix}\right) C\left(\begin{smallmatrix} b_3 \\ b_1 \end{smallmatrix}\right) C\left(\begin{smallmatrix} b_3 \\ G \end{smallmatrix}\right) \underbrace{C\left(\begin{smallmatrix} z_1 \\ b_1 \end{smallmatrix}\right) C\left(\begin{smallmatrix} z_1 \\ G \end{smallmatrix}\right)}_{=-1 \text{ from (6.49)}} C\left(\begin{smallmatrix} G \\ b_1 \end{smallmatrix}\right) C\left(\begin{smallmatrix} G \\ G \end{smallmatrix}\right) \\ &= -C\left(\begin{smallmatrix} b_2 \\ b_1 \end{smallmatrix}\right) C\left(\begin{smallmatrix} b_3 \\ b_1 \end{smallmatrix}\right) C\left(\begin{smallmatrix} 1 \\ G \end{smallmatrix}\right) C\left(\begin{smallmatrix} b_1 \\ G \end{smallmatrix}\right) C\left(\begin{smallmatrix} b_2 \\ G \end{smallmatrix}\right) C\left(\begin{smallmatrix} b_3 \\ G \end{smallmatrix}\right) \\ C\left(\begin{smallmatrix} B^1 \\ z_2 \end{smallmatrix}\right) &= C\left(\begin{smallmatrix} z_2 \\ b_2 \end{smallmatrix}\right) C\left(\begin{smallmatrix} z_2 \\ b_3 \end{smallmatrix}\right) C\left(\begin{smallmatrix} z_2 \\ z_1 \end{smallmatrix}\right) C\left(\begin{smallmatrix} z_2 \\ G \end{smallmatrix}\right) \\ &= -C\left(\begin{smallmatrix} b_2 \\ b_1 \end{smallmatrix}\right) C\left(\begin{smallmatrix} b_3 \\ b_1 \end{smallmatrix}\right) C\left(\begin{smallmatrix} 1 \\ G \end{smallmatrix}\right) C\left(\begin{smallmatrix} b_1 \\ G \end{smallmatrix}\right) C\left(\begin{smallmatrix} b_2 \\ G \end{smallmatrix}\right) C\left(\begin{smallmatrix} b_3 \\ G \end{smallmatrix}\right), \end{aligned} \tag{6.52}$$

i.e. they are equal. Considering also projecting B^2 and B^3 we can therefore deduce

$$C\left(\begin{smallmatrix} b_1 \\ b_2 \end{smallmatrix}\right) = C\left(\begin{smallmatrix} b_1 \\ b_3 \end{smallmatrix}\right) = C\left(\begin{smallmatrix} b_2 \\ b_3 \end{smallmatrix}\right) \tag{6.53}$$

and

$$C\left(\begin{smallmatrix} 1 \\ G \end{smallmatrix}\right) C\left(\begin{smallmatrix} b_1 \\ G \end{smallmatrix}\right) C\left(\begin{smallmatrix} b_2 \\ G \end{smallmatrix}\right) C\left(\begin{smallmatrix} b_3 \\ G \end{smallmatrix}\right) = 1. \tag{6.54}$$

Finally, we can note that the GGSO phases that can project on the V^1 sector are

$$O_{V^1} = \left\{ C\left(\begin{smallmatrix} V^1 \\ z_1 \end{smallmatrix}\right), C\left(\begin{smallmatrix} V^1 \\ z_2 \end{smallmatrix}\right), C\left(\begin{smallmatrix} V^1 \\ b_1+G \end{smallmatrix}\right) \right\}, \tag{6.55}$$

and since $B^1 = V^1 + z_1$ these can be simplified using (6.52) and (6.49) to give

$$O_{V^1} = \left\{ C\left(\begin{smallmatrix} z_1 \\ G \end{smallmatrix}\right), C\left(\begin{smallmatrix} z_1 \\ G \end{smallmatrix}\right), -1 \right\}. \tag{6.56}$$

We can write the projection condition for all possible oscillators as

$$\#\left\{ x \in O_{V^1} | x = -1 \right\} \neq 1, \tag{6.57}$$

therefore we observe that $C\left(\begin{smallmatrix} z_1 \\ G \end{smallmatrix}\right) = -1$ for the projection of V^1. Using this in equations (6.49) and (6.50) and rewriting conditions (6.53) and (6.54) we get the full conditions for the Type $\bar{0}$ string vacua

$$\begin{aligned} &C\left(\begin{smallmatrix} z_1 \\ b_1 \end{smallmatrix}\right) = C\left(\begin{smallmatrix} z_1 \\ b_2 \end{smallmatrix}\right) = C\left(\begin{smallmatrix} z_1 \\ b_3 \end{smallmatrix}\right) = 1, \quad C\left(\begin{smallmatrix} z_1 \\ G \end{smallmatrix}\right) = -1, \\ &C\left(\begin{smallmatrix} b_1 \\ b_2 \end{smallmatrix}\right) = C\left(\begin{smallmatrix} b_1 \\ b_3 \end{smallmatrix}\right), \quad C\left(\begin{smallmatrix} b_2 \\ b_3 \end{smallmatrix}\right) = C\left(\begin{smallmatrix} b_1 \\ b_3 \end{smallmatrix}\right), \\ &C\left(\begin{smallmatrix} 1 \\ G \end{smallmatrix}\right) = C\left(\begin{smallmatrix} b_1 \\ G \end{smallmatrix}\right) C\left(\begin{smallmatrix} b_2 \\ G \end{smallmatrix}\right) C\left(\begin{smallmatrix} b_3 \\ G \end{smallmatrix}\right). \end{aligned} \tag{6.58}$$

Therefore we see that 7 GGSO phases are fixed and we have 14 free phases. Similar constraints were derived for Type 0 models in ref. [4] and Section 6.1 where it was shown that in a similar minimal basis to (6.41) there were 12 free phases giving $2^{12} = 4096$ versions of a single unique Type 0 partition function.

To check whether we have 2^{14} versions of a unique partition function or not in our Type $\bar{0}$ case we must analyse the partition function, which in free fermionic models is given by the integral

$$Z = \int_{\mathcal{F}} \frac{d^2\tau}{\tau_2^2} Z_B \sum_{\alpha,\beta} C\left(\begin{smallmatrix} \alpha \\ \beta \end{smallmatrix}\right) \prod_f Z\begin{bmatrix} \alpha(f) \\ \beta(f) \end{bmatrix} = \int_{\mathcal{F}} \frac{d^2\tau}{\tau_2^3} \sum_{n.m} a_{mn}\, q^m \bar{q}^n, \tag{6.59}$$

where $d^2\tau/\tau_2^2$ is the modular invariant measure and Z_B denotes the contribution from the worldsheet bosons. The product is over the free worldsheet fermions. On the right-hand side

of (6.59) we have expanded the partition function in terms of the parameters $q \equiv e^{2\pi i\tau}$ and $\bar{q} \equiv e^{-2\pi i\bar{\tau}}$, which allows us to read off the boson-fermion degeneracies at each mass level. That is, $a_{mn} = N_b - N_f$ at mass level (m, n) and so we expect that Type $\bar{0}$ models have large negative a_{00} due to the absence of twisted bosonic states. Throughout this section we will refer to the unintegrated sum as the partition function. The whole integrated expression (6.59) represents the one-loop worldsheet vacuum energy $\Lambda_{\rm WS}$ of our theory and thus is a dimensionless quantity. It is related to the 4D spacetime cosmological constant Λ via

$$\Lambda = -\frac{1}{2}\mathcal{M}^4\Lambda_{\rm WS}, \tag{6.60}$$

where $\mathcal{M}$ is given in terms of the string mass as $\mathcal{M} = M_S/2\pi$. In the following, when we refer to the cosmological constant, we implicitly mean the spacetime value, but for simplicity, we drop the factor of $\mathcal{M}^4/2$. This can be reinstated if needed based on dimensional analysis.

Performing the calculation of the partition function for the $2^{14} = 16384$ Type $\bar{0}$ configurations we find that they all share the partition function

$$Z = 2\,q^0\bar{q}^{-1} - 728\,q^0\bar{q}^0 + 288\,q^{1/2}\bar{q}^{-1/2} + 1088\,q^{-1/2}\bar{q}^{1/2} + 38400\,q^{1/2}\bar{q}^{1/2} + \cdots . \tag{6.61}$$

Note that the uniqueness of the partition function does not necessarily imply that the models are identical, it merely means that the state degeneracies match at each mass level. We see that there are no on-shell tachyons and the absence of twisted bosons ensures a large negative contribution at the massless level $N_b^0 - N_f^0 = -728$. We can calculate the cosmological constant now for this unique case. Due to the abundance of fermionic states compared to bosonic ones, we expect a positive cosmological constant, and performing the modular integral using the techniques of Section 4.3 we, indeed, find

$$\Lambda = 238.38 \times \mathcal{M}^4. \tag{6.62}$$

which is as expected dominated by the fermionic degrees of freedom and hence larger than usual.

In Section 6.1 it was shown that Type 0 models exhibit misaligned supersymmetry [84], and further details of this behaviour were given. Similarly, all Type $\bar{0}$ models presented in this section exhibit a form of misaligned supersymmetry, meaning that the boson-fermion degeneracies oscillate while ascending through the tower of massive states.

6.2.1 Classification of Type $\bar{0}$ $\tilde{S}$-Models

In order to do a more general search for Type $\bar{0}$ models we can generalise from the basis (6.41) to

$$\begin{aligned}
\mathbb{1} &= \{\psi^\mu,\ \chi^{1,\dots,6}, y^{1,\dots,6}, w^{1,\dots,6} \mid \overline{y}^{1,\dots,6}, \overline{w}^{1,\dots,6}, \overline{\psi}^{1,\dots,5}, \overline{\eta}^{1,2,3}, \overline{\phi}^{1,\dots,8}\},\\
\tilde{S} &= \{\psi^\mu, \chi^{1,\dots,6} \mid \overline{\phi}^{3,4,5,6}\},\\
T_1 &= \{y^{1,2}, w^{1,2} \mid \overline{y}^{1,2}, \overline{w}^{1,2}\},\\
T_2 &= \{y^{3,4}, w^{3,4} \mid \overline{y}^{3,4}, \overline{w}^{3,4}\},\\
T_3 &= \{y^{5,6}, w^{5,6} \mid \overline{y}^{5,6}, \overline{w}^{5,6}\},\\
b_1 &= \{\psi^\mu, \chi^{12}, y^{34}, y^{56} \mid \overline{y}^{34}, \overline{y}^{56}, \overline{\eta}^1, \overline{\psi}^{1,\dots,5}\},\\
b_2 &= \{\psi^\mu, \chi^{34}, y^{12}, w^{56} \mid \overline{y}^{12}, \overline{w}^{56}, \overline{\eta}^2, \overline{\psi}^{1,\dots,5}\},\\
b_3 &= \{\psi^\mu, \chi^{56}, w^{12}, w^{34} \mid \overline{w}^{12}, \overline{w}^{34}, \overline{\eta}^3, \overline{\psi}^{1,\dots,5}\},\\
z_1 &= \{\overline{\phi}^{1,\dots,4}\},
\end{aligned} \tag{6.63}$$

where introducing T_i, $i = 1, 2, 3$ allows for internal symmetric shifts around the 3 internal T^2 tori. Since we have 9 basis vectors there are $2^{9(9-1)/2} = 2^{36} \sim 6.87 \times 10^{10}$ independent GGSO phase configurations.

The bosonic sectors that need projecting in this basis are similar to (6.46), up to allowing for the shifts induced by T_i. Explicitly, there are 15 vectorial bosonic sectors

$$\begin{aligned}
V^1_{pq} &= b_2 + b_3 + T_1 + pT_2 + qT_3,\\
V^2_{pq} &= b_1 + b_3 + T_2 + pT_1 + qT_3,\\
V^3_{pq} &= b_1 + b_2 + T_3 + pT_1 + qT_2,\\
V^4 &= T_1 + T_2,\\
V^5 &= T_1 + T_3,\\
V^6 &= T_2 + T_3,
\end{aligned} \tag{6.64}$$

which come with a right–moving oscillator and $p, q = 0, 1$. Additionally, there are 30 fermionic spinorial sectors

$$\begin{aligned}
B^1_{pq} &= b_2 + b_3 + z_1 + T_1 + pT_2 + qT_3,\\
B^2_{pq} &= b_1 + b_3 + z_1 + T_2 + pT_1 + qT_3,\\
B^3_{pq} &= b_1 + b_2 + z_1 + T_3 + pT_1 + qT_2,\\
B^4_{pq} &= \mathbb{1} + b_1 + z_1 + T_1 + pT_2 + qT_3,\\
B^5_{pq} &= \mathbb{1} + b_2 + z_1 + T_2 + pT_1 + qT_3,\\
B^6_{pq} &= \mathbb{1} + b_3 + z_1 + T_3 + pT_1 + qT_2,\\
B^7 &= T_1 + T_2 + z_1,\\
B^8 &= T_1 + T_3 + z_1,\\
B^9 &= T_2 + T_3 + z_1,\\
B^{10} &= T_1 + T_2 + z_2,\\
B^{11} &= T_1 + T_3 + z_2,\\
B^{12} &= T_2 + T_3 + z_2.
\end{aligned} \tag{6.65}$$

Implementing the GGSO projection conditions on all the sectors and scanning over 10^8 random GGSO phase configurations resulted in uncovering 5676 Type $\bar{0}$ configurations that correspond to just two distinct tachyon–free and two distinct tachyonic partition functions. The first tachyon–free model has the partition function

$$Z = 2\,q^0\bar{q}^{-1} - 440\,q^0\bar{q}^0 + 32\,q^{1/4}\bar{q}^{-3/4} - 6080\,q^{1/4}\bar{q}^{1/4} + \cdots, \tag{6.66}$$

and cosmological constant

$$\Lambda = 213.27 \times \mathcal{M}^4. \tag{6.67}$$

Whereas the second tachyon–free model has the partition function

$$Z = 2\,q^0\bar{q}^{-1} - 504\,q^0\bar{q}^0 + 48\,q^{1/4}\bar{q}^{-3/4} - 12192\,q^{1/4}\bar{q}^{1/4} + \cdots, \tag{6.68}$$

and cosmological constant

$$\Lambda = 278.60 \times \mathcal{M}^4. \tag{6.69}$$

Both models contain the same gauge boson enhancement and additional scalars from the sectors z_1, z_2 and $z_1 + z_2$ as in the case with a minimal basis (6.41). Other than these untwisted bosons the two models contain only twisted fermionic states in their massless spectra, as required for Type $\bar{0}$ configurations.

Regarding the two tachyonic models, we have one model with the partition function

$$Z = 2\,q^0\bar{q}^{-1} + 32q^{-1/4}\bar{q}^{-1/4} - 1016\,q^0\bar{q}^0 + 4096\,q^{1/4}\bar{q}^{1/4} + \cdots, \tag{6.70}$$

which has 32 tachyonic states and one with the partition function

$$Z = 2\,q^0\bar{q}^{-1} + 48\,q^{-1/4}\bar{q}^{-1/4} - 1272\,q^0\bar{q}^0 + 5120\,q^{1/4}\bar{q}^{1/4} + \cdots, \tag{6.71}$$

which has 48 tachyonic states. Such models with a tachyonic instability should not be written off as of no interest. In particular, moving away from the free fermionic point

in the moduli space or considering the theory in a different background may stabilise the model. Furthermore, there may be ways to connect such unstable vacua to stable ones via interpolation.

6.2.2 Classification Type $\bar{0}$ S-Models

We can now do a similar exploration of Type $\bar{0}$ models within a class of models which include the SUSY generating basis vector S. We employ a very familiar choice of $SO(10)$ basis

$$\begin{aligned}
\mathbb{1} &= \{\psi^\mu,\ \chi^{1,\ldots,6}, y^{1,\ldots,6}, w^{1,\ldots,6} \mid \overline{y}^{1,\ldots,6}, \overline{w}^{1,\ldots,6}, \overline{\psi}^{1,\ldots,5}, \overline{\eta}^{1,2,3}, \overline{\phi}^{1,\ldots,8}\},\\
S &= \{\psi^\mu, \chi^{1,\ldots,6}\},\\
T_1 &= \{y^{1,2}, w^{1,2} \mid \overline{y}^{1,2}, \overline{w}^{1,2}\},\\
T_2 &= \{y^{3,4}, w^{3,4} \mid \overline{y}^{3,4}, \overline{w}^{3,4}\},\\
T_3 &= \{y^{5,6}, w^{5,6} \mid \overline{y}^{5,6}, \overline{w}^{5,6}\},\\
b_1 &= \{\chi^{3,4,5,6}, y^{34}, y^{56} \mid \overline{y}^{34}, \overline{y}^{56}, \overline{\eta}^1, \overline{\psi}^{1,\ldots,5}\},\\
b_2 &= \{\chi^{1,2,5,6}, y^{12}, y^{56} \mid \overline{y}^{12}, \overline{y}^{56}, \overline{\eta}^2, \overline{\psi}^{1,\ldots,5}\},\\
z_1 &= \{\overline{\phi}^{1,\ldots,4}\},\\
z_2 &= \{\overline{\phi}^{5,\ldots,8}\},
\end{aligned} \tag{6.72}$$

which is exactly the same as that used to classify non–SUSY string models in ref. [82]. We will note the important linear combination in this basis

$$x = 1 + S + \sum_{i=1,2,3} T_i + \sum_{k=1,2} z_k, \tag{6.73}$$

and then have the combination $b_3 = b_1 + b_2 + x$. As in the $\tilde{S}$-models we have 9 basis vectors and so the number of independent GGSO phase configurations is $2^{9(9-1)/2} = 2^{36} \sim 6.87\times10^{10}$.

A key difference between this basis and the basis (6.63) is that there exists a supersymmetric subspace of the full space for certain choices of GGSO phase. In particular, the S sector generates supersymmetry whenever

$$C\left(\begin{smallmatrix} S \\ T_i \end{smallmatrix}\right) = C\left(\begin{smallmatrix} S \\ z_k \end{smallmatrix}\right) = -1, \qquad i = 1,2,3 \text{ and } k = 1,2 \tag{6.74}$$

which, furthermore, automatically ensures the projection of tachyonic sectors through the S GGSO projection.

Now we turn to the massless bosonic vectorial sectors that in our S–models arise from

$$\begin{aligned}
&b_i + x + pT_j + qT_k,\\
&T_1 + T_2,\\
&T_1 + T_3,\\
&T_2 + T_3,
\end{aligned} \tag{6.75}$$

and the massless bosonic spinorial sectors from

$$\begin{aligned}
&b_i + pT_j + qT_k,\\
&b_i + x + z_1 + pT_j + qT_k,\\
&b_i + x + z_2 + pT_j + qT_k,\\
&T_1 + T_2 + z_1,\\
&T_1 + T_3 + z_1,\\
&T_2 + T_3 + z_1,\\
&T_1 + T_2 + z_2,\\
&T_1 + T_3 + z_2,\\
&T_2 + T_3 + z_2,
\end{aligned} \tag{6.76}$$

where $i \neq j \neq k \in \{1,2,3\}$ and $p,q \in \{0,1\}$. We can now search for Type $\bar{0}$ GGSO configurations by implementing the conditions for the GGSO projection of all these massless twisted bosonic sectors.

In a random scan of 10^8 independent GGSO phase configurations, we found one supersymmetric model which contains a very simple massless spectrum containing the untwisted gauge bosons from the NS sector and its gauginos from the S sector, along with gauge enhancements and additional scalars of some form from z_1, z_2, z_1+z_2 and x and their superpartners from $S+z_1, S+z_2, S+z_1+z_2$ and $S+x$, respectively. The other Type $\bar{0}$ models arising in our 10^8 scan are non–supersymmetric.

All the Type $\bar{0}$ models are summarised in Table 6.3 with their partition functions, key characteristics and frequency within the sample delineated. Where we recall that the frequency refers to the number of different GGSO phase configurations corresponding to the same partition function. The projected total number is simply how many we expect in the full space of 2^{36} independent GGSO phase configurations. In principle, the exact constraints on the GGSO phases for each model could be derived and the free phases found to derive the exact number of each model in the total space.

6.3 Discussion and Conclusion

In this section, we explored the existence of both Type 0 and Type $\bar{0}$ models in heterotic orbifold compactifications. We called Type 0 string vacua those that do not contain any massless fermionic states. They have been of interest in other string theory limits, e.g. the issue of tree-level stability has been studied in the framework of Type II orientifolds, whereas other authors have advocated that there is a holographic duality of the Type 0B string theory and four-dimensional non-supersymmetric Yang-Mills theory [122, 123]. In this work based on [4], we demonstrated the existence of Type 0 $\mathbb{Z}_2 \times \mathbb{Z}_2$ heterotic string orbifolds. We showed that there exists a large degree of redundancy in the space of GGSO projection coefficients when the Type 0 restrictions are implemented. We explored the existence of such configurations in several constructions. The one presented in Section 6.1 corresponds to essentially a unique configuration out of a priori 2^{21} discrete GGSO choices. We showed this uniqueness analytically in Section 6.1.1 as well as by the corresponding analysis of the

Partition Function	$\Lambda\,[\mathcal{M}^4]$	**Tachyons?**	**SUSY?**	**# Models in Sample**	**Total # Expected**
$Z = 0$	0	No	Yes	562	3.86×10^5
$Z = 2\bar{q}^{-1} - 632 + 48q^{1/4}\bar{q}^{-3/4} - 8096q^{1/4}\bar{q}^{1/4} + \cdots$	293.8	No	No	389	2.67×10^5
$Z = 2\bar{q}^{-1} - 120 + 32q^{1/4}\bar{q}^{-3/4} - 6080q^{1/4}\bar{q}^{1/4} + \cdots$	125.6	No	No	284	1.95×10^5
$Z = 2\bar{q}^{-1} - 568 + 32q^{1/4}\bar{q}^{-3/4} - 1984q^{1/4}\bar{q}^{1/4} + \cdots$	223.97	No	No	1163	7.99×10^5
$Z = 2\bar{q}^{-1} - 504 + 32q^{1/4}\bar{q}^{-3/4} + 4128q^{1/4}\bar{q}^{1/4} + \cdots$	158.64	No	No	715	3.91×10^5
$Z = 2\bar{q}^{-1} + 32q^{-1/4}\bar{q}^{-1/4} - 664 + 6144q^{1/4}\bar{q}^{1/4} + \cdots$	∞	Yes	No	287	1.97×10^5
$Z = 2\bar{q}^{-1} + 32q^{-1/4}\bar{q}^{-1/4} - 1272 + 5888^{1/4}\bar{q}^{1/4} + \cdots$	∞	Yes	No	290	1.99×10^5
$Z = 2\bar{q}^{-1} + 32q^{-1/4}\bar{q}^{-1/4} - 632 - 512q^{1/4}\bar{q}^{1/4} + \cdots$	∞	Yes	No	301	2.07×10^5
$Z = 2\bar{q}^{-1} + 32q^{-1/4}\bar{q}^{-1/4} - 1528 + 4608q^{1/4}\bar{q}^{1/4} + \cdots$	∞	Yes	No	429	2.95×10^5
$Z = 2\bar{q}^{-1} + 32q^{-1/4}\bar{q}^{-1/4} - 1528 + 11008q^{1/4}\bar{q}^{1/4} + \cdots$	∞	Yes	No	395	2.71×10^5
$Z = 2\bar{q}^{-1} + 48q^{-1/4}\bar{q}^{-1/4} - 1016 - 1792q^{1/4}\bar{q}^{1/4} + \cdots$	∞	Yes	No	155	1.07×10^5
$Z = 2\bar{q}^{-1} + 144q^{-1/4}\bar{q}^{-1/4} - 504 + 9472^{1/4}\bar{q}^{1/4} + \cdots$	∞	Yes	No	153	1.05×10^5

TABLE 6.3: *Summary of Type* $\bar{0}$ *models arising from the basis (6.72). The cosmological constant* Λ *is expressed in units of* $\mathcal{M}^4$ *as in (6.60).*

partition function in Section 6.1.1. In Sections 6.1.2 and 6.1.3 we performed a wider classification in $\tilde{S}$–models and S–models, where the first class correspond to compactifications of a tachyonic ten-dimensional heterotic string vacuum, whereas the second correspond to compactifications of the ten-dimensional non–tachyonic $SO(16) \times SO(16)$. We showed that the Type 0 models in both cases contain physical tachyons at the free fermionic point in the moduli space. These vacua are therefore necessarily unstable. we demonstrated the existence of misaligned supersymmetry in the Type 0 models that guarantee the finiteness of the one-loop amplitude, aside from the divergence due to the tachyonic states. Given their rather restrictive structure, the Type 0 models may be useful in exploring the string dynamics in cosmological scenarios in the spirit of the analysis performed in ref. [82].

We also explored the existence of $Z_2 \times Z_2$ heterotic string orbifolds that do not contain any massless spacetime scalar bosons from the twisted sectors. In analogy with the Type 0 models that were, we dubbed such configurations Type $\bar{0}$ models. We presented two classes of such

models, where the first are of the $\tilde{S}$–models Type, whereas the second belong to the class of S–models. We note that the second class also contains supersymmetric models that have a vanishing cosmological constant, whereas all other Type $\bar{0}$ models found in both classes are non–supersymmetric and necessarily have an excess of fermionic over bosonic states and therefore have a positive cosmological constant. While our findings at this stage should be regarded as mere curiosities, it is plausible that they may contribute to the understanding of the string dynamics in the early universe. We have also found that in all the Type $\bar{0}$ models, there are no spinorial or anti–spinorial representations of the $SO(10)$ gauge group. This is necessarily the case in the supersymmetric $\bar{0}$ configurations, which therefore necessarily have a vanishing Euler characteristic. The non–supersymmetric $\bar{0}$ configurations may therefore be interpreted as supersymmetric $\bar{0}$ models, in which supersymmetry is maximally violated. A feature that may be explored by studying the interpolations between the two cases.

7 Non-Supersymmetric Asymmetric Heterotic Orbifolds

The classification methodology so far discussed has solely been developed for models with symmetric boundary conditions. The heterotic string in general, and the free fermionic models in particular, allow for more general assignments of boundary conditions, which are asymmetric between the left and the right-moving worldsheet fermions. These can be complicated assignments that realise the non-Abelian gauge symmetries at higher level Kac-Moody algebra [124, 125], or more mundane assignments that leave the gauge symmetries at level $k = 1$. Although symmetric in the $\mathbb{Z}_2 \times \mathbb{Z}_2$ twists, these asymmetric assignments produce asymmetric shift orbifold models, which amount to non-geometric compactifications, a review of which is given in ref. [126]. Completing a first step towards the extension of the classification methodology to such asymmetric orbifolds is the objective of this chapter. We choose to study models with Flipped $SU(5)$ (FSU5) gauge symmetry for both the $\mathcal{N} = 0$ and $\mathcal{N} = 1$ cases.

There are several profound phenomenological implications of choosing such asymmetric boundary condition assignments rather than symmetric ones. Of crucial importance to us is how they help to realise moduli fixing [67], top-quark Yukawa couplings from the untwisted sector [127] and doublet-triplet splitting [128]. Furthermore, we note that the early free fermionic constructions [129, 130] do utilise asymmetric boundary conditions, which gave rise to a stringy explanation of the hierarchical top-bottom quark mass splitting [131, 132].

The fixing of some of the three complex and Kähler structures that comprise the moduli space of the $\mathbb{Z}_2 \times \mathbb{Z}_2$ orbifold is of particular significance in the context of investigating the one-loop potential generating the (leading order) vacuum energy of a string model. This is of key interest in this work since we classify non-supersymmetric configurations. Various works on non-supersymmetric string vacua have attempted to use Scherk-Schwarz supersymmetry breaking [61, 63, 133–135] and a so-called 'super no-scale' condition [51, 113, 136] to argue for a suppression of the one-loop cosmological constant. Florakis and Rizos demonstrated the existence of free fermion models with positive vacuum energy at the minimum of the potential for one of the radii [82, 83, 108]. However, in order to argue for the stability of the vacua one needs to incorporate all moduli into the analysis, which is far too cumbersome in the symmetric orbifold case to be performed. This is where asymmetric orbifolds come into their own, as they give some control over the fixing of certain moduli.

This chapter is organised as follows, in Section 2 we overview the key aspects of free fermionic model building. In Section 3 we explain the translation of free fermionic constraints into the language of Boolean algebra. Then we turn to explain the construction of Flipped $SU(5)$ asymmetric orbifold models for classification in Section 4. In Section 5 we classify the asymmetric pairings of the internal fermions according to key characteristics such as the number of untwisted moduli they preserve. Following this, Section 6 details generic features of the FSU5 models we classify including the structure of their partition functions, whilst

Section 7 and Section 8 deal with classifying specific example Classes of models and their classification results. Finally, in Section 9 we give conclusions.

7.1 Asymmetric Orbifolds via Free Fermions

In this section, we begin the task of extending the classification methodology to the space of asymmetric orbifolds. We can take the NAHE-set [120] as the starting point for classifying large spaces of asymmetric orbifolds, which is defined by the set of basis vectors

$$\begin{aligned}
\mathbb{1} &= \{\psi^\mu,\ \chi^{1,\dots,6}, y^{1,\dots,6}, w^{1,\dots,6} \mid \overline{y}^{1,\dots,6}, \overline{w}^{1,\dots,6}, \overline{\psi}^{1,\dots,5}, \overline{\eta}^{1,2,3}, \overline{\phi}^{1,\dots,8}\},\\
S &= \{\psi^\mu, \chi^{1,\dots,6}\ \}\\
b_1 &= \{\psi^\mu, \chi^{12}, y^{34}, y^{56} \mid \overline{y}^{34}, \overline{y}^{56}, \overline{\psi}^{1,\dots,5}, \overline{\eta}^{1}\},\\
b_2 &= \{\psi^\mu, \chi^{34}, y^{12}, w^{56} \mid \overline{y}^{12}, \overline{w}^{56}, \overline{\psi}^{1,\dots,5}, \overline{\eta}^{2}\},\\
b_3 &= \{\psi^\mu, \chi^{56}, w^{12}, w^{34} \mid \overline{w}^{12}, \overline{w}^{34}, \overline{\psi}^{1,\dots,5}, \overline{\eta}^{3}\}
\end{aligned} \tag{7.1}$$

which gives rise to an $SO(10)$ symmetric GUT and due to the S vector can realise $\mathcal{N}=1$ supersymmetry for appropriate choices of GGSO phases. We will then choose to add the additional basis vectors:

$$\begin{aligned}
x &= \{\bar{\psi}^{1,\dots,5}, \bar{\eta}^{1,2,3}\}\\
z_1 &= \{\bar{\phi}^{1,\dots,4}\}
\end{aligned} \tag{7.2}$$

such that z_1 reduces the dimension of the Hidden gauge group and the x vector induces the enhancement $SO(10)\times U(1)\to E_6$ for certain choices of GGSO phases which can be seen as taking us from the space of vacua with $(2,0)$ worldsheet supersymmetry to those with $(2,2)$. The untwisted gauge group is

$$SO(10)\times SO(4)^3\times U(1)^3\times SO(8)\times SO(8) \tag{7.3}$$

at this level, with the three $SO(4)$ factors arising from the three groups of internal fermions from the b_k, $k=1,2,3$, such that the NS sector gauge bosons can be written

$$\begin{aligned}
&\psi^\mu\{\bar{y}^{3,4,5,6}\}\{\bar{y}^{3,4,5,6}\}\left|0\right\rangle_{NS},\\
&\psi^\mu\{\bar{y}^{1,2},\bar{w}^{5,6}\}\{\bar{y}^{1,2},\bar{w}^{5,6}\}\left|0\right\rangle_{NS}\\
&\psi^\mu\{\bar{w}^{1,2,3,4}\}\{\bar{w}^{1,2,3,4}\}\left|0\right\rangle_{NS}.
\end{aligned} \tag{7.4}$$

The NAHE-set naturally implements a $\mathbb{Z}_2\times\mathbb{Z}_2$ orbifolding through the twist vectors b_k that leave an untwisted moduli space of

$$\left(\frac{SO(2,2)}{SO(2)\times SO(2)}\right)^3 \tag{7.5}$$

where each of the three factors is parameterised by the moduli scalar fields from the NS sector

$$h_{ij} = \left|\chi^i\right\rangle_L \otimes \left|\bar{y}^j\bar{w}^j\right\rangle_R = \begin{cases}(i,j=1,2)\\(i,j=3,4)\\(i,j=5,6)\end{cases}. \tag{7.6}$$

In free fermionic models, as discussed extensively in Section 4.2, these untwisted moduli are in one-to-one correspondence with marginal operators that generate Abelian Thirring Interactions. For the NAHE-set the only such marginal operators left invariant are

$$J_L^i(z)\bar{J}_R^j(\bar{z}) =: y^i w^i :: \bar{y}^j \bar{w}^j := \begin{cases} (i,j=1,2) \\ (i,j=3,4) \\ (i,j=5,6). \end{cases} \tag{7.7}$$

From this it is straightforward to observe that the projection or retention of moduli is governed by the boundary conditions of the set of 12 internal real fermions $\{y^I, w^I \mid \bar{y}^I, \bar{w}^I\}$. In particular, we note that if the basis remains left-right symmetric in these internal fermions then all the untwisted moduli of the NAHE-set are retained. This is a central reason for attempting to classify asymmetric orbifolds models where the internal real fermions $\{y^I, w^I \mid \bar{y}^I, \bar{w}^I\}$ are not left-right symmetric.

In order to make the connection between the fields h_{ij} and the familiar three Kähler and three complex structure moduli of the $\mathbb{Z}_2 \times \mathbb{Z}_2$ orbifold we can construct six complex moduli from the six real ones of eq. (7.6). For the first complex plane, we can write

$$\begin{aligned} H_1^{(1)} &= \frac{1}{\sqrt{2}}(h_{11} + ih_{21}) = \frac{1}{\sqrt{2}} \left|\chi^1 + i\chi^2\right\rangle_L \otimes \left|\bar{y}^1\bar{w}^1\right\rangle_R \\ H_2^{(1)} &= \frac{1}{\sqrt{2}}(h_{12} + ih_{22}) = \frac{1}{\sqrt{2}} \left|\chi^1 + i\chi^2\right\rangle_L \otimes \left|\bar{y}^2\bar{w}^2\right\rangle_R, \end{aligned} \tag{7.8}$$

which can then be combined to define the Kähler and complex structure moduli for the first complex plane

$$\begin{aligned} T^{(1)} &= \frac{1}{\sqrt{2}}(H_1^{(1)} - iH_2^{(1)}) = \frac{1}{\sqrt{2}} \left|\chi^1 + i\chi^2\right\rangle_L \otimes \left|\bar{y}^1\bar{w}^1 - i\bar{y}^2\bar{w}^2\right\rangle_R \\ U^{(1)} &= \frac{1}{\sqrt{2}}(H_1^{(1)} + iH_2^{(1)}) = \frac{1}{\sqrt{2}} \left|\chi^1 + i\chi^2\right\rangle_L \otimes \left|\bar{y}^1\bar{w}^1 + i\bar{y}^2\bar{w}^2\right\rangle_R \end{aligned} \tag{7.9}$$

and similarly for $T^{(2),(3)}$ and $U^{(2),(3)}$.

We choose to classify Flipped SU(5) models such that a single basis vector both breaks the $SO(10)$ GUT and assigns asymmetric pairings to the internal fermions. This vector can then be taken to be of the general form

$$\boldsymbol{\gamma} = \boldsymbol{A} + \{\bar{\psi}^{1,\ldots,5} = \bar{\eta}^{1,2,3} = \bar{\phi}^{1,2,6,7} = \frac{1}{2}\} + \boldsymbol{B}. \tag{7.10}$$

where $\boldsymbol{A}$ ensures that the internal fermions are not symmetrically paired and $\boldsymbol{B}$ assigns appropriate boundary conditions to the hidden complex fermions

$$\boldsymbol{B} = \{B(\bar{\phi}^3), B(\bar{\phi}^4), B(\bar{\phi}^5), B(\bar{\phi}^8)\}, \tag{7.11}$$

where we choose real boundary conditions $B(\bar{\phi}^{3,4,5,8}) = 0, 1$ so as to be consistent with the modular invariance rules

$$\begin{aligned} N_\gamma \boldsymbol{\gamma} \cdot \boldsymbol{\gamma} &= 0 \bmod 8 \\ N_{z_1\gamma} z_1 \cdot \boldsymbol{\gamma} &= 0 \bmod 4, \end{aligned} \tag{7.12}$$

where N_γ is the smallest positive integer for which $N_\gamma \boldsymbol{\gamma} = 0$ and $N_{z_1\gamma}$ is the least common multiple of N_{z_1} and N_γ.

The supercurrent constraint (3.47) imposes a different constraint on these boundary conditions depending on whether $\boldsymbol{\gamma}$ is fermionic or bosonic. In the bosonic case we can write $\boldsymbol{A}$ as

$$\boldsymbol{A} = \{A(y^1), ..., A(y^6), A(w^1), ..., A(w^6) \mid A(\bar{y}^1), ..., A(\bar{y}^6), A(\bar{w}^1), ..., A(\bar{w}^6)\} \tag{7.13}$$

and (3.47) thus imposes that the boundary condition of the holomorphic internal fermions are

$$(y^I, w^I) = (1,1) \text{ or } (0,0), \quad I = 1, ..., 6 \tag{7.14}$$

to ensure a consistent supercurrent. On the other hand, if $\boldsymbol{\gamma}$ is fermionic then we choose $\boldsymbol{A}$ to be of the form

$$\boldsymbol{A} = \{\psi^\mu, \chi^{12}, A(y^1), ..., A(y^6), A(w^1), ..., A(w^6) \mid A(\bar{y}^1), ..., A(\bar{y}^6), A(\bar{w}^1), ..., A(\bar{w}^6)\} \tag{7.15}$$

and the supercurrent consistency imposes that

$$(y^I, w^I) = \begin{cases} (0,0) \text{ or } (1,1), & I = 1,2 \\ (1,0) \text{ or } (0,1), & I = 3, ..., 6 \end{cases} \tag{7.16}$$

and similar for the cases where $A(\chi^{34}) = 1$ or $A(\chi^{56}) = 1$ and $A(\chi^{12}) = 0$.

The next step towards classifying Flipped SU(5) asymmetric orbifolds is the addition of the symmetric shift vectors

$$e_i = \{y^i, w^i \mid \bar{y}^i, \bar{w}^i\}, \quad i = 1, ..., 6 \tag{7.17}$$

so long as they are consistent with the choice of $\boldsymbol{\gamma}$, in the sense that they satisfy the modular invariance rule

$$N_{\gamma e_i} \boldsymbol{\gamma} \cdot e_i = 0 \mod 4. \tag{7.18}$$

In the previous classifications of symmetric orbifolds all six e_i's are present in the basis to impose the 12 symmetric pairings between $\{y^I, w^I\}$ and $\{\bar{y}^I, \bar{w}^I\}$ to form 12 Ising model operators. One corollary of this symmetric pairing is that the rank of the untwisted gauge group from the holomorphic sector takes its minimal value of 16. However, asymmetric pairings will generate up to six additional $U(1)$'s from the pairing of two anti-holomorphic internal fermions $\{\bar{y}^I, \bar{w}^I\}$.

Putting this all together, we can write the basis we take as a starting point for exploring the space of asymmetric orbifolds as

$$\begin{aligned}
\mathbb{1} &= \{\psi^\mu,\ \chi^{1,\dots,6}, y^{1,\dots,6}, w^{1,\dots,6} \mid \overline{y}^{1,\dots,6}, \overline{w}^{1,\dots,6}, \overline{\psi}^{1,\dots,5}, \overline{\eta}^{1,2,3}, \overline{\phi}^{1,\dots,8}\},\\
S &= \{\psi^\mu, \chi^{1,\dots,6}\ \}\\
e_i &= \{y^i, w^i \mid \bar{y}^i, \bar{w}^i\}, \quad i \subset \{1,2,3,4,5,6\}\\
b_1 &= \{\psi^\mu, \chi^{12}, y^{34}, y^{56} \mid \overline{y}^{34}, \overline{y}^{56}, \overline{\psi}^{1,\dots,5}, \overline{\eta}^1\},\\
b_2 &= \{\psi^\mu, \chi^{34}, y^{12}, w^{56} \mid \overline{y}^{12}, \overline{w}^{56}, \overline{\psi}^{1,\dots,5}, \overline{\eta}^2\},\\
b_3 &= \{\psi^\mu, \chi^{56}, w^{12}, w^{34} \mid \overline{w}^{12}, \overline{w}^{34}, \overline{\psi}^{1,\dots,5}, \overline{\eta}^3\}\\
z_1 &= \{\bar{\phi}^{1,2,3,4}\}\\
x &= \{\bar{\psi}^{1,\dots,5}, \bar{\eta}^{1,2,3}\}\\
\boldsymbol{\gamma} &= \boldsymbol{A} + \{\bar{\psi}^{1,\dots,5} = \bar{\eta}^{1,2,3} = \bar{\phi}^{1,2,5,6} = \frac{1}{2}\} + \boldsymbol{B}
\end{aligned} \tag{7.19}$$

We furthermore note the existence of the following important linear combination of hidden fermions

$$z_2 = \mathbb{1} + \sum_{k=1}^{3} b_k + z_1 = \{\bar{\phi}^{5,6,7,8}\}. \tag{7.20}$$

and the combination generating the internal fermions

$$G = S + \sum_{k=1}^{3} b_k + x = \{y^I, w^I \mid \bar{y}^I, \bar{w}^I\}, \quad I = 1,2,3,4,5,6. \tag{7.21}$$

Our approach towards this classification will be two-fold. The first step is to classify the asymmetric pairings within $\boldsymbol{\gamma}$ given through the $\boldsymbol{A}$ vector in both the bosonic case (7.13) and fermionic case (7.15) with respect to their impact on important characteristics of the resultant models such as the number of retained moduli. The details are presented in the next section. This step is new to the classification program due to asymmetric orbifolding. The second step is to pick a particular pairing and perform a classification of the resultant space of vacua according to their phenomenological features, such as the number of particle generations at the Flipped $SU(5)$ level.

The exact relation between asymmetric fermionic constructions, achieved by asymmetric pairings of worldsheet fermions encapsulated in the basis vector $\boldsymbol{\gamma}$, and asymmetric Narain orbifolds, achieved by asymmetric orbifolding, is beyond the scope of this thesis. However, it is important to note that in-depth discussions of asymmetric orbifolds in the bosonic picture do exist [137–139]. An interesting aspect of those works is the notion that it is only asymmetric twists that can project geometric moduli. Hence in what follows, we will refer to the asymmetric pairing of fermions which project moduli as twists and those that do-not as shifts. A more in-depth look at the relationship between the asymmetric orbifold in the bosonic and fermionic pictures remains to be done.

7.2 Classification of Asymmetric Pairings

Due to the centrality of the pairings of the internal fermions $\{y^I, w^I \mid \bar{y}^I, \bar{w}^I\}$ in determining important features of the class of asymmetric orbifold models, a useful first step towards classifying the asymmetric orbifolds is to classify their possible pairings defined through the vector $\boldsymbol{A}$. The key criteria we can classify these pairings according to will be the untwisted moduli they retain and their number of possible chiral generations.

A convenient tool for classifying these pairings is to use machine learning tools such as an SAT/SMT solver as discussed in [19]. These tools provide a fast and convenient way to solve the constraints on the allowed basis vectors. Imposing the relevant supercurrent constraint and ensuring the pairing is asymmetric and consistent with the NAHE set allows us to generate all possible pairings as output from the SAT/SMT solver. More detailed discussions on machine learning tools in the string landscape are beyond the scope of this thesis, but we refer the reader to [6, 19] for reference.

Asymmetric Pairings and Three Generations

One key phenomenological feature impacted by the choice of pairings in $\boldsymbol{A}$ is the number of observable spinorial sectors that are required to give rise to the particle generations. In order to explore this further it will be helpful to define two quantities which result from a choice of pairings $\boldsymbol{A}$. Firstly we have

$$\boldsymbol{E} = (E_1, E_2, E_3, E_4, E_5, E_6) \;\text{ s.t. }\; \begin{cases} E_i = 1 \;\text{ if }\; A(y^i) = A(w^i) = A(\bar{y}^i) = A(\bar{w}^i) = 0 \\ E_i = 0 \text{ else} \end{cases} \tag{7.22}$$

for $i = 1, ..., 6$. This simply quantifies which of the e_i symmetric shift vectors remain in the basis. We can note that any asymmetric pairing automatically makes two e_i incompatible with modular invariance constraints and therefore

$$\max\left(\sum_i E_i\right) = 4. \tag{7.23}$$

The second quantity we can define is

$$\boldsymbol{\Delta} = (\Delta_1, \Delta_2, \Delta_3) \;\text{ s.t. }\; \begin{cases} \Delta_1 = 0 \;\text{ if } A(y^{3456}) = A(\bar{y}^{3456}) \\ \Delta_1 = 1 \;\text{ else} \end{cases} \tag{7.24}$$

$$\tag{7.25}$$

and similarly for Δ_2 and Δ_3. This notation has been employed, for example, in [67] and [121]. With this notation defined we can now consider the fermion generations.

At the level of the NAHE-set $\{\mathbb{1}, S, b_1, b_2, b_3\}$, the sectors b_1, b_2 and b_3, if present in the massless spectrum, give rise to sixteen copies of the **16** or $\overline{\mathbf{16}}$ of $SO(10)$ due to the degeneracy of the sets of internal fermions $\{y^{3,4,5,6} \mid \bar{y}^{3,4,5,6}, \bar{\eta}^1\}$, $\{y^{1,2}, w^{5,6} \mid \bar{y}^{1,2}, \bar{w}^{5,6}, \bar{\eta}^2\}$ and $\{w^{1,2,3,4} \mid \bar{w}^{1,2,3,4}, \bar{\eta}^3\}$, respectively. The addition of x reduces the degeneracy to eight copies of **16** or $\overline{\mathbf{16}}$ by separating out the $\bar{\eta}^k$ for each plane.

In the classification program for symmetric orbifolds, the basis contains all six symmetric shift e_i vectors. These symmetric shifts completely remove the degeneracy on the three orbifold planes and the sectors giving rise to observable spinorial states from the $\mathbf{16}/\overline{\mathbf{16}}$ of $SO(10)$ are

$$\begin{aligned}\boldsymbol{F}^1_{pqrs} &= b_1 + pe_3 + qe_4 + re_5 + se_6\\ \boldsymbol{F}^2_{pqrs} &= b_2 + pe_1 + qe_2 + re_5 + se_6\\ \boldsymbol{F}^3_{pqrs} &= b_3 + pe_1 + qe_2 + re_3 + se_4.\end{aligned} \tag{7.26}$$

such that any sector $\boldsymbol{F}^k_{pqrs}$, $k = 1, 2, 3$, in the massless spectrum produces exactly one $\mathbf{16}$ or $\overline{\mathbf{16}}$. This picture requires adjustment for the case of the Flipped $SU(5)$ asymmetric orbifolds generated by the basis of eq. (7.19). In particular, the number and degeneracy of each group of sectors $\boldsymbol{F}^k_{pqrs}$ will vary according to the pairing choice $\boldsymbol{A}$. More specifically, we will see that the degeneracies of each plane can be written as a function of $\boldsymbol{E}$ and $\boldsymbol{\Delta}$.

The impact of the inclusion of an e_i vector in the basis (7.19) on the degeneracy of each orbifold plane can be seen to reduce the degeneracy of the orbifold plane $k = 1, 2, 3$ by a factor two if $e_i \cap b_k \neq \emptyset$. Similarly, an asymmetric pairing in one of the three planes, *i.e.* $\Delta_k = 1$, will also reduce the degeneracy by a factor 2. We can now write the degeneracies as a vector

$$\boldsymbol{D} = (D_1, D_2, D_3) \tag{7.27}$$

for each orbifold plane such that

$$D_1 = \frac{8}{2^{\Delta_1+E_3+E_4+E_5+E_6}} \tag{7.28}$$

$$D_2 = \frac{8}{2^{\Delta_2+E_1+E_2+E_5+E_6}} \tag{7.29}$$

$$D_3 = \frac{8}{2^{\Delta_3+E_1+E_2+E_3+E_4}}, \tag{7.30}$$

and we note that

$$\min\left(D_k\right) = \frac{1}{2} \tag{7.31}$$

which when true tells us that the sectors $\boldsymbol{F}^k_{pqrs}$ will give rise to one component of the FSU5 representations of the $\mathbf{16}$ or $\overline{\mathbf{16}}$ and not the whole $SO(10)$ representation. In particular, since the decomposition under $SU(5) \times U(1)$ is

$$\begin{aligned}\mathbf{16} &= \left(\mathbf{10}, +\frac{1}{2}\right) + \left(\overline{\mathbf{5}}, -\frac{3}{2}\right) + \left(\mathbf{1}, \ \ \frac{5}{2}\right)\\ \overline{\mathbf{16}} &= \left(\overline{\mathbf{10}}, -\frac{1}{2}\right) + \left(\mathbf{5}, +\frac{3}{2}\right) + \left(\mathbf{1}, -\frac{5}{2}\right)\end{aligned} \tag{7.32}$$

sectors $\boldsymbol{F}^k_{pqrs}$ with $D_k = \frac{1}{2}$ will generate either the states with representation $\left(\mathbf{10}, +\frac{1}{2}\right)$ or those transforming under $\left(\overline{\mathbf{5}}, -\frac{3}{2}\right) + \left(\mathbf{1}, \frac{5}{2}\right)$, in the case of the sector being from $\mathbf{16}$.

Once we calculate the degeneracies (D_1, D_2, D_3) from $\boldsymbol{A}$ we can immediately check a necessary, but certainly not sufficient, condition for the presence of odd and, in particular, three

generations, which is simply

$$\exists\ k \in \{1,2,3\} :\ D_k \leq 1. \tag{7.33}$$

A sufficient condition for the presence of three generations is presented in Section 7.3 but the condition (7.33) can be checked immediately from the pairing choice $\boldsymbol{A}$ so will be tested for in the classification of pairings performed in this section.

Asymmetric Pairings and Retained Moduli

As mentioned in Section 7.1, the moduli scalar fields (7.6) are in one-to-one correspondence with the marginal operators (7.7). From the form of these operators, we can immediately derive conditions on their retention/projection depending on the boundary condition assignments from $\boldsymbol{A}$. The result is

$$J_L^i(z)\bar{J}_R^j(\bar{z}) \begin{cases} \text{retained if} & [A(y^i)+A(w^i)+A(\bar{y}^j)+A(\bar{w}^j)] \mod 2 = 0 \\ \text{projected if} & [A(y^i)+A(w^i)+A(\bar{y}^j)+A(\bar{w}^j)] \mod 2 = 1. \end{cases} \tag{7.34}$$

It will be useful when constructing the pairing classification Tables 7.1 and 7.2 to write the number of retained moduli in each orbifold plane as a triple

$$\boldsymbol{M} = (M_1, M_2, M_3). \tag{7.35}$$

Results for Classification of Pairings

The result of the classification of asymmetric pairings with a bosonic $\boldsymbol{A}$ are summarised in Table 7.1 and with fermionic $\boldsymbol{A}$ for Table 7.2. The data most important to consider is the number of untwisted moduli retained in each plane (7.35) and whether odd number generations are possible through checking (7.33). The Z3 SMT classifies all the asymmetric pairings in each case, bosonic and fermionic, in approximately 20 seconds.

Having classified the possible FSU5 pairings we can now move to the second step of the asymmetric orbifold classification where we fix the pairing and, therefore, the basis vectors and then classify the space of asymmetric orbifold models in reference to phenomenological characteristics.

7.3 Class-Independent Analysis

A class of Flipped $SU(5)$ models is defined through the basis (7.19) with a specific choice of $\boldsymbol{A}$. This choice of $\boldsymbol{A}$ tells us a concomitant consistent $\boldsymbol{B}$ and the number of e_i vectors quantified by $\boldsymbol{E}$. Two such classes will be investigated in Section 7.4 and Section 7.5. Before inspecting a specific class, it is worth seeing what we can say about all classes of models derived from the generic basis (7.19) since several features will be the same for all models.

7.3.1 Supersymmetry Constraints and Class Parameter Space

We seek to classify both $\mathcal{N} = 0$ and $\mathcal{N} = 1$ models and so it is important to define a necessary and sufficient condition for the presence of $\mathcal{N} = 1$ supersymmetry. To do this we

Untwisted Moduli in each Torus	Odd Number Generations Possible	Frequency
(2, 2, 0)	No	992
(2, 0, 2)	No	992
(0, 2, 2)	No	992
(4, 2, 2)	No	824
(2, 4, 2)	No	824
(2, 2, 4)	No	824
(0, 0, 0)	No	256
(4, 0, 0)	No	244
(0, 4, 0)	No	244
(0, 0, 4)	No	244
(4, 4, 0)	No	200
(4, 2, 2)	Yes	200
(4, 0, 4)	No	200
(2, 4, 2)	Yes	200
(2, 2, 4)	Yes	200
(0, 4, 4)	No	200
(4, 4, 4)	No	146
(4, 4, 4)	Yes	94
(4, 4, 0)	Yes	56
(4, 0, 4)	Yes	56
(0, 4, 4)	Yes	56
(2, 2, 0)	Yes	32
(2, 0, 2)	Yes	32
(0, 2, 2)	Yes	32
(4, 0, 0)	Yes	12
(0, 4, 0)	Yes	12
(0, 0, 4)	Yes	12

TABLE 7.1: *Possible moduli and whether odd number generations are possible for all bosonic type asymmetric pairings of internal fermions.*

first note that the gravitini and gaugini arise from

$$\partial\overline{X}^{\mu}\,|S\rangle \tag{7.36}$$

$$\{\bar{\lambda}^{a}\}\{\bar{\lambda}^{b}\}\,|S\rangle \tag{7.37}$$

respectively. Therefore the following GGSO phases are fixed as follows

$$C\binom{S}{e_i} = C\binom{S}{z_1} = C\binom{S}{x} = C\binom{S}{\gamma} = -1 \tag{7.38}$$

in order to preserve one gravitino. Furthermore we note that the phases $C\binom{\mathbb{1}}{S}$ and $C\binom{S}{b_k}$, $k = 1, 2, 3$, determine the chirality of the degenerate Ramond vacuum $|S\rangle$ and the gravitino is retained so long as

$$C\binom{\mathbb{1}}{S} = C\binom{S}{b_1}\,C\binom{S}{b_2}\,C\binom{S}{b_3} \tag{7.39}$$

which can, without loss of generality, be fixed to

$$C\binom{\mathbb{1}}{S} = C\binom{S}{b_1} = C\binom{S}{b_2} = C\binom{S}{b_3} = -1 \tag{7.40}$$

for a scan of $\mathcal{N} = 1$ vacua.

Untwisted Moduli in each Torus	Odd Number Generations Possible	Frequency
(2, 4, 2)	No	1024
(2, 2, 4)	No	1024
(2, 2, 0)	No	1024
(2, 0, 2)	No	1024
(0, 2, 2)	No	1024
(4, 2, 2)	No	976
(0, 4, 4)	No	256
(0, 4, 0)	No	256
(0, 0, 4)	No	256
(0, 0, 0)	No	256
(4, 4, 0)	No	244
(4, 0, 4)	No	244
(4, 0, 0)	No	244
(4, 4, 4)	No	228
(4, 2, 2)	Yes	48
(4, 4, 4)	Yes	12
(4, 4, 0)	Yes	12
(4, 0, 4)	Yes	12
(4, 0, 0)	Yes	12

TABLE 7.2: *Possible moduli and whether odd number generations are possible for all fermionic type asymmetric pairings of internal fermions.*

The number of independent GGSO phases for a class of models will be determined from the number of basis vectors, N, which can be written as

$$N = 8 + \sum_i E_i. \tag{7.41}$$

Taking into account the constraints (7.38) and (7.39) for $\mathcal{N} = 1$ models there are

$$\frac{N(N-1)}{2} - 7 - \sum_i E_i \tag{7.42}$$

independent GGSO phases[1]. The space of $\mathcal{N} = 0$ vacua can be defined as the space of models violating either condition (7.38) or (7.39). In ref. [110] breaking supersymmetry with different phases is discussed and it is noted how different breakings affect the spectra. If desired, we can restrict the breaking to just shifts beyond the $\mathbb{Z}_2 \times \mathbb{Z}_2$ orbifold sectors by preserving condition (7.39), such that b_1, b_2 and b_3 still preserve supersymmetry, then breaking would originate from the vectors beyond the NAHE-set through violating condition (7.38).

7.3.2 Phenomenological Features

Observable Spinorial Representations

As discussed in Section 7.2 the twisted sectors such as those giving rise to the spinorial $\mathbf{16}/\overline{\mathbf{16}}$ representations of $SO(10)$ are impacted by the choice of $\boldsymbol{A}$. To write these $\boldsymbol{F}^k_{pqrs}$ for

[1]We can fix $C(\frac{\mathbb{1}}{\mathbb{1}}) = +1$ without loss of generality and all other phases are determined from modular invariance rules

a particular $\boldsymbol{A}$ we must first note the presence of the following possible linear combinations of the vector (7.21), arising for certain $\boldsymbol{E}$

$$\begin{cases} e_{3456} = G + e_1 + e_2 = \{y^{3456}, w^{3456} \mid \bar{y}^{3456}, \bar{w}^{3456}\} & \text{for } \boldsymbol{E} = (1,1,0,0,0,0) \\ e_{1256} = G + e_3 + e_4 = \{y^{1256}, w^{1256} \mid \bar{y}^{1256}, \bar{w}^{1256}\} & \text{for } \boldsymbol{E} = (0,0,1,1,0,0) \\ e_{1234} = G + e_5 + e_6 = \{y^{1234}, w^{1234} \mid \bar{y}^{1234}, \bar{w}^{1234}\} & \text{for } \boldsymbol{E} = (0,0,0,0,1,1). \end{cases} \tag{7.43}$$

Then we can write the sectors giving rise to the fermion generations as

$$\begin{aligned} \boldsymbol{F}^1_{pqrst} =& b_1 + pE_3e_3 + qE_4e_4 + rE_5e_5 + sE_6e_6 \\ &+ tE_1E_2(1-E_3)(1-E_4)(1-E_5)(1-E_6)e_{3456} \\ \boldsymbol{F}^2_{pqrst} =& b_2 + pE_1e_1 + qE_2e_2 + rE_5e_5 + sE_6e_6 \\ &+ tE_3E_4(1-E_1)(1-E_2)(1-E_5)(1-E_6)e_{1256} \\ \boldsymbol{F}^3_{pqrst} =& b_3 + pE_1e_1 + qE_2e_2 + rE_3e_3 + sE_4e_4 \\ &+ tE_5E_6(1-E_1)(1-E_2)(1-E_3)(1-E_4)e_{1234}. \end{aligned} \tag{7.44}$$

where $p,q,r,s,t \in \{0,1\}$.

In order to write down the number of **16** and $\overline{\mathbf{16}}$, N_{16} and $N_{\overline{16}}$, as a function of the GGSO coefficients we can construct the generalised projectors for these sectors $\mathbb{P}_{\boldsymbol{F}^k_{pqrst}}$, $k = 1,2,3$, such that

$$\begin{aligned} \Upsilon(\boldsymbol{F}^1_{pqrst}) &= \{x + 2\boldsymbol{\gamma}, z_1, z_2, E_1e_1, E_2e_2\} \\ \Upsilon(\boldsymbol{F}^2_{pqrst}) &= \{x + 2\boldsymbol{\gamma}, z_1, z_2, E_3e_3, E_4e_4\} \\ \Upsilon(\boldsymbol{F}^3_{pqrst}) &= \{x + 2\boldsymbol{\gamma}, z_1, z_2, E_5e_5, E_6e_6\} \end{aligned} \tag{7.45}$$

where we recall that the vector $z_2 = \{\overline{\phi}^{5,6,7,8}\}$ is the combination defined in eq. (7.20). In order to determine whether a sector will give rise to a **16** or a $\overline{\mathbf{16}}$ we can first define the chirality phases

$$\boldsymbol{X}^1_{pqrs0} = -\mathrm{ch}(\psi^\mu) C \begin{pmatrix} \boldsymbol{F}^1_{pqrs0} \\ b_2 + rE_5e_5 + sE_6e_6 \end{pmatrix}^* \tag{7.46}$$

$$\boldsymbol{X}^2_{pqrs0} = -\mathrm{ch}(\psi^\mu) C \begin{pmatrix} \boldsymbol{F}^2_{pqrs0} \\ b_1 + rE_5e_5 + sE_6e_6 \end{pmatrix}^* \tag{7.47}$$

$$\boldsymbol{X}^3_{pqrs0} = -\mathrm{ch}(\psi^\mu) C \begin{pmatrix} \boldsymbol{F}^3_{pqrs0} \\ b_1 + pE_3e_3 + qE_4e_4 \end{pmatrix}^* \tag{7.48}$$

where $\mathrm{ch}(\psi^\mu)$ is the spacetime fermion chirality and we note that the sectors $\boldsymbol{F}^k_{00001}$ do not have a chirality and, instead, give rise to $D_k/2$ copies of both the **16** and the $\overline{\mathbf{16}}$.

With these definitions, we can write compact expressions for N_{16} and $N_{\overline{16}}$

$$\begin{aligned} N_{16} &= \frac{1}{2} \sum_{\substack{k=1,2,3 \\ p,q,r,s=0,1}} D_k \mathbb{P}_{\boldsymbol{F}^k_{pqrs0}} \left(1 + \boldsymbol{X}^k_{pqrs0}\right) + \frac{D_k}{2} \mathbb{P}_{F^k_{00001}} \\ N_{\overline{16}} &= \frac{1}{2} \sum_{\substack{k=1,2,3 \\ p,q,r,s=0,1}} D_k \mathbb{P}_{\boldsymbol{F}^k_{pqrs0}} \left(1 - \boldsymbol{X}^k_{pqrs0}\right) + \frac{D_k}{2} \mathbb{P}_{F^k_{00001}}. \end{aligned} \tag{7.49}$$

Since the $SO(10)$ breaking projection $\boldsymbol{\gamma}$ decomposes the $\mathbf{16}/\overline{\mathbf{16}}$ representations into those of $SU(5)\times U(1)$ according to eq. (7.32), we can write a compact expression for each of the FSU5 quantum numbers. These of course depend on the degeneracies (7.28) and can be written

$$\begin{aligned}
n_{10} &= \sum_{\substack{k=1,2,3\\ p,q,r,s=0,1}} \frac{1}{2^{2-\Delta_k}} D_k \mathbb{P}_{\boldsymbol{F}^k_{pqrs0}} \left(1+\boldsymbol{X}^k_{pqrs0}\right)\left(1+(1-\Delta_k)C\begin{pmatrix}\boldsymbol{F}^k_{pqrs0}\\ \boldsymbol{\gamma}\end{pmatrix}\right) + \frac{D_k}{2}\mathbb{P}_{F^k_{00001}} \\
n_{\bar{5}} &= \sum_{\substack{k=1,2,3\\ p,q,r,s=0,1}} \frac{1}{2^{2-\Delta_k}} D_k \mathbb{P}_{\boldsymbol{F}^k_{pqrs0}} \left(1+\boldsymbol{X}^k_{pqrs0}\right)\left(1-(1-\Delta_k)C\begin{pmatrix}\boldsymbol{F}^k_{pqrs0}\\ \boldsymbol{\gamma}\end{pmatrix}\right) + \frac{D_k}{2}\mathbb{P}_{F^k_{00001}} \\
n_{\overline{10}} &= \sum_{\substack{k=1,2,3\\ p,q,r,s=0,1}} \frac{1}{2^{2-\Delta_k}} \mathbb{P}_{\boldsymbol{F}^k_{pqrs0}} \left(1-\boldsymbol{X}^k_{pqrs0}\right)\left(1+(1-\Delta_k)C\begin{pmatrix}\boldsymbol{F}^k_{pqrs0}\\ \boldsymbol{\gamma}\end{pmatrix}\right) + \frac{D_k}{2}\mathbb{P}_{F^k_{00001}} \\
n_{5} &= \sum_{\substack{k=1,2,3\\ p,q,r,s=0,1}} \frac{1}{2^{2-\Delta_k}} D_k \mathbb{P}_{\boldsymbol{F}^k_{pqrs0}} \left(1-\boldsymbol{X}^k_{pqrs0}\right)\left(1-(1-\Delta_k)C\begin{pmatrix}\boldsymbol{F}^k_{pqrs0}\\ \boldsymbol{\gamma}\end{pmatrix}\right) + \frac{D_k}{2}\mathbb{P}_{F^k_{00001}}.
\end{aligned} \tag{7.50}$$

The number of generations for a model is then

$$n_g = n_{10} - n_{\overline{10}} = n_{\bar{5}} - n_5. \tag{7.51}$$

From this, we can construct a necessary condition for three-generation models to exist once $\boldsymbol{A}$ is specified

$$\begin{aligned}
\exists\, C\begin{pmatrix}\boldsymbol{b}_i\\ \boldsymbol{b}_j\end{pmatrix}: \quad & \sum_{\substack{k=1,2,3\\ p,q,r,s=0,1}} \frac{1}{2^{1-\Delta_k}} D_k \mathbb{P}_{\boldsymbol{F}^k_{pqrs0}} \boldsymbol{X}^k_{pqrs0}\left(1+(1-\Delta_k)C\begin{pmatrix}\boldsymbol{F}^k_{pqrs0}\\ \boldsymbol{\gamma}\end{pmatrix}\right) = 3 \\
\text{and} \quad & \sum_{\substack{k=1,2,3\\ p,q,r,s=0,1}} 2^{\Delta_k} D_k \mathbb{P}_{\boldsymbol{F}^k_{pqrs0}} \boldsymbol{X}^k_{pqrs0}(1-\Delta_k)C\begin{pmatrix}\boldsymbol{F}^k_{pqrs0}\\ \boldsymbol{\gamma}\end{pmatrix} = 0.
\end{aligned} \tag{7.52}$$

Checking that there exists a solution to this equation for a class of models and enumerating such solutions can be done easily by inputting this constraint into an SMT solver such as Z3.

Tachyonic Sectors

Since we include non-supersymmetric models in our classification it is vital we check for the absence of on-shell tachyons in order to ensure the stability of our models for a 4D Minkowski background. In order to do this we encode the GGSO projections for all on-shell tachyonic sectors. Many tachyonic sectors can arise due to e_i vectors, certain $\boldsymbol{\gamma}$ combinations and other class-dependent combinations and therefore are dependent on the choice of $\boldsymbol{A}$ and require class-by-class analysis. However, we will always have the untwisted tachyon

$$\{\bar{\lambda}\}\,|0\rangle_{NS} \tag{7.53}$$

that is projected for all models through the S projection. In addition, the following on-shell tachyonic sectors arise for all classes of models

$$T = \big\{|z_1\rangle \quad |z_2\rangle \quad |x+2\boldsymbol{\gamma}\rangle\, |z_1+x+2\boldsymbol{\gamma}\rangle \quad |z_2+x+2\boldsymbol{\gamma}\rangle \quad |z_1+z_2+x+2\boldsymbol{\gamma}\rangle\big\} \tag{7.54}$$

All of these sectors, $\boldsymbol{t} \in T$, must be projected from the spectrum through appropriate definitions of their generalised projectors $\mathbb{P}_{\boldsymbol{t}} = 0$. Once we specify the vector $\boldsymbol{A}$ we can then determine the further class-dependent tachyonic sectors and ensure their projection.

Enhancements

Additional space-time vector bosons may arise in all models derived from the basis (7.19). The following enhancements arise independently of the class

$$\begin{Bmatrix} \psi^\mu\{\bar{\lambda}\}_{\frac{1}{2}}: & |z_1\rangle & |z_2\rangle & |x+2\boldsymbol{\gamma}\rangle & |z_1+x+2\boldsymbol{\gamma}\rangle & |z_2+x+2\boldsymbol{\gamma}\rangle \\ \psi^\mu: & |x\rangle & |z_1+z_2\rangle & & & \end{Bmatrix} \tag{7.55}$$

with the following subset being enhancements to the observable gauge factors

$$H = \begin{Bmatrix} \psi^\mu\{\bar{\psi}^a\}: & |z_1\rangle & |z_2\rangle & |x+2\boldsymbol{\gamma}\rangle \\ \psi^\mu\{\bar{\psi}^a\}: & |z_1+x+2\boldsymbol{\gamma}\rangle & |z_2+x+2\boldsymbol{\gamma}\rangle & |x+2\boldsymbol{\gamma}+z_1+z_2\rangle \\ \psi^\mu: & |x\rangle & & \end{Bmatrix}. \tag{7.56}$$

with $a = 1,2,3,4,5$. Therefore, from these sectors, we can restrict our analysis to models with observable gauge group $SU(5)\times U(1)\times U(1)_{i=1,2,3}$ by imposing

$$\forall\ \boldsymbol{h} \in H:\ \mathbb{P}_{\boldsymbol{h}} = 0. \tag{7.57}$$

In this case, for these generalised projectors we have

$$\begin{aligned}
\Upsilon(z_1) &= \{S, E_1e_1, E_2e_2, E_3e_3, E_4e_4, E_5e_5, E_6e_6, x, b_1, b_2, z_2\} \\
\Upsilon(z_2) &= \{S, E_1e_1, E_2e_2, E_3e_3, E_4e_4, E_5e_5, E_6e_6, x, b_1, b_2, z_1\} \\
\Upsilon(x+2\boldsymbol{\gamma}) &= \{S, E_1e_1, E_2e_2, E_3e_3, E_4e_4, E_5e_5, E_6e_6, x, x+2\boldsymbol{\gamma}+z_1+z_2\} \\
\Upsilon(x+2\boldsymbol{\gamma}+z_1) &= \{S, E_1e_1, E_2e_2, E_3e_3, E_4e_4, E_5e_5, E_6e_6, x, x+2\boldsymbol{\gamma}+z_2\} \\
\Upsilon(x+2\boldsymbol{\gamma}+z_2) &= \{S, E_1e_1, E_2e_2, E_3e_3, E_4e_4, E_5e_5, E_6e_6, x, x+2\boldsymbol{\gamma}+z_1\} \\
\Upsilon(x+2\boldsymbol{\gamma}+z_1+z_2) &= \{S, E_1e_1, E_2e_2, E_3e_3, E_4e_4, E_5e_5, E_6e_6, x, x+2\boldsymbol{\gamma}\} \\
\Upsilon(x) &= \{S, E_1e_1, E_2e_2, E_3e_3, E_4e_4, E_5e_5, E_6e_6, z_1, z_2\}
\end{aligned} \tag{7.58}$$

Additional enhancements may arise depending on the specific form of $\boldsymbol{\gamma}$ which can be analysed class-by-class.

Exotics

Another important consideration for ensuring reasonable phenomenology is the absence of chiral exotics. The exotics sectors in general depend on the class, in particular on the exact form of $\boldsymbol{\gamma}$ since combinations of $\boldsymbol{\gamma}$ will be those that can generate exotics. However, we can

note here the following exotic sectors with $(\boldsymbol{\alpha}_L \cdot \boldsymbol{\alpha}_L, \boldsymbol{\alpha}_R \cdot \boldsymbol{\alpha}_R) = (4,4)$

$$\left\{ \{\bar{\psi}^a\}_{\frac{1}{2}} : \quad |S+z_1\rangle \quad |S+z_2\rangle \quad |S+x+2\boldsymbol{\gamma}\rangle \quad |S+z_1+x+2\boldsymbol{\gamma}\rangle \quad |S+z_2+x+2\boldsymbol{\gamma}\rangle \right\} \tag{7.59}$$

where $a \in [1,...,5]$. We note that these are the would-be gaugini of the enhancements (7.55). These sectors will not contribute to a chiral anomaly as they are automatically vector-like. It will then be necessary to analyse the other exotics at the level of a particular class of vacua.

7.3.3 Partition Function and Cosmological Constant

The analysis of the partition function for asymmetric orbifolds constructed in the free fermionic formulation as described in Section 7.1 is largely similar to the symmetric case presented in Chapter 4. However, there are some key differences and subtleties which are important to explicitly discuss. These arise for two main reasons, namely the asymmetric pairings introduced by the basis vector γ and the appearance of half boundary conditions in the basis set (7.19).

From the point of view of the partition function, the asymmetric pairings introduce imaginary GGSO phases, meaning that the fermionic partition function

$$Z = \sum_{\boldsymbol{\alpha},\boldsymbol{\beta}} C\begin{pmatrix}\boldsymbol{\alpha}\\ \boldsymbol{\beta}\end{pmatrix} \prod_f Z\begin{bmatrix}\alpha(f)\\ \beta(f)\end{bmatrix}, \tag{7.60}$$

will have imaginary terms which have to cancel. This cancellation is, however, ensured by modular invariance. In the case of symmetric orbifolds, since $Z\left[\begin{smallmatrix}a\\ b\end{smallmatrix}\right] = \sqrt{\vartheta\left[\begin{smallmatrix}a\\ b\end{smallmatrix}\right]}$, the fermionic part of the partition function can be expressed using the four standard Jacobi theta functions (A.5) with characteristics $a, b \in \{0,1\}$. In the presence of half boundary conditions, there will be sixteen such theta functions with a and b now taking values in the set $a, b \in \{-1/2, 0, 1/2, 1\}$.

To express the partition function of the models under consideration in the classification setup, it is beneficial to use the notation developed in 4.1. This makes many properties immediately readable from the form of the partition function and allows us to economically express all models used in this chapter in one compact form. Since the classification of asymmetric shifts and twists depends on the exact form of the vector $\boldsymbol{\gamma}$ it is instructive to first write down the partition function of the subset $\{\mathbb{1}, e_i, S, b_1, b_2, b_3, z_1, x\}$ without γ. In this case, all e_i are compatible and so we have 13 basis vectors giving

$$\begin{aligned} Z =& \frac{1}{\eta^{10}\bar{\eta}^{22}} \frac{1}{2^3} \sum_{\substack{a,k,r\\ b,l,s}} \frac{1}{2^6} \sum_{\substack{H_i\\ G_i}} \frac{1}{2^4} \sum_{\substack{h_1,h_2,P_1,P_2\\ g_1,g_2,Q_1,Q_2}} (-1)^{\Phi\left[\begin{smallmatrix}a & k & r & H_i & h_i & P_i\\ b & l & s & G_i & g_i & Q_i\end{smallmatrix}\right]} \\ & \times \vartheta\left[\begin{smallmatrix}a\\ b\end{smallmatrix}\right] \vartheta\left[\begin{smallmatrix}a+h_1\\ b+g_1\end{smallmatrix}\right] \vartheta\left[\begin{smallmatrix}a+h_2\\ b+g_2\end{smallmatrix}\right] \vartheta\left[\begin{smallmatrix}a-h_1-h_2\\ b-g_1-g_2\end{smallmatrix}\right] \\ & \times \Gamma_{(6,6)}\left[\begin{smallmatrix}r & H_i & h_1 & h_2\\ s & G_i & g_1 & g_2\end{smallmatrix}\right] \\ & \times \bar{\vartheta}\left[\begin{smallmatrix}k\\ l\end{smallmatrix}\right]^5 \bar{\vartheta}\left[\begin{smallmatrix}k+h_1\\ l+g_1\end{smallmatrix}\right] \bar{\vartheta}\left[\begin{smallmatrix}k+h_2\\ l+g_2\end{smallmatrix}\right] \bar{\vartheta}\left[\begin{smallmatrix}k-h_1-h_2\\ l-g_1-g_2\end{smallmatrix}\right] \bar{\vartheta}\left[\begin{smallmatrix}k+P_1\\ l+Q_1\end{smallmatrix}\right]^4 \bar{\vartheta}\left[\begin{smallmatrix}k+P_2\\ l+Q_2\end{smallmatrix}\right]^4, \end{aligned} \tag{7.61}$$

where all indices are summed over the set $\{0,1\}$. The phase Φ, which is a polynomial in the summation indices, is chosen such that the entire partition function is modular invariant. The choice of this phase translates to a choice of GGSO matrix in the classification setup. Indices k,l represent the sixteen complex right-moving fermions giving the fermionic representation of the $E_8 \times E_8$ lattice of the underlying 10D heterotic theory. The non-freely acting $\mathbb{Z}_2 \times \mathbb{Z}_2$ orbifold is represented by the parameters h_i and g_i, where the h_i give the various twists, while the g_i implement the orbifold projections. The H_i and G_i correspond to the basis vectors $\mathbf{e_i}$ and hence are responsible for orbifold shifts along the six internal dimensions of the T^6. Finally, P_i and Q_i break one of the E_8 factors in the hidden sector by a $\mathbb{Z}_2$ twist.

The internal lattice $\Gamma_{(6,6)}$ which corresponds to the T^6 is given by

$$\begin{aligned}\Gamma_{(6,6)}\left[\begin{smallmatrix} r & H_i & h_1 & h_2 \\ s & G_i & g_1 & g_2 \end{smallmatrix}\right] = \Big| & \vartheta\left[\begin{smallmatrix} r+h_1+H_1 \\ s+g_1+G_1 \end{smallmatrix}\right]_{y\bar{y}^1} \vartheta\left[\begin{smallmatrix} r+h_1+H_2 \\ s+g_1+G_2 \end{smallmatrix}\right]_{y\bar{y}^2} \vartheta\left[\begin{smallmatrix} r+h_2+H_3 \\ s+g_2+G_3 \end{smallmatrix}\right]_{y\bar{y}^3} \\ & \times \vartheta\left[\begin{smallmatrix} r+h_2+H_4 \\ s+g_2+G_4 \end{smallmatrix}\right]_{y\bar{y}^4} \vartheta\left[\begin{smallmatrix} r+h_2+H_5 \\ s+g_2+G_5 \end{smallmatrix}\right]_{y\bar{y}^5} \vartheta\left[\begin{smallmatrix} r+h_2+H_6 \\ s+g_2+G_6 \end{smallmatrix}\right]_{y\bar{y}^6} \\ & \times \vartheta\left[\begin{smallmatrix} r-h_1-h_2+H_1 \\ s-g_1-g_2+G_1 \end{smallmatrix}\right]_{w\bar{w}^1} \vartheta\left[\begin{smallmatrix} r-h_1-h_2+H_2 \\ s-g_1-g_2+G_2 \end{smallmatrix}\right]_{w\bar{w}^2} \vartheta\left[\begin{smallmatrix} r-h_1-h_2+H_3 \\ s-g_1-g_2+G_3 \end{smallmatrix}\right]_{w\bar{w}^3} \\ & \times \vartheta\left[\begin{smallmatrix} r-h_1-h_2+H_4 \\ s-g_1-g_2+G_4 \end{smallmatrix}\right]_{w\bar{w}^4} \vartheta\left[\begin{smallmatrix} r+h_1+H_5 \\ s+g_1+G_5 \end{smallmatrix}\right]_{w\bar{w}^5} \vartheta\left[\begin{smallmatrix} r+h_1+H_6 \\ s+g_1+G_6 \end{smallmatrix}\right]_{w\bar{w}^6} \Big|,\end{aligned} \tag{7.62}$$

where $|\vartheta\left[\begin{smallmatrix} a \\ b \end{smallmatrix}\right]| = \sqrt{\vartheta\left[\begin{smallmatrix} a \\ b \end{smallmatrix}\right]\bar{\vartheta}\left[\begin{smallmatrix} a \\ b \end{smallmatrix}\right]}$. The subscript on the ϑ's denote which worldsheet fermions the terms correspond to. We see that with this basis the internal lattice is left-right symmetric, meaning that all left moving y's and w's are paired with a right moving $\bar{y}$ or $\bar{w}$. This is why the internal lattice can be written as a magnitude.

The introduction of asymmetric pairings via the vector $\boldsymbol{\gamma}$ introduces further complexity to the above partition function. Recall the notation introduced in Section 7.1, where the most general consistent form of $\boldsymbol{\gamma}$ is written as in (7.10)

$$\boldsymbol{\gamma} = \boldsymbol{A} + \{\bar{\psi}^{1,\ldots,5} = \bar{\eta}^{1,2,3} = \bar{\phi}^{1,2,6,7} = \frac{1}{2}\} + \boldsymbol{B}, \tag{7.63}$$

where

$$\begin{aligned} \boldsymbol{B} &= \{B(\bar{\phi}^3), B(\bar{\phi}^4), B(\bar{\phi}^5), B(\bar{\phi}^8)\}, \\ \boldsymbol{A} &= \begin{cases} \{A(y^1), \cdots, A(w^6) \mid A(\bar{y}^1), \cdots, A(\bar{w}^6)\} & \text{if } \boldsymbol{\gamma} \text{ bosonic;} \\ \{\psi^\mu, \chi^{12}, A(y^1), \cdots, A(w^6) \mid A(\bar{y}^1), \cdots, A(\bar{w}^6)\} & \text{if } \boldsymbol{\gamma} \text{ fermionic.} \end{cases} \end{aligned} \tag{7.64}$$

Also recall the vector $\boldsymbol{E} = (E_1, E_2, E_3, E_4, E_5, E_6)$ of (7.22), which qualifies which of the e_i are compatible with a specific choice of $\boldsymbol{\gamma}$ and hence appear in the basis set. That is, if $E_i = 0$ then $e_i \notin \mathcal{B}$ and vice-versa.

In terms of the above quantities we can now examine the effect of $\boldsymbol{\gamma}$ on the partition function (7.61) within the frame of the general classification setup. For simplicity, we consider the case where $\boldsymbol{\gamma}$ is bosonic and hence has no action on ψ^μ and χ^{1-6}. The anti-holomorphic hidden worldsheet fermions are affected by the choice of $\boldsymbol{B}$, while the specific choice of $\boldsymbol{A}$ will only change how the internal lattice is structured. Thus the partition function takes the

form

$$
\begin{aligned}
Z = \frac{1}{\eta^{10}\bar{\eta}^{22}}\,\frac{1}{2^4}\sum_{\substack{a,k,r,\rho\\ b,l,s,\sigma}}\frac{1}{2^{\sum_i E_i}}\sum_{\substack{H_i\\ G_i}}\frac{1}{2^3}\sum_{\substack{h_1,h_2,H\\ g_1,g_2,G}}\frac{1}{4}\sum_{\substack{H'\\ G'}}(-1)^{\Phi\left[\begin{smallmatrix} a & k & \rho & r & H_i & h_1 & h_2 & H & H'\\ b & l & s & \sigma & G_i & g_1 & g_2 & G & G'\end{smallmatrix}\right]}\\
&\times\vartheta\left[\begin{smallmatrix}a\\ b\end{smallmatrix}\right]\vartheta\left[\begin{smallmatrix}a+h_1\\ b+g_1\end{smallmatrix}\right]\vartheta\left[\begin{smallmatrix}a+h_2\\ b+g_2\end{smallmatrix}\right]\vartheta\left[\begin{smallmatrix}a-h_1-h_2\\ b-g_1-g_2\end{smallmatrix}\right]\\
&\times\Gamma^{\gamma}_{(6,6)}\left[\begin{smallmatrix} r & H_i & h_1 & h_2 & H'\\ s & G_i & g_1 & g_2 & G'\end{smallmatrix}\right]\\
&\times\bar{\vartheta}\left[\begin{smallmatrix}k+H'\\ l+G'\end{smallmatrix}\right]^5\bar{\vartheta}\left[\begin{smallmatrix}k+h_1+H'\\ l+g_1+G'\end{smallmatrix}\right]\bar{\vartheta}\left[\begin{smallmatrix}k+h_2+H'\\ l+g_2+G'\end{smallmatrix}\right]\bar{\vartheta}\left[\begin{smallmatrix}k-h_1-h_2+H'\\ l-g_1-g_2+G'\end{smallmatrix}\right]\\
&\times\bar{\vartheta}\left[\begin{smallmatrix}k+P_1+H'\\ l+Q_1+G'\end{smallmatrix}\right]^2\bar{\vartheta}\left[\begin{smallmatrix}k+P_2+H'\\ l+Q_2+G'\end{smallmatrix}\right]^2\bar{\vartheta}\left[\begin{smallmatrix}k+P_1+2B(\bar{\phi}^3)H'\\ l+Q_1+2B(\bar{\phi}^3)G'\end{smallmatrix}\right]\bar{\vartheta}\left[\begin{smallmatrix}k+P_1+2B(\bar{\phi}^4)H'\\ l+Q_1+2B(\bar{\phi}^4)G'\end{smallmatrix}\right]\\
&\times\bar{\vartheta}\left[\begin{smallmatrix}k+P_2+2B(\bar{\phi}^5)H'\\ l+Q_2+2B(\bar{\phi}^5)G'\end{smallmatrix}\right]\bar{\vartheta}\left[\begin{smallmatrix}k+P_2+2B(\bar{\phi}^8)H'\\ l+Q_2+2B(\bar{\phi}^8)G'\end{smallmatrix}\right],
\end{aligned}
\tag{7.65}
$$

where the sum in the new indices H' and G' run over $\{-1/2, 0, 1/2, 1\}$ as opposed to the other indices which still take values in $\{0, 1\}$. This is because the half boundary conditions in $\boldsymbol{\gamma}$ introduce a new $\mathbb{Z}_4$ orbifold to the picture. The factor of two in front of some indices is a result of having both half and integer boundary conditions within the same basis vector, and hence this factor ensures that integer boundary conditions are correctly accounted for.

The form of the internal lattice $\Gamma^{\gamma}_{(6,6)}$ depends on the choice of asymmetric shifts and twists in the internal degrees of freedom, i.e. $\boldsymbol{A}$. Consequently, this determines which of the symmetric $\mathbb{Z}_2$ shifts e_i are compatible with this choice, which fixes $\boldsymbol{E}$. The asymmetric shifts and twists introduced by $\boldsymbol{\gamma}$ break the left-right symmetry of the lattice (7.62). To examine this further, we have to look at what happens to a set of internal fermions corresponding to one of the orbifold planes. If we take , for example, the fermions $\{y^{3,4,5,6} \mid \bar{y}^{3,4,5,6}\}$, the corresponding part of the lattice is

$$
\begin{aligned}
\Gamma = \;&\vartheta\left[\begin{smallmatrix}r+h_2+H_3\\ s+g_2+G_3\end{smallmatrix}\right]^{1/2}_{y^3}\vartheta\left[\begin{smallmatrix}r+h_2+H_4\\ s+g_2+G_4\end{smallmatrix}\right]^{1/2}_{y^4}\vartheta\left[\begin{smallmatrix}r+h_2+H_5\\ s+g_2+G_5\end{smallmatrix}\right]^{1/2}_{y^5}\vartheta\left[\begin{smallmatrix}r+h_2+H_6\\ s+g_2+G_6\end{smallmatrix}\right]^{1/2}_{y^6}\\
&\times\vartheta\left[\begin{smallmatrix}r+h_2+H_3\\ s+g_2+G_3\end{smallmatrix}\right]^{1/2}_{\bar{y}^3}\bar{\vartheta}\left[\begin{smallmatrix}r+h_2+H_4\\ s+g_2+G_4\end{smallmatrix}\right]^{1/2}_{\bar{y}^4}\bar{\vartheta}\left[\begin{smallmatrix}r+h_2+H_5\\ s+g_2+G_5\end{smallmatrix}\right]^{1/2}_{\bar{y}^5}\bar{\vartheta}\left[\begin{smallmatrix}r+h_2+H_6\\ s+g_2+G_6\end{smallmatrix}\right]^{1/2}_{\bar{y}^6}.
\end{aligned}
\tag{7.66}
$$

Since the asymmetric shifts and twists cannot mix the orbifold planes, we either have 0, 1 or 2 such shifts and twists affecting these fermions. As an example, we consider what happens when $\boldsymbol{A}$ contains one such pairing, say y^5y^6. Firstly, this imposes that $\boldsymbol{E} = (1, 1, 1, 1, 0, 0)$, *i.e.* $e_{5,6}$ are no longer in the basis, so that $H_{5,6}$ and $G_{5,6}$ are not present. Secondly, it breaks the left-right symmetry of the $(y^5\bar{y}^5)$ and $(y^6\bar{y}^6)$ pairings which become $(y^5\bar{y}^5)(y^6\bar{y}^6) \to (y^5y^6)(\bar{y}^5\bar{y}^6)$. Given the above factors, the internal lattice of the first orbifold plane becomes

$$
\begin{aligned}
\Gamma^{\gamma} = \;&\vartheta\left[\begin{smallmatrix}r+h_2+H_3\\ s+g_2+G_3\end{smallmatrix}\right]^{1/2}_{y^3}\vartheta\left[\begin{smallmatrix}r+h_2+H_4\\ s+g_2+G_4\end{smallmatrix}\right]^{1/2}_{y^4}\vartheta\left[\begin{smallmatrix}r+h_2+2H'\\ s+g_2+2G'\end{smallmatrix}\right]_{y^{5,6}}\\
&\times\vartheta\left[\begin{smallmatrix}r+h_2+H_3\\ s+g_2+G_3\end{smallmatrix}\right]^{1/2}_{\bar{y}^3}\bar{\vartheta}\left[\begin{smallmatrix}r+h_2+H_4\\ s+g_2+G_4\end{smallmatrix}\right]^{1/2}_{\bar{y}^4}\bar{\vartheta}\left[\begin{smallmatrix}r+h_2\\ s+g_2\end{smallmatrix}\right]_{\bar{y}^{5,6}}.
\end{aligned}
\tag{7.67}
$$

If there are two such asymmetric holomorphic pairings in the first plane then, regardless of the specific pairing, the lattice simply becomes

$$\Gamma^{\gamma} = \vartheta \begin{bmatrix} r+h_2+2H' \\ s+g_2+2G' \end{bmatrix}^2_{y^{3456}} \bar{\vartheta} \begin{bmatrix} r+h_2 \\ s+g_2 \end{bmatrix}^2_{\bar{y}^{3456}} . \tag{7.68}$$

The construction of the partition function for the remaining two planes is equivalent and can be straightforwardly done once a specific basis is taken.

Once a model is chosen and the partition function is fixed according to the above considerations, the cosmological constant can be calculated according to methods used in Section 4.3. This entails performing a q-expansion of the theta functions, which will result in the partition function taking the form

$$Z = \sum_{n,m} a_{mn} q^m \bar{q}^n, \tag{7.69}$$

where the η-functions have also been q-expanded. Written in this form, the a_{mn} correspond to $a_{mn} = n_b - n_f$ at the mass level with conformal weights of (m, n) for the holomorphic and anti-holomorphic sector respectively. The one-loop cosmological constant Λ is then given by the integral of this partition function over the fundamental domain of the modular group as discussed extensively in Section 4.3. Since the models under consideration are void of physical tachyons, the series expansion contains only finite terms and converges exponentially fast. It is important to note the difference between the worldsheet vacuum energy Λ_{WS} which is unitless and the spacetime cosmological constant Λ_{ST}. The spacetime cosmological constant is obtained by introducing the string-scale via

$$\Lambda_{\mathrm{ST}} = -\frac{1}{2}\mathcal{M}^4 \Lambda_{\mathrm{WS}}. \tag{7.70}$$

It is also interesting to note that all of the above models considered in the classification exhibit a form of misaligned supersymmetry discovered in [69, 84]. This is not unexpected as this phenomenon is a direct consequence of modular invariance [69, 84, 85], or a smaller subgroup of the modular group in some cases [21, 23], and so heterotic asymmetric orbifolds should also respect this mechanism.

7.4 Asymmetric Orbifold of Class A

The first Class of models we will choose is a pairing choice where all untwisted moduli are retained, *i.e.* $\boldsymbol{M} = (4, 4, 4)$. The pairing we choose is inspired by that used in the model of [129, 130, 140] and is given by $\boldsymbol{A} = \{y^3 y^6, y^1 w^6, w^1 w^3\}$. The basis for this class of models is

then

$$\begin{aligned}
\mathbb{1} &= \{\psi^\mu, \chi^{1,\ldots,6}, y^{1,\ldots,6}, w^{1,\ldots,6} \mid \overline{y}^{1,\ldots,6}, \overline{w}^{1,\ldots,6}, \overline{\psi}^{1,\ldots,5}, \overline{\eta}^{1,2,3}, \overline{\phi}^{1,\ldots,8}\},\\
S &= \{\psi^\mu, \chi^{1,\ldots,6}\},\\
e_2 &= \{y^2, w^2 \mid \overline{y}^2, \overline{w}^2\},\\
e_4 &= \{y^4, w^4 \mid \overline{y}^4, \overline{w}^4\},\\
e_5 &= \{y^5, w^5 \mid \overline{y}^5, \overline{w}^5\},\\
b_1 &= \{\psi^\mu, \chi^{12}, y^{34}, y^{56} \mid \overline{y}^{34}, \overline{y}^{56}, \overline{\eta}^1, \overline{\psi}^{1,\ldots,5}\},\\
b_2 &= \{\psi^\mu, \chi^{34}, y^{12}, w^{56} \mid \overline{y}^{12}, \overline{w}^{56}, \overline{\eta}^2, \overline{\psi}^{1,\ldots,5}\},\\
b_3 &= \{\psi^\mu, \chi^{56}, w^{1234} \mid \overline{w}^{1234}, \overline{\eta}^3, \overline{\psi}^{1,\ldots,5}\},\\
z_1 &= \{\overline{\phi}^{1,\ldots,4}\},\\
x &= \{\overline{\psi}^{1,\ldots,5}, \overline{\eta}^{1,2,3}\},\\
\boldsymbol{\gamma} &= \{y^3y^6, y^1w^6, w^1w^3 \mid \bar{\psi}^{1,2,3,4,5} = \bar{\eta}^{1,2,3} = \frac{1}{2}, \bar{\phi}^{1,2,6,7} = \frac{1}{2}\}
\end{aligned} \tag{7.71}$$

Based on the general definitions in Section 7.3, we can immediately note the following quantities for this class

$$\begin{aligned}
\boldsymbol{E} &= (0,1,0,1,1,0)\\
\boldsymbol{\Delta} &= (1,1,1)\\
\boldsymbol{D} &= (1,1,1)
\end{aligned} \tag{7.72}$$

which will help us easily determine the key characteristics of the models.

The vector bosons from the untwisted sector of these models generate the gauge symmetry group

$$\text{Observable:}\quad SU(5)\times U(1)\times U(1)_{k=1,2,3}\times U(1)_{l=4,5,6} \tag{7.73}$$

$$\text{Hidden:}\quad SU(2)\times U(1)_{H_1}\times SO(4)^2\times SU(2)\times U(1)_{H_2}. \tag{7.74}$$

where we note that $U(1)_{k=1,2,3}$ are generated by the anti-holomorphic currents $\bar{\eta}^k\bar{\eta}^{k*}$ and the $U(1)_{l=4,5,6}$ are horizontal symmetries arising from the asymmetric pairings: $\bar{y}^3\bar{y}^6, \bar{y}^1\bar{w}^6$ and $\bar{w}^1\bar{w}^3$. Another important note is that for this Class of models we can apply eq. (7.7) and see that all the untwisted moduli are, indeed, retained.

From the discussion in Section 7.3.1 we note that the space of $\mathcal{N}=1$ vacua is $2^{45}\sim 3.52\times 10^{13}$. It is important to note at this point that there are two imaginary phases $C\binom{\mathbb{1}}{\boldsymbol{\gamma}} = \pm i$ and $C\binom{z_1}{\boldsymbol{\gamma}} = \pm i$, consistent with modular invariance, and all other phases are real. Furthermore, we note that the latter of these, $C\binom{z_1}{\boldsymbol{\gamma}}$, and the following four phases do not play a role in the phenomenological constraints

$$C\binom{\mathbb{1}}{b_1},\ C\binom{\mathbb{1}}{b_2}, C\binom{\mathbb{1}}{b_3},\ C\binom{\mathbb{1}}{z_1}. \tag{7.75}$$

This leaves a space of $2^{40}\sim 1.1\times 10^{12}$ $\mathcal{N}=1$ GGSO phase configurations.

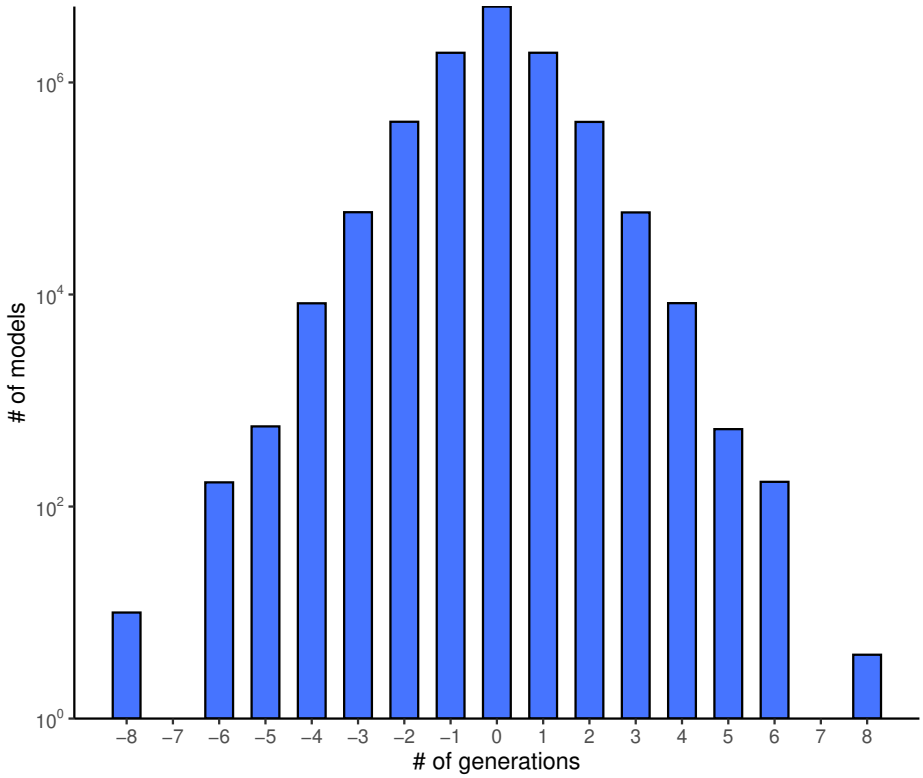

FIGURE 7.1: *Frequency plot for number of generations from a sample of* 10^7 *Class A vacua.*

7.4.1 Class A Phenomenological Features

Observable Spinorial Representations

From eq. (7.44) we can write the sectors producing fermions generations

$$\begin{aligned} \boldsymbol{F}^1_{qr} &= b_1 + qe_4 + re_5 \\ \boldsymbol{F}^2_{qr} &= b_2 + qe_2 + re_5 \\ \boldsymbol{F}^3_{qs} &= b_3 + qe_2 + se_4 \end{aligned} \tag{7.76}$$

and $\boldsymbol{D} = (1,1,1)$ means that any of these sectors will produce one copy of all states in the **16** or $\overline{\mathbf{16}}$ when present in the massless spectrum. Therefore the number of generations (7.51) simplifies to

$$n_g = N_{16} - N_{\overline{16}}. \tag{7.77}$$

Encoding the condition for 3 generations (7.52) for this class of models into Z3 returns `sat` to confirm 3 generation models are present for this class. In order to see the spread of generation number, n_g, we can generate a bar graph of generations for a random scan of Class A models. This graph is shown in Figure 7.1 for a sample of 10^7 vacua with $N_{16} \geq N_{\overline{16}}$ so that models with $n_g \geq 0$ are plotted. From this sample, we find 3 generation models with a probability of approximately 6×10^{-3}.

Tachyonic Sector Analysis

When classifying the $\mathcal{N}=0$ models we must ensure the projection of all on-shell tachyonic sectors. In addition to the model-independent tachyonic sectors (7.54), we have the following on-shell tachyonic sectors for Class A models that require an anti-holomorphic oscillator

$$T_1 = \left\{ \begin{array}{llll} \{\bar{\lambda}\}_{\frac{1}{2}}: & |e_2\rangle & |e_4\rangle & |e_5\rangle \\ \{\bar{\lambda}\}_{\frac{1}{2}}: & |e_2+e_4\rangle & |e_2+e_5\rangle & |e_4+e_5\rangle \\ \{\bar{\lambda}\}_{\frac{1}{2}}: & |e_2+e_4+e_5\rangle & |G+e_2+e_4+e_5\rangle & \\ \{\bar{\lambda}\}_{\frac{1}{2}}: & |(3)\boldsymbol{\gamma}\rangle & |x+(3)\boldsymbol{\gamma}\rangle & \\ \{\bar{\lambda}\}_{\frac{1}{4}}: & |z_1+(3)\boldsymbol{\gamma}\rangle & |z_2+(3)\boldsymbol{\gamma}\rangle & |z_1+x+(3)\boldsymbol{\gamma}\rangle \quad |z_2+x+(3)\boldsymbol{\gamma}\rangle \end{array} \right\} \tag{7.78}$$

As well as the following on-shell tachyonic sectors which arise with no oscillator

$$T_2 = \left\{ \begin{array}{cc} |z_1\rangle & |z_2\rangle \\ |e_i+z_1\rangle & |e_i+z_2\rangle \\ |e_i+e_j+z_1\rangle & |e_i+e_j+z_2\rangle \\ |e_i+e_j+e_k+z_1\rangle & |e_i+e_j+e_k+z_2\rangle \\ |G+e_2+e_4+e_5+z_1\rangle & |G+e_2+e_4+e_5+z_2\rangle \\ \\ |x+2\boldsymbol{\gamma}\rangle & |z_1+x+2\boldsymbol{\gamma}\rangle \\ |e_i+x+2\boldsymbol{\gamma}\rangle & |e_i+z_1+x+2\boldsymbol{\gamma}\rangle \\ |e_i+e_j+x+2\boldsymbol{\gamma}\rangle & |e_i+e_j+z_1+x+2\boldsymbol{\gamma}\rangle \\ |e_2+e_4+e_5+x+2\boldsymbol{\gamma}\rangle & |e_2+e_4+e_5+z_1+x+2\boldsymbol{\gamma}\rangle \\ |G+e_2+e_4+e_5+x+2\boldsymbol{\gamma}\rangle & |G+e_2+e_4+e_5+z_1+x+2\boldsymbol{\gamma}\rangle \\ \\ |z_2+x+2\boldsymbol{\gamma}\rangle & |z_1+z_2+x+2\boldsymbol{\gamma}\rangle \\ |e_i+z_2+x+2\boldsymbol{\gamma}\rangle & |e_i+z_1+z_2+x+2\boldsymbol{\gamma}\rangle \\ |e_i+e_j+z_2+x+2\boldsymbol{\gamma}\rangle & |e_i+e_j+z_1+z_2+x+2\boldsymbol{\gamma}\rangle \\ |e_2+e_4+e_5+z_2+x+2\boldsymbol{\gamma}\rangle & |e_2+e_4+e_5+z_1+z_2+x+2\boldsymbol{\gamma}\rangle \\ |G+e_2+e_4+e_5+z_2+x+2\boldsymbol{\gamma}\rangle & |G+e_2+e_4+e_5+z_1+z_2+x+2\boldsymbol{\gamma}\rangle \\ \\ |z_1+z_2+(3)\boldsymbol{\gamma}\rangle & |z_1+z_2+x+(3)\boldsymbol{\gamma}\rangle \end{array} \right\} \tag{7.79}$$

where $i \neq j \in \{2,4,5\}$. All of these sectors, $\boldsymbol{t} \in T_1$ and $\boldsymbol{t} \in T_2$, must be projected from the spectrum through appropriate definitions of their generalised projectors $\mathbb{P}_{\boldsymbol{t}} = 0$. Since there are so many sectors this is generally the most computationally expensive aspect of the classification methodology and is a key reason for introducing SMT methods into the program.

For reasons of efficiency in projecting the tachyonic sectors, we can split the projection into two steps. Firstly, since the SUSY generating vector S acts as a projector on all tachyonic sectors, we can implement this projection on all tachyonic sectors and see which sectors remain. Then we can construct and perform the other projections for the remaining sectors.

Enhancements

In classifying the Class A models we should ensure the absence of enhancements to the observable gauge factors coming from the class-Independent sectors given in eq. (7.56) using the generalised projectors discussed in Section 7.3. We have further sectors giving possible

observable enhancements through combinations with $\boldsymbol{\gamma}$. At the level $(\boldsymbol{\alpha}_L \cdot \boldsymbol{\alpha}_L, \boldsymbol{\alpha}_R \cdot \boldsymbol{\alpha}_R) = (0, 6)$ we have the following sectors

$$\psi^\mu \{\bar{\lambda}\}_{\frac{1}{4}} \begin{cases} |e_{136} + (3)\boldsymbol{\gamma}\rangle =: \boldsymbol{O_1} \\ |e_{136} + x + (3)\boldsymbol{\gamma}\rangle =: \boldsymbol{O_2} \end{cases} \tag{7.80}$$

and at level $(0, 8)$ there are the sectors

$$\psi^\mu \begin{cases} |e_{136} + z_1 + (3)\boldsymbol{\gamma}\rangle =: \boldsymbol{O_3} \\ |e_{136} + z_1 + x + (3)\boldsymbol{\gamma}\rangle =: \boldsymbol{O_4} \\ |e_{136} + z_2 + (3)\boldsymbol{\gamma}\rangle =: \boldsymbol{O_5} \\ |e_{136} + z_2 + x + (3)\boldsymbol{\gamma}\rangle =: \boldsymbol{O_6} \end{cases} \tag{7.81}$$

which should be projected to ensure the absence of observable enhancements. In order to construct the projectors we note that

$$\begin{aligned} \Upsilon(\boldsymbol{O_{1,2}}) =& \{S, e_2, e_4, e_5, z_1 + z_2 + x + 2\boldsymbol{\gamma}\} \\ \Upsilon(\boldsymbol{O_{3,4}}) =& \{S, e_2, e_4, e_5, z_2 + x + 2\boldsymbol{\gamma}\} \\ \Upsilon(\boldsymbol{O_{5,6}}) =& \{S, e_2, e_4, e_5, z_1 + x + 2\boldsymbol{\gamma}\} \end{aligned} \tag{7.82}$$

and the projectors have the form

$$\begin{aligned} \mathbb{P}_{\boldsymbol{O}_{1,2}} &= \prod_{\boldsymbol{\xi} \in \Upsilon(\boldsymbol{O}_{1,2})} \frac{1}{2}\left(1 + \delta_{\boldsymbol{O}_{1,2}} \delta_{\boldsymbol{\xi}}^{\psi^\mu} \delta_{\boldsymbol{\xi}}^{\bar{\lambda}} C\left(\begin{smallmatrix} \boldsymbol{O}_{1,2} \\ \boldsymbol{\xi} \end{smallmatrix}\right)\right) \\ \mathbb{P}_{\boldsymbol{O}_{3,4,5,6}} &= \prod_{\boldsymbol{\xi} \in \Upsilon(\boldsymbol{O}_{3,4,5,6})} \frac{1}{2}\left(1 + \delta_{\boldsymbol{O}_{3,4,5,6}} \delta_{\boldsymbol{\xi}}^{\psi^\mu} C\left(\begin{smallmatrix} \boldsymbol{O}_{3,4,5,6} \\ \boldsymbol{\xi} \end{smallmatrix}\right)\right). \end{aligned} \tag{7.83}$$

which gives three unique projectors from (7.82), on which we impose

$$\forall\ \bar{\lambda},\ \forall\ i \in [1, 6]: \quad \mathbb{P}_{\boldsymbol{O_i}} = 0. \tag{7.84}$$

.

Exotic Sectors

Another important consideration for ensuring reasonable phenomenology is the absence of chiral exotics. Along with the sectors (7.59) there are 124 sectors at the level $(4, 6)$ that can produce exotic massless states with a right moving oscillator such that $\nu_f = \frac{1}{2}$ or $\nu_{f^*} = -\frac{1}{2}$. These all arise in pairs with $+\boldsymbol{\gamma}$ and $+3\boldsymbol{\gamma}$ which contribute equal and opposite gauge charges and therefore do not contribute to any chiral anomaly. Similarly for the 212 exotic sectors at level $(4, 8)$. Therefore we conveniently do not need to implement a condition on chiral exotics in the classification for this class of models.

7.4.2 Class A Results

Having defined the key phenomenological characteristics for models in Class A we now seek to classify a large space of both $\mathcal{N} = 0$ and $\mathcal{N} = 1$ vacua with reference to the following key

	Total models in sample: 10^9				
	SUSY or Non-SUSY:	$\mathcal{N}=1$	Probability	$\mathcal{N}=0$	Probability
	Total	15624051	1.56×10^{-2}	984375949	0.984
(1)	+ Tachyon-Free			30779240	3.08×10^{-2}
(2)	+ No Observable Enhancements	15135704	1.51×10^{-2}	28581301	2.86×10^{-2}
(3)	+ Complete Generations	15135704	1.51×10^{-2}	28581301	2.86×10^{-2}
(4)	+ Three Generations	89930	8.99×10^{-5}	195716	1.96×10^{-4}
(5)	+ Heavy Higgs	89820	8.98×10^{-5}	129233	1.29×10^{-4}
(7)	+ TQMC	89820	8.98×10^{-5}	129233	1.29×10^{-4}
(8)	+ $a_{00}=N_b^0-N_f^0=0$			388	3.88×10^{-7}

TABLE 7.3: *Phenomenological statistics from sample of* 10^8 *Class A models. Note that the number of* $a_{00}=0$ *models is an estimate based on extrapolating from a sample of* 2×10^3 *of the 129233* $\mathcal{N}=0$ *models satisfying (1)-(7).*

classification criteria

$$\begin{aligned}
&(1)\ \text{No On-Shell Tachyons as discussed in Section 7.3.2 and 7.4.1}\\
&(2)\ \text{No Observable Enhancements as given by eq. (7.57) and (7.84)}\\
&(3)\ \text{Complete Generations: } n_g\neq0 \text{ and } n_{10}-n_{\overline{10}}=n_{\bar5}-n_5\\
&(4)\ \text{Three generations: } n_g=3\\
&(5)\ \text{Presence of Heavy Higgs: } n_{10H}\geq1\\
&(6)\ \text{Presence of viable Top Quark Mass Coupling}\\
&(7)\ \text{Super No-Scale Condition: } a_{00}=N_b^0-N_f^0=0
\end{aligned}\tag{7.85}$$

These conditions were discussed in previous sections other than (5) and (6) which are additional constraints coming from phenomenological considerations. More details on these can be found in [6]. The results of a classification of 10^9 Class A models created through random generation is presented in Table 7.3.

As mentioned in Section 7.2 we can employ machine learning techniques to efficiently find models satisfying the phenomenological criteria as well as to inform us of when criteria are in contradiction and no solutions can be found. As a test of efficiency we ran the algorithm for 1 hour to see how many models it finds satisfying the criteria (1)-(7) in Table 7.3 and compared it with the random generation method over the same time. The result of this comparison is displayed in Figure 7.2. We find that the SMT is approximately 322 times faster than the random scan after 3 minutes but after 1 hour it levels out at approximately 93 times faster. This demonstrates that the machine learning tool is especially effective as a fishing algorithm in finding pools of solutions very quickly, whereas its efficiency in complete enumeration of solutions reduces.

We can also perform a statistical analysis at the level of the partition function. This includes the calculation of the q-expanded partition function and the evaluation of the one-loop cosmological constant. In Figure 7.3, we present the distribution of the cosmological constant for a sample of Class A models evaluated at the free fermionic point. This shows that there is a tendency towards negative values, even though positive values are not excluded. It is important to note that this is not guaranteed to be a stable point in moduli space as there may be flat directions, however, the analysis of the potential is outside the scope of this

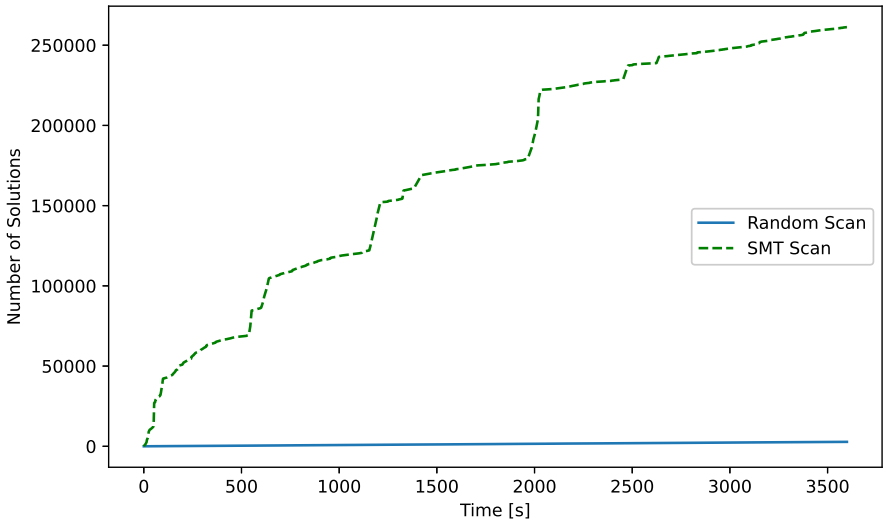

FIGURE 7.2: *Rate at which the Z3 SMT finds solutions satisfying constraints (1)-(7) compared with a random generation approach over a 1-hour period.*

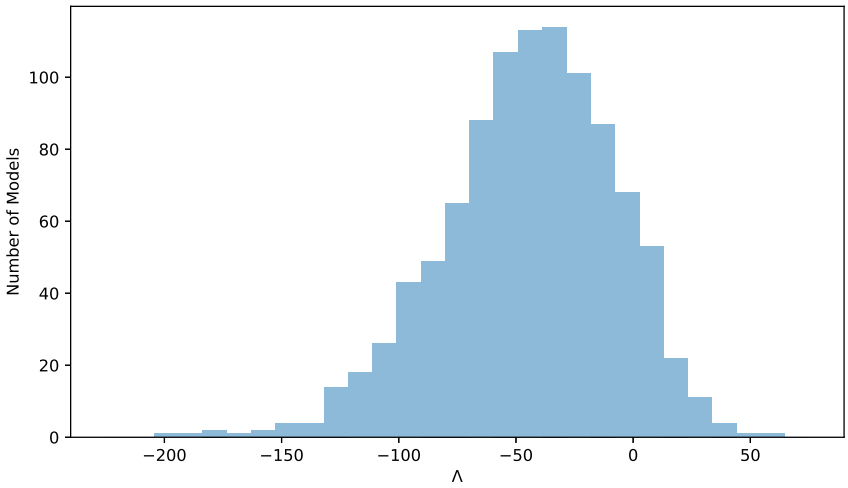

FIGURE 7.3: *The distribution of the cosmological constant Λ_{ST} for a sample off 10^3 Class A models satisfying conditions (1)-(7) of Table 7.3. To gain the physical value, a factor of $\mathcal{M}^4$ must be reinstated. These values are evaluated at the free fermionic point using methods discussed in Section 7.3.3.*

thesis and is left for future work. It is also interesting to compare the effectiveness of the SMT and random scan algorithms in finding unique models from the point of view of the partition function. Form Figure 7.4 we see that the SMT algorithm has a tendency to find more degenerate solutions as compared to a random scan. However, this does not conclude that random scans are more efficient. Indeed, comparing this to Figure 7.2, we see that SMT algorithms still vastly outperform random scans by more than 2 orders of magnitude.

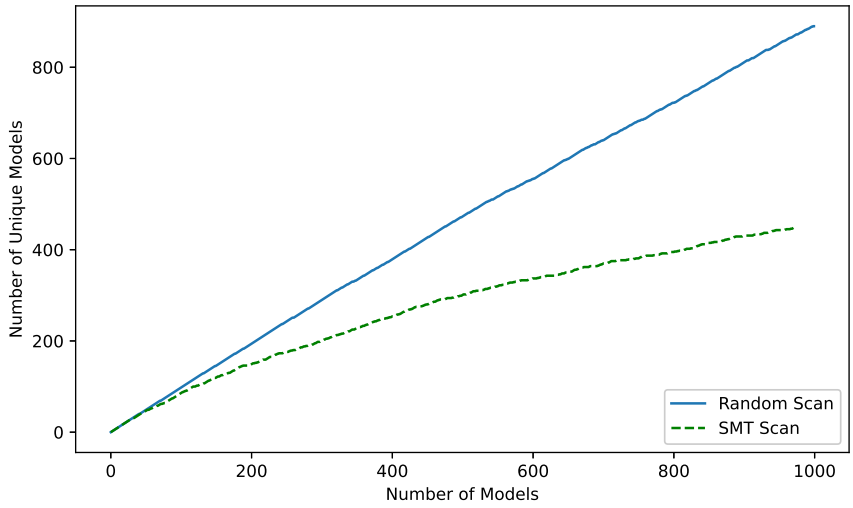

FIGURE 7.4: *The degeneracy of models in a Random versus an SMT scan for Class A as seen from the partition function.*

7.4.3 Class A Example Model

Having classified a random sample of Class A vacua, we can provide an example model satisfying criteria (1)-(7) of (7.85). Consider a model defined by the basis set (7.71) and choice of GGSO phases given by

$$C\left(\begin{smallmatrix}\boldsymbol{b}_i\\ \boldsymbol{b}_j\end{smallmatrix}\right) = \begin{array}{c} \\ \mathbf{1} \\ S \\ e_2 \\ e_4 \\ e_5 \\ b_1 \\ b_2 \\ b_3 \\ z_1 \\ x \\ \boldsymbol{\gamma} \end{array} \begin{array}{c} \begin{array}{cccccccccccc} \mathbf{1} & S & e_2 & e_4 & e_5 & b_1 & b_2 & b_3 & z_1 & x & \boldsymbol{\gamma} \end{array} \\ \left(\begin{array}{cccccccccccc} 1 & 1 & -1 & -1 & -1 & 1 & -1 & 1 & 1 & 1 & i \\ 1 & 1 & -1 & 1 & 1 & 1 & 1 & 1 & 1 & -1 & 1 \\ -1 & -1 & 1 & 1 & -1 & -1 & -1 & -1 & 1 & -1 & -1 \\ -1 & 1 & 1 & 1 & -1 & 1 & -1 & 1 & -1 & -1 & -1 \\ -1 & 1 & -1 & -1 & 1 & -1 & -1 & -1 & -1 & -1 & 1 \\ 1 & -1 & -1 & 1 & -1 & 1 & -1 & -1 & 1 & 1 & 1 \\ -1 & -1 & -1 & -1 & -1 & -1 & -1 & -1 & -1 & 1 & -1 \\ 1 & -1 & -1 & 1 & -1 & -1 & -1 & 1 & 1 & -1 & -1 \\ 1 & 1 & 1 & -1 & -1 & 1 & -1 & 1 & 1 & -1 & i \\ 1 & -1 & -1 & -1 & -1 & -1 & -1 & 1 & -1 & -1 & -1 \\ 1 & 1 & -1 & -1 & 1 & -1 & 1 & 1 & -1 & -1 & -1 \end{array}\right) \end{array} \tag{7.86}$$

This model has 3 fermion generations arising from $b_1 + e_4$, $b_2 + e_2$ and $b_3 + e_2 + e_4$.

The partition function for Class A models can be found using the methods discussed in Section 7.3.3. Specifically, the internal lattice can be constructed by noting that the form of $\boldsymbol{A}$ introduces exactly one asymmetric pairing in each of the three orbifold planes. Thus the

internal lattice takes the form

$$\begin{aligned}\Gamma^{\gamma}_{(6,6)} = &\vartheta\left[\begin{smallmatrix} r+h_2+H_4 \\ s+g_2+G_4 \end{smallmatrix}\right]^{1/2}_{y^4} \vartheta\left[\begin{smallmatrix} r+h_2+H_5 \\ s+g_2+G_5 \end{smallmatrix}\right]^{1/2}_{y^5} \vartheta\left[\begin{smallmatrix} r+h_2+2H' \\ s+g_2+2G' \end{smallmatrix}\right]_{y^{3,6}} \\ &\times \vartheta\left[\begin{smallmatrix} r+h_2+H_4 \\ s+g_2+G_4 \end{smallmatrix}\right]^{1/2}_{\bar{y}^4} \bar{\vartheta}\left[\begin{smallmatrix} r+h_2+H_5 \\ s+g_2+G_5 \end{smallmatrix}\right]^{1/2}_{\bar{y}^5} \bar{\vartheta}\left[\begin{smallmatrix} r+h_2 \\ s+g_2 \end{smallmatrix}\right]_{\bar{y}^{3,6}} \\ &\times \vartheta\left[\begin{smallmatrix} r+h_2+H_2 \\ s+g_2+G_2 \end{smallmatrix}\right]^{1/2}_{y^2} \vartheta\left[\begin{smallmatrix} r+h_2+H_5 \\ s+g_2+G_5 \end{smallmatrix}\right]^{1/2}_{w^5} \vartheta\left[\begin{smallmatrix} r+h_2+2H' \\ s+g_2+2G' \end{smallmatrix}\right]_{y^1 w^6} \\ &\times \vartheta\left[\begin{smallmatrix} r+h_1+H_2 \\ s+g_1+G_2 \end{smallmatrix}\right]^{1/2}_{\bar{y}^2} \bar{\vartheta}\left[\begin{smallmatrix} r+h_1+H_5 \\ s+g_1+G_5 \end{smallmatrix}\right]^{1/2}_{\bar{w}^5} \bar{\vartheta}\left[\begin{smallmatrix} r+h_1 \\ s+g_1 \end{smallmatrix}\right]_{\bar{y}^1 \bar{w}^6} \\ &\times \vartheta\left[\begin{smallmatrix} r-h_1-h_2+H_2 \\ s-g_1-g_2+G_2 \end{smallmatrix}\right]^{1/2}_{w^2} \vartheta\left[\begin{smallmatrix} r-h_1-h_2+H_4 \\ s-g_1-g_2+G_4 \end{smallmatrix}\right]^{1/2}_{w^4} \vartheta\left[\begin{smallmatrix} r-h_1-h_2+2H' \\ s-g_1-g_2+2G' \end{smallmatrix}\right]_{w^{1,3}} \\ &\times \vartheta\left[\begin{smallmatrix} r-h_1-h_2+H_2 \\ s-g_1-g_2+G_2 \end{smallmatrix}\right]^{1/2}_{\bar{w}^2} \bar{\vartheta}\left[\begin{smallmatrix} r-h_1-h_2+H_4 \\ s-g_1-g_2+G_4 \end{smallmatrix}\right]^{1/2}_{\bar{w}^4} \bar{\vartheta}\left[\begin{smallmatrix} r-h_1-h_2 \\ s-g_1-g_2 \end{smallmatrix}\right]_{\bar{w}^{1,3}} .\end{aligned} \tag{7.87}$$

We can then use this expression together with (7.65) and (7.69) to gain the q-expanded partition function of this model which is

$$\begin{aligned}Z = &\, 2\,q^0\bar{q}^{-1} - 8\,q^{1/4}\bar{q}^{-3/4} - 16\,q^{1/2}\bar{q}^{-1/2} + 8\,q^{-1/2}\bar{q}^{1/2} \\ &+ 176\,q^{1/8}\bar{q}^{1/8} + 976\,q^{1/4}\bar{q}^{1/4} + 2048\,q^{3/8}\bar{q}^{3/8} + 2560\,q^{1/2}\bar{q}^{1/2},\end{aligned} \tag{7.88}$$

including all terms up to at most $\mathcal{O}(q^{1/2})$ and $\mathcal{O}(\bar{q}^{1/2})$. The top line gives the off-shell tachyonic states required by modular invariance, while the bottom line gives all on-shell states. Note the presence of the off-shell model-independent term $2\,q^0\bar{q}^{-1}$ obtained from the so-called 'proto-graviton' resulting from the state $\psi^\mu\,|0\rangle_L \otimes |0\rangle_R$. This provides a neat check to confirm the correct normalisation of the partition function. We also see that this model is indeed of the super no-scale type, *i.e.*s has $a_{00} = n_b^0 - n_f^0 = 0$. Integrating this expansion over the fundamental domain of the modular group via (4.67) yields the spacetime cosmological constant

$$\Lambda_{\rm ST} = 13.34 \times \mathcal{M}^4, \tag{7.89}$$

which was calculated to $4^{\rm th}$ order q and $\bar{q}$. It is important to note that this value is not calculated at a minimum in the moduli space, but rather at a maximally symmetric point where the orbifold theory admits a free fermionic description.

Whether the cosmological constant can indeed be suppressed requires more in-depth analysis. In these Class A models, all untwisted moduli being retained complicates this analysis, which motivates the study of a different class of models where some moduli are projected. Such a model is described in the next section. Moreover, through a translation to a $\mathbb{Z}_2^n$ orbifold in the bosonic picture the dependence on some of these geometric moduli can be reinstated and a systematic investigation of the one-loop potential can be attempted as done in [7, 82, 83, 108] for symmetric orbifolds, however, its implementation for asymmetric models is left for future work.

7.5 Asymmetric Orbifold of Class B

The second Class of models we study is an example where all untwisted moduli on the second and third tori are projected and only h_{11}, h_{12}, h_{21} and h_{22} are retained. From Table 7.1 and 7.2 we can see there are 12 possible pairings in both the bosonic and fermionic cases that

give rise to just h_{11}, h_{12}, h_{21} and h_{22}, whilst allowing for odd number generations. These all have $\boldsymbol{E} = (1,1,0,0,0,0)$. The possible pairings can be grouped into 3 types according to their $\boldsymbol{\Delta} = (\Delta_1, \Delta_2, \Delta_3)$ and degeneracies $\boldsymbol{D} = (D_1, D_2, D_3)$, which for the bosonic case are

$$\boldsymbol{A} = \begin{cases} \{\bar{w}^{3456}\}, \{y^{34}, w^{34}, \bar{y}^{34}, \bar{w}^{56}\}, & \boldsymbol{\Delta} = (0,1,1), \quad \boldsymbol{D} = (8,1,1) \\ \{y^{3456}, w^{3456}, \bar{y}^{3456}\}, \{y^{56}, w^{56}, \bar{y}^{56}, \bar{w}^{34}\} & \\ \{\bar{y}^{56}, \bar{w}^{34}\}, \{y^{56}, w^{56}, \bar{w}^{3456}\}, & \boldsymbol{\Delta} = (1,0,1), \quad \boldsymbol{D} = (4,2,1) \\ \{y^{34}, w^{34}, \bar{y}^{3456}\}, \{y^{3456}, w^{3456}, \bar{y}^{34}, \bar{y}^{56}\} & \\ \{\bar{y}^{34}, \bar{w}^{56}\}, \{y^{34}, w^{34}, \bar{y}^{34}\bar{w}^{56}\}, & \boldsymbol{\Delta} = (1,1,0), \quad \boldsymbol{D} = (4,1,2) \\ \{y^{3456}, w^{3456}, \bar{y}^{3456}\}, \{y^{56}, w^{56}, \bar{y}^{56}, \bar{w}^{34}\} & \end{cases} \tag{7.90}$$

As mentioned in Section 7.3, the condition for odd number generations 7.33 is a necessary but not sufficient condition for the possibility of having 3 generation models within a class. We can check which of the 3 pairing possibilities in (7.90) can give rise to 3 generations by checking whether eq. (7.52) is satisfiable with our SMT solver for each $\boldsymbol{A}$. Doing this tells us that none of the pairings can give rise to 3 generation models. Despite this we will choose the pairing $\boldsymbol{A} = \{\bar{w}^{34}, \bar{w}^{56}\}$ with $\boldsymbol{D} = (4,2,1)$ to classify systematically and in Section 7.5.1 we will demonstrate the origin of the absence of three generations.
The basis for this class of models will then be

$$\mathbb{1} = \{\psi^\mu, \chi^{1,\dots,6}, y^{1,\dots,6}, w^{1,\dots,6} \mid \overline{y}^{1,\dots,6}, \overline{w}^{1,\dots,6}, \overline{\psi}^{1,\dots,5}, \overline{\eta}^{1,2,3}, \overline{\phi}^{1,\dots,8}\}, \tag{7.91}$$

$$S = \{\psi^\mu, \chi^{1,\dots,6}\}, \tag{7.92}$$

$$e_1 = \{y^1, w^1 \mid \overline{y}^1, \overline{w}^1\}, \tag{7.93}$$

$$e_2 = \{y^2, w^2 \mid \overline{y}^2, \overline{w}^2\}, \tag{7.94}$$

$$b_1 = \{\psi^\mu, \chi^{12}, y^{34}, y^{56} \mid \overline{y}^{34}, \overline{y}^{56}, \overline{\eta}^1, \overline{\psi}^{1,\dots,5}\}, \tag{7.95}$$

$$b_2 = \{\psi^\mu, \chi^{34}, y^{12}, w^{56} \mid \overline{y}^{12}, \overline{w}^{56}, \overline{\eta}^2, \overline{\psi}^{1,\dots,5}\}, \tag{7.96}$$

$$b_3 = \{\psi^\mu, \chi^{56}, w^{1234} \mid \overline{w}^{1234}, \overline{\eta}^3, \overline{\psi}^{1,\dots,5}\}, \tag{7.97}$$

$$z_1 = \{\overline{\phi}^{1,\dots,4}\}, \tag{7.98}$$

$$x = \{\overline{\psi}^{1,\dots,5}, \overline{\eta}^{1,2,3}\}, \tag{7.99}$$

$$\boldsymbol{\gamma} = \{\bar{y}^{56}, \bar{w}^{34}, \bar{\psi}^{1,\dots,5} = \bar{\eta}^{1,2,3} = \bar{\phi}^{1,2,6,7} = \frac{1}{2}, \bar{\phi}^8\} \tag{7.100}$$

where we have the same z_2 combination as eq. (7.20) and the untwisted gauge group is

$$\text{Observable:} \quad SU(5) \times U(1) \times U(1)_{i=1,2,3} \times U(1)_{j=4,5} \tag{7.101}$$

$$\text{Hidden:} \quad SU(2) \times U(1)_{H_1} \times SO(4) \times U(1)_{H_2} \times SU(2) \times U(1)_{H_3} \times U(1)_{H_4}. \tag{7.102}$$

There are two horizontal symmetries associated to the anti-holomorphic currents from the pairings $\bar{y}^{5,6}$ and $\bar{w}^3\bar{w}^4$. Since there are 10 basis vectors we naively have 2^{45} independent GGSO configurations but the following 10 phases do not affect the projection criteria for the phenomenological criteria we investigate

$$C\binom{\mathbb{1}}{b_1}, C\binom{\mathbb{1}}{b_2}, C\binom{\mathbb{1}}{b_3}, C\binom{\mathbb{1}}{z_1}, C\binom{\mathbb{1}}{\boldsymbol{\gamma}}, C\binom{S}{\boldsymbol{\gamma}}, C\binom{b_1}{\boldsymbol{\gamma}}, C\binom{b_3}{\boldsymbol{\gamma}}, C\binom{z_1}{\boldsymbol{\gamma}}, C\binom{x}{\boldsymbol{\gamma}}. \tag{7.103}$$

This leaves just 35 free GGSO phases generating a space of $2^{35} \sim 3.4 \times 10^{10}$ independent configurations to classify. The supersymmetric subspace of which is subject to conditions (7.38) and (7.39).

7.5.1 Class B Phenomenological Features

Observable Spinorials Representations and Three Generation

The following sectors give rise to the fermion generations

$$\boldsymbol{F}_t^1 = b_1 + te_{3456} \tag{7.104}$$
$$\boldsymbol{F}_{pq}^2 = b_2 + pe_1 + qe_2 \tag{7.105}$$
$$\boldsymbol{F}_{pq}^3 = b_3 + pe_1 + qe_2 \tag{7.106}$$

and the degeneracies $\boldsymbol{D}$ tell us that $\boldsymbol{F}_0^1$ generate 4 copies of the **16** or $\overline{\mathbf{16}}$, $\boldsymbol{F}_1^1$ generate 2 copies of the **16** *and* 2 copies of the $\overline{\mathbf{16}}$, whilst $\boldsymbol{F}_{pq}^2$ generate 2 copies of either $\left(\mathbf{10}, +\frac{1}{2}\right)$, $\left(\bar{\mathbf{5}}, -\frac{3}{2}\right) + \left(\mathbf{1}, \frac{5}{2}\right)$, $\left(\overline{\mathbf{10}}, -\frac{1}{2}\right)$ or $\left(\mathbf{5}, +\frac{3}{2}\right) + \left(\mathbf{1}, -\frac{5}{2}\right)$. Lastly, $\boldsymbol{F}_{pqrs}^3$ generates 1 copy of the **16** or $\overline{\mathbf{16}}$.

As mentioned above, three-generation models do not arise in this class, and to see why it will be useful to write the projection equations for these spinorial sectors. We can first construct the projectors for these sectors by utilising eq. (7.45)

$$\mathbb{P}_{\boldsymbol{F}_t^1} = \frac{1}{2^5} \prod_{i=1,2} \left(1 - C\left(\begin{smallmatrix} \boldsymbol{F}_t^{(1)} \\ e_i \end{smallmatrix}\right)\right) \left(1 - C\left(\begin{smallmatrix} \boldsymbol{F}_t^{(1)} \\ \mathbf{2\gamma + x} \end{smallmatrix}\right)\right) \prod_{a=1,2} \left(1 - C\left(\begin{smallmatrix} \boldsymbol{F}_t^{(1)} \\ z_a \end{smallmatrix}\right)\right) \tag{7.107}$$

$$\mathbb{P}_{\boldsymbol{F}_{pq}^2} = \frac{1}{2^3} \left(1 - C\left(\begin{smallmatrix} \boldsymbol{F}_{pq}^2 \\ \mathbf{2\gamma + x} \end{smallmatrix}\right)\right) \prod_{a=1,2} \left(1 - C\left(\begin{smallmatrix} \boldsymbol{F}_{pq}^2 \\ z_a \end{smallmatrix}\right)\right) \tag{7.108}$$

$$\mathbb{P}_{\boldsymbol{F}_{pq}^3} = \frac{1}{2^3} \left(1 - C\left(\begin{smallmatrix} \boldsymbol{F}_{pq}^3 \\ \mathbf{2\gamma + x} \end{smallmatrix}\right)\right) \prod_{a=1,2} \left(1 - C\left(\begin{smallmatrix} \boldsymbol{F}_{pq}^3 \\ z_a \end{smallmatrix}\right)\right) \tag{7.109}$$

Next, we can apply eq. (7.46) to get the chirality phases

$$\boldsymbol{X}_{t=0}^1 = -C\left(\begin{smallmatrix} \boldsymbol{F}_0^1 \\ b_2 \end{smallmatrix}\right)^*,$$
$$\boldsymbol{X}_{pq}^2 = -C\left(\begin{smallmatrix} \boldsymbol{F}_{pq}^2 \\ b_1 \end{smallmatrix}\right)^*$$
$$\boldsymbol{X}_{pq}^3 = -C\left(\begin{smallmatrix} \boldsymbol{F}_{pq}^3 \\ b_1 \end{smallmatrix}\right)^*$$

where we have chosen $\mathrm{ch}(\psi^\mu) = +1$ for the spacetime fermion chirality and note the $\boldsymbol{F}_1^1$ does not have a chirality operator as it gives rise to 2 copies of the **16** and the $\overline{\mathbf{16}}$. By applying

eq. (7.50) we can write the quantum numbers of the $SU(5) \times U(1)$ representations as

$$\begin{aligned}
n_{10} &= \sum_{t=0,1} 2\mathbb{P}_{\boldsymbol{F}_t^1} \frac{1}{2}\left(1 + t + (1-t)\boldsymbol{X}_t^1\right) + \sum_{p,q=0,1} 2\mathbb{P}_{\boldsymbol{F}_{pq}^2} \frac{1}{4}\left(1 + \boldsymbol{X}_{pq}^2\right)\left(1 + C\left(\begin{smallmatrix}\boldsymbol{F}_{pq}^2\\ \boldsymbol{\gamma}\end{smallmatrix}\right)\right) \\
&\quad + \sum_{p,q=0,1} \mathbb{P}_{\boldsymbol{F}_{pq}^3} \frac{1}{2}\left(1 + \boldsymbol{X}_{pq}^3\right) \\
n_{\bar{5}} &= \sum_{t=0,1} 2\mathbb{P}_{\boldsymbol{F}_t^1} \frac{1}{2}\left(1 + t + (1-t)\boldsymbol{X}_t^1\right) + \sum_{p,q=0,1} 2\mathbb{P}_{\boldsymbol{F}_{pq}^2} \frac{1}{4}\left(1 + \boldsymbol{X}_{pq}^2\right)\left(1 - C\left(\begin{smallmatrix}\boldsymbol{F}_{pq}^2\\ \boldsymbol{\gamma}\end{smallmatrix}\right)\right) \\
&\quad + \sum_{p,q=0,1} \mathbb{P}_{\boldsymbol{F}_{pq}^3} \frac{1}{2}\left(1 + \boldsymbol{X}_{pq}^3\right) \\
n_{\overline{10}} &= \sum_{t=0,1} 2\mathbb{P}_{\boldsymbol{F}_t^1} \frac{1}{2}\left(1 + t - (1-t)\boldsymbol{X}_t^1\right) + \sum_{p,q=0,1} 2\mathbb{P}_{\boldsymbol{F}_{pq}^2} \frac{1}{4}\left(1 - \boldsymbol{X}_{pq}^2\right)\left(1 + C\left(\begin{smallmatrix}\boldsymbol{F}_{pq}^2\\ \boldsymbol{\gamma}\end{smallmatrix}\right)\right) \\
&\quad + \sum_{p,q=0,1} \mathbb{P}_{\boldsymbol{F}_{pq}^3} \frac{1}{2}\left(1 - \boldsymbol{X}_{pq}^3\right) \\
n_5 &= \sum_{t=0,1} 2\mathbb{P}_{\boldsymbol{F}_t^1} \frac{1}{2}\left(1 + t - (1-t)\boldsymbol{X}_t^1\right) + \sum_{p,q=0,1} 2\mathbb{P}_{\boldsymbol{F}_{pq}^2} \frac{1}{4}\left(1 - \boldsymbol{X}_{pq}^2\right)\left(1 - C\left(\begin{smallmatrix}\boldsymbol{F}_{pq}^2\\ \boldsymbol{\gamma}\end{smallmatrix}\right)\right) \\
&\quad + \sum_{p,q=0,1} \mathbb{P}_{\boldsymbol{F}_{pq}^3} \frac{1}{2}\left(1 - \boldsymbol{X}_{pq}^3\right),
\end{aligned} \tag{7.110}$$

where we note the singlets have the same projection as **5** and $\bar{\mathbf{5}}$. Imposing the condition for complete generations $n_{10} - n_{\overline{10}} = n_{\bar{5}} - n_5$ results in the condition

$$\sum_{p,q} \mathbb{P}_{\boldsymbol{F}_{pq}^2} C\left(\begin{smallmatrix}\boldsymbol{F}_{pq}^2\\ \boldsymbol{\gamma}\end{smallmatrix}\right) X_{pq}^2 = 0 \tag{7.111}$$

and $n_{10} - n_{\overline{10}} = 3$ for three generations tells us

$$3 = \sum_t 2\mathbb{P}_{F_t^1} X_t^1 + \sum_{p,q} 2\mathbb{P}_{F_{pq}^2} \frac{1}{2}\left(1 + C\left(\begin{smallmatrix}\boldsymbol{F}_{pq}^2\\ \boldsymbol{\gamma}\end{smallmatrix}\right)\right) X_{pq}^2 + \sum_{p,q} \mathbb{P}_{\boldsymbol{F}_{pq}^3} X_{pq}^3 \tag{7.112}$$

which is only possible if

$$\sum_{p,q} \mathbb{P}_{\boldsymbol{F}_{pq}^3} X_{pq}^3 \in \{1, 3\} \tag{7.113}$$

but $\sum_{p,q} \mathbb{P}_{\boldsymbol{F}_{pq}^3} X_{pq}^3 = 3$ we can show is impossible by inspecting (7.109) which only depends on nine phases

$$C\left(\begin{smallmatrix}b_3\\ z_1\end{smallmatrix}\right),\ C\left(\begin{smallmatrix}b_3\\ z_2\end{smallmatrix}\right),\ C\left(\begin{smallmatrix}b_3\\ x\end{smallmatrix}\right),\ C\left(\begin{smallmatrix}e_1\\ z_1\end{smallmatrix}\right),\ C\left(\begin{smallmatrix}e_1\\ z_2\end{smallmatrix}\right),\ C\left(\begin{smallmatrix}e_1\\ x\end{smallmatrix}\right),\ C\left(\begin{smallmatrix}e_2\\ z_1\end{smallmatrix}\right),\ C\left(\begin{smallmatrix}e_2\\ z_2\end{smallmatrix}\right),\ C\left(\begin{smallmatrix}e_2\\ x\end{smallmatrix}\right) \tag{7.114}$$

and if 3 of the 4 sectors $\boldsymbol{F}_{pq}^3$ have $\mathbb{P}_{\boldsymbol{F}_{pq}^3} = 1$ then all 9 phases are fixed and ensures the fourth also has $\mathbb{P}_{\boldsymbol{F}_{pq}^3} = 1$.

Therefore the only way to satisfy (7.112) is if $\sum_{p,q} \mathbb{P}_{\boldsymbol{F}_{pq}^3} X_{pq}^3 = 1$. This further implies $\sum_{p,q} \mathbb{P}_{\boldsymbol{F}_{pq}^2} C\left(\begin{smallmatrix}\boldsymbol{F}_{pq}^2\\ \boldsymbol{\gamma}\end{smallmatrix}\right) X_{pq}^2 \in \{2, 4\}$ from (7.111). If we assume $\sum_{p,q} \mathbb{P}_{\boldsymbol{F}_{pq}^2} C\left(\begin{smallmatrix}\boldsymbol{F}_{pq}^2\\ \boldsymbol{\gamma}\end{smallmatrix}\right) X_{pq}^2 = 2$ then

the constraints this imposes on the phases in $\mathbb{P}_{\boldsymbol{F}^2_{pq}}$ necessitates

$$\sum_{p,q} \mathbb{P}_{\boldsymbol{F}^3_{pq}} X^3_{pq} \in \{0, 2\} \tag{7.115}$$

making 3 generations impossible. Similarly if $\sum_{p,q} \mathbb{P}_{\boldsymbol{F}^2_{pq}} C\left(\begin{smallmatrix}\boldsymbol{F}^2_{pq}\\ \boldsymbol{\gamma}\end{smallmatrix}\right) X^2_{pq} = 4$ this imposes

$$\sum_{p,q} \mathbb{P}_{\boldsymbol{F}^3_{pq}} X^3_{pq} \in \{0, 4\} \tag{7.116}$$

which again makes 3 generations impossible.

Tachyonic Sector Analysis

Class A models have significantly fewer tachyonic sectors than Class B. Specifically there are 27 sectors producing on-shell tachyons for Class B, compared with the 78 of Class A. The following 3 sectors will produce on-shell tachyons with a right-moving oscillator should they be present in the spectrum of a model

$$T_1 = \begin{Bmatrix} \{\bar{\lambda}\}_{\frac{1}{2}}: & |e_1\rangle & |e_2\rangle \\ \{\bar{\lambda}\}_{\frac{1}{2}}: & |e_1 + e_2\rangle & \end{Bmatrix} \tag{7.117}$$

Further to this, the following on-shell tachyonic sectors arise with no oscillator

$$T_2 = \left\{ \begin{array}{ccc} |z_1\rangle & |z_2\rangle & |x + 2\boldsymbol{\gamma}\rangle \\ |e_i + z_1\rangle & |e_i + z_2\rangle & |e_i + x + 2\boldsymbol{\gamma}\rangle \\ |e_1 + e_2 + z_1\rangle & |e_1 + e_2 + z_2\rangle & |e_1 + e_2 + x + 2\boldsymbol{\gamma}\rangle \\ & & \\ |z_1 + x + 2\boldsymbol{\gamma}\rangle & |z_2 + x + 2\boldsymbol{\gamma}\rangle & |z_1 + z_2 + x + 2\boldsymbol{\gamma}\rangle \\ |e_i + z_1 + x + 2\boldsymbol{\gamma}\rangle & |e_i + z_2 + x + 2\boldsymbol{\gamma}\rangle & |e_i + z_1 + z_2 + x + 2\boldsymbol{\gamma}\rangle \\ |e_1 + e_2 + z_1 + x + 2\boldsymbol{\gamma}\rangle & |e_1 + e_2 + z_2 + x + 2\boldsymbol{\gamma}\rangle & |e_1 + e_2 + z_1 + z_2 + x + 2\boldsymbol{\gamma}\rangle \end{array} \right\} \tag{7.118}$$

where $i \in \{1, 2\}$. The condition for the absence of such tachyonic sectors can be compactly written

$$\forall\ t \in T_1 \cup T_2: \quad \mathbb{P}_t = 0. \tag{7.119}$$

Enhancements

As in Class A models, we will ensure the absence of enhancements to the observable gauge factors given from sectors listed in eq. (7.56) as well as the model-dependent sectors

$$\psi^\mu \{\bar{\lambda}\}_{\frac{1}{4}} \begin{cases} |z_1 + (3)\boldsymbol{\gamma}\rangle =: \mathbf{O}_1 \\ |z_1 + x + (3)\boldsymbol{\gamma}\rangle =: \mathbf{O}_2 \\ |z_1 + z_2 + (3)\boldsymbol{\gamma}\rangle =: \mathbf{O}_3 \\ |z_1 + z_2 + x + (3)\boldsymbol{\gamma}\rangle =: \mathbf{O}_4 \end{cases} \tag{7.120}$$

and we ensure the generalised projectors of these sectors are zero, which can be written as

$$\forall\ i \in [1, 4]: \quad \mathbb{P}_{\mathbf{O}_i} = 0. \tag{7.121}$$

	Total models in sample: $2^{31} = 2147483648$				
	SUSY or Non-SUSY:	$\mathcal{N}=1$	Probability	$\mathcal{N}=0$	Probability
	Total	134217728	6.25×10^{-2}	2013265920	9.38×10^{-1}
(1)	+ Tachyon-Free			518921216	2.42×10^{-1}
(2)	+ No Obs. Enhancements	121896960	5.68×10^{-2}	478915840	2.23×10^{-1}
(3)	+ Complete Generations	74317824	3.46×10^{-2}	271702016	1.27×10^{-1}
(8)	+ $a_{00} = N_b^0 - N_f^0 = 0$			326042	1.51×10^{-4}

TABLE 7.4: *Phenomenological statistics from a complete scan of* 2^{31} *Class B models. Note that the number of* $a_{00} = 0$ *models is an estimate based on extrapolating from a sample of* 2.5×10^3 *of the 1245265024* $\mathcal{N} = 0$ *models satisfying (1)-(3).*

Exotics

Along with the $(\boldsymbol{\alpha}_L \cdot \boldsymbol{\alpha}_L, \boldsymbol{\alpha}_R \cdot \boldsymbol{\alpha}_R) = (4, 4)$ exotic sectors (7.59), there are 112 sectors at the level $(4, 6)$ that can produce exotic massless states with a right moving oscillator with $\nu_f = \frac{1}{2}$ or $\nu_{f^*} = -\frac{1}{2}$. As in Model A these all arise in pairs with $+\boldsymbol{\gamma}$ and $+3\boldsymbol{\gamma}$ with equal and opposite gauge charges and therefore do not contribute to any chiral anomaly. Similarly for 176 sectors at level $(4, 8)$. Therefore we conveniently do not need to implement a condition on chiral exotics in the classification.

7.5.2 Class B Results

We wish to implement the constraints listed in (7.85) for the case of Class B. However, the absence of 3 generation models in this class means all models break at constraint (4). For completeness, we still present the reduced results in Table 7.4. In order to do a complete scan, we choose to impose condition (7.40) such that for $\mathcal{N} = 0$ models SUSY is broken by phases beyond the NAHE-set. This condition reduces the parameter space to $2^{31} \sim 2.15 \times 10^9$. We then enumerate all possible configurations of these 31 phases that give both $\mathcal{N} = 1$ and $\mathcal{N} = 0$ models.
In order to compare the efficiency of the SMT solver to that of a random scan we can search for four generation models rather than three that satisfy criteria (1)-(3) and (5)-(7) from (7.85). The results of this comparison are shown in Figure 7.5. We see that the efficiency gained from the SMT is lower for Class B than the Class A case with efficiency approximately 5.5 times higher compared to the random approach after 3 minutes, reducing to approximately 1.5 times after 1 hour. This reduced efficiency for Class B seems to result from the fewer constraints imposed from the absence of tachyons evidenced by the probability 2.42×10^{-1} for Table 7.4 compared to 3.08×10^{-2} for Table 7.3, as well as the smaller space of models and higher degeneracy meaning the SMT algorithm's search saturates more quickly than in Class A.

As in the case of Class A models, it is also interesting to perform a statistical analysis at the level of the partition function. Figure 7.6 shows the distribution of the cosmological constant for a batch of 1.5×10^3 Class B models satisfying conditions (1)-(3) of Table 7.4. We again note the slight tendency to negative values even though positive values are not excluded. Similarly to Figure 7.4 in the class A case, the SMT find a larger number of degenerate models. This is mostly due to the reduced number of constraints on the GGSO phases and the increased frequency of solutions as discussed above.

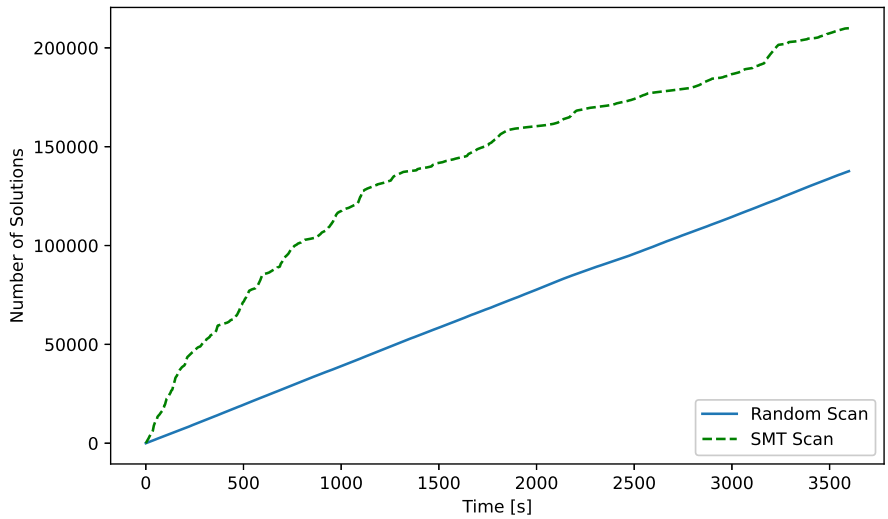

FIGURE 7.5: *Rate at which the Z3 SMT finds 4 generation models satisfying constraints (1)-(3) and (5)-(7) compared with a random generation approach over a 1 hour period.*

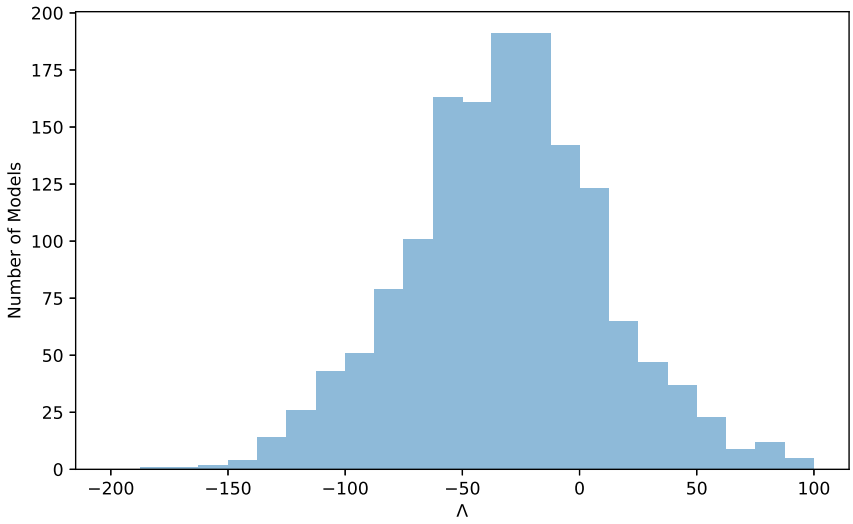

FIGURE 7.6: *The distribution of the cosmological constant Λ_{ST} for a sample off 1.5×10^3 Class B models satisfying conditions (1)-(3) of Table 7.4. To gain the physical value, a factor of $\mathcal{M}^4$ must be reinstated. These values are evaluated at the free fermionic point using methods discussed in Section 7.3.3.*

7.5.3 Class B Example Model with 4 Generations

Having discussed the absence of three-generation models in this class, we give an example four generation model and discuss its key characteristics. We emphasize that, although this class of models is not phenomenological, they are of particular interest due to the fact that the untwisted moduli of the 2nd and 3rd tori are fixed. The chosen model is defined by the

basis (7.91) and the GGSO phases

$$C\left(\begin{smallmatrix}\boldsymbol{b}_i\\ \boldsymbol{b}_j\end{smallmatrix}\right) = \begin{array}{c} \\ \mathbf{1} \\ S \\ e_1 \\ e_2 \\ b_1 \\ b_2 \\ b_3 \\ z_1 \\ x \\ \boldsymbol{\gamma} \end{array} \begin{array}{c} \begin{array}{cccccccccc} \mathbf{1} & S & e_1 & e_2 & b_1 & b_2 & b_3 & z_1 & x & \boldsymbol{\gamma} \end{array} \\ \begin{pmatrix} 1 & -1 & 1 & 1 & -1 & -1 & -1 & -1 & 1 & -i \\ -1 & -1 & 1 & 1 & -1 & -1 & -1 & 1 & 1 & -1 \\ 1 & 1 & -1 & 1 & -1 & 1 & -1 & -1 & 1 & 1 \\ 1 & 1 & 1 & -1 & -1 & 1 & 1 & 1 & 1 & 1 \\ -1 & 1 & -1 & -1 & -1 & -1 & -1 & -1 & -1 & -1 \\ -1 & 1 & 1 & 1 & -1 & -1 & 1 & 1 & -1 & -i \\ -1 & 1 & -1 & 1 & -1 & 1 & -1 & -1 & 1 & -1 \\ -1 & 1 & -1 & 1 & -1 & 1 & -1 & -1 & 1 & -i \\ 1 & 1 & 1 & 1 & 1 & 1 & -1 & 1 & -1 & -1 \\ 1 & -1 & 1 & 1 & -1 & -1 & -1 & 1 & -1 & -i \end{pmatrix} \end{array} \tag{7.122}$$

The states from sector b_1 generate four copies of fermion generations in the **16**. There is a hidden sector gauge boson from $\psi^\mu\{\bar{y}^1\}\,|z_1\rangle$ which enhances the hidden gauge group

$$\begin{aligned} &SU(2)\times U(1)_{H_1}\times SO(4)\times U(1)_{H_2}\times SU(2)\times U(1)_{H_3}\times U(1)_{H_4} \\ &\to\ U(1)_{H_1}\times SO(5)\times SU(2)\times U(1)_{H_2}\times SU(2)\times U(1)_{H_3}\times U(1)_{H_4}. \end{aligned} \tag{7.123}$$

The partition function for this model can be calculated similarly to the Class A model presented in Section 7.4.3. The main difference, in this case, is that the asymmetric shifts and twists introduced by $\boldsymbol{A}$ only explicitly include the anti-holomorphic part of the internal lattice in the first and third orbifold plane. That is, the lattice becomes

$$\begin{aligned} \Gamma^{\gamma}_{(6,6)} = \quad & \vartheta\left[\begin{smallmatrix} r+h_2 \\ s+g_2 \end{smallmatrix}\right]_{y^{3,4}} \vartheta\left[\begin{smallmatrix} r+h_2 \\ s+g_2 \end{smallmatrix}\right]_{y^{5,6}} \vartheta\left[\begin{smallmatrix} r+h_2 \\ s+g_2 \end{smallmatrix}\right]_{\bar{y}^{3,4}} \bar{\vartheta}\left[\begin{smallmatrix} r+h_2+2H' \\ s+g_2+2G' \end{smallmatrix}\right]_{\bar{y}^{5,6}} \\ & \times \vartheta\left[\begin{smallmatrix} r+h_1+H_1 \\ s+g_1+G_1 \end{smallmatrix}\right]^{1/2}_{y^1} \vartheta\left[\begin{smallmatrix} r+h_1+H_2 \\ s+g_1+G_2 \end{smallmatrix}\right]^{1/2}_{y^2} \vartheta\left[\begin{smallmatrix} r+h_1 \\ s+g_1 \end{smallmatrix}\right]_{w^{5,6}} \\ & \times \bar{\vartheta}\left[\begin{smallmatrix} r+h_1+H_1 \\ s+g_1+G_1 \end{smallmatrix}\right]^{1/2}_{\bar{y}^1} \bar{\vartheta}\left[\begin{smallmatrix} r+h_1+H_2 \\ s+g_1+G_2 \end{smallmatrix}\right]^{1/2}_{\bar{y}^2} \bar{\vartheta}\left[\begin{smallmatrix} r+h_1 \\ s+g_1 \end{smallmatrix}\right]_{\bar{w}^{5,6}} \\ & \times \vartheta\left[\begin{smallmatrix} r-h_1-h_2+H_1 \\ s-g_1-g_2+G_1 \end{smallmatrix}\right]^{1/2}_{w^1} \vartheta\left[\begin{smallmatrix} r-h_1-h_2+H_2 \\ s-g_1-g_2+G_2 \end{smallmatrix}\right]^{1/2}_{w^2} \vartheta\left[\begin{smallmatrix} r-h_1-h_2 \\ s-g_1-g_2 \end{smallmatrix}\right]_{w^{3,4}} \\ & \times \vartheta\left[\begin{smallmatrix} r-h_1-h_2+H_1 \\ s-g_1-g_2+G_1 \end{smallmatrix}\right]^{1/2}_{\bar{w}^1} \bar{\vartheta}\left[\begin{smallmatrix} r-h_1-h_2+H_2 \\ s-g_1-g_2+G_2 \end{smallmatrix}\right]^{1/2}_{\bar{w}^2} \bar{\vartheta}\left[\begin{smallmatrix} r-h_1-h_2+2H' \\ s-g_1-g_2+2G' \end{smallmatrix}\right]_{\bar{w}^{3,4}}. \end{aligned} \tag{7.124}$$

We see that indeed part of the lattice remains left-right symmetric and that the lack of $e_{3,4,5,6}$ simplifies the lattice. Based on this lattice, we can gain the q-expansion of the model, which is now given by

$$\begin{aligned} Z =& \, 2\,q^0\bar{q}^{-1} + 56\,q^{1/2}\bar{q}^{-1/2} + 208\,q^{-1/2}\bar{q}^{1/2} \\ & + 8\,q^0\bar{q}^0 - 192\,q^{1/8}\bar{q}^{1/8} + 1280\,q^{1/4}\bar{q}^{1/4} - 5632\,q^{1/2}\bar{q}^{1/2}, \end{aligned} \tag{7.125}$$

including all terms up to at most $\mathcal{O}(q^{1/2})$ and $\mathcal{O}(\bar{q}^{1/2})$. We note again the presence of the proto-graviton term with the correct factor and the presence of a constant term $q^0\bar{q}^0$. There was no model found with $N_b = N_f$ in a sample of 2.5×10^3 4 generation models. Integrating this expansion over the fundamental domain of the modular group gives the spacetime cosmological constant

$$\Lambda_{\rm ST} = 31.86\times\mathcal{M}^4, \tag{7.126}$$

which was calculated to $\mathcal{O}(q^4\bar{q}^4)$. As in the Class A case, this value is evaluated at the free fermionic self-dual point in moduli space. While some moduli are projected by the asymmetric twists, some of the geometric moduli remain unfixed and require further analysis.

7.6 Discussion and Conclusion

In this section, we initiated the extension of the fermionic $\mathbb{Z}_2 \times \mathbb{Z}_2$ orbifold classification method to string vacua with asymmetric boundary conditions. There are notable phenomenological advantages for string models with asymmetric boundary conditions. Perhaps most notable is the fact that asymmetric boundary conditions fix many of the untwisted moduli by projecting out the moduli fields from the massless spectrum [67]. In this respect, we note that there exist cases in which all the untwisted moduli are projected out, as well as cases in which it has been argued the string vacuum is entirely fixed, i.e. cases in which the twisted, as well as the supersymmetric moduli, are fixed [112]. We note that from the point of view of the free fermionic classification methodology, these cases are futile because it entails that they are not compatible with any of the e_i vectors discussed in Section 7.2. Our purpose here was therefore to analyse configurations in which some of the moduli are fixed. This approach is particularly suited in the search for string vacua with a positive cosmological constant, á la references [82, 108]. In these cases, the potential of some of the remaining unfixed moduli is analysed away from the self-dual point with the aim of finding a vacuum state with a positive vacuum energy at a stable minimum. Thus, whereas in the case of [82, 108] the other moduli are unfixed, in the case of vacua with asymmetric boundary conditions the possibility exists of finding such vacua in which the other moduli are fixed.

In the classification of vacua with asymmetric boundary conditions, there exists a variation in the pairings of the holomorphic worldsheet fermions. We presented a complete classification of all the possible pairings, consistent with modular invariance and worldsheet supersymmetry, and picked two of these choices for detailed classification. We showed the existence of three-generation quasi-realistic models in the first case, whereas the second case did not produce any three-generation models. In both cases, the incorporation of asymmetric boundary conditions was done in a single basis vector, whereas the remaining basic set, aside from the set of the e_i basis vectors that are compatible with the given pairings, were identical in the two cases. We note that in principle this can be relaxed, e.g. by not including the vector z_1 in the basis, and that a three-generation model might be obtainable with this variation, we leave such variations for future work. We note, however, that the program initiated herein opens the door to the systematic investigation of quasi-realistic vacua that are intrinsically non-geometric. We furthermore demonstrated effective applications of SMT algorithms to the space of free fermionic models under investigation. Not only do they provide significant efficiency increases, as demonstrated in Figure 7.2 and 7.5, but they also allowed for an immediate evaluation of unsatisfiable constraints, such as proving the absence of three-generation models in Class B.

Other than the systematic study of the one-loop potential for asymmetric models mentioned as a key motivation for this work, future work classifying Standard-like models (SLMs) with asymmetric boundary conditions is a natural extension of this work. The space of asymmetric SLMs will be larger and phenomenologically viable models more sparsely distributed, thus the application of SMT algorithms could prove instrumental in effective searches of

this landscape. The analysis of Section 7.2 can be extended so that the SMT can explicitly interpret phenomenological constraints as a function of all asymmetric pairings and provide generic results, including no-go theorems, over a varied space of models. It will furthermore be interesting to explore different possibilities for how to implement the asymmetric boundary conditions other than solely through the $SO(10)$ breaking vector as studied in this work.

8 Conclusion

In this thesis, we discussed various aspects of non-supersymmetric heterotic string vacua through the lens of the fermionic worldsheet construction. Following a quick introduction to string theory and its formulation in terms of free worldsheet fermions in Chapters 2 and 3 we developed key tools and methods to analyse the phenomenological features of four-dimensional string models. A central element of the thesis has been the partition function and one-loop potential extensively discussed in Chapter 4. This proves to be a pivotal element in the analysis of non-supersymmetric vacua as the specific form and convergence of the one-loop partition function give us key insights into the structure of the physical structure and stability of sting models. One of these intriguing features is the emergence of misaligned supersymmetry which manifests as an oscillation in the excess of bosonic and fermionic states over the massive spectrum of closed string theories. We also extensively discussed the modular invariance properties of string theory and its implications for the finiteness of string amplitudes and its relation with misaligned supersymmetry.

In Chapter 5, we uncovered new possibilities in the landscape for constructing viable four-dimensional non-supersymmetric models that arise from the less studied ten-dimensional tachyonic heterotic vacua. This opens up a new avenue in string phenomenology and shows that higher-dimensional tachyonic vacua should be considered on an equal footing in discussions of string phenomenology. We showed that such models have interesting phenomenological features and proved that there are indeed consistent configurations in which all tachyons are projected. Moreover, we find models with a physical spectrum that is Bose-Fermi degenerate at the massless level. This may provide a starting point for constructing models where the cosmological constant is exponentially suppressed. After an analysis of the tachyonic sectors that may arise, we gave an exhaustive classification of the phenomenological features of models in this class. We then gave an example of a model with desirable features that is also Bose-Fermi degenerate. These kinds of models are not well studied and more work is needed to provide more understanding of their scope. Another interesting question is the general structure of the $\tilde{S}$-map and how these models could be connected to other parts of the landscape via interpolations.

Over the past four decades, much of the focus has been to construct realistic string models that can produce some of the phenomenological features observed today. However, there are other parts of the string landscape containing models with interesting features that may provide useful in some cosmological scenarios. In Chapter 6 we provide some examples of models from these "corners" of the landscape. We show the existence of two new classes of four-dimensional heterotic models, one with no massless fermions in its physical spectrum and one with no massless twisted bosons. We call these the heterotic Type-0 and Type-$\bar{0}$ models respectively and they provide an interesting insight into the possible boundaries of the heterotic landscape. We show that the conditions of the lack of massless fermions or bosons are very restrictive on the possible choices of GGSO coefficient and in some cases produce a unique model with these given characteristics. Even though we fail to find any Type-0

models without on-shell tachyons these constructions lead us to discover that misaligned supersymmetry is still present in tachyonic models. This shines a new light on discussions about the relation between the finiteness of closed string theories and misaligned supersymmetry. In the case of Type-$\bar{0}$ models, we did find some configurations in which all physical tachyons are projected and so we gain a finite value for the vacuum energy. Interestingly, due to the large abundance of fermions at the massless level which provides the dominant contribution to the vacuum energy, we found that all models have a large positive value for the cosmological constant.

The string constructions considered in Chapters 5 and 6 correspond to symmetric orbifoldings of toroidal heterotic compactifications. However, one can consider compactifications in which the left and right-moving sectors are not treated identically. Such models are called asymmetric orbifolds which we turned to discuss in Chapter 7. Even though these are special constructions from the geometric point of view, the free fermionic formulation is fully applicable and gives a powerful tool for exploring the possible phenomenological features that arise. Perhaps the most important feature of these asymmetric models is the ability to project some of the moduli of the underlying toroidal geometry. This makes them good candidates to produce stable non-supersymmetric four-dimensional models. We provided an exhaustive enumeration of allowed pairings of the internal fermions and derived the implications this has towards the retainment or projection of the moduli. Then working with a very general basis, we developed classification methods for two separate classes of asymmetric orbifolds. We also provided examples of models in each class and discussed their phenomenological features. We focused on models in which some of the moduli are left unfixed. This provides the possibility of employing the methods of Chapter 4 to deform the models away from the fermionic point thereby examining the stability in the free parameters of the moduli space.

Overall, in this thesis, we provided a snapshot of various interesting parts of the landscape of heterotic orbifold compactifications. The tools developed here give us the opportunity to uncover some of the features of string models and draw conclusions regarding the finiteness, stability and viability of many different configurations. There is yet still much left to discover and mapping the entirety of the string landscape remains a daunting task that requires much more work.

A Theta Functions and Poisson Resummation

In this appendix, we summarise some definitions and results concerning the Jacobi ϑ and Dedekind η-functions. These definitions, identities and relations are used throughout the thesis and so it is useful to gather them in one place. We will not provide mathematical proof for the equalities stated, however, these are readily available in the standard resources on θ-functions and modular forms [141–144].

In this appendix, and indeed the entire thesis, we often express quantities in their q-expanded form. For this, we must define

$$q \coloneqq e^{2\pi i\tau}\,, \qquad \bar{q} \coloneqq e^{-2\pi i\bar{\tau}}, \tag{A.1}$$

where $\tau \in \mathbb{C}$ is a complex parameter in the upper half-plane. In fact, for our purposes, τ is usually taken to be in the fundamental domain of the modular group $\mathrm{SL}(2,\mathbb{Z})$ given by

$$\mathcal{F} = \{\tau \in \mathbb{C} \mid |\tau| > 1\,,\, |\tau_1| < 1/2\}. \tag{A.2}$$

Hence, for the rest of this appendix, we assume that $\tau \in \mathcal{F}$ and therefore make no further reference to the range of τ.

The Dedekind η-function is defined via an infinite product as

$$\eta(\tau) \coloneqq q^{1/24}\prod_{n=1}^{\infty}(1-q^n)\,, \tag{A.3}$$

which under the modular group transforms as

$$\begin{aligned} T:&\quad \eta(\tau+1) = e^{i\pi/12}\,\eta(\tau) \\ S:&\quad \eta(-\frac{1}{\tau}) = \sqrt{-i\tau}\,\eta(\tau). \end{aligned} \tag{A.4}$$

Another set of pivotal functions when discussing string theory is the Jacobi ϑ-functions with characteristics $a, b \in \mathbb{R}$ defined as

$$\vartheta\left[\begin{smallmatrix} a \\ b \end{smallmatrix}\right](\tau,u) \coloneqq \sum_{n\in\mathbb{Z}} q^{\frac{1}{2}(n-\frac{a}{2})^2} e^{2\pi i(u-\frac{b}{2})(n-\frac{a}{2})}, \tag{A.5}$$

where $u \in \mathbb{C}$ is a new complex parameter. The series is convergent for any choice of $u \in \mathbb{C}$ and is hence well defined. Under modular transformations, the ϑ-functions transform as

$$\begin{aligned} T: \quad & \vartheta\left[\begin{smallmatrix} a \\ b \end{smallmatrix}\right](\tau+1,u) = e^{\frac{-i\pi}{4}a(a-2)}\vartheta\left[\begin{smallmatrix} a \\ a+b-1 \end{smallmatrix}\right](\tau,u) \\ S: \quad & \vartheta\left[\begin{smallmatrix} a \\ b \end{smallmatrix}\right](-\frac{1}{\tau},u) = \sqrt{-i\tau}\, e^{\frac{i\pi}{2}ab+i\pi\frac{u^2}{\tau}}\vartheta\left[\begin{smallmatrix} b \\ -a \end{smallmatrix}\right](\tau,u). \end{aligned} \tag{A.6}$$

In general, for the expression used in this thesis, we always require the form of these functions with $u = 0$, and so we denote

$$\vartheta\left[\begin{smallmatrix} a \\ b \end{smallmatrix}\right] = \vartheta\left[\begin{smallmatrix} a \\ b \end{smallmatrix}\right](\tau,0), \tag{A.7}$$

where the dependence on τ is implicitly understood. The ϑ-functions also exhibit additional periodicity properties in their characteristic arguments

$$\begin{aligned} \vartheta\left[\begin{smallmatrix} a+2 \\ b \end{smallmatrix}\right] &= \vartheta\left[\begin{smallmatrix} a \\ b \end{smallmatrix}\right] \\ \vartheta\left[\begin{smallmatrix} a \\ b+2 \end{smallmatrix}\right] &= e^{i\pi ab}\vartheta\left[\begin{smallmatrix} a \\ b \end{smallmatrix}\right], \end{aligned} \tag{A.8}$$

which can easily be deduced from the definition (A.5).

The ϑ-functions with characteristics restricted to $a, b \in \{0,1\}$ play a special role and are hence separately defined as

$$\begin{aligned} \vartheta_1 &\coloneqq \vartheta\left[\begin{smallmatrix} 1 \\ 1 \end{smallmatrix}\right] = i\sum_{n\in\mathbb{Z}}(-1)^n q^{(n+1/2)^2/2} = 0 \\ \vartheta_2 &\coloneqq \vartheta\left[\begin{smallmatrix} 1 \\ 0 \end{smallmatrix}\right] = \sum_{n\in\mathbb{Z}} q^{(n+1/2)^2/2} = 2\sum_{n\in\mathbb{Z}^+} q^{(n+1/2)^2/2} \\ \vartheta_3 &\coloneqq \vartheta\left[\begin{smallmatrix} 0 \\ 0 \end{smallmatrix}\right] = \sum_{n\in\mathbb{Z}} q^{n^2/2} = 1 + 2\sum_{n\in\mathbb{Z}^+} q^{n^2/2} \\ \vartheta_4 &\coloneqq \vartheta\left[\begin{smallmatrix} 0 \\ 1 \end{smallmatrix}\right] = \sum_{n\in\mathbb{Z}}(-1)^n q^{n^2/2} = 1 + 2\sum_{n\in\mathbb{Z}^+}(-1)^n q^{n^2/2}. \end{aligned} \tag{A.9}$$

For these special theta functions, we can also write down a product representation which expresses the sums (A.9) in terms of infinite products via

$$\begin{aligned} \vartheta_2 &= 2\,q^{1/8}\prod_{n=1}^{\infty}(1-q^n)(1+q^n)(1+q^n) \\ \vartheta_3 &= \prod_{n=1}^{\infty}(1-q^n)(1+q^{n-1/2})(1+q^{n-1/2}) \\ \vartheta_4 &= \prod_{n=1}^{\infty}(1-q^n)(1-q^{n-1/2})(1-q^{n-1/2}). \end{aligned} \tag{A.10}$$

These will be helpful in deriving the partition function of free fermions.

There are a number of intriguing identities these four functions satisfy. The most important of which are the *Jacobi identity*

$$\vartheta_1^4 - \vartheta_2^4 + \vartheta_3^4 - \vartheta_4^4 = 0, \tag{A.11}$$

and the *triple product identity*

$$\vartheta_2\,\vartheta_3\,\vartheta_4 = 2\eta^3. \tag{A.12}$$

The former is a powerful identity that underlies the structure of supersymmetry cancellations in string theory and the latter provides an elegant relation between the ϑ and η-functions which will provide some notational simplification.

One can also derive the *generalised Jacobi identity* which generalises the above equation to theta functions with general characteristics

$$\begin{aligned}\frac{1}{2}\sum_{a,b\in\{0,1\}}(-1)^{a(1+G)+b(1+H)}&\vartheta\left[\begin{smallmatrix}a\\b\end{smallmatrix}\right]\vartheta\left[\begin{smallmatrix}a+h_1\\b+g_1\end{smallmatrix}\right]\vartheta\left[\begin{smallmatrix}a+h_2\\b+g_2\end{smallmatrix}\right]\vartheta\left[\begin{smallmatrix}a-h_1-h_2\\b-g_1-g_2\end{smallmatrix}\right]\\ &=\vartheta\left[\begin{smallmatrix}1+H\\1+G\end{smallmatrix}\right]\vartheta\left[\begin{smallmatrix}1+H+h_1\\1+G+g_1\end{smallmatrix}\right]\vartheta\left[\begin{smallmatrix}1+H+h_2\\1+G+g_2\end{smallmatrix}\right]\vartheta\left[\begin{smallmatrix}1+H-h_1-h_2\\1+G-g_1-g_2\end{smallmatrix}\right].\end{aligned} \tag{A.13}$$

In the manipulation of toroidal lattice sums and partition functions, it is key to make use of the so-called *Poisson resummation* formula

$$\sum_{w_i\in\mathbb{Z}} e^{-\pi A_{ij}w^iw^j+\pi B_iw_i} = \frac{1}{\sqrt{\det A}}\sum_{m_i\in\mathbb{Z}} e^{-\pi(m_i+\frac{i}{2}B_i)(A^{-1})_{ij}(m_j+\frac{i}{2}B_j)}, \tag{A.14}$$

which provides a neat way to map expressions between their Hamiltonian and Lagrangian forms.

Bibliography

[1] Alon E. Faraggi, Viktor G. Matyas, and Benjamin Percival. "Stable Three Generation Standard–like Model From a Tachyonic Ten Dimensional Heterotic–String Vacuum". In: *The European Physical Journal C* 80.4 (2020), p. 337. arXiv: 1912.00061.

[2] Alon E. Faraggi, Viktor G. Matyas, and Benjamin Percival. "Towards the Classification of Tachyon-Free Models From Tachyonic Ten-Dimensional Heterotic String Vacua". In: *Nuclear Physics B* 961 (2020), p. 115231. arXiv: 2006.11340.

[3] Alon E. Faraggi, Viktor G. Matyas, and Benjamin Percival. "Classification of Non-Supersymmetric Pati-Salam Heterotic String Models". In: *Physical Review D* 104.4 (2021), p. 046002. arXiv: 2011.04113.

[4] Alon E. Faraggi, Viktor G. Matyas, and Benjamin Percival. "Type 0 $\mathbb{Z}_2 \times \mathbb{Z}_2$ Heterotic String Orbifolds and Misaligned Supersymmetry". In: *International Journal of Modern Physics A* 36.24 (2021), p. 2150174. arXiv: 2010.06637.

[5] Alon E. Faraggi, Viktor G. Matyas, and Benjamin Percival. "Type $\bar{\mathbf{0}}$ Heterotic String Orbifolds". In: *Physics Letters B* 814 (2021), p. 136080. arXiv: 2011.12630.

[6] Alon E. Faraggi, Viktor G. Matyas, and Benjamin Percival. "Towards classification of $\mathcal{N} = 1$ and $\mathcal{N} = 0$ flipped $SU(5)$ asymmetric $\mathbb{Z}_2 \times \mathbb{Z}_2$ heterotic string orbifolds". In: *Physical Review D* 106.2 (2022), p. 026011. arXiv: 2202.04507.

[7] Alonzo R. Diaz Avalos, Alon E. Faraggi, Viktor G. Matyas, and Benjamin Percival. "Fayet-Iliopoulos D-Term in Non-Supersymmetric Heterotic String Orbifolds". In: (2023). arXiv: 2302.10075.

[8] Federica Albertini, Michele Del Zotto, Iñaki Garca Etxebarria, and Saghar S. Hosseini. "Higher Form Symmetries and M-theory". In: *JHEP* 12 (2020), p. 203. arXiv: 2005.12831.

[9] Michele Del Zotto, Iñaki Garca Etxebarria, and Saghar S. Hosseini. "Higher form symmetries of Argyres-Douglas theories". In: *JHEP* 10 (2020), p. 056. arXiv: 2007.15603.

[10] Saghar S. Hosseini and Robert Moscrop. "Maruyoshi-Song flows and defect groups of $D_p^b(G)$ theories". In: *JHEP* 10 (2021), p. 119. arXiv: 2106.03878.

[11] Fabio Apruzzi, Federico Bonetti, Iñaki Garca Etxebarria, Saghar S. Hosseini, and Sakura Schafer-Nameki. "Symmetry TFTs from String Theory". In: (2021). arXiv: 2112.02092.

[12] Gabriel Arenas-Henriquez, Olivera Miskovic, and Rodrigo Olea. "Vacuum Degeneracy and Conformal Mass in Lovelock AdS Gravity". In: *JHEP* 11 (2017), p. 128. arXiv: 1710.08512.

[13] Gabriel Arenas-Henriquez, Robert B. Mann, Olivera Miskovic, and Rodrigo Olea. "Mass in Lovelock Unique Vacuum gravity theories". In: *Phys. Rev. D* 100.6 (2019), p. 064038. arXiv: 1905.10840.

[14] Gabriel Arenas-Henriquez. "Black Hole Energy in Lovelock Unique Vacuum theories". MA thesis. Andres Bello Natl. U., 2019. arXiv: 1909.06716.

[15] Gabriel Arenas-Henriquez, Ruth Gregory, and Andrew Scoins. "On acceleration in three dimensions". In: *JHEP* 05 (2022), p. 063. arXiv: 2202.08823.

[16] Gabriel Arenas-Henriquez, Felipe Diaz, and Per Sundell. "Logarithmic corrections, entanglement entropy, and UV cutoffs in de Sitter spacetime". In: *JHEP* 08 (2022), p. 261. arXiv: 2206.10427.

[17] Gabriel Arenas-Henriquez, Felipe Diaz, and Yerko Novoa. "Thermal fluctuations of black holes with non-linear electrodynamics and charged Renyi entropy". In: (2022). arXiv: 2211.06355.

[18] Alon E. Faraggi, Glyn Harries, Benjamin Percival, and John Rizos. "Doublet-Triplet Splitting in Fertile Left-Right Symmetric Heterotic String Vacua". In: *Nucl. Phys. B* 953 (2020), p. 114969. arXiv: 1912.04768.

[19] Alon E. Faraggi, Benjamin Percival, Sven Schewe, and Dominik Wojtczak. "Satisfiability modulo theories and chiral heterotic string vacua with positive cosmological constant". In: *Phys. Lett. B* 816 (2021), p. 136187. arXiv: 2101.03227.

[20] Susha Parameswaran and Flavio Tonioni. "Non-supersymmetric String Models from Anti-D3-/D7-branes in Strongly Warped Throats". In: *JHEP* 12 (2020), p. 174. arXiv: 2007.11333.

[21] Niccolò Cribiori, Susha Parameswaran, Flavio Tonioni, and Timm Wrase. "Misaligned Supersymmetry and Open Strings". In: *JHEP* 04 (2021), p. 099. arXiv: 2012.04677.

[22] Ander Retolaza, Jamie Rogers, Radu Tatar, and Flavio Tonioni. "Branes, fermions, and superspace dualities". In: *JHEP* 10 (2021), p. 243. arXiv: 2106.02090.

[23] Niccolò Cribiori, Susha Parameswaran, Flavio Tonioni, and Timm Wrase. "Modular invariance, misalignment and finiteness in non-supersymmetric strings". In: *JHEP* 01 (2022), p. 127. arXiv: 2110.11973.

[24] Gary Shiu, Flavio Tonioni, Vincent Van Hemelryck, and Thomas Van Riet. "AdS scale separation and the distance conjecture". In: (2022). arXiv: 2212.06169.

[25] Gary Shiu, Flavio Tonioni, and Hung V. Tran. "Accelerating universe at the end of time". In: (2023). arXiv: 2303.03418.

[26] M. Medevielle, T. Mohaupt, and G. Pope. "Type-II Calabi-Yau compactifications, T-duality and special geometry in general spacetime signature". In: *JHEP* 02 (2022), p. 048. arXiv: 2111.09017.

[27] Harold Erbin and Maxime Médevielle. "Closed string theory without level-matching at the free level". In: *JHEP* 03 (2023), p. 091. arXiv: 2209.05585.

[28] Bruno Valeixo Bento, Dibya Chakraborty, Susha L. Parameswaran, and Ivonne Zavala. "Dark Energy in String Theory". In: *PoS* CORFU2019 (2020), p. 123. arXiv: 2005.10168.

[29] Bruno Valeixo Bento, Dibya Chakraborty, Susha L. Parameswaran, and Ivonne Zavala. "A new de Sitter solution with a weakly warped deformed conifold". In: *JHEP* 12 (2021), p. 124. arXiv: 2105.03370.

[30] Bruno Valeixo Bento, Fay Dowker, and Stav Zalel. "If time had no beginning: growth dynamics for past-infinite causal sets". In: *Class. Quant. Grav.* 39.4 (2022), p. 045002. arXiv: 2109.10749.

[31] Bruno Valeixo Bento and Stav Zalel. "If time had no beginning". In: (2021). arXiv: 2109.11953.

[32] Bruno Valeixo Bento, Dibya Chakraborty, Susha Parameswaran, and Ivonne Zavala. "Gravity at the tip of the throat". In: *JHEP* 09 (2022), p. 208. arXiv: 2204.02086.

[33] Bruno Valeixo Bento, Dibya Chakraborty, Susha Parameswaran, and Ivonne Zavala. "A guide to frames, 2π's, scales and corrections in string compactifications". In: (2023). arXiv: 2301.05178.

[34] A. E. Faraggi, S. Groot Nibbelink, and M. Hurtado-Heredia. "Uncovering a spinorvector duality on a resolved orbifold". In: *Nucl. Phys. B* 969 (2021), p. 115473. arXiv: 2103.13442.

[35] A. E. Faraggi, S. Groot Nibbelink, and M. Hurtado Heredia. "Constraint on spinorvector dualities in six dimensions". In: *Phys. Rev. D* 103.12 (2021), p. 126016. arXiv: 2103.14684.

[36] A. E. Faraggi, S. Groot Nibbelink, and M. Hurtado Heredia. "Taming triangulation dependence of $T^6/\mathbb{Z}_2 \times \mathbb{Z}_2$ resolutions". In: *JHEP* 01 (2022), p. 169. arXiv: 2111.10407.

[37] A. E. Faraggi, S. Groot Nibbelink, and M. Hurtado Heredia. "The fate of discrete torsion on resolved heterotic Z2×Z2 orbifolds using (0,2) GLSMs". In: *Nucl. Phys. B* 988 (2023), p. 116111. arXiv: 2211.01397.

[38] Joseph Polchinski. *String Theory: Volume 1: An Introduction to the Bosonic String*. Vol. 1. Cambridge: Cambridge University Press, 1998.

[39] Joseph Polchinski. *String Theory: Volume 2: Superstring Theory and Beyond*. Vol. 2. Cambridge: Cambridge University Press, 1998.

[40] Thomas Mohaupt. *A Short Introduction to String Theory*. en. Cambridge University Press, 2022, p. 283.

[41] Ralph Blumenhagen, Dieter Lüst, and Stefan Theisen. *Basic Concepts of String Theory*. en. Berlin, Heidelberg: Springer, 2013.

[42] Elias Kiritsis. *String Theory in a Nutshell*. en. Princeton University Press, 2019, p. 883.

[43] Steven Abel. "Cargese lectures: A String phenomenology primer". In: *PoS* CARGESE2007 (2007), p. 001.

[44] Ignatios Antoniadis, C. P. Bachas, and C. Kounnas. "Four-Dimensional Superstrings". In: *Nucl. Phys. B* 289 (1987), p. 87.

[45] Ignatios Antoniadis and C. Bachas. "4-D Fermionic Superstrings with Arbitrary Twists". In: *Nucl. Phys. B* 298 (1988), pp. 586–612.

[46] Hikaru Kawai, David C. Lewellen, and S. H. Henry Tye. "Construction of Fermionic String Models in Four-Dimensions". In: *Nucl. Phys. B* 288 (1987), p. 1.

[47] Luis Alvarez-Gaume, Gregory W. Moore, Cumrun Vafa, and M. Stone. "Theta Functions, Modular Invariance and Strings". In: *Commun. Math. Phys.* 106 (1986), pp. 1–40.

[48] A. N. Schellekens. "Multiloop Modular Invariance of the Covariant Lattice Construction of Fermionic Strings". In: *Phys. Lett. B* 199 (1987), pp. 427–431.

[49] S. Ferrara, C. Kounnas, and M. Porrati. "Multiloop Modular Invariance in Spontaneously Broken Superstrings". In: *Phys. Lett. B* 197 (1987), pp. 135–138.

[50] H. Kawai, D. C. Lewellen, J. A. Schwartz, and S. H. H. Tye. "The Spin Structure Construction of String Models and Multiloop Modular Invariance". In: *Nucl. Phys. B* 299 (1988), pp. 431–470.

[51] Steven Abel, Keith R. Dienes, and Eirini Mavroudi. "Towards a Non-Supersymmetric String Phenomenology". In: *Physical Review D* 91.12 (2015), p. 126014. arXiv: 1502.03087.

[52] David J. Gross, Jeffrey A. Harvey, Emil J. Martinec, and Ryan Rohm. "The Heterotic String". In: *Phys. Rev. Lett.* 54 (1985), pp. 502–505.

[53] David J. Gross, Jeffrey A. Harvey, Emil J. Martinec, and Ryan Rohm. "Heterotic String Theory. 1. The Free Heterotic String". In: *Nucl. Phys. B* 256 (1985), p. 253.

[54] Lance J. Dixon and Jeffrey A. Harvey. "String Theories in Ten-Dimensions Without Space-Time Supersymmetry". In: *Nucl. Phys. B* 274 (1986). Ed. by B. Schellekens, pp. 93–105.

[55] Luis Alvarez-Gaume, Paul H. Ginsparg, Gregory W. Moore, and C. Vafa. "An O(16) x O(16) Heterotic String". In: *Phys. Lett. B* 171 (1986), pp. 155–162.

[56] N. Seiberg and Edward Witten. "Spin Structures in String Theory". In: *Nucl. Phys. B* 276 (1986), p. 272.

[57] H. Kawai, D. C. Lewellen, and S. H. H. Tye. "Classification of Closed Fermionic String Models". In: *Phys. Rev. D* 34 (1986), p. 3794.

[58] Herbert K. Dreiner, Jorge L. Lopez, Dimitri V. Nanopoulos, and David B. Reiss. "String Model Building in the Free Fermionic Formulation". In: *Nucl. Phys. B* 320 (1989), pp. 401–439.

[59] Michael Blaszczyk, Stefan Groot Nibbelink, Orestis Loukas, and Saul Ramos-Sanchez. "Non-supersymmetric heterotic model building". In: *JHEP* 10 (2014), p. 119. arXiv: 1407.6362.

[60] P. Athanasopoulos, A. E. Faraggi, S. Groot Nibbelink, and V. M. Mehta. "Heterotic free fermionic and symmetric toroidal orbifold models". In: *Journal of High Energy Physics* 2016.4 (2016), pp. 1–51. arXiv: 1602.03082.

[61] Sergio Ferrara, Costas Kounnas, and Massimo Porrati. "Superstring Solutions With Spontaneously Broken Four-dimensional Supersymmetry". In: *Nucl. Phys. B* 304 (1988), pp. 500–512.

[62] Sergio Ferrara, Costas Kounnas, and Massimo Porrati. "$N = 1$ Superstrings With Spontaneously Broken Symmetries". In: *Phys. Lett. B* 206 (1988), pp. 25–31.

[63] Sergio Ferrara, Costas Kounnas, Massimo Porrati, and Fabio Zwirner. "Superstrings with Spontaneously Broken Supersymmetry and their Effective Theories". In: *Nucl. Phys. B* 318 (1989), pp. 75–105.

[64] Costas Kounnas and Bruno Rostand. "Coordinate Dependent Compactifications and Discrete Symmetries". In: *Nucl. Phys. B* 341 (1990), pp. 641–665.

[65] Benedict Aaronson, Steven Abel, and Eirini Mavroudi. "On interpolations from SUSY to non-SUSY strings and their properties". In: *Physical Review D* 95.10 (2017), p. 106001. arXiv: 1612.05742.

[66] Jonathan Bagger, Dennis Nemeschansky, Nathan Seiberg, and Shimon Yankielowicz. "Bosons, Fermions and Thirring Strings". In: *Nucl. Phys. B* 289 (1987), pp. 53–86.

[67] Alon E. Faraggi. "Moduli Fixing in Realistic String Vacua". In: *Nuclear Physics B* 728.1-3 (2005), pp. 83–108. arXiv: hep-th/0504016.

[68] A. Gregori, C. Kounnas, and J. Rizos. "Classification of the N=2, Z(2) x Z(2) symmetric type II orbifolds and their type II asymmetric duals". In: *Nucl. Phys. B* 549 (1999), pp. 16–62.

[69] Keith R. Dienes, Moshe Moshe, and Robert C. Myers. "String theory, misaligned supersymmetry, and the supertrace constraints". In: *Phys. Rev. Lett.* 74 (1995), pp. 4767–4770. arXiv: hep-th/9503055.

[70] Carlo Angelantonj, Ioannis Florakis, and Boris Pioline. "A new look at one-loop integrals in string theory". In: *Commun. Num. Theor. Phys.* 6 (2012), pp. 159–201.

[71] Carlo Angelantonj, Ioannis Florakis, and Boris Pioline. "One-Loop BPS amplitudes as BPS-state sums". In: *JHEP* 06 (2012), p. 070. arXiv: 1203.0566.

[72] Carlo Angelantonj, Ioannis Florakis, and Boris Pioline. "Rankin-Selberg methods for closed strings on orbifolds". In: *JHEP* 07 (2013), p. 181. arXiv: 1304.4271.

[73] Ioannis Florakis and Boris Pioline. "On the Rankin-Selberg method for higher genus string amplitudes". In: *Commun. Num. Theor. Phys.* 11 (2017), pp. 337–404. arXiv: 1602.00308.

[74] Michael B. Green, Michael B. Green, John H. Schwarz, and Edward Witten. *Superstring Theory: Volume 2, Loop Amplitudes, Anomalies and Phenomenology*. en. Cambridge University Press, 1988, p. 608.

[75] Iraj Kani and Cumrun Vafa. "Asymptotic Mass Degeneracies in Conformal Field Theories". In: *Commun. Math. Phys.* 130 (1990), pp. 529–580.

[76] G. H. Hardy and S. Ramanujan. "Asymptotic Formulaæ in Combinatory Analysis". en. In: *Proceedings of the London Mathematical Society* s2-17.1 (1918), pp. 75–115.

[77] W. Fischler and Leonard Susskind. "Dilaton Tadpoles, String Condensates and Scale Invariance". In: *Phys. Lett. B* 171 (1986), pp. 383–389.

[78] Willy Fischler and Leonard Susskind. "Dilaton Tadpoles, String Condensates and Scale Invariance. 2." In: *Phys. Lett. B* 173 (1986), pp. 262–264.

[79] Ralph Blumenhagen and Anamaria Font. "Dilaton tadpoles, warped geometries and large extra dimensions for nonsupersymmetric strings". In: *Nucl. Phys. B* 599 (2001), pp. 241–254. arXiv: hep-th/0011269.

[80] E. Dudas and J. Mourad. "Brane solutions in strings with broken supersymmetry and dilaton tadpoles". In: *Phys. Lett. B* 486 (2000), pp. 172–178. arXiv: hep-th/0004165.

[81] Michele Cicoli et al. "String Cosmology: from the Early Universe to Today". In: (2023). arXiv: 2303.04819.

[82] Ioannis Florakis and John Rizos. "Chiral Heterotic Strings with Positive Cosmological Constant". In: *Nuclear Physics B* 913 (2016), pp. 495–533. arXiv: 1608.04582.

[83] Ioannis Florakis, John Rizos, and Konstantinos Violaris-Gountonis. "Three-Generation Super No-Scale Models in Heterotic Superstrings". In: *Physics Letters B* 833 (2022), p. 137311. arXiv: 2206.09732.

[84] Keith R. Dienes. "Modular invariance, finiteness, and misaligned supersymmetry: New constraints on the numbers of physical string states". In: *Nucl. Phys. B* 429 (1994), pp. 533–588.

[85] Carlo Angelantonj, Matteo Cardella, Shmuel Elitzur, and Eliezer Rabinovici. "Vacuum stability, string density of states and the Riemann zeta function". In: *JHEP* 02 (2011), p. 024. arXiv: 1012.5091.

[86] Carlo Angelantonj, Ioannis Florakis, and Giorgio Leone. "Tachyons and Misaligned Supersymmetry in Closed String Vacua". In: (2023). arXiv: 2301.13702.

[87] Alon E. Faraggi. "String Phenomenology From a Worldsheet Perspective". In: *Eur. Phys. J. C* 79.8 (2019), p. 703.

[88] Alon E. Faraggi and Mirian Tsulaia. "Interpolations Among NAHE-based Supersymmetric and Nonsupersymmetric String Vacua". In: *Phys. Lett. B* 683 (2010), pp. 314–320. arXiv: 0911.5125.

[89] Paul H. Ginsparg and C. Vafa. "Toroidal Compactification of Nonsupersymmetric Heterotic Strings". In: *Nucl. Phys. B* 289 (1987), p. 414.

[90] Alon E. Faraggi, Costas Kounnas, and John Rizos. "Chiral family classification of fermionic Z(2) x Z(2) heterotic orbifold models". In: *Phys. Lett. B* 648 (2007), pp. 84–89.

[91] Alon E. Faraggi, Costas Kounnas, and John Rizos. "Spinor-Vector Duality in fermionic Z(2) X Z(2) heterotic orbifold models". In: *Nucl. Phys. B* 774 (2007), pp. 208–231.

[92] Alon E. Faraggi, Costas Kounnas, and John Rizos. "Spinor-vector duality in N=2 heterotic string vacua". In: *Nucl. Phys. B* 799 (2008), pp. 19–33. arXiv: 0712.0747.

[93] Tristan Catelin-Jullien, Alon E. Faraggi, Costas Kounnas, and John Rizos. "Spinor-Vector Duality in Heterotic SUSY Vacua". In: *Nucl. Phys. B* 812 (2009), pp. 103–127. arXiv: 0807.4084.

[94] Carlo Angelantonj, Alon E. Faraggi, and Mirian Tsulaia. "Spinor-Vector Duality in Heterotic String Orbifolds". In: *JHEP* 07 (2010), p. 004. arXiv: 1003.5801.

[95] Alon E. Faraggi, Ioannis Florakis, Thomas Mohaupt, and Mirian Tsulaia. "Conformal Aspects of Spinor-Vector Duality". In: *Nucl. Phys. B* 848 (2011), pp. 332–371. arXiv: 1101.4194.

[96] Panos Athanasopoulos and Alon E. Faraggi. "Niemeier Lattices in the Free Fermionic Heterotic-String Formulation". In: *Adv. Math. Phys.* 2017 (2017), p. 3572469. arXiv: 1610.04898.

[97] A. E. Faraggi, C. Kounnas, S. E. M. Nooij, and J. Rizos. "Classification of the chiral Z(2) x Z(2) fermionic models in the heterotic superstring". In: *Nucl. Phys. B* 695 (2004), pp. 41–72.

[98] Alon E. Faraggi, Glyn Harries, and John Rizos. "Classification of left-right symmetric heterotic string vacua". In: *Nucl. Phys. B* 936 (2018), pp. 472–500. arXiv: 1806.04434.

[99] Alon E. Faraggi, John Rizos, and Hasan Sonmez. "Classification of standard-like heterotic-string vacua". In: *Nucl. Phys. B* 927 (2018), pp. 1–34. arXiv: 1709.08229.

[100] Benjamin Assel, Kyriakos Christodoulides, Alon E. Faraggi, Costas Kounnas, and John Rizos. "Exophobic Quasi-Realistic Heterotic String Vacua". In: *Phys. Lett. B* 683 (2010), pp. 306–313. arXiv: 0910.3697.

[101] Benjamin Assel, Kyriakos Christodoulides, Alon E. Faraggi, Costas Kounnas, and John Rizos. "Classification of Heterotic Pati-Salam Models". In: *Nucl. Phys. B* 844 (2011), pp. 365–396. arXiv: 1007.2268.

[102] Kyriakos Christodoulides, Alon E. Faraggi, and John Rizos. "Top Quark Mass in Exophobic Pati-Salam Heterotic String Model". In: *Phys. Lett. B* 702 (2011), pp. 81–89. arXiv: 1104.2264.

[103] Alon Faraggi, John Rizos, and Hasan Sonmez. "Classification of Flipped SU(5) Heterotic-String Vacua". In: *Nucl. Phys. B* 886 (2014), pp. 202–242. arXiv: 1403.4107.

[104] Hasan Sonmez. "Flipped SU(5) string vacua classification: A variation of the SO(10) breaking basis vector". In: *Phys. Rev. D* 93.12 (2016), p. 125002. arXiv: 1603.03504.

[105] Gerald B. Cleaver and Alon E. Faraggi. "On the anomalous U(1) in free fermionic superstring models". In: *Int. J. Mod. Phys. A* 14 (1999), pp. 2335–2356. arXiv: hep-ph/9711339.

[106] Alon E. Faraggi. "Generation mass hierarchy in superstring derived models". In: *Nucl. Phys. B* 407 (1993), pp. 57–72. arXiv: hep-ph/9210256.

[107] Alon E. Faraggi. "Higgs-matter splitting in quasi-realistic orbifold string GUTs". In: *Eur. Phys. J. C* 49 (2007), pp. 803–813.

[108] Ioannis Florakis, John Rizos, and Konstantinos Violaris-Gountonis. "Super No-Scale Models with Pati-Salam Gauge Group". In: *Nuclear Physics B* 976 (2022), p. 115689. arXiv: 2110.06752.

[109] Alon E. Faraggi, Costas Kounnas, and Herve Partouche. "Large volume susy breaking with a solution to the decompactification problem". In: *Nucl. Phys. B* 899 (2015), pp. 328–374. arXiv: 1410.6147.

[110] Johar M. Ashfaque, Panos Athanasopoulos, Alon E. Faraggi, and Hasan Sonmez. "Non-Tachyonic Semi-Realistic Non-Supersymmetric Heterotic String Vacua". In: *Eur. Phys. J. C* 76.4 (2016), p. 208.

[111] Stefan Groot Nibbelink, Orestis Loukas, Andreas Mütter, Erik Parr, and Patrick K. S. Vaudrevange. "Tension Between a Vanishing Cosmological Constant and Non-Supersymmetric Heterotic Orbifolds". In: *Fortsch. Phys.* 68.7 (2020), p. 2000044. arXiv: 1710.09237.

[112] Gerald B. Cleaver, Alon E. Faraggi, Elisa Manno, and Cristina Timirgaziu. "Quasi-realistic heterotic-string models with vanishing one-loop cosmological constant and perturbatively broken supersymmetry?" In: *Phys. Rev. D* 78 (2008), p. 046009. arXiv: 0802.0470.

[113] Costas Kounnas and Herve Partouche. "Super no-scale models in string theory". In: *Nucl. Phys. B* 913 (2016), pp. 593–626. arXiv: 1607.01767.

[114] Alon E. Faraggi. "Fractional charges in a superstring derived standard like model". In: *Phys. Rev. D* 46 (1992), pp. 3204–3207.

[115] Sanghyeon Chang, Claudio Coriano, and Alon E. Faraggi. "Stable superstring relics". In: *Nucl. Phys. B* 477 (1996), pp. 65–104. arXiv: hep-ph/9605325.

[116] L. Delle Rose, A. E. Faraggi, C. Marzo, and J. Rizos. "Wilsonian dark matter in string derived Z' model". In: *Phys. Rev. D* 96.5 (2017), p. 055025. arXiv: 1704.02579.

[117] Costas Kounnas. "Massive Boson-Fermion Degeneracy and the Early Structure of the Universe". In: *Fortsch. Phys.* 56 (2008), pp. 1143–1156. arXiv: 0808.1340.

[118] Ioannis Florakis and Costas Kounnas. "Orbifold Symmetry Reductions of Massive Boson-Fermion Degeneracy". In: *Nucl. Phys. B* 820 (2009), pp. 237–268. arXiv: 0901.3055.

[119] Ioannis Florakis, Costas Kounnas, and Nicolaos Toumbas. "Marginal Deformations of Vacua with Massive boson-fermion Degeneracy Symmetry". In: *Nucl. Phys. B* 834 (2010), pp. 273–315. arXiv: 1002.2427.

[120] Alon E. Faraggi and Dimitri V. Nanopoulos. "Naturalness of three generations in free fermionic Z(2)-n x Z(4) string models". In: *Phys. Rev. D* 48 (1993), pp. 3288–3296.

[121] Alon E. Faraggi. "Toward the classification of the realistic free fermionic models". In: *Int. J. Mod. Phys. A* 14 (1999), pp. 1663–1702. arXiv: hep-th/9708112.

[122] F. Bigazzi, L. Girardello, and A. Zaffaroni. "A Note on regular type 0 solutions and confining gauge theories". In: *Nucl. Phys. B* 598 (2001), pp. 530–542. arXiv: hep-th/0011041.

[123] Mohammad Akhond, Adi Armoni, and Stefano Speziali. "Phases of $\mathbf{U}(N_c)$ QCD from Type 0 Strings and Seiberg Duality". In: *JHEP* 09 (2019), p. 111.

[124] David C. Lewellen. "Embedding Higher Level Kac-Moody Algebras in Heterotic String Models". In: *Nucl. Phys. B* 337 (1990), pp. 61–86.

[125] Keith R. Dienes and John March-Russell. "Realizing higher level gauge symmetries in string theory: New embeddings for string GUTs". In: *Nucl. Phys. B* 479 (1996), pp. 113–172. arXiv: hep-th/9604112.

[126] Erik Plauschinn. "Non-geometric backgrounds in string theory". In: *Phys. Rept.* 798 (2019), pp. 1–122. arXiv: 1811.11203.

[127] Alon E. Faraggi. "Yukawa couplings in superstring derived standard like models". In: *Phys. Rev. D* 47 (1993), pp. 5021–5028.

[128] Alon E. Faraggi. "Doublet triplet splitting in realistic heterotic string derived models". In: *Phys. Lett. B* 520 (2001), pp. 337–344. arXiv: hep-ph/0107094.

[129] Alon E. Faraggi, Dimitri V. Nanopoulos, and Ka-jia Yuan. "A Standard Like Model in the 4D Free Fermionic String Formulation". In: *Nucl. Phys. B* 335 (1990), pp. 347–362.

[130] Alon E. Faraggi. "A New standard - like model in the four-dimensional free fermionic string formulation". In: *Phys. Lett. B* 278 (1992), pp. 131–139.

[131] Alon E. Faraggi. "Hierarchical top - bottom mass relation in a superstring derived standard - like model". In: *Phys. Lett. B* 274 (1992), pp. 47–52.

[132] Alon E. Faraggi. "Top quark mass prediction in superstring derived standard - like model". In: *Phys. Lett. B* 377 (1996), pp. 43–47. arXiv: hep-ph/9506388.

[133] Joel Scherk and John H. Schwarz. "Spontaneous Breaking of Supersymmetry Through Dimensional Reduction". In: *Phys. Lett. B* 82 (1979), pp. 60–64.

[134] Joel Scherk, John H. Schwarz, A. Salam, and E. Sezgin. "How to Get Masses from Extra Dimensions". In: *Nucl. Phys. B* 153 (1979), pp. 61–88.

[135] Costas Kounnas and Massimo Porrati. "Spontaneous Supersymmetry Breaking in String Theory". In: *Nucl. Phys. B* 310 (1988), pp. 355–370.

[136] Steven Abel and Richard J. Stewart. "On exponential suppression of the cosmological constant in non-SUSY strings at two loops and beyond". In: *Physical Review D* 96.10 (2017), p. 106013. arXiv: 1701.06629.

[137] K. S. Narain, M. H. Sarmadi, and C. Vafa. "Asymmetric Orbifolds". In: *Nucl. Phys. B* 288 (1987), p. 551.

[138] Stefan Groot Nibbelink and Patrick K. S. Vaudrevange. "T-duality orbifolds of heterotic Narain compactifications". In: *JHEP* 04 (2017), p. 030. arXiv: 1703.05323.

[139] Stefan Groot Nibbelink. "A worldsheet perspective on heterotic T-duality orbifolds". In: *JHEP* 04 (2021), p. 190. arXiv: 2012.02778.

[140] G. B. Cleaver, A. E. Faraggi, and Dimitri V. Nanopoulos. "String derived MSSM and M theory unification". In: *Phys. Lett. B* 455 (1999), pp. 135–146. arXiv: hep-ph/9811427.

[141] David Mumford. *Tata Lectures on Theta II*. en. Boston, MA: Birkhäuser, 2007.

[142] David Mumford. *Tata Lectures on Theta I*. en. Boston, MA: Birkhäuser, 2007.

[143] S. Kharchev and A. Zabrodin. "Theta vocabulary I". en. In: *Journal of Geometry and Physics* 94 (2015), pp. 19–31. arXiv: 1502.04603.

[144] S. Kharchev and A. Zabrodin. "Theta vocabulary II. Multidimensional case". In: *J. Geom. Phys.* 104 (2016), pp. 112–120. arXiv: 1510.02699.